VNIVERSITAT DE VALÈNCIA

Doctoral programme in Biomedicine and Biotechnology

Subcellular distribution of calpain-1 and calpain-2 as a key event for calpain-mediated functions in physiological and neoplastic mammary models.

Doctoral thesis presented by:

Lucía Rodríguez Fernández

Directors:

Dr. Juan Viña Ribes

Dr. Elena Ruiz García-Trevijano

Dr. Rosa Zaragozá Colom

VNIVERSITAT DE VALÈNCIA Facultat de Medicina i Odontologia

Departament de Bioquímica
i Biologia Molecular

Dr. JUAN VIÑA RIBES, Catedrático de Bioquímica y Biología Molecular de la Universitat de València.

Dra. ELENA RUIZ GARCÍA-TREVIJANO, Profesora titular de Bioquímica y Biología Molecular de la Universitat de València.

Dra. ROSA ZARAGOZÁ COLOM, Profesora ayudante doctor de Anatomía y Embriología Humana de la Universitat de València.

CERTIFICAN:

Que Dña. LUCÍA RODRÍGUEZ FERNÁNDEZ, Licenciada en Farmacia por la Universitat de València, ha realizado bajo nuestra dirección y asesoramiento el presente trabajo de investigación, titulado "SUBCELLULAR DISTRIBUTION OF CALPAIN-1 AND CALPAIN-2 AS A KEY EVENT FOR CALPAIN-MEDIATED FUNCTION IN PHYSIOLOGICAL AND NEOPLASTIC MAMMARY MODELS", que será presentado como tesis doctoral para optar al grado de Doctor en Biomedicina y Biotecnología.

Y para que conste a todos los efectos, firman la presente certificación:

Fdo. Prof. Juan Viña Ribes

Fdo. Prof. Elena Ruiz García-Trevijano

Fdo. Prof. Rosa Zaragozá Colom

Valencia, 28 de Noviembre 2018

This thesis has been supported by funding from Ministerio de Economía y Competitividad (BFU2013-46434-P to Juan Viña Ribes and Rosa Zaragozá Colom), Generalitat Valenciana (GVPROMETEO 2014- 055 to Juan Viña Ribes) and Generalitat Valenciana (GVPROMETEO 2018- 167 to Juan Viña Ribes).

AGRADECIMIENTOS

En primer lugar, quiero agradecer a mis directores de tesis, el Dr. Juan Viña, la Dra. Elena Ruiz y a la Dra. Rosa Zaragozá, el haberme brindado la oportunidad de realizar la tesis doctoral bajo vuestra dirección. Han sido años de mucho trabajo, pero a la vez años emocionantes y de mucho aprendizaje, y deseo agradeceros todo lo que me habéis enseñado y el haber fomentado mi formación como investigadora. Al Dr. Juan Viña un especial agradecimiento por abrirme las puertas de su laboratorio, por su apoyo durante estos años, por sus sabios consejos, tanto científicos como personales y por transmitirme su experiencia en todos los niveles. A la Dra. Elena Ruiz por enseñarme a desarrollar el pensamiento científico y crítico, a plantear experimentos con criterio y organizar las ideas e información. Gracias por todo lo que me has enseñado, por esas conversaciones tan interesantes y por transmitirme tu pasión por la investigación. A la Dra. Rosa Zaragozá, agradecerte todo lo que me has enseñado y ayudado estos años, especialmente tu apoyo y ayuda en estos difíciles últimos meses. Finalmente, quiero reiterar mi agradecimiento a todos por vuestra comprensión, apoyo y ayuda, dadas las complicadas circunstancias, en estos últimos meses. Muchas gracias a los tres por todo.

Sumar un particular agradecimiento a Concha García, por toda su ayuda y perfecta organización durante estos años, por salvarme de más de un apuro y por hacerme el trabajo mucho más fácil. Muchas gracias por todo.

Durante estos años, he tenido la grandísima suerte de haber conocido y convivido con personas maravillosas, mis compañeros de laboratorio, que me han hecho los días más alegres y llevaderos, me han ayudado a sacar fuerza de flaqueza, han conseguido hacerme reír en momentos de desesperación, y siempre han estado para tenderme una mano en cualquier momento.

A Marcelino, mi Marce, compañero de batalla, poco queda por añadir que no nos hayamos dicho ya. Agradecerte enormemente tu apoyo día a día, tanto dentro como fuera del laboratorio. Los dos hemos vivido momentos muy intensos durante este tiempo, tanto laborales como personales, y he tenido la grandísima suerte de tenerte siempre ahí, animándome, escuchándome y dándome fuerza. Eres una grandísima persona y nada hubiese sido igual de no haberte tenido a mi lado (literalmente). Echo de menos las risas, los cafés, las meriendas, las cervezas, las cenas, las fiestas, los viajes y las horas y horas de

bancada juntos, hablando de tonterías la mayoría de las veces, pero que nos han unido y convertido en grandes amigos. Para siempre, ¡Calpaína amor! Gracias por todo.

A Pepa, persona a la que admiro especialmente, trabajadora incansable, atenta, dispuesta siempre a ayudar, y con un corazón que no le cabe en el pecho. Agradecerte todo lo que me has enseñado, tu apoyo y ánimo en los peores momentos y por todos los buenos consejos que me has dado durante estos años y que recordaré siempre. He aprendido mucho de ti, y he disfrutado mucho del tiempo que hemos pasado juntas. Gracias por todo.

A Paco… ¡ay, Paco! El hombre que está en todo, el del ascensor y los pasillos, el de la eterna sonrisa, que contagia energía y positivismo allá donde va. Qué buenos momentos hemos pasado juntos, y cuantísimas risas. Ha sido maravilloso tenerte estos meses en Londres y se te echa muchísimo de menos. Me quedo con buenísimos recuerdos, que espero revivir en un futuro. Paco, ¡vuelve!.

A Pitu, ha sido genial compartir tantísimos buenos momentos contigo. Gracias por las risas (que no han sido pocas), por transmitir tanta energía positiva y alegría y por tu ayuda siempre que la he necesitado (principalmente por enseñarme a “limpiar”).

A Ángela, muchas gracias por tan buenos momentos juntas y por esas conversaciones tan interesantes, he aprendido mucho de ti. Gracias también por tu ayuda, apoyo y consejos que me has dado siempre que los he necesitado.

A Laura, fue un auténtico placer compartir contigo los últimos meses de laboratorio. Muchas gracias por tu trabajo y alegría y por aguantarme en los momentos de mayor estrés. Eres una persona muy noble, lista y trabajadora y te deseo lo mejor durante tu tesis.

A Carlos, porque has sido imprescindible durante estos años, y parte de esto te lo debo a ti. Gracias por tu ayuda constante, apoyo, y todos los buenos momentos juntos. Gracias por todo.

También, tengo mucho que agradecer a Teresa e Iván por su ayuda en mi incorporación al laboratorio. Especialmente, quiero agradecerle a Teresa el haberme enseñado los primeros meses a trabajar en el laboratorio, por

ayudarme a la hora de buscar estancia y por acogerme durante esos meses en Londres. Muchas gracias por todo.

Agradecer también a todas las personas que he conocido durante estos años en la Universidad de Valencia e Incliva, y con las que he compartido tan buenos momentos: a Ray (eres una máquina), Antonio, Bea, Javi, Edu, Bego, Ana, Paula, Iris, Birlipta, Roberto, Lidia, Valentina, Guadalupe, Sonia. Gracias a todos.

I would like to thank Dr. Richard Grose, not only for giving me the opportunity to do a wonderful stay in your laboratory, but also for allowing me to continue the exciting work I started during that time. I would also wish to thank my wonderful lab colleagues, Abi, Reza, Demi, Tash, for your support during these months. Special thanks to Ed, for teaching me and for your support and help during both, my stay and now in my return. Thank you also for passing all your positivity and dedication to science on to me. Agradecer también a todos mis compañeros de BCI, Gabriel, Marina, José, Jesús, Ana, Lorena y Bea por hacerme sentir como en casa, por hacer los días más alegres y por animarme día a día estos últimos meses.

A mis amigas y amigos, Susa, Raquel, Marta, Blanca, Clara, María, Marina, Marta, Alba, Jolís, Bea, Ampa, Javi y Miriam, gracias por vuestra amistad, cariño y apoyo durante estos años. Me habéis dado fuerza y alegría en mis peores momentos y habéis sido imprescindibles a lo largo de todo este proceso. Muchísimas gracias por todo.

Finalmente, el agradecimiento que para mí es el más importante, el agradecimiento a mi familia. A toda ella en general, mis tíos, abuelo y primos, gracias por preocuparos por mí y estar siempre atentos. Pero, por encima de todo, el agradecimiento a mis padres y mi hermano. Sin ellos, sin su ayuda constante, su apoyo y cariño, no hubiese conseguido nada. Todo lo que soy os lo debo a vosotros. Gracias.

INDEX

FIGURES INDEX

TABLES INDEX

ABBREVIATIONS

ALLN	N-acetyl-Leu-Leu-Norleu-al
BCS	Bovine calf serum
BSA	Bovine serum albumin
CAPN	Calpain
CAPN1	Calpain-1
CAPN2	Calpain-2
CAPNS1	Calpain regulatory subunit
CAST	Calpastatin
CBS	Calcium binding site
CEBP	CCAAT/enhancer-binding protein
cDNA	Complementary DNA
CDKs	Cyclin-dependent kinase
Ct	Carboxy-terminal end
CysPC	cysteine-protease core domain
C2L	C2-like domain
DAPI	4’,6-Diamino-2-phenylindole
DMD	Duchenne’s muscular dystrophy
DMEM	Dulbecco’s Modified Eagle’s Medium
DMSO	Dimethyl sulfoxide
E-Cdh	E-cadherin
ECM	Extracellular matrix
ED	Early differentiation
EGF	Epidermal growth factor

EGFR	Epidermal growth factor receptor
EMT	Epithelial to mesenchymal transition
ER	Oestrogen receptor
ERBB2	Erb-b2 receptor tyrosine kinase 2
esiRNA	Endoribonuclease-prepared small interfering RNA
FAK	Focal adhesion kinase
FBS	Fetal bovine serum
GA	Growth arrested
GAPDH	Glyceraldehyde 3-phosphate dehydrogenase
GR	Glycin rich
HER2	Human epidermal growth factor receptor -2
hTOP1	Human DNA topoisomerase I
IF	Immunofluorescence
IBMX	Methylisobutylxanthine
LAMP2A	Lysosome associated membrane protein 2
LGMD2A	Limb-girdle muscular dystrophy type 2A
MCE	Mitotic clonal expansion
MDIR	1-Isobutyl 3-metylxanthine, dexamethasone, insulin, rosiglitazone
MMP	Matrix metalloprotease
NF-κB	Nuclear factor kappa-light-chain-enhancer of activated B cells
NLS	Nuclear localization signals
NoLS	Nucleolar localization signals
No	Nucleolar
No-less	Nucleolar-less

Nt	Amine (N)-terminal end
NUP	Nucleoporin
OMM	Outer mitochondria membrane
PBS	Phosphate buffered saline
PC	Protease core
PEF(L)	Penta EF-hand (Large)
PEF(S)	Penta EF-hand (Small)
PG	Progesterone receptor
PIP_2	Phosphatidylinositol 4,5-bisphosphate
PKA	Protein kinase A
PKC	Protein kinase C
PLA	Proximity ligation assay
PPAR	Peroxisome proliferator-activated receptor
PR	Progesterone receptor
rDNA	Ribosomal DNA
rRNA	Ribosomal RNA
RT	Room temperature
RT-qPCR	Reverse transcription quantitative polymerase chain reaction
Sc	Scramble
SEM	Standard error of the mean
TD	Terminal differentiation
TNBC	Triple negative breast cancer
VATB2	Vacuolar type-ATPase subunit B2
VEGF	Vascular endothelial growth factor

INTRODUCTION

INTRODUCTION

1. THE CALPAIN SYSTEM

Calpains (CAPNs) (Clan CA, family C02; EC 3.4.22.17) are a family of calcium-dependent proteases, characterized by a cystein-protease domain called CysPc motif[1]. CAPNs, first identified in 1964[2], were named after the acronym standing for "calcium-dependent papain-like enzyme"[3]. These intracellular proteases are found in almost every eukaryote organism and in some bacteria and yeast[4].

The peculiarity of these enzymes lies in not being merely degrading proteases but modifying proteases. They produce specific cleaves on their substrates, modifying them and altering their original function or ways of regulation. Although the physiological functions of CAPNs are not completely understood, more than 100 CAPN substrates have been identified *in vitro*, including: membrane proteins, cytoskeleton proteins, transcription factors and kinases. This wide variety of substrates explains why CAPNs are involved in a large number of cellular functions, such as cytoskeleton remodelling, cell signalling, cell migration, cell cycle control, gene expression regulation, cell differentiation, apoptosis, etc[5–12]. Consequently, CAPNs dysfunctions are also related to a number of pathological processes, such as type 2 diabetes mellitus, Alzheimer's disease and other neurodegenerative disorders, myocardial infarction, some types of muscular dystrophy and cancer[1,13–15].

Among the fifteen members of the CAPN family identified [16], calpain-1 (CAPN1) and calpain-2 (CAPN2) are the best characterized isoforms. Both proteases are ubiquitously expressed in mammals. Classically, these CAPNs have always been known as μ-calpain and m-calpain (CAPN1 and CAPN2, respectively). This terminology was based on the calcium (Ca^{2+}) requirements of each isoform for their activation *in vitro*[17]. However, CAPN nomenclature has been unified and are named by the gene that encodes them: CAPN1, CAPN2, etc…[16]. CAPN1 and CAPN2 proteases share a 62% homology in their amino acidic sequence. Both isoforms form heterodimers composed of an 80 KDa size catalytic subunit (encoded by CAPN1 or CAPN2 genes) and a small regulatory subunit of 28 KDa size, common to both of them and encoded by CAPNS1, also known as CAPN4. The other main regulatory

component of the CAPN system is calpastatin (CAST), the only specific endogenous inhibitor of CAPNs known so far[1].

1.1 STRUCTURE OF CALPAINS

Classification of the different CAPN family members is based on structure similarities with CAPN1 and CAPN2.

1.1.1 Structure of ubiquitous CAPNs.

CAPN1 and CAPN2 have the same structure and domain distribution. As depicted in Figure 1, both catalytic subunits are divided into four domains (I-IV). Whilst the regulatory subunit CAPNS1 is composed by two domains (V and VI). Dimerization of the catalytic and the regulatory subunits occurs through the interaction between PEF motives present in both of them. The characteristics of each domain are explained below:

(i) *Domain I or anchor α-helix*: This is the N-terminal domain and anchors the catalytic subunit to the CAPNS1. This domain is not structurally part of the protease core.

(ii) *Domain II or CysPc domain (cysteine protease core domain)*: This domain is divided into PC1 and PC2 'protease core' independent domains. These domains contain the three amino acidic residues which constitute the catalytic triad: Cys (115/105), His (272/262) and Asn (296/286) (number in parenthesis indicates the amino acid residue in CAPN1 or CAPN2, respectively)[1]. When CAPN2 molecule was crystallized, PC1 and PC2 domains were revealed to contain two Ca^{2+}-binding sites (CBS), CBS-1 and CBS-2[18]. As explained later, Ca^{2+}-binding to CBSs is responsible for triggering CAPN activation.

(iii) *Domain III or C2L domain (C2-like domain):* The structure of this domain includes eight β-sheets, similar to the β-sandwich tertiary structure found in C2 type domains. The conserved C2 domain, identified in several signalling proteins such as protein kinase C (PKC), has Ca^{2+} and phospholipid-binding sites, which suggested that the C2L domain of CAPNs might also bind these ligands[19]. However, when the CAPN2 structure was obtained, it was shown that the β-sheets disposition in the C2L domain was different from that in C2 domains. Moreover, Ca^{2+}-binding to C2L had no effect on CAPN activity[20].

(iv) *Domain IV or PEF(L) domain (penta-EF-hand)*: This domain is the C-terminal end of the catalytic subunit. It comprises five EF-hand domains, four of them capable of binding Ca^{2+}. The fifth EF domain does not bind Ca^{2+} but is involved in the dimerization with the small regulatory subunit CAPNS1. Ca^{2+}-binding to PEF(L) domain, induces only slight conformational changes with no influence on the catalytic triad reorganization.

(v) *Domain V or GR (Glycin Rich) domain*: It is included into the N-terminal end of the CAPNS1. This is a glycine-rich hydrophobic domain which is autolysed upon CAPNs activation.

(vi) *Domain VI or PEF(S) domain*: it is found at the C-terminal end of CAPNS1. Just as the above mentioned PEF(L) domain, it contains five EF-hand motives: four of them bind Ca^{2+}, and the fifth is involved in the catalytic subunit binding.

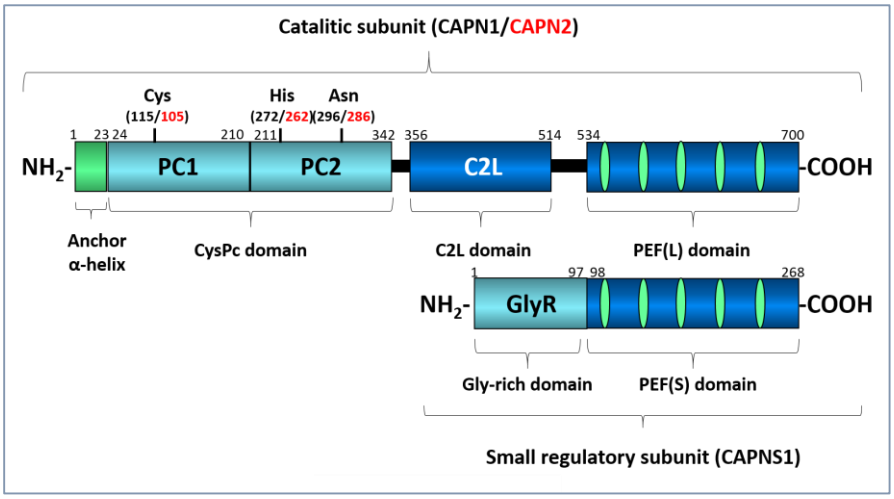

Figure 1: Schematic structure of CAPN1/CAPN2 catalytic subunit and CAPNS1 regulatory subunit. *CAPN1 and CAPN2 are heterodimers of a catalytic subunit (upper structure) and a small regulatory subunit (CAPNS1) (lower structure). The catalytic triad residues of CAPN1 and CAPN2 catalytic subunits are shown in black and red, respectively. PC1 and PC2, protease core domains 1 and 2; CysPc, cysteine protease core domain; C2L, C2-like domain; PEF(L) and PEF(S), penta-EF-hand (Large) and (Small) domain; GlyR, glycine-rich domain. The figure was modified from Moretti D. et al. 2014.*

1.1.2 Structure of calpastatin.

CAST, unlike conventional CAPNs and despite its high specificity, is poorly conserved among species. Moreover, although there is only one CAST gene, at least nine different CAST isoforms are known. These are products of alternative splicing in the N-terminal domain (L domain) and/or different promoters that control gene expression[21,22].

CAST structure, as shown in Figure 2, has five domains: one N-terminal domain (L domain), with no inhibitory activity, and four homologous inhibitory domains (I-IV). Each inhibitory domain can inhibit, with greater or lesser efficiency, one CAPN molecule. These domains contain in turn three well-conserved subdomains: A, B and C[23].

CAST/CAPN interaction is a complex process in which CAST subdomains specifically interact with CAPN domains as follows: subdomain A/(PEF(L)) CAPN domain, subdomain B/CysPc CAPN domain and subdomain C/(PEF(S)) CAPNS1 domain[24]. The stability provided by the interactions of subdomains A and C with PEFs domains is required for the inhibitory activity of the B subdomain[25,26].

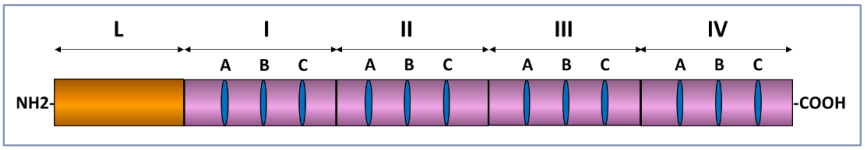

Figure 2: CAST structure. *CAST structure consist of four consecutive inhibitory domains (I-IV) and an N-terminal domain (L domain) with no inhibitory activity. A-, B- and C-regions in each inhibitory domain are important for CAST/CAPN interaction. The figure was modified from Wendt A. et al. 2004.*

1.2 CALPAIN CLASSIFICATION

There are fifteen genes known to codify different CAPN catalytic subunits, named as CAPNn (n = 1, 2, 3 and 5-16)[14]. These CAPNs can be classified according to two different criteria: structure and expression profile in the organism.

Attending to their expression profile in the organism, CAPNs are classified as ubiquitous or tissue-specific proteases. Ubiquitous CAPNs have been reported to play central roles in any cell type. In fact, defects in

ubiquitous CAPNs may be lethal, as shown in the embryonically lethal *Capn2* or *CapnS1* knockout mice[27,28]. On the other hand, tissue-specific CAPNs carry out defined functions within a cellular type or tissue. Defects in these CAPNs may cause tissue-specific symptoms or pathologies.

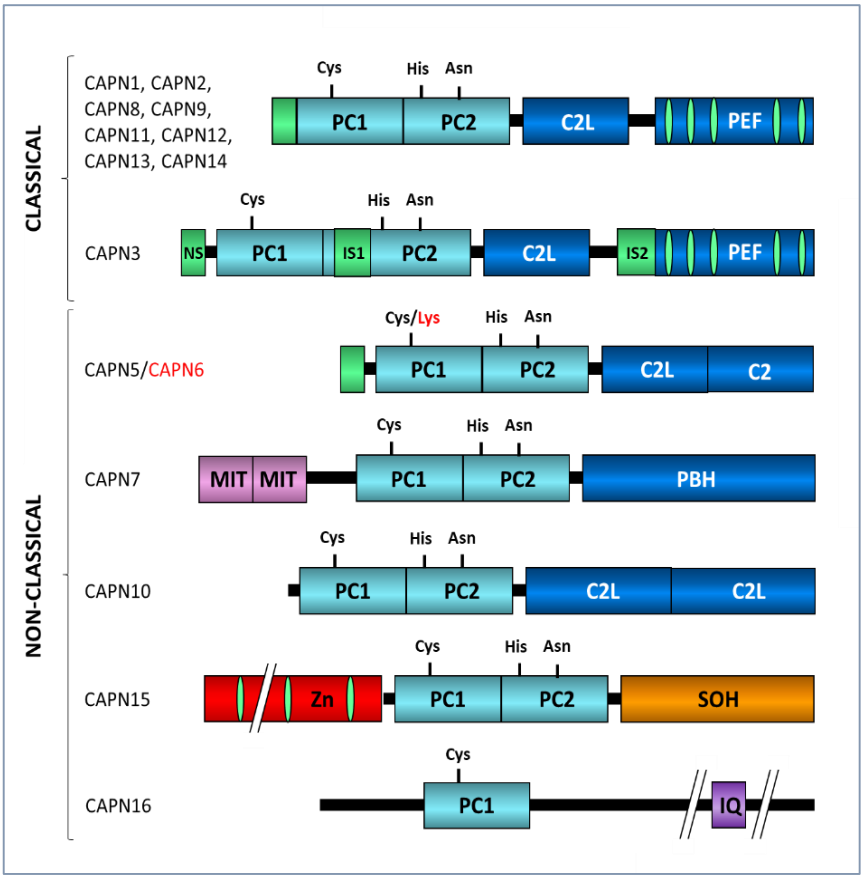

Figure 3: Structure of CAPN family members. *CAPNs are classified on the basis of their structure: "classical" with domain structures that are identical to those of CAPN1 and CAPN2, and "non-classical" that differ from CAPN1 or CAPN2 structure. PC1 and PC2, protease core domain 1 and 2; C2L, C2-like domain; PEF(L) and PEF, penta-EF-hand domain, GlyR, glycine-rich domain; NS, N-terminal addition sequence; IS, insertion sequence; MIT, microtubule interacting and transport motif; PBH, protease PalB homologous domain; Zn, Zn-finger motif; SOH, SOL-homology domain; IQ: calmodulin-interacting domain. The figure was modified from Sorimachi H. et al. 2011.*

Classification of CAPNs according to their structure, divides CAPN family into 'classical' and 'non-classical' members. As mentioned, the principle of this classification is based on the similarity to CAPN1 and CAPN2 structures, since they were the first CAPNs to be characterized. In broad terms, 'classical' CAPNs are defined by the presence of a PEF domain at the C-terminal end, whereas 'non-classical' CAPNs lack this domain and have additional domains different from the 'classical' ones. 'Classical' CAPNs also contain the C2L and CysPc domain. Among all human CAPN genes, nine are included into the 'classical' category. The others are considered as 'non-classical' and can be further subdivided into several subfamilies according to their domain structures. As shown in Figure 3, the organization of these domains in CAPN homologs is diverse. Consequently, their function and regulation strongly differs from those of 'classical' CAPNs.

1.3 CALPAIN ACTIVATION AND REGULATION

As the knowledge about CAPNs increases, it reveals how complex the CAPN system is. It has been demonstrated that homology sequence is not enough to predict the activation mechanism of the different isoforms. All these limitations bring up the special need to further study the structure of each isoform and the nature of its activity[29,30]. In this sense, several mechanisms have been postulated to regulate CAPN activation:

1.3.1 Calcium-binding.

Crystallization and elucidation of CAPN2/CAPNS1 structure was a breakthrough in the field of CAPN research. This achievement gave a plausible theory with regard to CAPN activation by Ca^{2+}-binding[18,31]. As previously explained, the amino acids comprising the catalytic triad (CAPN1/CAPN2: $Cys^{115/105}$, $His^{272/262}$ and $Asn^{296/286}$), are found in PC1 and PC2 within the active site of the enzyme[32], and both PC have their own CBS[33]. In the absence of Ca^{2+}, the catalytic triad is not catalytically active. Upon Ca^{2+}-binding to PC1 and PC2, a conformation change of the polypeptidic chains brings the three residues together into an active catalytic cleft[20,34,35] (Figure 4).

Previous to the crystallization of CAPN2/CAPNS1, former theories pointed to the Ca^{2+}-binding sites located in the PEF domains as the main regulators of the enzymatic activity[36]. Nevertheless, now it is known that Ca^{2+}-binding to PEF domains barely changes the enzyme conformation. Therefore,

it has been suggested that both PEF and C2L domains might provide an additional level of safeguard to prevent spontaneous CAPN activation[20].

All in all, these findings indicate that CAPNs always depend on Ca^{2+} for their activation, remaining inactive in its absence. This rigorous regulation prevents undesired proteolysis of a large number of proteins in close contact with CAPNs[16]. However, the Ca^{2+} concentrations required for CAPN activation determined *in vitro* were much higher than the physiological Ca^{2+} concentrations within the cell. Indeed, while the concentration required for the activation *in vitro* of CAPN1 and CAPN2 is ~ 50 µM and ~ 500 µM, respectively, intracellular Ca^{2+} concentration throughout the cytoplasm is around 0.1 µM[37]. Therefore, it is reasonable to think that CAPNs might use different strategies *in vivo* to overcome these excessive Ca^{2+} requirements. Moreover, in addition to Ca^{2+} binding, other mechanisms have been shown to regulate CAPN activity.

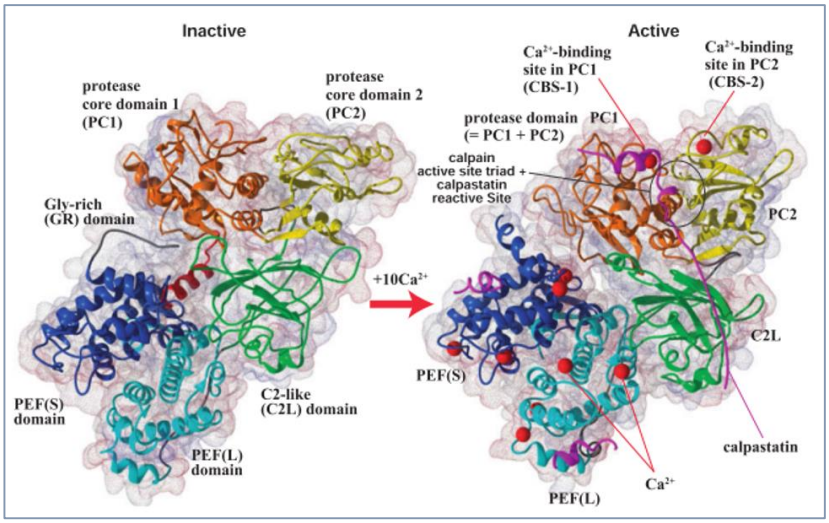

Figure 4: CAPN2 activation mechanism. *This scheme shows the Ca^{2+}-binding sites of PC1 and PC2 and PEFs domains. Upon Ca^{2+}-binding to PC1 and PC2, CAPN2 structure reorganizes and the catalytic triad are brought in contact. The figure was obtained from Sorimachi H. et al 2011.*

1.3.2 Phospholipids-binding.

Membrane phospholipids are mainly involved in docking CAPNs to cellular membranes. However, besides directing CAPNs localization,

different groups have reported that phospholipids are capable of lowering Ca^{2+} requirements for CAPN activation[38,39]. However, the *in vivo* relevance of this finding is unknown since high phospholipid concentrations are needed to exert influence on CAPN activation. It seems that CAPN binding to membranes might favour its activation due to a local increase in Ca^{2+} influx caused by the high concentration of Ca^{2+} channels in the proximity. Another explanation would be that the charged head of PIP_2 could electrostatically modify CAPN structure triggering Ca^{2+} activation. Surprisingly, in a recent study it was determined that PIP_2 worked as a CAPN2 cofactor, demonstrating that PIP_2 is also actively involved in CAPN2 activation[40].

1.3.3 Inhibition of CAPN activity by calpastatin.

CAST binding to CAPNs is one of the most important mechanisms for CAPN activity regulation. It has been evidenced that the only known endogenous CAPN inhibitor modulates CAPN1, CAPN2, CAPN8 and CAPN9 but not CAPN3[41,42]. For the CAPN and CAST interaction to occur, a previous CAPN conformational change induced by Ca^{2+}-activation is needed. CAST binding to Ca^{2+}-activated CAPNs, suggest that CAST might be part of an attenuating rather than preventive mechanism of CAPN activity regulation[43].

In physiological conditions, CAPNs are activated in a limited manner. However, under stress conditions CAPN proteolysis is over-activated and needs to be regulated by CAST to avoid cell damage, acting the inhibitor as a "safe-guard"[20]. This hypothesis would explain why *Cast* knockout mice show no symptoms under normal conditions. Nevertheless, when excitotoxicity in hippocampus was induced in these mice, the apoptotic response was increased in CAST-deficient mice, indicating that under pathological conditions, CAST-induced CAPN inhibition weakens and is not sufficient to regulate CAPNs activity[44]. Indeed CAST has been determined to be downregulated in some diseases[45–47].

CAST inhibitory functions are regulated by several mechanisms:

- After intracellular Ca^{2+} elevation, CAST is sequentially degraded by CAPNs. In the early phase CAST proteolysis renders CAST fragments with inhibitory activity. These fragments amplify the inhibitory effect by binding to other CAPN molecules. After prolonged CAPN activation, CAST is completely degraded and its inhibition activity is impaired[48,49].

- Decreased CAST levels are compensated by an upregulation in CAST mRNA expression. Once CAST protein levels are restored, its mRNA transcription is repressed[49,50].
- CAST accessibility and inhibitory capacity can be reversibly regulated by phosphorylation. The L-domain of CAST can by phosphorylated by either PKA or PKC, promoting either activation or inhibition, respectively[50–53].

1.3.4 Small regulatory subunit.

CAPNS1 is the regulatory subunit of both CAPN1 and CAPN2, traditionally claimed as essential for their activity. However, several studies concluded that the catalytic subunits have intrinsic and CAPNS1-independent protease activity[54,55]. Nevertheless, CAPNS1 has been reported to be important for the stability and folding of CAPN1 and CAPN2[56]. Studies with *Capns1*$^{-/-}$ mice seem to support this chaperone-like function of CAPNS1. These mice are embryonically lethal, as a result of a down-regulation in both CAPN1 and CAPN2 proteins[27,57].

CAPNS1 dissociation has been proposed as a possible reversible mechanism for CAPN activation. In the presence of Ca^{2+}, this dissociation could facilitate the realignment of the protease core, favouring its activation. In turn, it would render the catalytically active CAPN subunit on one side, and on the other CAPNS1 subunit. CAPNS1 subunits would then form homodimers[58,59]. On the other hand, some works have reported several reasons to support that this dissociation is not likely to occur and that CAPN/CAPNS1 remain associated during catalysis[60,61]. Briefly:

- The area of interaction between the PEF domains of both subunits is extensive and hydrophobic; thus, the reversibility of this dissociation would need the intervention of a chaperone or a denaturing condition[20]. Besides, the shift of PEFs domain after Ca^{2+}-binding is so subtle that seems not to be sufficient to disrupt CAPN/CAPNS1 interaction[26,43].
- As previously explained, CAST binds to the Ca^{2+}-activated CAPN/CAPNS1 dimer. In this scenario, the small subunit dissociation would prevent CAST binding and inhibition of CAPN/CAPNS1[43].
- After the analysis of active CAPN/CAPNS1 by anion-exchange chromatography, pure CAPNS1 homodimers expected from subunit dissociation were not obtained. Conversely, heterodimers of domains IV

and VI of CAPN and CAPNS1 were obtained instead, confirming that CAPNS1 stays bound to the large subunit during catalysis[62].

1.3.5 Autoproteolysis.

Autoproteolysis has been for years the main theory to explain CAPN activation *in vivo*[38]. CAPNs were thought to be activated following a general mechanism described for other proteases such as cathepsines or papains: autoproteolysis of a pro-peptide within their catalytic site triggers the activation of the pro-enzyme[63]. In agreement with this, several studies have demonstrated that cleavage of the N-terminal anchor helix of CAPN1 and CAPN2 lowers Ca^{2+} requirements for their activation. Cleavage of N-terminal anchor helix would release the enzyme from movement restrictions, facilitating the conformational change of the core domains PC1 and PC2[38,64–66].

It is important to point out that most of the autoproteolysis studies were focused on CAPN1, and even though this mechanism seems to be true for CAPN1 activation, several evidences contradict this fact for CAPN2. To begin with, CAPN1 anchor peptide is longer than the CAPN2 one, and thus, more feasible to be cleaved. In fact, when the CAPN2/CAPNS1 heterodimer was crystallized, it showed that the N-terminal region was not a pro-peptide blocking the enzyme active site cleft[20]. Moreover, it was revealed that the intramolecular cleavage sites of the N-terminal anchor helix in CAPN2 are far away from the active cleft[31].

Another contradictory argument is that autolysis is an irreversible process. The advantage of a non-proteolytic activation is that after Ca^{2+} activation, CAPN could return to the inactive state as an undamaged and fully responsive enzyme. Thereby, autolysis would be a very unfavourable mechanism for the cell[68]. A recent *in vitro* study about the rate of autolysis at different sites in CAPN2, determined that autolysis of the N-terminal anchor helix happens at the same time as the proteolysis of other sites in domain III. The domain III cleavage would lead to CAPN inactivation; thus autolytic activation would overlap with inactivation. Taking all this reasons into consideration, they concluded that autolysis is probably a consequence of CAPN concentration after purification and extraction procedures rather than an *in vivo* activation phenomena[62].

1.3.6 Phosphorylation.

In addition to these regulatory mechanisms, CAPNs have several phosphorylation sites that can regulate CAPN activity. Nine and eight different phosphorylation sites have been identified in CAPN1 and CAPN2, respectively. Not all sites are phosphorylated in all molecules and some sites are phosphorylated more frequently than others[1]. Indeed, the phosphorylation pattern of CAPNs will affect their activity and thus their functions.

It has been shown that some growth factors such as Epidermal Growth Factor (EGF) are able to activate CAPN2 through its phosphorylation at Ser50. This ERK1/2-mediated phosphorylation takes place even in the absence of Ca^{2+}[69]. Conversely, CAPN1 lacks this Ser50 phosphorylation site, which would explain why its activity is not modified by ERK. Both CAPN isoforms have PKC phosphorylation sites[1]. PKC activation by nicotine has been involved in phosphorylation of both CAPN isoforms, enhancing motility of tumour cells[70]. Also, endothelial CAPN1 is activated by PKC in type 1 diabetic vasculature, leading to upregulation of proteins involved in intercellular adhesion[71].

On the other hand, phosphorylation can also inhibit CAPN activity. Phosphorylation of CAPN2 at Ser369 and Tyr370 by PKA, constricts the conformational change of domain III, retaining CAPN2 in an inactive state[72,73]. This phosphorylation can also inhibit CAPN2 indirectly by preventing its binding to PIP_2[40].

1.4 CALPAIN SUBSTRATE RECOGNITION

CAPNs substrate recognition, just like other intracellular proteases such as the proteasome proteins, lysosomal peptidases or caspases, is strictly regulated. However, major differences exist between these intracellular proteolytic systems and CAPNs. First of all, the proteasome or lysosomal peptidases recognise substrates that have been previously tagged by other systems, like ubiquitination[74] or autophagosome formation[75,76]. With regard to caspases, their substrate recognition is based on the identification of specific amino acid residues located in particular positions[77]. On the contrary, CAPNs substrate recognition is far more complex. CAPNs do not use any external system for their substrate identification, participating themselves in target recognition. Despite CAPNs being highly specific for their substrates

targeting, the basis of this recognition is not completely understood. Nevertheless, some determinants for this recognition have been proposed:

1.4.1 Substrate specificity.

Initial studies suggested that CAPNs had certain cleavage preferences for some regions rich in proline (P), glutamate (E), serine (S), and threonine (T) within the amino acidic sequence. The so-called PEST sequence seemed to be the intramolecular signal for CAPN-proteolytic degradation[78]. However, further studies discarded this hypothesis, proving that PEST sequence does not make a big difference in CAPN targets identification. Indeed, different well known CAPN substrates lack PEST sequence[79,80]. More recently, two different methods were taken to find the consensus sequences recognised by CAPNs. Both approaches estimated the preferred amino acid residues sequence for positions (P) P4-P3-P2-P1-X-P1′-P2′-P3′ (X: cleavage site) for CAPN cleavage. However, the results were completely different and thus inconclusive[81,82].

An important observation derived from the CAPN2/CAPNS1 crystallization was that the active site cleft within the CysPc domains was deeper and narrower than in papain-like cysteine proteases[83]. This implies that CAPN substrates conformation must be ´malleable´ or extended so that it fits in the cleavage site. Somehow, this could explain why CAPNs preferentially proteolyze inter-domain unstructured regions[26,43]. Therefore, the overall three-dimensional conformation or higher order structures have been pointed as the main determinants for substrate recognition instead of a specific primary amino acidic sequence[84,85].

1.4.2 CAPN subcellular localization.

Since both CAPNs isoforms have potentially the same ability of cleaving the same substrates, it has been suggested that substrates recognition *in vivo* might be delimited by their subcellular location. After certain stimuli, CAPNs can translocate from one cell compartment to another in an isoform-specific manner. Indeed, CAPNs are able to translocate to several cellular compartments such as endoplasmic reticulum (ER), Golgi apparatus (GA), caveolae, plasma membranes, nucleus and nucleolus[86–93]. This compartmentalization narrows the variety of possible CAPN targets and therefore, regulates CAPN function.

Distinctive subcellular localization and compartmentalization might be defined by the following determinants:

(i) Phosphorylation

In addition to CAPNs activation, phosphorylation may also influence on CAPNs spatial distribution. As previously explained, ERK exclusively phosphorylates CAPN2, and induces CAPN2 translocation to plasma membrane. This membrane-binding is reversed by PKA-mediated phosphorylation of CAPN2. Therefore the phosphorylation pattern of CAPN2 regulates the redistribution of this protease[40].

(ii) Phospholipid binding

CAPNs translocation to cell membranes is mostly mediated by the CAPN phospholipid-binding domains within domain III. Through this domain CAPNs attach to membrane phosphatidylinositol (PI) or phosphatidylinositol 4,5-bisphosphate (PIP_2)[94]. This CAPN-PIP_2 binding is determinant for CAPNs subcellular redistribution to some cellular organelles like ER, GA[90,95] or plasma membrane. In the latter case, CAPNs binding to PIP_2 is a key event for cell motility. As will be further explained, this process is regulated by asymmetrical distribution of PIP_2[96,97]. This targeting mechanism has been shown to be more important for CAPN2 than for CAPN1 distribution[40,97].

(iii) Sequence and structural determinants

Some targeting sequences might rule CAPNs localization. In this sense, CAPN1 is the only isoform found in the inner mitochondria membrane. This localization is specifically determined by a mitochondrial targeting sequence located in the N-terminus of CAPN1, which is absent in the CAPN2 sequence[98].

In addition, differences in specific domains may influence CAPNs localization. For example, the dissimilar localization of CAPN1 and CAPN2 in the cytosolic membrane of the ER and GA is also conditioned by differences in specific domains. CAPN1 is preferentially located in the cytosolic surface of the GA, while CAPN2 is found in the cytosolic membrane of both organelles. Membrane-targeting specificity of CAPN1 and CAPN2 may be dependent on differences in the total negative charge of their acidic loops in Domain III, involved in phospholipids binding. The resulting

electrostatic interactions, in presence or absence of Ca^{2+}, with certain membrane phospholipids also explains why CAPN2 and not CAPN1 preferentially binds to PIP_2[90].

Interestingly, CAPN2 is also found in the lumen of ER and GA organelles. CAPN2 entrance to the lumen is also explained by structural changes, since CAPN2 lacks an N-terminal signal for its targeting. CAPN2 might include an internal topogenic signal sequence that modifies its intramolecular conformation and in turn targets CAPN2 into the lumen[90].

(iv) Protein-protein interactions

CAPNs compartmentalization might also be determined by protein-protein interactions. It has been postulated that the association of CAPNs with membranes is further mediated by binding to CAST and CAPNS1. Both regulatory subunits are capable of associating with membranes through their hydrophobic motifs. Once there, they provide a docking site for nascent CAPN molecules[99]. Another study indicated that CAPN1 interaction with the heat shock protein 90 (HSP90) facilitates CAPN1 recruitment at specific cellular sites[100].

Other members of the CAPN family show specific cellular compartmentalization directed by protein-protein interactions. For example, CAPN3 has been found in the nucleolus of cancer cell lines, where it favours p53 degradation. CAPN3 nucleolar localization is mediated by the interaction with a nucleolar protein called Def (Digestive organ expansion factor)[101–103]. Recently, CAPN2 has also been found to be distributed in nucleoli of colorectal cancer cell lines[93]. Nevertheless, the determinants for CAPN2 nucleolar internalization are still unknown.

1.5 SUBCELLULAR DISTRIBUTION AND CALPAIN FUNCTIONS

In terms of functions, there are great differences between CAPNs and other proteolytic systems. The proteasome function is purely degrading and its aim is protein removal[104]. Lysosome peptidases are involved in removal of non-specific cell components such as proteins or microorganisms in order to recycle or eliminate them[105]. Caspases, despite being involved in other cellular processes like cell differentiation, inflammation, and proliferation, their main role is related to apoptosis[106]. Conversely, CAPNs cleave their substrates in a precise and limited way, modifying their target structure irreversibly and

changing its original properties, which may entail a variation in the protein activity, function, specificity or localization. For this reason, CAPNs are considered as intracellular 'modulator proteases' rather than merely degrading proteases[16].

More than 100 CAPN targets have been identified, connecting CAPNs with several cellular functions like cell proliferation, cell cycle progression, cell differentiation, gene expression, cytoskeleton remodelling, cell motility and apoptosis[5,88,107–111]. Nevertheless, the precise physiological functions of CAPNs and substrate recognition need to be addressed. Moreover, information found in the literature about CAPNs functions is often confusing. Many studies do not discern between the specific implication of CAPN1 or CAPN2 isoforms, connecting them indistinctly with redundant functions[112]. The main reason for this misapprehension is the lack of accuracy in the studies of CAPNs functions. Most of the studies are based on CAPN activity inhibitors, which are non-specific and act on different CAPN isoforms and some of them can even inhibit other proteases[113]. Other commonly used approximations are CAPNS1 knocking-down or CAST overexpression, common regulators of both CAPN1 and CAPN2[114–116]. Furthermore, several CAPNs substrates have been identified by *in vitro* digestions using recombinant CAPNs and higher concentrations of Ca^{2+} than the physiologic ones[117,118]. However, these *in vitro* studies do not resemble the precise *in vivo* recognition because *in vitro* both isoforms can recognise the same proteins as substrates. Therefore, results obtained from such approaches should be cautiously interpreted.

It is important to highlight that even though both CAPNs have the same ability to cleave *in vitro* the same substrates, *in vivo* each CAPN is responsible for the cleavage of certain targets, and hence they may have specific roles[119]. Strong evidences derived from knockout mice studies support that both isoforms do not perform interchangeable functions. *CapnS1* knockout mice are embryonically lethal[57]. However, *Capn1* knockout mice generate viable and fertile mice[120] while *Capn2* knockout mice are not viable[28]. This demonstrate that both isoforms are differentially regulated *in vivo* and are responsible for specific functions.

For that reason, it has been proposed that the specificity of CAPNs substrate recognition *in vivo* is mediated by their subcellular localization. This CAPNs compartmentalization restricts access to their substrates, and thus

limits CAPN functions within the cell depending on the cell type and cell context.

1.5.1 Plasma membrane and cell adhesion.

CAPNs are important modulators of **cell migration**. In particular, CAPNs are important for cell adhesion formation and cell adhesion disassembly. In this sense, cell migration is dependent on the asymmetrical spatial distribution of CAPN1 and CAPN2, which are compartmentalized at the leading edge and at the rear of the cell, respectively[7]. CAPN1 is an upstream activator of small GTPases like Rac and Rho, which control the formation of new focal adhesion complexes, cytoskeletal reorganization and lamellipodia formation at the leading edge[7,12,121]. Also, CAPN1 cleaves different focal adhesion proteins, like talin-1, ezrin, focal adhesion kinase (FAK) and the cytoplasmic tails of β1 and β3 integrin, regulating adhesion turnover[121–125]. The activation of CAPN1 at the leading edge seems to be mainly regulated by Ca^{2+} influxes[126].

On the other hand, CAPN2 is involved in tail detachment by cleaving several proteins found within focal adhesions, including talin-1, paxillin, FAK, Src, α-actinin, and tensin[111]. This specific cleavage is regulated by the coordination of two mechanisms: through the activation of CAPN2 by phosphorylation via ERK/MAP Kinase pathway and by asymmetric CAPN2 binding to PIP_2. ERK-mediated phosphorylation of CAPN2 at Ser50 induces CAPN2 translocation to the plasma membrane, favouring CAPN2 activation near the adhesion complex targets[91,92]. Moreover, CAPN2 localization at the rear of the cell is mainly determined by its binding to membrane PIP_2. During cell motility, PIP_2 is depleted in lamellipodia and concentrated at the cell rear by a turnover mechanism. This binding to PIP_2 favours not only a polarised CAPN2 distribution but also allows its phosphorylation, because only membrane-proximal CAPN2 is activated by ERK[96,97].

It is noteworthy that depending on the cell context, cell adhesion disassembly entails a different cell fate. **Anoikis** is a type of cell death induced by loss of cell-extracellular matrix (ECM) attachment. CAPNs favour this type of cell death by cleaving specific plasmatic membrane proteins involved in cell anchoring, such as vimentin, p130Cas, FAK and talin-1[127,128]. For example, it has been determined that in breast cancer cell lines, CAPNs activation by Disulfiram, favours anoikis by disruption of focal adhesion complexes[129].

1.5.2 Cytoplasm: apoptosis, differentiation or cytoskeleton remodelling.

Many CAPNs substrates are located at the cytosolic compartment, relating CAPNs with different cell functions like apoptosis, cell cycle control or cytoskeleton remodelling. Regarding **apoptosis**, CAPN1 and CAPN2 process and modulate caspases in the cytoplasmic compartment. In this sense, proteolysis of pro-apoptotic pro-caspase 3, 7, 8 and 9 by CAPNs inactivates them[130,131]. CAPNs can also switch cell fate from autophagy to apoptosis[132,133]. CAPN cleavage of Atg5, a protein that genuinely is involved in autophagosome formation, changes its localization from cytosol to mitochondria, where it associates with Bcl-xL and triggers cytochrome c release. This Atg truncation was observed in several cell types subjected to different apoptotic stimulus[132].

CAPN-mediated switch cell fate is also important during myoblast **differentiation**. c-Myc transcriptionally inhibits myoblast differentiation. However, CAPN cleavage of c-Myc at the cytosolic compartment, removes its nuclear localization signals and DNA binding domain, retaining the proteolytic product (Myc-nick) in the cytosol and modifying its functions. Then, Myc-nick favours muscle differentiation by regulating α-tubulin acetylation[134]. Moreover, CAPNs can also regulate cell localization of other **transcription factors**. In mouse lymphoma cells under oxidative stress conditions, it was observed that CAPNs were responsible for Iκ-Bα proteolysis, the cytosolic NF-κB inhibitor, allowing translocation of the transcription factor to the nuclear compartment[135]. This cytosolic mechanism of nuclear NF-κB activation mediated by CAPNs has also been involved during cardiac dysfunction in septic mice[136], in B lymphocytes activation[137] and in ceramine-induced pro-survival pathway in mouse embryonic fibroblasts[138].

Finally, CAPNs are important effectors of **cytoskeleton remodelling** during cell migration or wound-healing processes by cleaving actin-associated proteins such as spectrin[6,139,140].

1.5.3 Mitochondria and apoptosis.

Within mitochondria CAPNs have been found in both, the outer mitochondria membrane (OMM) and the mitochondrial intermembrane space. CAPNs are involved in the cleavage of different Bcl-2 family members in the

cytosolic face of the OMM. Cleavage of anti-apoptotic proteins, like Bcl-xL and Bcl-2[141], favours cell death. In cisplatin-treated melanoma cells CAPNs cleave Bid, causing oligomerization of Bax and/or Bak and thus cytochrome c release[142]. Furthermore, Bax cleavage by CAPNs[143,144] generates a more potent pro-apoptotic protein (Bax/p18) which is no longer able to heterodimerize with anti-apoptotic proteins[145].

Besides, several research groups have identified the presence of CAPN1 within mitochondrial intermembrane space (mit-CAPN1)[146,147]. One of the main mit-CAPN1 targets is apoptosis-inducing factor (AIF), involved in caspase-independent apoptosis. Truncated product of AIF (tAIF), detaches from the mitochondrial membrane and relocates to the nuclei, where it triggers DNA fragmentation by recruiting endonucleases[148,149].

1.5.4 Lysosome and lysosomal cell death.

Lysosomal membrane permeabilization is a type of cell death whereby lysosomes release their content (mostly cathepsins) to the cytosol[150]. CAPN1 is the isoform that has been related to this process via the cleavage of lysosome membrane proteins[147,151]. In mammary gland involution, CAPN1 translocate to lysosomes of epithelial cells where it cleaves LAMP2A (Lysosome associated membrane protein 2) and VATB2 (Vacuolar type-ATPase subunit B2), leading to lysosome membrane permeability[147].

1.5.5 Golgi apparatus and autophagy.

Golgi apparatus is a source of autophagosome membranes. For the autophagosome vesicle to form, late endosomes must detach from the rest of the Golgi complex. CAPNs favours this autophagosome formation in osteosarcoma cell lines by cleaving Bif-1, a protein involved in vesicle formation that lies on Golgi apparatus[152,153].

1.5.6 Endoplasmic reticulum (ER) and ER-stress response.

CAPNs participate in the execution of ER stress-induced cell death, which results from a collapse of important cell functions controlled by the ER, such as protein folding or modifying and Ca^{2+} storage and signalling. Disturbances in any of these functions triggers and increase in Ca^{2+} influx, resulting in activation of the ER-membrane bound CAPN2. Active CAPN2 cleaves the ER-membrane pro-caspase-12, activating it and triggering apoptosis[87,130,131].

1.5.7 Nuclear compartment.

CAPNs have also been reported to enter the nucleus, where they modulate many cell functions. CAPNs do not diffusely distribute within the nucleus but rather they accumulate on specific localizations, where they modulate different functions:

(i) *Nucleoplasm*

Within nucleoplasm, CAPNs can regulate different functions, such as **cell death processes** among others. In rat cardiomyocytes under oxidative stress conditions, CAPN2 translocates to the nucleus where it cleaves specifically a Ca^{2+}/calmodulin-dependent protein kinase II δ_B (CaMK II δ_B). This cleavage downregulates Bcl-2, altering the Bcl-2/Bax ratio and triggering apoptosis[154].

Furthermore, CAPN2 is involved in cell protection from camptothecin-induced cytotoxicity after ionomycin stimulation. Ionomycin-induced Ca^{2+} influx triggers CAPN2 nuclear translocation in colon carcinoma cell lines, where it cleaves human DNA topoisomerase I (hTOP I). This cleavage also increased hTOP I DNA relaxation activity, important for **DNA replication and transcription**[155].

Nuclear CAPNs have also been related to **differentiation** processes. In the involuting mammary gland, CAPN1 translocates to the nucleus of differentiating adipocytes, where it is involved in the cleavage of the N-tail of histone H3, favouring gene expression and differentiation[88]. Additionally, CAPNs also proteolyze transcription factors involved in cell differentiation. During adipocyte differentiation, inhibition of CAPN activity prevents the expression of C/EBP-α, impairing adipocyte differentiation. C/EBP-β is the transcriptional activator of C/EBP-α. In pre-adipocytes, C/EBP-β is sequestered by CHOP-10, a dominant-negative isoform of C/EBP-β[156]. After the induction of differentiation, CAPN cleaves CHOP-10, releasing C/EBP-β to bind to the C/EBP-α promoter[157].

Regarding **cell cycle and proliferation processes**, CAPNs have been related to the cleavage of cyclins (cyclin D1 and E)[158–160], cyclin-dependent kinases inhibitors ($p19^{Ink4d}$ and $p27^{Kip1}$) and transcription factors such as p53[161], c-Jun and c-Fos[161–164]. CAPNs are required for the degradation of $p27^{Kip1}$, important for triggering the mitotic clonal expansion phase of pre-adipocytes differentiation. Indeed, CAPN activity inhibition prevents pre-

adipocytes to re-enter into the cell cycle and start differentiation[108]. Unfortunately, most of these studies do not examine the implication of a particular CAPN isoform in these processes nor determine the precise compartment in which CAPNs are acting. For example, many transcription factors are thought to be cleaved by CAPNs in the cytoplasmic compartment, such as c-Fos, c-Jun and p53. Nevertheless, in many cases, literature was published long ago, when CAPNs were thought to be mainly restricted to the cytosolic compartment, and were not accurate enough to make such statements.

(ii) Nuclear envelope and nuclear destabilization-induced cell death

The cleavage of different nuclear pore complex components like NUP98, NUP153 or Mab414 by CAPNs favours the loss of nuclear membrane integrity, which leads to cell death[88,165,166].

(iii) Chromosomes and mitosis

In HeLa cells, CAPN2 was observed to be involved in the correct chromosome alignment on the metaphase plate during mitosis. Inhibition of CAPN2 induced mitotic delay, probably caused by an impair in the formation of bipolar attachment of mitotic spindles to kinetochores of several chromosomes[167].

(iv) Nucleolus, ribosomal biogenesis and cell cycle control

Nucleolus is the largest nuclear subcompartment and is the site for ribosome biosynthesis[168] and for the regulation of other cellular functions such as mitosis regulation, cell cycle regulation, proliferation, DNA repair, ribonucleoproteins synthesis, stress responses and senescence[169–172]. Proteomics analysis have risen the number of proteins related to the nucleolus to more than 4500 proteins, and only 30% of these are involved in ribosome biosynthesis[173–175]. Furthermore, nucleolus functions are found deregulated in different diseases, such as cancer[174,176–178]. Therefore, uncovering all the processes in which the nucleolus is involved in and identifying new proteins related to such functions would reveal potential new targets for cancer therapy.

As previously mentioned, CAPN2 has been recently found for the first time to be compartmentalized within the nucleolus of colorectal cancer cells. CAPN2 was identified to bind to the rDNA-core promoter and intergenic spacer (IGS), and it was determined that in growth limiting conditions CAPN2

was involved in ribosomal biogenesis suppression[93]. Previous to CAPN2, CAPN3 was the only CAPN isoform that had been identified in nucleoli. It was first identified in melanoma cell lines and human melanoma biopsies. This nucleolar localization resulted from a Nuclear Localization Signal present in two CAPN3 splice variants[103]. In different studies performed in zebrafish and human tumoral cell lines, it was observed that CAPN3 was involved in p53 nucleolar degradation, which was determined to be essential for the development of digestive organs and cell cycle control during organogenesis[102].

1.6 PATHOLOGICAL IMPLICATIONS OF CALPAINS

The wide range of physiological processes in which CAPNs are involved highlights the importance of an accurate regulation of the CAPN system to ensure cell homeostasis. In fact, deregulations in the CAPN system are linked to the development of different diseases. On one side, CAPN alterations can be the leading cause of a group of diseases commonly known as calpainopathies (Table 1). These diseases include muscular dystrophies, spastic paraplegia, gastric ulcer, retinopathy and oesophagitis[14,15].

GENE	EXPRESSION PROFILE	TYPE OF ALTERATION	DISEASE
CAPN1	Ubiquitous	Loss of CAPN1 function	Spactic paraplegia 76[179]
CAPN3	Skeletal muscle	Missense mutations in CAPN3 gene that result in protein defects	Limb-girdle muscular dystrophy type 2A (LGMD2A)[180]
CAPN5	Ubiquitous (abundant in testis and brain)	Mutations in CAPN5 gene that lads to CAPN5 hyperactivation	Autosomal dominant neovascular inflammatory vitreoretinopathy[181,182]
CAPN8/ CAPN9	Gastrointestinal tract	Gene downregulation	Stress-induced gastric ulcer[183]
CAPN10	Ubiquitous	CAPN10 gene polymorphism that alter the gene expression or	Increase risk in developing type 2 diabetes[184,185]

		induces alternative splicing mechanisms	
CAPN12	Hair follicle and skin	Mutations in CAPN12 gene that leads to protein deficiency	Congenital ichthyosis[186]
CAPN14	Ubiquitous	Gene upregulation	Eosinophilic oesophagitis[187]

Table 1: Calpainopathies. *This table summarizes different calpainopathies, group of diseases in which particular CAPN genes are altered.*

In addition to calpainopathies, deregulation of CAPNs has also been classically considered as an aggravating factor for many other pathologies, such as: neurodegenerative disorders, cardiovascular diseases, myopathies, ischaemic disorders, diabetes and cancer. As a result, CAPNs are becoming promising therapeutic targets for the treatment of those diseases CAPNs are involved in[14,15,30].

Pathologies such as neurodegenerative diseases, ischaemic disorders, myocardial injury and muscular dystrophy are associated with alterations in Ca^{2+} homeostasis[47,188–196]. This Ca^{2+} misbalance leads to CAPNs overactivation in such conditions. Cleavage of neuronal substrates after pathological CAPN activation harms neuron structure and function. During Alzheimer's disease abnormal CAPN processing of the amyloid precursor protein leads to the generation of amyloid-β peptide aggregates[197]. CAPNs also favour the formation of tau aggregates[198]. In ischaemic disorders, CAPNs activation during brain ischemia increases neuronal cell death, which can be prevented by CAPN inhibitors administration[193].

CAPNs are also involved in cardiac injury after acute cardiovascular disorders such as heart failure. The CAPN system participate in apoptotic processes and in the degradation of heart myofibrillar proteins, sarcolemma proteins, sarcoplasmic reticulum proteins and regulatory enzymes, favouring myocytes and cardiomyocytes death[194–196]. The resulting protein homeostasis imbalance causes the dysfunctional symptomatology after heart failure.

CAPN upregulation activity is also involved in Duchenne's muscular dystrophy (DMD). This disease is the most common muscular dystrophy and

is caused by a mutation in DMD gene that encodes the protein dystrophin. This cytoskeletal protein links the plasma membrane of the skeletal muscle to the ECM[199]. The lack of dystrophin leads to plasmatic membrane weakening, an increase in Ca^{2+} influx and thus CAPN activation. Once activated, CAPNs increase muscle protein proteolysis and necrosis, exacerbating DMD symptoms[188].

1.6.1 CAPNs deregulation in cancer.

In recent years, the interest in exploring the role of CAPNs in cancer development and progression has raised. Several studies have demonstrated that CAPN expression is altered during tumorigenesis and have related CAPN activity to the progression of different types of cancer[13,14,200]. Correlation between CAPN up-regulation and a more aggressive cancer phenotype has also been documented in clinical investigations. Table 2 shows the involvement of different CAPNs genes in several types of cancers, both in basic research and clinical studies.

CAPN	CANCER	EXPRESSION	SAMPLE	IMPLICATIONS
CAPN1	Breast cancer	Overexpressed	Patients	Adverse relapse free survival[201]
	OSCC	Overexpressed.[202]	Patients	Reduced overall survival in patients.
			Cell lines	Increased migration and proliferation
	SCC and BCC	mRNA upregulation but reduced protein levels	Patients	Not conclusive[203]
	Renal carcinoma	mRNA upregulation	Patients	Correlation of high expression with increased malignancy(Braun et al., 1999)
CAPN2	CCR	Overexpressed	Patients Cell lines	Tumour progression[204]
			Animal model	Tumour progression[205]
			Cell lines	Increased migration and proliferation[206]
	Prostate cancer	Overexpressed	Cell lines	Increased migration and invasion[207,208]
	RMS	Increased activity	Cell lines	Increased migration and invasiveness[209]

	Breast cancer	Overexpressed in TNBC	Patients	Adverse breast cancer survival[210]
CAPNS1	HCC	Overexpressed	Patients	HCC recurrence after liver transplantation, invasion and metastasis[211].
	Ovarian cancer	Overexpressed	Patients	Poor prognosis[212]
	Glioma	Overexpressed[213]	Patients	Overexpression in higher tumour grade
			Cell lines	Increased invasion, migration and proliferation
CAPN3	Melanoma	Overexpressed	Patients	Not reported[214]
		Downregulation of determinant CAPN3 variants	Cell lines	Tumour progression[103]
CAPN6	Uterine cancer	Overexpressed	Patients	Development LSIL and progression to HSIL.[215]
CAPN9	Gastric cancer	Decreased expression	Patients	Poor prognosis[216]
	Breast cancer	Decreased expression	Patients	Adverse survival in endocrine therapy treated patients[217]
CAPN10	Laryngeal cancer	Determinant haplotype	Patients	Poor prognosis[218] or protective[219]
	Colorectal carcinoma	Determinant haplotype	Patients	Protective[220]

Table 2: Deregulation of CAPN isoforms in different cancers. *This table shows the implication of CAPNs alterations in different types of cancer. In each case is indicated the type of cancer, the type of alteration, the type of sample and the implication of that CAPN gene deregulation. OSCC: Oral squamous cell carcinoma; SCC: Squamous cell carcinoma; BCC: Basal cell carcinoma; CCR: colorectal carcinoma; RMS: Rhabdomiosarcoma; TNBC: triple-negative breast cancer; HCC: Hepatocellular carcinoma; LSIL: low-grade squamous intraepithelial lesion; HSIL: high-grade squamous intraepithelial lesion.*

CAPNs play crucial roles in oncogenic processes like cell proliferation, survival mechanisms, angiogenesis, cell migration and invasion[13,221]. The pathological processes of oncogenic cell transformation are orchestrated by several oncogenes, such as v-Src, v-Myc, v-Jun, v-Fos or k-Ras[13]. Most of these oncogenic proteins are upstream activators of CAPNs. In

v-Src-transformed cells, CAPN2 expression is induced, while CAST is degraded, leading to an increase in cell motility and acceleration of cell cycle progression[222]. This enhanced CAPN2 activity was also observed in v-Myc, v-Jun, v-Fos or k-Ras transformed fibroblasts[223].

Nevertheless, this regulation between oncogenes and CAPNs is bi-directional, since it has been demonstrated that CAPNs are also involved in the proteolysis of some of these oncogenes, like c-Fos, c-Jun[163] or c-myc[224]. In this sense, the product of CAPN-mediated cleavage of c-myc, Myc-nick, has also been observed in cancer cell lines and tumours biopsies. In colon cancer cells, CAPN-cleaved Myc-nick favours cell survival under stress conditions. Additionally, Myc-nick also promotes cell survival in colon cancer cells after treatment with chemotherapeutic drugs such as etoposide, cisplatin, and imatinib. The cell survival mechanisms of Myc-nick derive from its acetyltranferases-recruiting functions, which drive to modifications of cytoplasmic proteins[225].

Regarding cell survival, CAPNs can exert different pro-survival activities by regulating both p53 and NF-κB[226,227]. In hepatocarcinoma and colorectal cancer cell lines, cleavage of p53 by CAPNs diminished p53 stability, decreasing p53-dependent apoptosis[228]. Furthermore, in breast cancer cell lines that overexpress human epidermal growth factor receptor 2 (HER2), the nuclear translocation of NF-κB is increased, favouring cell survival. It was determined that NF-κB nuclear translocation was mediated by CAPN cleavage of IκBα[226].

In addition to cell survival, CAPNs are also important for angiogenesis. The angiogenic vascular endothelial growth factor (VEGF) stimulates CAPN2 activation, which in turn favours endothelial cells motility and angiogenesis. CAPN inhibition has proved to be effective in blocking tumour neovascularization [229,230].

This information regarding CAPNs involvement in several tumorigenic processes makes clear record of CAPNs as possible therapeutic targets in cancer diseases[14]. However, different studies have shown contradictory results after CAPN inhibition, and therefore, the prognosis value and benefits of the therapeutic inhibition of CAPNs has not been clearly established. This is mainly because these proteases are also required for the apoptosis induced by some anticancer drugs. For example, CAPNs are important mediators of the apoptotic cell response to anticancer treatments such as genistein, cisplatin and oxaliplatin chemotherapies[231–236]. Thus, CAPN

unspecific inhibition could be both, beneficial and detrimental for tumour progression, depending on the type of tumour, the therapeutic agent or the tumour progression stage[13]. Besides, as previously mentioned, the mechanisms of CAPN regulation or deregulation and its targets in pathological conditions are still unknown. In addition, data about CAPNs deregulation in cancer are incomplete; most clinical data describe the aberrant expression of CAPNs, which is not necessarily related to an increase in enzymatic activity and substrate processing in tumour cells. Neither a clear specific isoform has been established to be associated with each tumorigenic process. Consequently, increasing knowledge of CAPN substrate recognition, isoform specificity and activity/spatial regulation, are necessary to design new specific anticancer therapeutic strategies.

1.6.2 CAPNs in tumour cell migration and invasion.

In contrast to the afore-mentioned tumorigenic processes, in which CAPNs participation is ambiguous, the positive role played by CAPNs in tumour cells migration and invasion has been well ascertained. CAPNs are important modulators of cellular migration, function that is enhanced in tumorigenic processes. During cancer cell dissemination CAPN activity is necessary for the cleavage and formation of focal adhesion complexes and the proteolysis of cell adhesion proteins. In many clinical investigations correlations between CAPNs upregulation and a more aggressive tumour phenotype have been described[202,210,237]. Nevertheless, the involvement of CAPNs in cell migration and invasiveness has been mainly demonstrated in experimental models of cultured cells, in which CAPN inhibition or silencing significantly reduces both processes. As an example, in breast cancer cell lines CAPN2 has been shown to be involved in c-Src-mediated invadopodia dynamics, through the proteolysis and activation of PTP1B, a phosphatase that positively regulates c-Src activation[238]. Other studies performed in prostate cancer cells, demonstrated that CAPN inhibition prevented EGF-induced cell motility, effect that was also accomplished by CAPN2 downregulation. Tumour xenografts of prostate cancers treated with leupeptin, a specific inhibitor of CAPN activity, also reduced cell invasion *in vivo*, and showed that prostate cancer cell migration was dependent on EGF and CAPN2 activity[208]. This EGF-induced CAPN2 activation is critical in cancer cells migration as

EGFR (Epidermal growth factor receptor) is overexpressed in a wide variety of cancers[239].

According to this, CAPNs are involved in migration of different types of cancer, like colon, lung cancer, rabdomyosarcoma, bladder carcinoma, renal carcinoma or hepatocellular carcinoma[70,206,209,240–242]. In the latter case, downregulation of both CAPN1 and CAPN2 expression led to a reduction in migration and invasiveness of hepatoma cells. Besides, concomitant with CAPNs downregulation, the secretion of matrix metalloprotease-2 (MMP-2) and MMP-9 also diminished, suggesting that CAPNs might control directly or indirectly cell migration[240]. Indeed, different studies suggest that CAPNs regulate MMPs expression and secretion[243,244]. Degradation of ECM components is necessary for cells to migrate, so CAPNS might also be involved in cell migration by regulating indirectly ECM remodelling[245,246].

One of the main mechanisms for dissemination and metastasis initiation in cancer cells is epithelial-to-mesenchymal transition (EMT). This cell transformation is induced by a cross-talk of different signalling pathways that changes the epithelial cell phenotype into a mesenchymal one[247]. EMT is characterized by the loss of cell-cell adhesion complexes, like E-cadherin and cytokeratins, and upregulation of mesenchymal markers, like vimentin and fibronectin [248]. In normal epithelial cells, transmembrane E-cadherins form complexes with other proteins, like catenins (p120-, α-, β-, and γ-catenin) and other regulatory proteins, and all together form epithelial adherens junctions[249]. All these E-cadherin/catenin protein complexes have been identified as CAPN targets, and their proteolysis favours cell migration (Figure 5). Cleavage of E-cadherin by CAPNs was observed in prostate and mammary epithelial cells. Indeed, this E-cadherin proteolysis was linked to an increased migration in prostate cancer cells[250].

As previously mentioned, one of the main substrates of CAPNs in plasma membrane are proteins involved in focal adhesions, which mediate contacts between cells and the ECM, such as FAK, talin-1, ezrin and integrins (Figure 5). In human colon cancer cells, integrin-α2 signalling is activated when cells attach to collagen IV, which enhances CAPN1 activation. The increase in CAPN activity resulted in FAK cleavage and increased cell motility[251]. In breast cancer cell lines, downregulation of filamin A, a protein that mediates cell-ECM connections and integrin signalling, increased CAPN activity. As a result, increased cleavage of talin-1, FAK and paxillin, led to focal adhesion disassembly and increased cell motility[252]. In this sense,

CAPN-mediated cleavage of talin-1 has been demonstrated to be essential for focal adhesion disassembly and a rate-limiting step during adhesion turnover[253].

It would be important to mention that most of the studies on cell migration were carried out on two dimensional cell culture. However, these

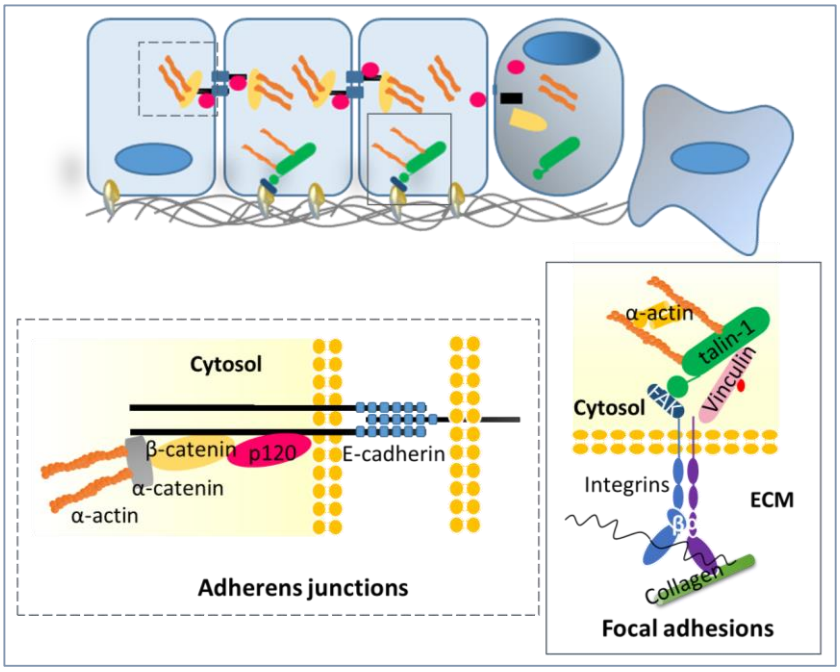

Figure 5. Cell–cell adherens junctions and cell–ECM focal adhesions scheme. *Adherens junctions are mediated by transmembrane protein E-cadherin, whose extracellular domain mediates specific homophilic interactions with neighbouring cells. The intracellular domain of E-cadherin associates with catenins, which tether these complexes to the actin cytoskeleton forming stable adhesion junctions. Focal adhesions are multi-protein complexes that mediate cells-ECM contacts. Heterodimers of α- and β-integrins are the membrane receptors of focal adhesions. They form multi-protein complexes that are linked to the actin cytoskeleton. Key players that link integrins to the actin cytoskeleton include talin-1, vinculin and a-actinin. The tyrosine FAK are also part of the integrin complexes and are key mediators of signalling downstream of integrins. All these proteins involved in both adhesion complexes are CAPNs targets. CAPNs-mediated cleavage of those proteins favours cell migration and invasion.*

models do no recapitulate neither the cancer environment nor the complexity of polarized tissue structure or cross-talk between different cell types[254]. Actually, invasive cells can follow different modes of migration, including amoeboid-like or mesenchymal single-cell migration to multicellular streaming or collective invasion[255,256]. On this subject, only a few studies on cell invasion mediated by CAPNs have been performed in tree-dimensional (3D) models. 3D studies with fibrosarcoma cells revealed that CAPN2 was necessary for mesenchymal but not for amoeboid invasion. Contrary to amoeboid-like migration, which is modulated by Rho/ROCK pathway, mesenchymal migration is dependent on integrin-mediated adhesion and MMPs-mediated matrix remodelling. In this study it was demonstrated that Src-induced CAPN2 activation, favoured integrin cleavage and thus, mesenchymal migration[257]. This highlights the importance of finding models that could simulate an environment and reproduce tridimensional tissue structuring much closer to reality[254].

Despite this, most of the information that is now available regarding the role of CAPNs in cell migration and invasion comes from studies with cell lines and cohort studies in patients' tumours. In this sense, breast cancer has been one of the most frequent models to study deregulation of CAPNs in invasive processes. In addition to migration, CAPNs deregulation in breast cancer has been also associated with tumour progression or antitumor resistance therapies.

1.6.3 Breast cancer.

(i) Breast cancer classification

Breast cancer is the most common cancer in women worldwide. Breast cancer is a heterogeneous group of diseases, encompassing diseases of different genetic and epigenetic alterations that result in dissimilar molecular, histopathological and clinical features[258]. Gene expression profiling techniques like microarrays and RNA-Seq have allowed a more accurate classification of breast cancers subtypes, according to a set of certain genes differently expressed between those groups. Consistent with their intrinsic molecular characteristics, breast cancer tumours can been classified in: luminal A, luminal B, ERBB2+ (also known as HER2), basal-like, claudin-low and normal-like subtypes[259–262].

Patients belonging to each group show significantly different outcomes and treatment-response. In brief, luminal tumours own an expression profile that resembles luminal epithelial cells features. Luminal tumours are also characterized by the expression of hormone receptors: oestrogen receptor (ER), progesterone receptor (PR) and human epidermal growth factor 2 (HER2). Luminal A tumours have higher expression of ER-related genes and lower expression of HER2 than luminal B cancers[259,263]. Overall, the luminal subtypes carry a good prognosis, having luminal A subtype tumours significantly better prognosis than luminal B tumours[264,265].

The ERBB2+ (Erb-b2 receptor tyrosine kinase 2) group is characterized by ER negative, PR negative and HER2 positive tumour expression. These tumours also overexpress other genes in the ERBB2 amplicon[259,263]. Despite having good chemotherapy response, patients with these tumours show poor prognosis due to a higher risk of early relapse[264,265].

Basal-like subtype has basal-like profile, mimicking basal epithelial cells or myoepithelial cells gene expression. Most of these tumours are characterized by the lack of ER, PR, and HER2 expression and, thus, are clinically referred to as 'triple negative' breast cancers (TNBC)[261,266]. Nevertheless, not all basal-like tumours show TNBC profile (30% of basal-like tumours are not TNBC)[267]. Basal-like tumours show high aggressiveness and bad prognosis. This is partly due to the high mutational rate in genes like TP53 and BRCA1 (Breast cancer type 1)[259].

The last subtype identified was the claudin-low subtype, characterized by low expression of tight junction proteins claudin 3, 4 and 7 and E-cadherin. This group express mesenchymal and stem cells-associated genes, and genes involved in immune system responses[262]. Due to these features, claudin-low subtype shows bad prognosis. Immunohistochemical analysis classify the claudin-low subtype as TNBC. However, as for basal-like subtypes, not all claudin-low tumours are TNBC[268]. Basal-like and claudin-low breast cancer subtypes have a significant overlap with the triple negative subtype. The TNBC group is the most heterogeneous among all subtypes and has been further subdivided[269]. These tumours follow aggressive clinical course and are associated with a lower survival. Their poor prognosis also results from the relatively few treatment options available for triple negative tumours[265,270].

In addition, there is another breast cancer subgroup known as normal-like. These tumours are poorly characterized and show an intermediate prognosis between luminal and basal-like tumours. They are also triple-negative for ER, PR and HER2 expression. However, they are excluded from

the basal-like subtype due to the lack of cytokeratin 5 and EGFR expression[259,260,271,272].

(ii) *Breast cancer cell lines*

A large proportion of current knowledge on breast carcinomas is derived from *in vivo* and *in vitro* studies performed using breast cancer cell lines, given that they offer an unlimited source of homogenous materials. Cell lines are representative of breast tumours subtypes and can also be categorized based on gene expression[273,274].

Luminal cell lines are more differentiated than other cell lines subtypes[275,276]. These cells maintain tight cell-cell junctions and thus have less tendency to migrate. Luminal B cell lines are more invasive and consequently more aggressive than luminal A cells[277]. ERBB2+ cells are more aggressive

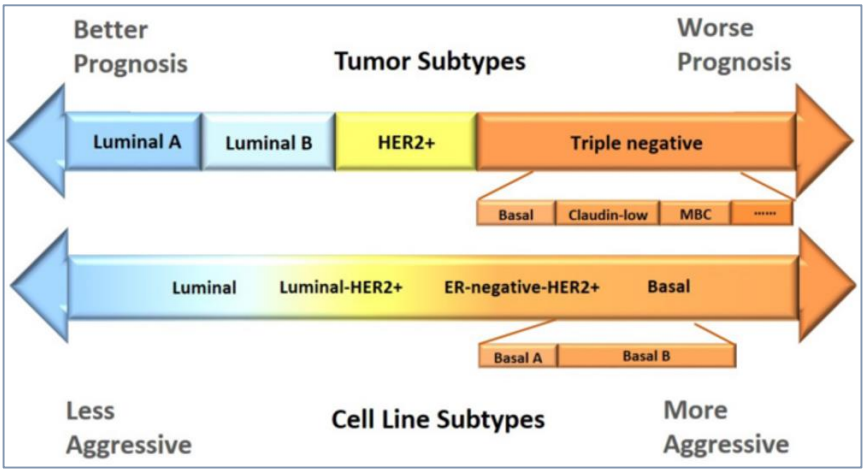

Figure 6. Breast tumours and cancer cell lines classification. *The scheme shows a gradual prognosis/aggressiveness comparison between breast tumours and cancer cell lines subtypes. Breast cancer tumours can be classified as luminal A, luminal B, HER2 positive, and triple negative breast cancer (TNBC), according to the status of ER, PR, HER2. TNBC tumours can be further sub-classify into: basal, claudin-low, MBC (metaplastic breast cancer) and interferon-rich. Lower diagram shows breast cancer cells lines classification, representative of breast tumours subtypes. TNBC cells are called the 'Basal' subtype, with basal A and basal B being further differentiated to represent the basal tumours and claudin-low, respectively. In terms of prognosis, luminal tumours have better prognosis than TNBC tumours, and luminal cell lines are less aggressive than TNBC cell lines. The figure was obtained from Dai X. et al. 2017.*

with respect to cell migration as compared with luminal cells, since HER2 over-expression is associated with the breakdown of cell–cell junctions[277]. Triple negative A (basal A) lines are called basal-like as they are enriched with basal markers and resemble the basal tumour subtype. Triple negative B (basal B) cell lines, include the mesenchymal cluster or normal-like/claudin-low, which over-expresses genes associated with tumour invasiveness and aggressive features[273,274,278]. Figure 6 shows a comparison between breast cancer cell lines and tumours subtypes[273].

(iii) CAPNs and breast cancer

Different clinical and basic *in vivo* and *in vitro* studies have reported the importance of the CAPN system in breast cancer progression[279]. Studies of CAPN1, CAPN2 and CAST levels in patients' breast tumours tried to establish a correlation between CAPN levels with specific breast cancer subtypes. Immunohistochemical analysis of CAPN1, CAPN2 and CAST in early-stage invasive breast cancer tissue microarrays demonstrated an association between CAPN2 expression and a significant worse prognosis in TNBC and basal-like subgroups. CAPN2 expression was significantly linked to lymphovascular invasion. In fact, patients with TNBC or basal-like tumours expressing lower CAPN2 levels, showed breast cancer-specific survival similar to non-basal or hormonal receptors-positive counterparts. Therefore, CAPN2 expression was proposed as a putative prognosis factor for triple negative or basal-like breast cancer patients[210]. In the same study, the expression of CAPN1 was associated with ER and PR positive tumours and low tumour grade[210]. Nevertheless, in a recent study CAPN1 was significantly expressed in TNBC tissues varying from low to high. A correlation between high CAPN1 levels with lymph node metastasis was observed. Conversely, no correlation with the proliferating/apoptotic index or other clinical variables were proved[280].

The involvement of the CAPN system in lymphovascular invasion was also corroborated by *in vivo* and *in vitro* experiments. A low CAST expression was associated with lymphovascular invasion, supporting that CAPNs might be involved in the initial metastatic dissemination of breast cancer[45]. *In vitro*, CAPN was involved in spheroidogenesis and lymphovascular emboli in models of inflammatory breast cancer. The generation of lymphovascular emboli was a result of E-cadherin cleavage by CAPN activity. Nevertheless, no specific isoform was related to this process[281]. Finally, high CAPN1 expression has been linked to worse free survival in trastuzumab-treated patients with HER2-positive tumours[282].

These observations were further confirmed in a subsequent study, suggesting that CAPN1 might be a marker of relapse-free survival in HER2-positive patients treated with trastuzumab[201].

On the whole, differences in the localization or activity of both CAPNs have not been studied in breast tumours, and although CAPNs are good targets for cancer therapy, there is no evidence for the role of a particular CAPN isoform in breast cancer progression. Reports about the isoform-specific function of CAPNs in cell migration use cultured cells that do not resemble the polarized structure of mammary epithelium[88,238,253,283,284]. Regarding this, mammary gland provides an excellent model that allows the study of invasion and migration processes within the tissue context. During mammary gland development, epithelial ducts branch and expand in a process that implies epithelial cell invasion into the surrounding fat pad, for which the invading epithelial cells display some characteristics and increase the expression of EMT genes[285–287]. Additionally, during post-lactation involution, the epithelial layer suffers anoikis and remodelling processes, which both require the cleavage of cell-cell junctions and cell anchors, events that precede cell migration[288]. In this sense, the mammary gland during the pregnancy/lactation cycle has been used as a unique approach to investigate the early events during breast tumour progression[289–291].

2. THE CALPAIN SYSTEM IN PHYSIOLOGIC AND NEOPLASTIC MAMMARY GLAND PROCESSES

2.1 MAMMARY GLAND AS AN EXPERIMENTAL MODEL

Mammary gland is the tissue responsible for milk production during lactation that provides nourishment and immune protection of the new-born. Mammary gland architecture consists of a compound tubule-alveolar gland embedded within connective tissue. The basic components of the mammary gland are the alveoli, which are the secretory units; these alveoli join through small ducts to form lobules that show a collecting duct which ends in the nipple. The histology of this gland consist of bilayered ducts of two different epithelial cells types: luminal and myoepithelial (Figure 7). Luminal cells are

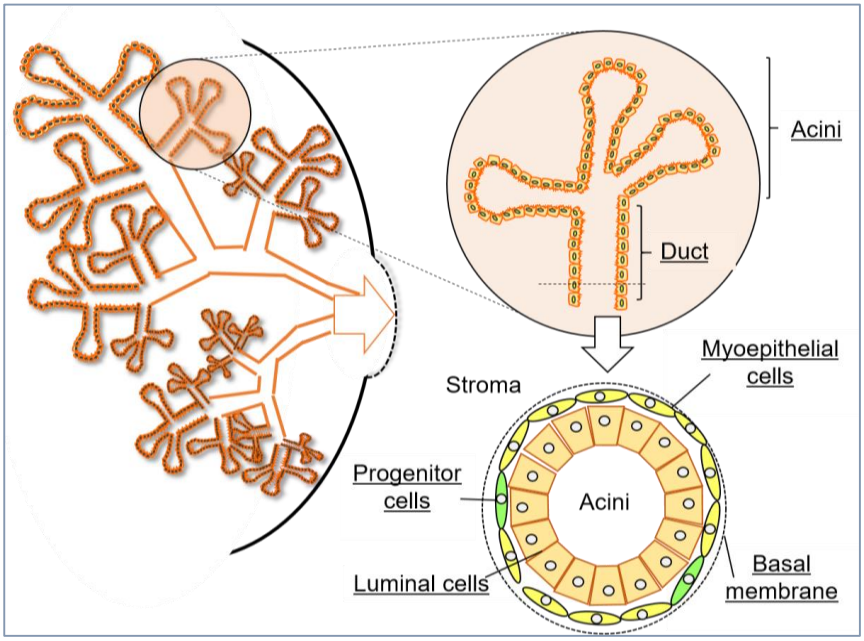

Figure 7. Mammary gland anatomical structure. *Mammary gland is organized in lobule-alveolar structures which are sustained within the stroma. Acini are the globular structures that secrete milk during lactation, which is drained thought ducts to the nipple. Cross section of the acinar structure shows the bilayered ductal composition of luminal and myoepithelial cells. Myoepithelial layer is surrounded by the basal membrane.*

located in the inner side, oriented towards the lumen. The myoepithelial layer is found surrounding the luminal layer, which is also in contact with the basal membrane. This ductal structure is sustained by the stroma, connective tissue composed by different cells of mesenchymal origin, like fibroblasts, adipocytes, macrophages, and which also includes blood and lymph vessels[292].

This gland is a unique glandular organ since its main development occurs in different phases after birth, reaching its maximum degree of development and differentiation during lactation[292]. All through the different developmental phases, the cells that configure the mammary gland experiment different processes of proliferation, differentiation, invasion and apoptosis so that the tissue adapts to the requirements of each physiological stage[293]. During puberty, epithelial ducts expand and branch in response to hormonal changes and growth factors[294]. The virgin mammary gland expands and branches further during pregnancy. At late pregnancy, luminal and basal progenitor's mammary stem cells differentiate into secretory alveolar cells and the contractile myoepithelial cells, respectively[295–297].

After weaning or litter removal, begins a physiologic process known as involution, in which all the structures and adaptations that were developed during pregnancy and lactation are removed. The aim of this stage is to return the mammary gland to a pre-gestational state and remodel it for a subsequent pregnancy-lactation cycle. Different signalling pathways finely coordinate this complex phase that includes programmed cell death mechanisms of epithelia, tissue and ECM remodelling and cell differentiation processes within the surrounding stroma[298].

Therefore, all the processes that converge in the mammary gland along the pregnancy-lactation-involution cycle, turn this tissue into a useful tool for the study of physiological functions like cell death, cell detachment, tissue remodelling, cell differentiation, cell polarity, cell fate, intertissue flux of nutrients and cell signalling mechanisms. Moreover, the mammary gland during involution has been used as a unique approach to investigate the early events that take place in breast tumour progression[290]. Many signalling pathways and genes that coordinately orchestrate the involution process, are de-regulated in breast cancer[289,299]. Furthermore, macrophages influx generates a proinflamatory environment that renders the perfect niche for the development of oncogenic events[300]. The remodelling mammary gland stroma has also been related to carcinogenesis development[301]. In this sense, the expression profile of extracellular proteases in the remodelling gland[302],

fibrillar collagen deposition, and release of bioactive fragments of fibronectin and laminin is similar to that found in developing breast tumours[303].

Indeed, post-lactation mammary gland involution is considered a pro-tumorigenic factor due to the proinflammatory microenvironment generated during this process[304,305]. In the 5 year-window following pregnancy the risk of developing an oncogenic event increases, known as pregnancy-associated breast cancer. This risk is directly correlated with the mother's age[306]. Pregnancy-associated breast cancers are characterized by having poorer outcome and are highly metastatic[307,308]. Therefore, understanding the mechanisms regulating the physiological mammary gland involution might shed some light in deciphering how those mechanisms are altered in breast malignant processes.

2.2 MAMMARY GLAND INVOLUTION

Knowledge about mammary gland development and the involution process results primarily from studies performed in mice, providing insight into the biology of the human breast. The murine experimental model of mammary gland involution is based on an artificial weaning. Physiological murine lactation spans for 21 days. In this model, the offspring withdrawal at mid process (9-11 days) triggers involution drastically in such a way that all death and remodelling processes initiate synchronously[147]. Murine mammary gland involution occurs in two phases:

2.2.1 First phase.

Covers the first 48h after weaning and is controlled by local signals triggered by milk stasis. This phase is reversible and can be reverted by resuming sucking. Several signalling pathways regulate the first phase of involution, being JAK/STAT, TGF-β, PI3K/AKT and NF-κB the principal signalling nodes involved[289,298,305]. During this period, the secretory alveolar epithelium is eliminated by programmed cell death processes. A distinguishing feature of this phase is the cell detachment from the luminal layer. These cells are then shed into the lumen where they die from anoikis[288] (Figure 8). In addition, macrophages massively infiltrate the involuting mammary gland for the removal of dying cells and cellular debris.

2.2.2 Second phase.

This irreversible phase begins at approximately 48 h after weaning and is controlled by hormonal factors. During this phase, macrophages

infiltration is coupled with collapse and removal of lobule-alveolar structures in a process of tissue remodelling[288]. Tissue remodelling processes implies extracellular matrix (ECM) degradation and adipocytes differentiation for the replacement of the epithelium that is being removed. Proteases like metalloproteinases and cathepsins are the main effectors of the ECM remodelling[298].

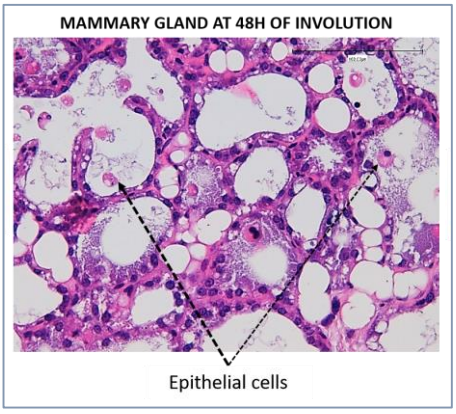

Figure 8: Luminal cells detachment in mammary gland involution. *Haematoxylin and eosin stained sections of 48h involuting mammary gland showing epithelial cells shed into the alveolar lumen. Scale bars 100µm.*

2.3 ROLE OF CALPAINS IN MAMMARY GLAND INVOLUTION

One of the important regulatory nodes during involution is controlled by the transcription factor NF-κB, which regulates cell proliferation and inflammatory processes. Besides, the aberrant regulation of this transcription factor is involved in oncogenesis[309–311]. Due to its importance during involution, our laboratory focused on the study of this transcription factor during weaning. Target genes of NF-κB at 48h of mammary gland involution were determined by the ChIP-on-chip technology. After analysing the targets by the disease filter (MeSH), it was revealed that 81% of those genes were included in the neoplasm category. Two of the overexpressed genes whose expression is controlled by this transcription factor are CAPN1 and CAPN2[312].

Further CAPN activity analysis showed that CAPNs are gradually activated along the involution time course[147]. This finding opened the door to new lines of research to explore the role of CAPNs during the process of mammary gland involution. Since it was known that CAPNs regulate

programmed cell death processes, the involvement of CAPNs in these processes during mammary gland involution was studied. At this point, it was demonstrated that CAPNs triggered epithelial cell death in involuting mammary gland by different mechanisms. Results obtained from this research revealed that, once activated, CAPNs relocated to different subcellular organelles, like lysosomes, mitochondria or nuclear envelope. Once there, CAPNs were involved in the cleavage of certain membrane proteins. In lysosomes, CAPNs cleaved the lysosome membrane proteins LAMP2A and VATB2. This proteolysis caused lysosomal membrane destabilization and release of hydrolytic lysosomal content to the cytosol, favouring cell death[313,314]. Furthermore, CAPN translocation to mitochondrial membrane increased membrane permeability and release of cytochrome c, which triggered caspase-mediated apoptosis[147]. Finally, CAPNs were also linked to the proteolysis of different peripheral nucleoporins of the nuclear pore complex, causing nuclear membrane destabilization[88].

As previously explained, during the early and reversible phase of involution, luminal cells detach from the ECM and are shed into the lumen of alveoli where they are cleared by different mechanisms (Figure 8). For this

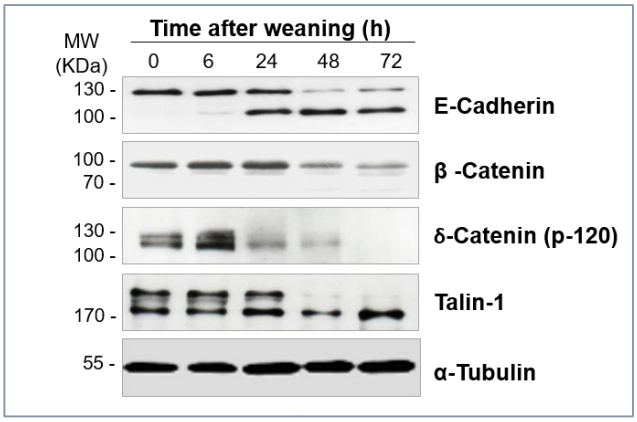

Figure 9: Cleavage of adhesion proteins along mammary gland involution. *Western blot of protein samples from mammary gland at the peak of lactation (0 h) and during the time course of involution (6, 24, 48 and 72 h) shows the cleavage of E-cadherin, β-catenin, δ-catenin (p-120) and talin-1 along involution. α-tubulin was used as loading control. The figure was obtained from Rodríguez-Fernández L. et al. 2016.*

cell detachment, cells need to cleave the cell-cell adhesion complexes that maintain the structure of the epithelial layer. Previous experiments performed in our laboratory showed that adherens and focal adhesion proteins such as E-cadherin, β-catenin, δ-catenin (p120), and talin-1 were cleaved along the time course of involution (Figure 9). Nevertheless, CAPN involvement in the cleavage of these proteins needs further study.

In addition to epithelial cells, in which CAPNs seemed to have a role on cell death during involution, it was also observed that CAPN1 was localized at the nuclear compartment of adipocytes that were differentiating and repopulating the mammary gland during the remodelling phase of involution (Figure 10). In this sense, CAPN1 was found to be involved in the cleavage of the N-tail of histone H3, modulating the epigenetic program during adipocyte differentiation. Furthermore, CAPN1 presence in adipogenic genes promoters, such as leptin and C/EBP-α, was verified by ChIP-assay experiments[88].

On the basis of these results, a dual role for CAPNs during mammary gland involution was proposed, since CAPNs were ruling different functions depending on the cell type. In epithelial cells CAPNs regulated programmed cell death processes, while in adipocytes they were involved in cell differentiation. Those functions were, in turn, conditioned by CAPNs subcellular localization.

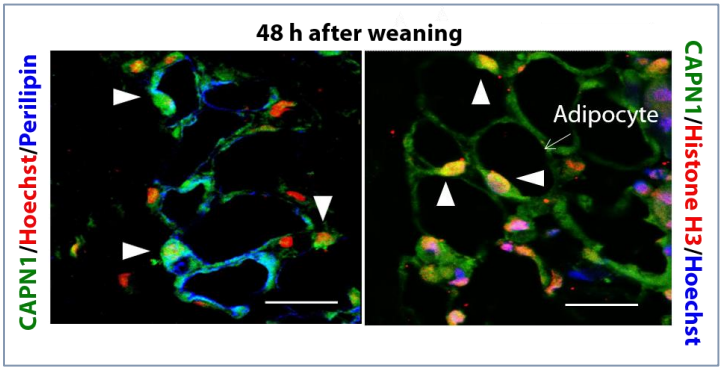

Figure 10: CAPN1 in the nucleus of differentiating adipocytes during involution. *Co-immunofluorescence analysis of CAPN1/perilipin and CAPN1/histone H3 in mammary gland tissue sections at 48h of involution, indicate that CAPN1 accumulates in nuclei of differentiating adipocytes during mammary gland involution. Scale bar 21 μm. The figure was obtained from Arnandis T. et al. 2014.*

AIMS

AIMS

CAPNs deregulations have been determined as an aggravating factor of different diseases, including cancer. Nevertheless, there are no clear records about the particular contribution of each CAPN isoform in physiological processes and how these isoforms are deregulated in pathological conditions. *In vivo*, each CAPN isoform recognizes specific proteins as substrates, and it has been suggested that CAPNs subcellular localization might determine this substrate recognition and consequently their functions.

Therefore, the general goal of this thesis project was to evaluate the relationship between CAPN isoforms localization and their role in specific biological processes and whether their localization is different depending on the cell context. Regarding the specific aims, they are described as follows:

1. TO EVALUATE WHETHER THE ISOFORM-SPECIFIC FUNCTIONS AND LOCALIZATION OF CALPAINS IS DEPENDENT ON THE BIOLOGICAL CONTEXT

For this purpose, mammary gland during involution and breast cancer cell lines will be used as physiological and pathological models. It is well known that cleavage of adhesion proteins is the first step for physiological clearance of undesired cells during postlactational regression of the mammary gland. Our group has previously established by *in vitro* studies that proteolysis of adhesion proteins is CAPN-mediated. Similarly, these proteins are also CAPN-targets in breast cancer models. However, in this pathological process cells do not die, but rather migrate after cell adhesion disruption. Hence, our first objective is to identify the CAPN specific isoform involved in the proteolysis of adhesion complexes in both models.

2. TO EVALUATE WHETHER THE ISOFORM-SPECIFIC FUNCTION AND LOCALIZATION OF CALPAINS IS DEPENDENT ON THE CELL CONTEXT

In previous studies, CAPN1 was found at the nuclear compartment of differentiating adipocytes during the second phase of mammary gland involution. The second aim is to further explore the possible role of specific CAPNs isoforms in different cell types, since we postulated that CAPN1 might have different roles, depending on the cellular niche. As experimental

model, 3T3-L1 murine fibroblasts cell line was used. The dynamic changes taking place during pre-adipocytes to adipocytes differentiation could represent an excellent model to study the isoform-specific distribution of CAPNs in a progressively changing biological context within a gradually changing cell type.

3. TO STUDY THE STRUCTURAL AND SEQUENCE DETERMINANTS THAT MIGHT FAVOUR CALPAIN 2 NUCLEOLAR INTERNALIZATION

Different studies with confocal microscopy revealed that CAPNs where specifically concentrated in particular aggregates within the nuclei, that have turned out to be nucleoli. This novel CAPN localization was observed both in adipocytes and in breast and colon cancer cell lines. The last goal within this thesis is to elucidate those specific signals within CAPNs structure and sequence that are involved in their nucleolar translocation.

MATERIALS AND METHODS

MATERIALS AND METHODS

1. ANIMALS HUSBANDRY AND TISSUE EXTRACTION

C57BL/6 female mice (Taconic, Ejby, Denmark) were used for the study of physiological mammary gland involution. Animals were housed in a controlled environment (12 h light/12 h dark cycle) and received water and food *ad libitum*. Mice were cared for and handled attending to the National Institutes of Health guidelines and the Guiding Principles for Research Involving Animals and Humans approved by the Council of the American Physiological Society. Experimental protocols were approved by the Research Committee of the School of Medicine (University of Valencia, Valencia, Spain).

Virgin female mice (10 weeks old) were mated and males were subsequently removed at mid-gestation. Following parturition, litters were maintained with at least seven pups. Then, at the peak of lactation (days 9-11), mice were divided into different groups: control lactating mice (n=6) and weaned mice whose pups were removed 10 days after delivery to initiate involution. Weaning took place for 24, and 72 h before sacrifice (n=6, for each condition). To study in vivo the role of calpains during involution, a fourth group of mice was treated with a calpain inhibitor. Calpeptin (Sigma) (i.p. 40 mg/kg) was administered to 10-day lactating mice right after weaning of the pups. Mice received calpeptin or vehicle every 12 h during 3 days (n=4). Mice were killed by a single dose of sodium pentobarbital (i.p. 60 mg/kg). Inguinal mammary glands were removed and quickly freeze-clamped in liquid nitrogen or fixed in 4% formaldehyde for histological studies.

2. CELL CULTURE

The major bulk of the experimental work was carried out using cell line cultures for *in vitro* assays:

2.1 Human breast cancer cell lines.

Human breast cancer cell lines from luminal and triple-negative subtypes were used in the present study as representative models of breast cancer heterogeneity[273,278]. Breast tumours can be classified according to the expression status of certain hormonal receptors: oestrogen receptor (ER),

progesterone receptor (PR) and human epidermal growth factor receptor 2 (HER2) (Table 3). Two different luminal cell lines were chosen according to luminal subtypes classification: MCF-7 (luminal A) and BT-474 (luminal B). Two triple-negative cell lines, either basal or claudin-low, were also studied: MDA-MB468 (Triple negative A or basal-like) and MDA-MB-231 (Triple negative B or claudin-low). Breast cancer cell lines were purchased from American Type Culture Collection (ATCC). Cells were maintained in Dulbecco's Modified Eagle's Medium (DMEM) (Gibco) supplemented with 10% Fetal Bovine Serum (FBS) (Gibco, 16140-017), 1% penicillin/streptomycin (K952, Amresco), and L-glutamine (G7513, Sigma), and maintained in a humidified atmosphere at 37°C and 5% CO_2.

CELL LINE	ER	PR	HER2	SUBTYPE	TUMOUR	AGE
MCF-7	+	+	-	Luminal A	IDC	69
BT-474	+	+	+	Luminal B	IDC	60
MDA-MB-468	-	-	-	TNA	AC	51
MDA-MB-231	-	-	-	TNB	AC	51

Table 3. Breast cancer cell lines characteristics. *This table shows the expression of hormonal receptors (oestrogen receptor (ER), progesterone receptor (PR) and human epidermal growth factor receptor 2 (HER2)) for each cell line. The breast cancer subtype, the type of tumour where the cell lines were derived and the patient age are also indicated. TNA: triple-negative A; TNB: triple-negative A; IDC: invasive ductal carcinoma; AC: adenocarcinoma.*

2.2 Pre-adipocyte 3T3-L1 cell line.

Murine 3T3-L1 fibroblast cell line was also acquired form ATCC. Cells were maintained in the *Pre-adipocyte expansion medium*: DMEM high glucose (ATCC, 30-2002) supplemented with 10% Bovine Calf Serum (BCS) (ATCC, 30-2030), 1% Penicillin/streptomycin and L-glutamine. During maintenance, cells were never allowed to get confluent. For differentiation experiments, once cells reached 100% confluency, were kept for 2 days in *Pre-adipocyte expansion medium*. Then, differentiation was induced with the *Differentiation medium* (day 0): DMEM high glucose supplemented with 10% FBS, 1% penicillin/streptomycin, L-glutamine, 1.0 µg/mL insulin (I0516, Sigma Aldrich), 1.0 µM dexamethasone (API-04, G-Biosciences), 0.5 mM

methylisobutylxanthine (IBMX) (I5879, Sigma Aldrich) and rosiglitazone 2.0 µM (71740, Cayman Chemical)[315]. After 48 h (day 2), culture media was replaced with *Adipocyte maintenance medium* supplemented with insulin: DMEM high glucose supplemented with 10% FBS, 1% penicillin/streptomycin, L-glutamine and 1.0 µg/mL insulin. 48 h later, cells were maintained in *Adipocyte maintenance medium* (without insulin supplement) (Figure 11).

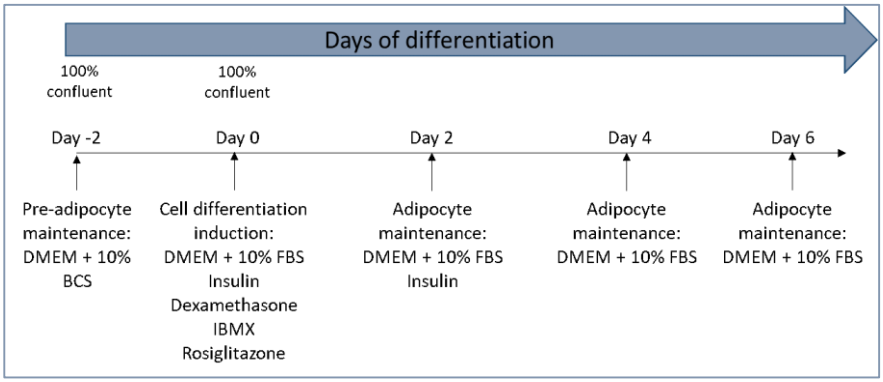

Figure 11. 3T3-L1 cell differentiation procedure: *Cells were seeded and maintained in pre-adipocyte expansion medium. Two-day post-confluent cells were stimulated to differentiate into adipocytes with differentiation medium. After 48 h cells were maintained in adipocyte maintenance medium supplemented with insulin and after that time with fresh adipocyte maintenance medium every 48 h.*

3. CAPN esiRNA TRANSFECTIONS

Both breast cancer cells and 3T3-L1 cells were transiently transfected with 30nM of CAPN1 or CAPN2 endoribonuclease-prepared small interfering RNA (esiRNA). esiRNA are pools of siRNA generated as a result of enzymatic digestion of long double stranded RNAs by *Escherichia coli RNase III*[316]. Different esiRNA were employed, depending on the experimental model or the gene to be silenced (Table 4). As transfection control (Scramble), cells were transfected with a Universal Negative Control #1 siRNA (SIC001).

Equal volumes of esiRNA and Lipofectamine were diluted separately in Opti-Mem medium (Gibco) and incubated for 5 min at room temperature (RT). esiRNA dilutions were then added to Lipofectamine dilution and incubated for 5 min at RT. After vigorous vortexing, the mixture was

incubated for another 20 min at RT. Then, cells were transfected following either forward or reverse transfection protocol. According to the forward transfection protocol, the transfection reagent dilutions are added to already seeded cells, while through reverse transfection protocol, cell were seeded on wells containing the transfection reagent.

MDA-MD-231 and MDA-MB-468 were transfected following the forward transfection protocol and using Lipofectamine 3000 (L3000008, Life Technologies) as Transfection reagent. Cells ($1.6x10^5$) were seeded in a 6 well plate and transfected 48h later, when cells reached 70% confluence. MCF-7 and BT-474 were reverse-transfected with Lipofectamine RNAiMAX (13778075, Life Technologies). In this case, $6x10^5$ cells were seeded onto 6 well plates that already had the transfection solution in the wells. 3T3-L1 cells were reversely-transfected 48h before the induction of differentiation, in such a way that CAPNs expression was silenced at the time of differentiation. Transfecting these cells as confluent pre-adipocytes, ensures that CAPN expression was silenced at the phase of growth arrested pre-adipocytes, when stimuli for differentiation were added.

For transfection, cells were incubated with the transfection mix and complete medium without antibiotics for 24 h. At this point, the transfection reaction was replaced with fresh media supplemented with antibiotics. esiRNA transfection efficiency was analysed by real-time quantitative PCR (RT-qPCR) and western blot at 72 h after transfection. In the case of 3T3-L1 samples, transfection efficiency was analysed after 96 h after induction of differentiation for mRNA and 72 h for western blot analysis.

GENE	ORGANISM	esiRNA REFERENCE
CAPN1	HUMAN	Sigma, EHU032581
CAPN2	HUMAN	Sigma, EHU025391
Capn1	MOUSE	Sigma, EMU057001
Capn2	MOUSE	Sigma, EMU080871
Negative control #1	UNIVERSAL	Sigma, SIC001

Table 4: Endoribonuclease-prepared esiRNAs for silencing experiments. *The table indicates the targeted gene, the organism and the product reference of each esiRNA used.*

4. PHARMACOLOGICAL CALPAIN ACTIVITY INHIBITION

In order to study the role of CAPN activity on adipocyte differentiation, confluent 3T3-L1 pre-adipocytes were treated for 24 h with two calpain inhibitors: 50 µM Calpeptin and 50 µM ALLN (N-Acetyl-L-leucyl-L-leucyl-L-norleucinal) (Calbiochem). Both inhibitors were dissolved in DMSO, thus, control cells were treated with the same volume of DMSO. Cells were treated 24 h before the induction of differentiation. Total protein extraction and total RNA isolation were carried out at day 3 and 4 of differentiation and analysed by RT-qPCR and western blot.

5. CALPAIN ACTIVITY ASSAY

CAPN protease activity was measured using the commercially available *Fluorogenic calpain activity assay kit* (QIA-120, Calbiochem) following the manufacturer's instructions. Total protein extracts from human breast cancer cell lines were obtained treating cells with CytoBuster™ Protein Extraction Reagent and incubated on ice for 20 min. Then cells were centrifuged 20 min at 14000 g and 4°C. The supernatant, containing the protein extract, was collected and quantified by the BCA Protein Assay Kit. Equal amounts of protein were incubated with the specific fluorogenic CAPN substrate (Suc Leu-Leu-Val-Tyr-AMC) in the presence of either activation (containing Ca^{2+} and TCEP reducing agent) or inhibition buffer (containing BAPTA) in a 96-well plate during 15 min at RT. A standard curve with increasing concentrations of AMC Standard incubated with activation buffer in the same conditions as the samples was also obtained. As an effective internal assay control, recombinant human CAPN1 was incubated with the CAPN substrate with either activation or inhibition buffer. All dilutions used in this protocol were prepared following the manufacturer's instructions. After incubation, fluorescence was measured using a fluorescence plate reader (ESPECTRAMAX-GEMINI XPS, Molecular Devices) at an excitation wavelength of ~360–380 nm and an emission wavelength of ~440–460 nm. CAPN activity was determined as the difference between the activity obtained after incubation with the activation buffer and that detected with the CAPN-inhibition buffer (BAPTA).

6. CELL MIGRATION AND INVASION

6.1 Wound healing assay.

MDA-MB-231 cells (16×10^4) were plated in six-well plates, cultured under standard conditions for further 24 h, and transfected as described above. MCF-7 cells (6×10^5) were simultaneously plated and reverse-transfected in six-well plates. The wound healing experiment was conducted in Scramble (control), CAPN1 esiRNA and CAPN2 esiRNA transfected cells. 24 h after transfection, both cell lines were serum-starved and 24 h later (48 h after silencing), confluent monolayers were scratched with a 1 ml pipette tip to induce a wound.

The wounded edges were imaged using an inverted microscope Nikon Eclipse Ti (×10 magnification). Images were collected at 48 h (MCF-7) or 28 h (MDA-MB-231) after scratch. The areas of five representative wounds for each condition were analysed and quantified by Image J software as the percentage of cells that migrated to the wound area after scratch.

6.2 Transwell assay.

Breast cancer cells migration ability after CAPN1 expression silencing was also analysed by Transwell assay, using 'Fluorimetric QCM 24-well (8µm) Chemotaxis Cell Migration Assay' (ECM509, Millipore) following manufacturer's instructions. Each insert contains an 8 µm pore size polycarbonate membrane. Migrating cells go through the pore membrane and attach to the bottom of the membrane. Then, these migrated cells are measured.

In brief, MCF-7 and MDA-MB-231 cells were transfected with scramble control siRNA or CAPN1 esiRNA as described for wound-healing experiments. Transfected cells were cultured for 48 h under standard conditions, and 24 h before starting Transwell assays cells were serum-starved. Cells were suspended in serum-free medium (DMEM 5% BSA) and placed in the upper chambers of Transwell plates (12×10^4 cells/well). DMEM 10% FBS was used as a chemoattractant in the lower chambers. Cell migration was measured by fluorescence using a fluorescence plate reader (ESPECTRAMAX-GEMINI XPS) after 8 and 24 h incubation for MCF-7 and MDA-MB-231, respectively. For this, migrated cells were detached from the polycarbonated membrane and then lysed with a lysis buffer that includes a

fluorescent dye CyQUANT® GR Dye that bounds to nucleic acids (Figure 12).

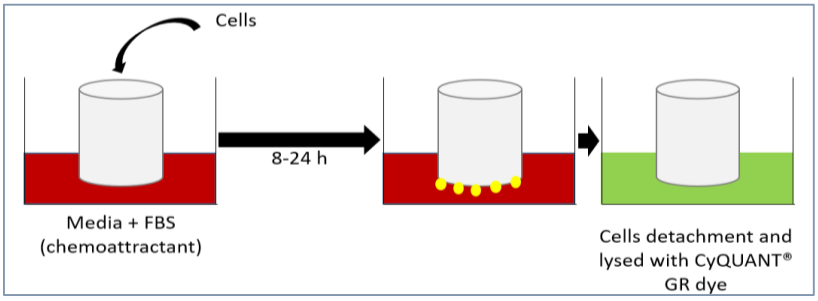

Figure 12: Transwell assay scheme. *Cells were loaded into the Transwell and cultured for 8 h for MDA-MB-231 and 24 h for MCF-7 cells. Invading cells migrate through and attach to the bottom of the membrane, while non-invading cells remain above. Then, cells are detached and lysed with CyQUANT® GR Dye.*

7. BACTERIAL TRANSFORMATION

Two CAPN2 overexpression vector constructs were commercially available from GenScrip. The cDNA of CAPN2 of 2115 bp gene length (0Hu23853C) and a truncated version of CAPN2 (ΔCAPN2) of 1356 pb (0Hu56639C) were cloned on pcDNA3.1(+)-N-DYK construct (Figure 13).

Competent cells SIG-10 5-alpha (#CMC0007, Sigma Aldrich) were transformed with both plasmids. After SIG-10 5-alpha cells were thaw on ice, 45 µl of cells were added to different 1.5ml Eppendorfs. Then, 5 µl of each cDNA were cautiously added to the competent cells and were incubated on ice for 30 min. Afterwards, cells were under heat shock (45 seconds at 42°C) and then were chilled again on ice for 2 min. Finally, 950 µl of *Recovery medium* were added to the cells, followed by 1.5 h at 37°C in a shaking device at 750 rpm.

Meanwhile, for growing bacteria, agar petri dishes were prepared as follows: 1.5% (p/v) Bactoagar (214010, BD) and Ampicillin (50 µg/ml) diluted on sterile LB Broth agar (2 % (p/v) on distilled water (L3022, Sigma)). After the incubation, 300 µl of the transformed bacteria were seeded on agar petri dishes and incubated overnight at 37°C. The plasmid construction included an Ampicillin resistant gene, thus, only bacteria that had incorporated the plasmid, would develop ampicillin resistance and grow.

The following day, selected individual colonies were picked and further grown in liquid LB Broth with 25 µg/ml Ampicillin in a shaking incubator at 750 rpm, overnight at 37°C.

Finally, bacteria were lysed and plasmids isolated with a plasmid extraction kit (#K0491 GeneJET Plasmid Maxiprep Kit, Thermo Scientific) following manufacturer's instructions.

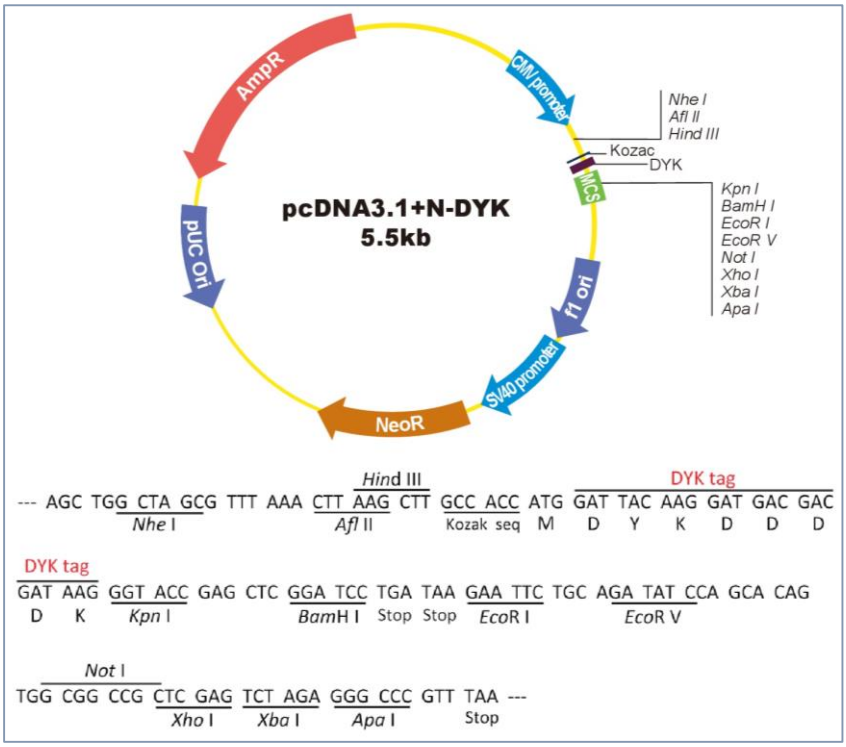

Figure 13: Cloning vector map of pcDNA3.1+N-DYK.

8. PLASMID TRANSFECTION

MDA-MB-231 and MCF-7 cells were plated on tissue culture dishes to reach 80% confluence after 48h post seeding. For total protein extraction, cells were seeded on 60 mm culture dishes and for immunofluorescence studies, on 8 chambered coverglass. Lipofectamine 3000 reagent was used as transfection vehicle following manufacturer's instructions. Transfection reagents were diluted in Opti-MEM (31985070, Gibco). Amounts of cDNA

and Lipofectamine volumes used are indicated on table 5. For transfection, cells were maintained in culture medium without antibiotics and 24 h later, the reaction dilution was replaced with fresh media supplemented with antibiotics. CAPN2 and ΔCAPN2 overexpression efficiency was analysed by western blot at 48 after transfection.

CULTURE DISH	cDNA	LIPOFECTAMINE
60 mm (21 cm^2)	4 µg	6 µl
8 chambered coverglass (0.7 cm^2)	0.5 µg	1 µl

Table 5: Transfection conditions. *The table includes the quantity of cDNA and the volume of Lipofectamine for each dish size used.*

9. IMMUNOFLUORESCENCE STAINING

To determine CAPN location within the cell, immunofluorescence (IF) studies were carried out. With this approach CAPN-mediated cleavage of E-cadherin in involuting mammary gland was analysed. Formalin-fixed paraffin-embedded tissue from DMSO and calpeptin-treated mice at 72h of involution was cut into thin sections of 5 µm and mounted onto microscope slides at the Department of Pathology in the School of Medicine. To remove paraffin, these sections were treated with xylene, rehydrated through a graded series of alcohol (100, 90, 70, 50, 30 % ethanol v/v) and washed with PBS. Antigen retrieval was achieved by 10 min boiling in 10mM tri-sodium citrate buffer, pH 6.0. After boiling, sections were cooled down with cold distilled water.

For the experiments performed with cell lines, protocol was as follows: Breast cancer cells (MCF-7: 6 x 10^5; BT-474: 6 x 10^5; MDA-MB-231: 4.2 x 10^5 ; MDA-MB-468: 4.2 x 10^5) and 3T3-L1 cells (5 x 10^5) were cultured onto 13 mm Ø borosilicate coverglass (VWR 631-0149) in 60mm dishes. First of all, the medium was carefully removed from the wells and cells were treated with 4% paraformaldehyde (Sigma) diluted in PBS for 10 min to be fixed. Then, cells were permeabilized by 10 min incubation with 0.3% Triton X-100 in PBS for breast cancer cells and cold 100% methanol for 3T3-L1 cells at RT.

Either tissue sections or cells grown and fixed on the coverglass were blocked in 5% normal goat serum (Dako, Glostrup, Denmark) for 1 h at RT.

Then, samples were incubated overnight at 4°C with the corresponding primary antibody, whose dilutions and references can be found in Table 6.

Subsequently, slides were washed three times with PBS and incubated 1 h at RT with secondary antibodies in the dark. Secondary fluorescent antibodies and dilutions used for detection are indicated in Table 7. Both primary and secondary antibodies were diluted in PBS + 0.3% Triton X-100. Antibody non-specific binding was minimized incubating one section merely with secondary antibody and the resultant image was used as negative control. Nuclei were counterstained with Hoechst DNA dye 33342 (Invitrogen) diluted 1:1000 in distilled water. Pictures were acquired in Leica TCS-SP 2 or Olympus FV1000 confocal microscope.

PRIMARY ANTIBODY	APLICATION	DILUTION	REFERENCE
CAPN1	IF	1/100	Abcam, ab39170
CAPN2	IF	1/50	Cell Signalling, 2539
CAPNS1	IF	1/100	Abcam, ab28237
Calpastatin	IF	1/100	Thermo Scientific, MA3-944
E-Cadherin	IF	1/100	BD Biosciences, 610182
β-Catenin	IF	1/100	Abcam, ab6301
δ-Catenin (p120)	IF	1/100	Abcam, ab11508
Talin-1	IF	1/100	Sigma-Aldrich, T3287
Fibrillarin	IF	1/100	NB300-269
Perilipin-1	IF	1/75	Progen Bio, 651156
Histone H3 N-terminal	IF	1/5000	Active Motif, 39763
DYKDDDDK tag	IF	1/500	GenScript, A00187-100

Table 6: Primary antibodies used for immunofluorescence analysis. *This table includes the dilution and reference of each primary antibody employed for immunofluorescence studies. Antibodies were diluted in PBS + 0.3% Triton X-100.*

SECONDARY ANTIBODY	APLICATION	DILUTION	REFERENCE
Alexa Fluor 488 anti-rabbit IgG	IF	1/200	Invitrogen, A11008
Cy3 anti-mouse IgG	IF	1/200	Sigma, C2181

Table 7: Secondary immunofluorescence antibodies. *The table shows the dilution and reference of the secondary immunofluorescence antibodies. Antibodies were diluted in PBS + 0.3% Triton X-100.*

10. OIL RED O STAINING

Oil Red O staining (Sigma-Aldrich) is a method used for easy estimation of lipid content and distribution within a tissue or cell. Through this technique, nuclei are stained in blue and lipids in red and mature adipocytes can be easily observed. 3T3-L1 cells pre-treated with CAPN inhibitors (Calpeptin and ALLN) 48h prior to differentiation induction, were stained with Oil Red O at day 3 differentiation. Briefly, cells were washed with PBS and fixed with 10% formaldehyde in PBS for 45 min. Cells were then washed with distilled water and incubated for 5 min with 60% isopropanol, followed by 5 min incubation with Oil Red O working solution (3:2, Oil Red O stock solution: Water). Oil Red O stock solution is obtained by adding 20 ml 99% isopropanol to 60 mg Oil Red O powder according to manufacturer's instructions. After several washes with water, haematoxylin was added for 1 min. Finally, cells were washed several times with water and imaged with a Leica DMI 3000 microscope.

11. PROXIMITY LIGATION ASSAY

Proximity Ligation Assay (PLA) allows visualization of two interacting proteins *in vivo*. The principle of this technique lies on the secondary antibody. In brief, samples are incubated with primary antibodies of different species that bind to the proteins of interest. Then, secondary antibodies or PLA probes are added. Each PLA probe, is labelled with an oligonucleotide. Only in the case that the two proteins are in close proximity (<40 nm) both oligonucleotides will hybridize by means of a ligase reaction. The ligated circle serves as a template for a polymerase which amplifies the circled product. In this amplification reaction the polymerase incorporates

fluorescently labelled nucleotides. The amplified signal is detected by fluorescent microscopy (Figure 14).

Mammary gland tissue sections from lactating (0 h), weaning mice (24 and 72 h involution) and 72 h weaning samples from mice treated with calpeptin or vehicle (DMSO) were used to detect *In situ* interaction between CAPN1/E-cadherin and CAPN2/E-cadherin. In breast cancer cells, the interactions between CAPN1/E-cadherin in MCF-7 and CAPN1/talin-1 in MDA-MB-231 cell lines, were also analysed with PLA approach. Finally, 3T3-L1 cells at day 2 and 5 of differentiation were selected to study CAPN1/histone H3-Nt and CAPN2/histone H3-Nt. All the samples (either tissue or cell lines) were fixed and permeabilized as described for immunofluorescence analysis.

To detect *in situ* interactions between the proteins of interest, the Duolink® In Situ assay (DUO92102, Sigma-Aldrich) based on PLA technique was used. Following permeabilization, tissue sections or cells were incubated with blocking solution provided in the kit for 30 min at 37°C. Afterwards, samples were incubated with primary antibodies (each from different host

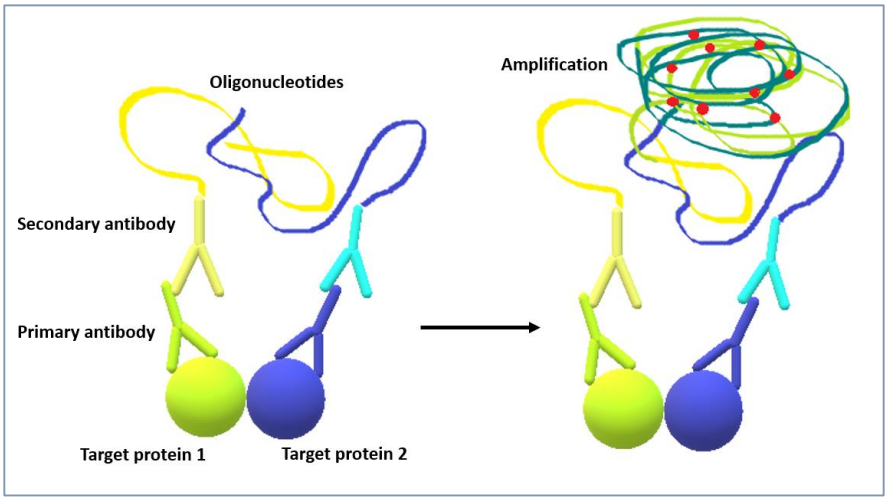

Figure 14. Proximity ligation assay principle. *Samples were incubated with primary antibodies of different host species that bind to the proteins of interest. Secondary antibodies are conjugated with oligonucleotides, which are hybridized by means of a ligase reaction and then amplified following a polymerase reaction. In the amplification reaction the polymerase incorporates fluorescently labelled nucleotides.*

species) over night at 4°C. On the next day, PLA probes dilutions were added and incubated for 1 h 37°C. Then, oligonucleotides labelled to the PLA probes were ligated by means of ligase incubation (30 min at 37°C). Finally, after amplifying the PLA signal by incubating with a polymerase 100 min at 37°C, tissue sections and cells were washed and mounted with Duolink in Situ Mounting Medium with DAPI. The steps on the described protocol that required incubation at 37°C were carried out in a pre-heated humidity chamber. All dilutions used in this protocol were prepared according to the manufacturer's instructions.

To visualize protein interaction, PLA signals in mammary gland tissue sections and cells were analysed in Leica TCS-SP 2 or Olympus FV1000 confocal microscope.

12. RNA ISOLATION AND REAL TIME RT-qPCR ANALYSIS

Total RNA from breast cancer cell lines was extracted by RNAeasy Mini Kit (Qiagen). Whereas, total RNA from 3T3-L1 was isolated with QIAzol lysis reagent (Qiagen) followed by additional column purification (RNeasy Lipid tissue Mini Kit, Qiagen). RNA quantity and purity were determined using the NanoDrop ND-2000 (NanoDrop Technologies). High RNA quality was determined by absorbance ratio values. RNA purity is considered when the ratios 260/280nm and 260/230 nm have a value between 2.0 - 2.2. Nucleic acids absorb at 260nm while proteins and phenols absorb at 280 nm. The second ratio, 260/230 is a secondary purity measure, as EDTA, phenols and carbohydrates absorb at 230 nm, and may interfere with the result.

Once RNA purity was checked, RNA (1 µg) was reverse-transcribed (RT) to cDNA using a High-Capacity RNA-to-cDNA kit (4387406, Applied Biosystems) on a thermocycler *Gene Amp PCR system 2700* (Applied Biosystems). RT program was as follows: 60 min at 37°C plus 5 min at 95°C.

Then, cDNA products were amplified by qPCR using the GeneAmp Fast PCR Master Mix (4362070, Applied Biosystems). All reactions were carried out in triplicate. Real time-qPCR was run in the 7900HT Fast Real-Time PCR System. Pre-developed TaqMan primers were purchased from Applied Biosystems (Table 8). Results were normalized according to 18S quantification in the same sample reaction. The threshold cycle (Ct) was determined, and the relative gene expression was expressed as follows:

$$Relative\ amount = 2^{-\Delta(\Delta Ct)}$$

where Ct = Ct(target) − Ct(18S) and Δ(ΔCt) = ΔCt (Sample) − ΔCt(Control).

GENE	ORGANISM	REFERENCE
CAPN1	HUMAN	Hs00559804_m1
CAPN2	HUMAN	Hs00965097_m1
Capn1	MOUSE	Mm00482964_m1
Capn2	MOUSE	Mm00486669_m1
Leptin	MOUSE	Mm00434759_m1
Perilipin-1	MOUSE	Mm00558672_m1
CEPB-α	MOUSE	Mm01194587_m1
18S rRNA Endogenous Control	EUKARYOTIC	4319413E

Table 8: Pre-developed Taqman probes employed for cDNA amplification. *The table indicates the gene, the organism and the product reference of each Taqman probe used.*

13. TOTAL PROTEIN EXTRACTION

Total proteins were extracted in RIPA buffer (1.8 mM NaH_2PO_4, 8.4 mM Na_2HPO_4, 0.1% (p/v) sodium dodecyl sulphate (SDS), 1.0% (v/v) Triton X-100, 0.1 M NaCl, 0.5% (p/v) sodium deoxycholate), in the presence of inhibitors (1mM phenylmethylsulfonyl fluoride (PMSF), 2µl/ml protease inhibitor cocktail and 5µl/ml phosphatase inhibitor cocktail (Calbiochem) at 4°C.

Mammary gland protein samples were obtained from frozen tissue, minced and homogenized with Ultra-Turrax T25 basic® (Ika-Werke GmbH & Co. KG. Germany). Total extracts from breast cancer cell lines and 3T3-L1 cell line were isolated from culture dishes of different size, depending on the experiment. Cells were collected using a cell scraper and uniformly lysed with the sonication device Bioruptor ® (Diagenode). After mammary gland and

cell lines extracts homogenization, samples were centrifuged 20 min at 14000 g and 4°C. The supernatant, containing the protein extract, was collected and stored at -80ºC. Proteins were quantified by the BCA Protein assay kit (23225 ThermoFisher) according to the manufacturer's instructions.

14. SUBCELLULAR FRACTIONATION

14.1 Nuclear and cytosolic fractions.

3T3-L1 cell line (1.3×10^6 cells) were platted on 100mm tissue culture dishes and cultured as indicated above. Nuclear and cytoplasmic factions were isolated using the Nuclear Extract kit (Active Motif, 40010) according to manufacturer's instructions. In brief, cells were pelleted in PBS and then treated with 1X hypotonic buffer supplemented with phosphatase inhibitor cocktail (50 µl/ml) and protease inhibitor cocktail (1 µl/ml). After 15 min incubation on ice, nuclear and cytoplasmic fractions were separated by centrifugation (14000 g for 30 seconds at 4°C). The supernatant, was stored as the cytoplasmic fraction. The pellet, including intact nuclei, was lysed with 1X lysis buffer supplemented with 10 mM DTT, phosphatase inhibitor cocktail (50 µl/ml) and protease inhibitor cocktail (1 µl/ml) in a rocking platform for 30 min with gentle agitation at 4ºC. The sample was then centrifuged (14000 g for 10 min at 4°C) and the supernatant was recovered as the nuclear fraction.

To quantify nuclear and cytoplasmic proteins the Bradford (Bio-Rad) method was used instead of the BCA reagent, since DTT present in lysis buffer interferes with the BCA reagent. α-Tubulin was used as marker of cytoplasmic fraction purity while fibrillarin, a nucleolar protein, was used as nuclear marker.

14.2 Nucleolar purification.

Breast cancer cells (MCF-7: 4×10^6; BT-474: 4×10^6; MDA-MB-231: 3×10^6; MDA-MB-468: 3×10^6) and 3T3-L1 cells (3.5×10^6) were seeded on 150mm tissue culture dishes and handled as previously described. Nucleoli purification was performed following a published protocol [317] based on sucrose gradients. Cells were washed 3 times with cold Solution I (0.5 M sucrose, 3 mM $MgCl_2$ with (50 µl/ml) and protease inhibitor cocktail (1 µl/ml) and collected with the help of cell scrapers. Then, cells were sonicated

(Sonics, VCV130), at 40% amplitude, 10 seconds on, 50 seconds off on ice. Number of sonication cycles varied depending on the cell type (MCF-7: 7 cycles; MDA-MB-231: 5 cycles; 3T3-L1: 5 cycles). Cell lysates contained intact nucleoli and solubilized nuclear and cytosolic proteins. With the help of a light microscope, it was checked that more than 90% of the cells and nuclei were broken.

In order to separate the nucleolar fraction from the rest of the cellular content, the lysate was laid on the same volume of Solution II (1.0 M sucrose, 3 mM $MgCl_2$, protease inhibitor cocktail 2 µl/ml; phosphatase inhibitor cocktail 5 µl/ml, PMSF 1 mM) and centrifuged (1800 g for 10 min at 4°C). The supernatant was collected as the nucleolar-less fraction (containing cytoplasmic and nuclear proteins excepting the nucleoli) and the pellet was resuspended in RIPA solution (supplemented with protease inhibitor cocktail 2 µl/ml; phosphatase inhibitor cocktail 5 µl/ml and PMSF 1 mM). This nucleolar fraction was sonicated again (at 40% amplitude, 10 seconds on, 50 seconds off on ice, 4 times). Both the nucleolar-less and the nucleolar fraction were centrifuged again at 14000 g, 10 min at 4°C and the respective supernatants were collected and stored at -80°C.

Fibrillarin was used as marker to assess the purity of nucleolar fractions and α-tubulin, a protein known to be present in both nuclear and cytoplasmic compartments but not in nucleoli [318], was also used to discard contamination between fractions.

15. WESTERN BLOT

Equal amounts of protein (15 µg for tissue extracts and 20 µg for cellular extracts) were prepared with a 5x loading reductive buffer (0.3 M Tris-HCl pH6.8, 50% (v/v) glycerol, 10% SDS, 25% 2-Mercaptoethanol and 0.05% bromophenol blue). Then, samples were boiled 5 min at 95 ºC.

Samples were subjected to SDS–PAGE of different acrylamide concentration depending on the molecular weight of the protein of interest. Proteins were resolved in electrophoresis buffer (25 mM Tris-HCl, 192 mM glycine, 0,1% (w/v) SDS, pH 8.3), at 120 V for 120 min. After the electrophoresis, proteins were electroblotted onto nitrocellulose membranes (88018 Protran® Whatman, Kent, UK), in transfer buffer (25 mM Tris-HCl, 192 mM glycine, 20% (v/v) methanol, pH 8.3) at 60 V for 120 min.

Equal loading was confirmed by Ponceau S staining (Sigma) of the membrane. Subsequently, membrane was blocked with freshly prepared 5% nonfat dried milk or BSA diluted in TBS-T (20mM Tris-HCl, 500mM NaCl, pH 7.5 added Tween20 to 1%) during 1 h at RT. After blocking, membranes were incubated with the corresponding primary antibody at 4°C overnight. Primary antibodies used are listed on the Table 9 with their corresponding dilutions (prepared in 1% BSA (p/v) in TBST). Then, membranes were washed (1% (p/v) BSA in TBST) three times and incubated with the HRP-conjugated secondary antibody 1 h at RT, followed by three washes with TBS-

ANTIBODY	APLICATION	DILUTION	REFERENCE
CAPN1	WB	1/2000	Abcam, ab39170
CAPN1-NH2	WB	1/1000	Abcam, ab28257
CAPN2	WB	1/1000	Cell Signalling, 2539
CAPNS1	WB	1/1000	Abcam, ab28237
Calpastatin	WB	1/1000	Thermo Scientific, MA3-944
E-Cadherin	WB	1/5000	BD Biosciences, 610182
β-Catenin	WB	1/5000	Abcam, ab6301
δ-Catenin (p120)	WB	1/10000	Abcam, ab11508
Talin-1	WB	1/400	Sigma-Aldrich, T3287
β-Actin	WB	1/2500	Abcam, ab8227
Fibrillarin	WB	1/1000	NB300-269
α-Tubulin	WB	1/5000	Abcam, ab52866
Perilipin-1	WB	1/1000	Progen Bio, 651156
GAPDH	WB	1/10000	Abcam, ab8245
Histone H3 C-terminal	WB	1/20000	Millipore, 07-690
DYKDDDDK tag	WB	1/5000	GenScript, A00187-100

Table 9: Primary antibodies used in western blot experiments. *The dilution and the product reference for each antibody used is listed in this table.*

T. All steps were carried out under shaking conditions. Finally, blots were developed by enhanced chemiluminescence reaction (ECL Detection Kit, GE Healthcare, UK).

The processor Curix60 (AGFA) was used for film development. Equal loading was confirmed by reprobing the blot against either α-tubulin, β-actin or GAPDH. The intensity of the bands was measured by densitometry using Image J, a public domain Java image processing program.

16. BIOINFORMATICS ANALYSIS

The structure characteristics responsible of CAPN2 nucleolar distribution were studied with different bioinformatics tools:

16.1 Nucleolar Localization Sequence detector.

The prediction of nucleolar signals (NoLS) within CAPNs sequence was achieved by the NoD (Nucleolar localization sequence detector)[319] platform, created by the Dundee University. The prediction tool is found in the webpage: http://www.compbio.dundee.ac.uk/www-nod/index.jsp. This tool is based on different NoLS sequences that have been experimentally validated. With this database they have created a network predictor that takes into consideration the protein sequence, length and secondary structure. For the software to predict a possible NoLS, 8 consecutive 13-residues sequences must have an average score of at least 0.8 /1.

16.2 Positively charged regions study.

The charge values of the CAPNs amino acidic sequence were analysed by the *EMBOSS: charge platform*, available on http://www.bioinformatics.nl/cgi-bin/emboss/charge. This bioinformatics tool generates a graph based on the amino acid properties. To this effect, the program assigns values to particular residues: D and E a charge of -1; K and R a charge of +1; and H a charge of +0.5.

16.3 Nuclear Localization Sequences detector.

For the estimation of possible Nuclear Localization Sequences (NLS) on the CAPN2 sequence, we used the platform *PSORT II predictor* (https://psort.hgc.jp/form2.html). Different consensus sequences have been identified as NLSs for nuclear protein import[320]. The program bases its

prediction on the detection of three established sequences, that can be: i) 4 residue pattern (pat4), that consist of 4 basic amino acids (K or R), or three basic amino acids (K or R) and either H or P; ii) 7 residue pattern (pat7), being the first residue a P, followed by basic residues (at least 3 K/R); iii) and bipartite: 2 basic residues, 10 residue spacer, and another basic region of at least 3 basic residues[321].

16.4 Analysis of protein folding and disorganized regions.

The platform FoldIndex©: Will this protein fold? (https://fold.weizmann.ac.il/fldbin/findex), allows estimation of grade of folding of a protein based on its sequence. This platform applies the algorithm of Uversky[322], which is based on the average residue hydrophobicity and net charge of the sequence[323].

16.5 Prediction of protein-protein interaction motifs.

The *Interaction Sites Identified from Sequence* (ISIS), is a network platform that identifies possible protein-protein interaction sites which operated with a 90% of accuracy. This tool is based on the combination of biophysical sequence features and structural characteristics with evolutionary information[324].

17. STATISTICAL ANALYSIS

The results presented in the graphs correspond to the arithmetic mean of the values obtained in each experiment ± the standard error of the mean (SEM) of at least three independent experiments. In the experiments in which the mean values of independent samples distributed normally were compared with reference to control samples mean, t-Student's test was used. Those groups of data in which there were significant differences (at least at $p \leq 0.05$) were indicated by asterisks.

Experiments with differences among groups were analysed, one-way ANOVA was used for statistical analysis with the statistic programme SPSS v9. Significant differences were determined by a Tukey–Kramer test. Different superscript letters indicate significant differences between groups. The letter 'a' always represents the lowest value within the group. Groups that do not share a letter are significantly different. Differences were considered significant at least at $p<0.05$.

RESULTS

RESULTS

1. ISOFORM-SPECIFIC ROLE OF CALPAINS IN CELL MEMBRANES

1.1 CALPAIN ISOFORMS IN A BREAST PHYSIOLOGICAL MODEL: MAMMARY GLAND INVOLUTION

During each pregnancy/lactation cycle, the mammary gland suffers a process of regression known as involution, where epithelial cell death is coupled to tissue remodelling. This process ensures removal of no-longer needed secretory cells from mammary epithelia, together with tissue remodelling of the gland.

1.1.1 Cell detachment and adhesion proteins cleavage by CAPNs.

Cell detachment is a key event triggering cell death in postlactational regression of mammary gland. Previous studies performed in our laboratory showed that adherens and focal adhesion proteins such as E-cadherin, β-catenin, δ-catenin (p-120) and talin-1 were proteolyzed as mammary gland involution progressed (Figure 9). *In vitro* digestion of lactating mammary gland samples by recombinant CAPNs showed that focal and adherens junctions were cleaved equally by both CAPN1 and CAPN2 isoforms. Furthermore, inhibitors of CAPN activity prevented this cleavage, demonstrating that both CAPN isoforms were able to recognize *in vitro* the same adhesion proteins from mammary gland epithelia[325].

In order to study *in vivo* CAPN-cleavage of adhesion proteins we inhibited CAPN activity in mice during weaning. The inhibitor calpeptin was injected into the mammary tissue of mice at the peak of lactation and litter was removed. Weaning lasted 72 h and studies were performed to compare 72 h involuting glands *versus* 72 h calpeptin treated glands[147]. Then, levels of adhesion proteins were analysed by western blot. For adherens junction disruption, proteolysis of E-cadherin, β-catenin and δ-catenin (p-120) was analysed. On the other hand, loss of focal adhesions with the basal membrane was analysed by means of talin-1 cleavage.

As shown in Figure 15, adherens junctions and focal adhesion proteins were processed after 72 h weaning. Furthermore, this cleavage was prevented

in samples of calpeptin-treated mice, where CAPN activity was inhibited. These results indicate that the proteolysis of different adhesion proteins during mammary gland involution is mediated by CAPN activity. Nevertheless, the isoform-specific functions of CAPNs in cell adhesion have never been elucidated in a physiological *in vivo* model. To discern which CAPN is responsible for this cleavage further approaches should be performed.

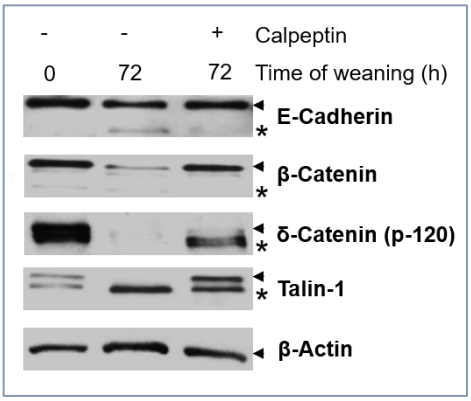

Figure 15: Adhesion proteins cleavage prevention of in calpeptin-treated mammary gland. *Cleavage of E-cadherin, β-catenin, δ-catenin (p-120), and talin-1 at 0 h and 72 h of weaning in DMSO or calpeptin-treated mice mammary gland extracts was assessed by western blot. Full length protein is pointed by arrow heads and the truncated fragments by asterisks. β-Actin was used as loading control. Representative immunoblots are shown (n ≥ 3).*

1.1.2 CAPN2 isoform-specific cleavage of E-cadherin.

Based on this former information we sought to examine which CAPN isoform was responsible for the proteolytic processing of adhesion proteins *in vivo* under physiological conditions. To achieve this, the interaction between CAPN1 or CAPN2 and E-cadherin was analysed by *in situ* Duolink Proximity Ligation Assay (PLA) in tissue sections from mammary gland during weaning. As mentioned in material and methods section, PLA assays can detect the direct interaction of two proteins *in vivo*. A fluorescent signal will be generated only when the plus and minus probes from antibodies recognizing both proteins are in close proximity[326].

As shown in Figure 16A, no CAPN1/E-cadherin interaction was detected during the course of involution (lactating control, 24 h and 72 h of involution). Conversely, although CAPN2/E-cadherin interaction was barely

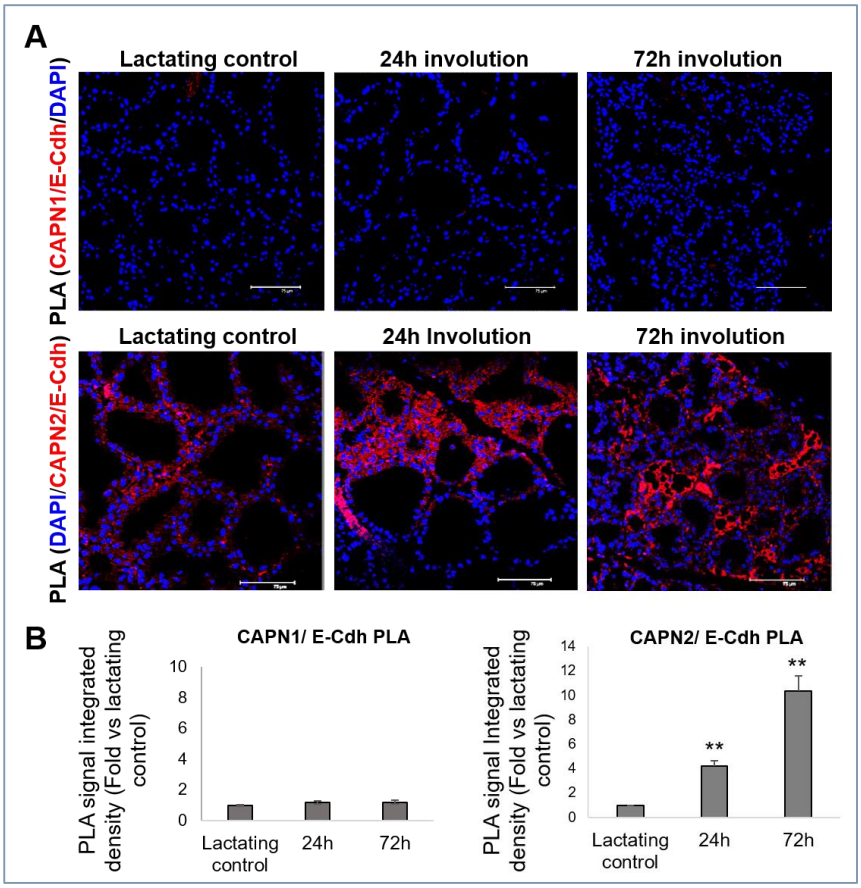

Figure 16: *In vivo* analysis of CAPN-mediated cleavage of E-cadherin during mammary gland involution. *(A) CAPN2/E-cadherin and CAPN1/E-cadherin in vivo interaction (red) was analysed by PLA in 5 µm tissue sections from mammary gland during the time course of involution (0h, 24 h and 72 h). Scale bar, 75 µm. Nuclei were stained with DAPI (blue). (B) Quantification of CAPNs/E-cadherin interaction analysed by PLA in tissue sections at different involution time-points (lactation, 24 h and 72 h). Integrated density of red spots was measured in three independent experiments for each condition and results are expressed as fold increase vs lactating control. Results (n≥3) are mean values ± SEM, Student's t-test was performed for the statistical analysis, **p≤0.01 vs lactating control.*

detected at the peak of lactation, as the involution progressed the interaction dramatically increased. The results obtained by IF imaging were quantified and represented on bar charts (Figure 16B). At 24 h involution, the interaction between CAPN2 and E-cadherin was already increased, and it was even more evident at 72 h weaning, with statistically significant differences at both time points compared to controls.

It is noteworthy that the fluorescence staining that indicates CAPN2/E-cadherin interaction, is not restricted to the cellular membrane. Instead there is a diffuse and punctate signalling in the cytosolic compartment during involution. This might be the product obtained from CAPN2-mediated cleavage of E-cadherin, which gradually accumulated in the cytoplasm. The only plausible explanation for the fluorescence increase along the time-course of mammary gland involution is given by the fact that cleaved E-cadherin remains bound to the active centre of CAPN2 and both proteins translocate to the cytosol. To confirm this hypothesis, the same PLA assay was performed in mammary gland sections from 72 h weaning mice treated with either vehicle DMSO (control) or calpeptin, a pharmacological competitive inhibitor of CAPNs (Figure 17). In agreement with the previous result, no interaction was observed for CAPN1 and E-cadherin at 72 h weaning, neither in DMSO- nor in calpeptin-treated mice (Figure 17A). On the other hand, CAPN2/E-cadherin interaction was observed in DMSO treated mice. However, calpeptin treatment prevented CAPN2/E-cadherin interaction at 72 h involution almost completely (Figure 17B). Since calpeptin remains bound to CAPN2 in calpeptin treated mice, the protease is no longer available to bind E-cadherin, and thus interaction between both proteins (estimated by PLA assay) falls up to 80% compared to control 72 h involuting glands.

Nevertheless, it has to be taken into consideration that tissue remodelling during involution, involves the loss of epithelial architecture and thus, total levels of E-cadherin dramatically decrease during weaning [298]. Therefore, loss of CAPN2/E-cadherin PLA signal in calpeptin-treated tissue could be due to an accelerated drop of E-cadherin levels after treatment, rather than by the specific inhibition of CAPN2/E-cadherin interaction. To discard this possibility, E-cadherin levels were analysed by IF in the same tissue sections used for previous PLA assays (Figure 18).

Concomitant with mammary gland involution, E-cadherin levels were dramatically diminished in DMSO control samples after 72 h involution. As can be observed in Figure 18, ductal architecture of the gland is reduced at this time point of weaning and epithelial cells are lost. On the contrary, calpeptin treatment delays the involution process, as previously reported[147].

Consequently, the acinar and ductal structure is conserved. Thus, in calpeptin-treated samples E-cadherin remains at cell–cell junctions, and its cleavage is prevented. Therefore, the loss of CAPN2/E-cadherin PLA signals results from an impaired interaction between both proteins and not from a decrease in E-cadherin levels. All in all, these results suggest that during mammary gland involution, the isoform involved specifically in E-cadherin cleavage is CAPN2.

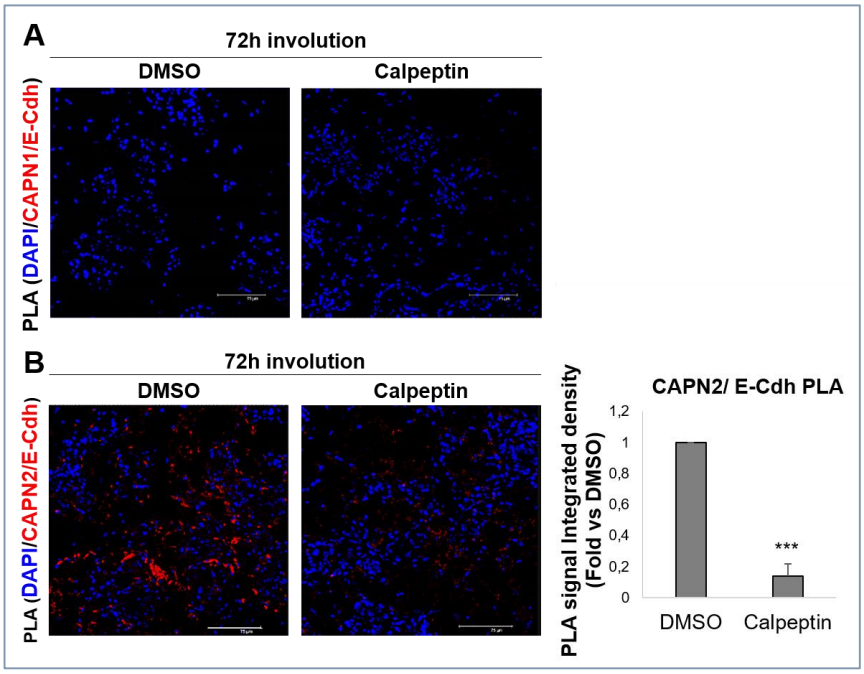

Figure 17: Specificity of CAPN2 and E-cadherin interaction in mammary gland involution. *(A) CAPN1/E-cadherin interaction analysed by PLA in tissue sections from DMSO (vehicle) or calpeptin-treated mammary gland at 72 h after weaning. No interaction was observed for CAPN1/E-cadherin. (B) The same analysis was performed for CAPN2/E-cadherin interaction (red) in tissue sections from DMSO or calpeptin-treated mammary gland at 72 h weaning (left panel). Graph (right panel) shows the quantification of PLA CAPN2/E-cadherin in vivo-interaction from 72 h weaned mammary tissue treated with CAPN inhibitor, calpeptin versus non-treated tissue (DMSO). Results are expressed as fold vs. DMSO-treated tissue. Nuclei were stained with DAPI (blue). Data (n≥3) are mean values ± SEM. Student's t-test was performed for the statistical analysis, ***p≤0.001 vs DMSO. Scale bar, 75 µm.*

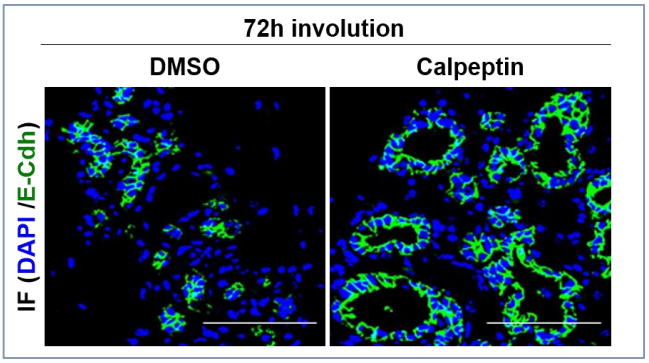

Figure 18: E-cadherin distribution analysis in involuting mammary gland. *Immunofluorescence staining of E-cadherin (green) in tissue sections from DMSO (vehicle) or calpeptin-treated mammary glands at 72 h weaning. Scale bar, 75 µm. Nuclei were stained with DAPI (blue). Representative images are shown (n ≥ 3).*

1.2 CALPAIN ISOFORMS IN A BREAST PATHOLOGICAL MODEL: BREAST CANCER CELL LINES

Several studies have underlined the implication of CAPNs in fundamental processes for cancer development and progression[13,14,200]. In particular, the role of CAPNs in the proteolytic processing of adhesion proteins to promote cell migration and metastasis has been extensively documented[70,92,97,206,250]. Nevertheless, as previously explained, the pattern of gene expression and subcellular localization of CAPNs is highly dependent on the cell context, and differences in the localization or activity of both CAPNs have not been studied in breast tumours. Even though CAPNs are good targets for cancer therapy, there is no evidence for the role of a particular CAPN isoform in each tumorigenic process.

1.2.1 Subcellular distribution of CAPN isoforms.

The context-dependent subcellular distribution of a CAPN isoform might specify its target-substrate to undertake a specific biological function. Consequently, the subcellular distribution of both CAPNs was analysed by IF staining in breast cancer cell lines cultured under standard conditions. To detect possible differences among breast cancer subtypes according to their intrinsic classification, a cell line from each subtype (luminal A, luminal B, triple negative A (Basal A) and triple negative B (claudin-low)) was used.

As can be observed in Figure 19 (upper panel), CAPN1 was distributed in cell membrane, cytosol and prominently in nuclei of breast cancer cells. CAPN2 (Figure 19, lower panel), barely detected in the cytosolic compartment, was found to be mainly localized in nuclei of all the cell lines tested. Interestingly, a more detailed analysis demonstrated that CAPN2 was not only compartmentalized into the nucleus, but also highly concentrated in a specific region inside the nucleus. Its shape and distribution resembles the nucleolar compartment, which is the largest and densest subnuclear structure within the nucleus.

It is also noteworthy that although no difference in CAPN distribution was observed among the cell lines from distinct breast cancer subtypes; cells apparently expressed different CAPN levels depending on the breast cancer subtype. According to the fluorescence intensity on Figure 19, luminal MCF-7 and BT-474 cell lines had higher levels of CAPN1 than triple-negative MDA-MB-231 and MDA-MB-468 cells. In contrast, CAPN2 was highly expressed in TNBC cells and weakly expressed in luminal cell lines. Nevertheless, a quantitative analysis would be needed to precisely determine those differences.

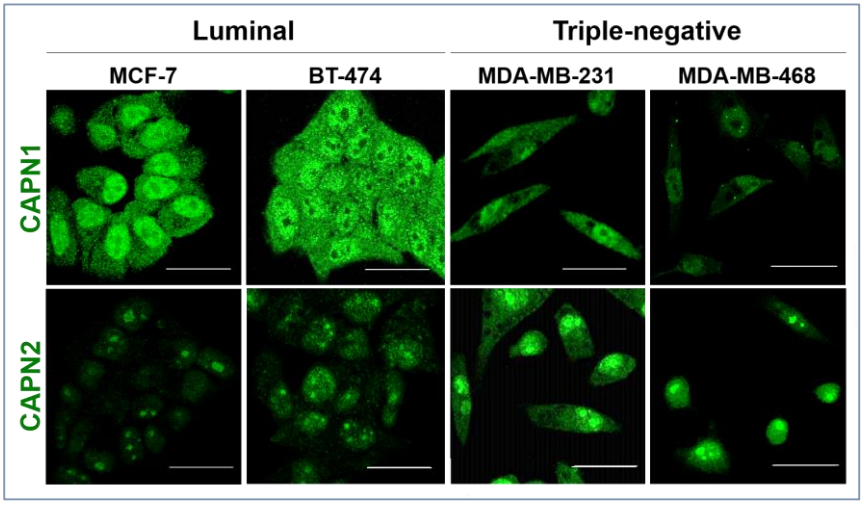

Figure 19: Subcellular distribution of CAPN1 and CAPN2 in breast cancer cell lines. *Immunostaining of CAPN1 (upper panels) and CAPN2 (lower panels) in MCF-7, BT-474, MDA-MB-231, and MDA-MB-468 breast cancer cell lines. Scale bars, 21µm. Representative images are shown (n ≥ 3).*

Once clarified the distribution of ubiquitous CAPNs, other regulatory components of the CAPN system were also studied. Subcellular location of the small regulatory subunit (CAPNS1) and calpastatin (CAST) was analysed by IF (Figure 20). CAPNS1 was diffusely distributed in the nuclei and cytoplasm of the four cell lines, although in TNBC it seemed to be more abundant within the nuclei. Regarding CAST, it was preferentially concentrated inside the nuclear compartment of TNBC and MCF-7 luminal cell lines. Surprisingly, in BT-474 cell line CAST was barely detected, and was only observed in a specific compartment within the nucleus, which also resembled the nucleolus.

CAPNS1 staining in the cytoplasm and in the nucleus indicates that CAPNs could be regulated by this regulatory subunit in both compartments. However, CAST concentration in the nuclear compartment suggests a major

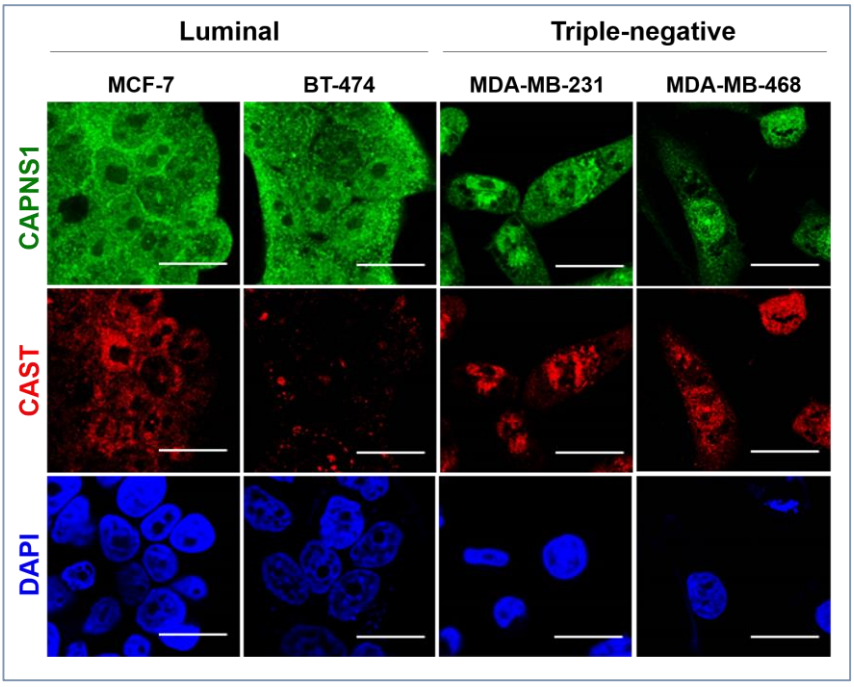

Figure 20: Subcellular localization of CAPNS1 and CAST in breast cancer cell lines. *Immunofluorescence staining of CAPNS1 (green) and CAST (red) in luminal cells (MCF-7 and BT-474) and TNBC (MDA-MB-231 and MDA-MB-468). Nuclei were stained with DAPI (blue). Scale bar 25µm. Data are (n≥3).*

inhibitory regulation of CAPN activity in the nuclear compartment than in cytoplasm and plasmatic membrane.

1.2.2 CAPN levels and activity in different breast cancer subtypes.

In the previous immunostaining studies, CAPN1 and CAPN2 levels seemed to be dependent on the breast cancer subtype. As observed in Figure 19, there is a switch on the levels of both CAPNs; CAPN1 is more abundant on luminal cells, whereas CAPN2 is increased in TNBC cell lines compared to luminal ones. To further evaluate these differences, an exhaustive analysis of CAPN expression and enzymatic activity was performed in all cell lines cultured under standard conditions. Gene expression and protein levels of CAPN1 and CAPN2 were quantitatively measured by RT-qPCR and western blot, respectively.

As shown in Figures 21, and 22, CAPN1 and CAPN2 were differentially expressed in the four cell lines according to their subtype. In agreement with immunostaining data, MCF-7 expressed the highest CAPN1 mRNA (Figure 21A) and protein levels (Figure 22A) compared to the other

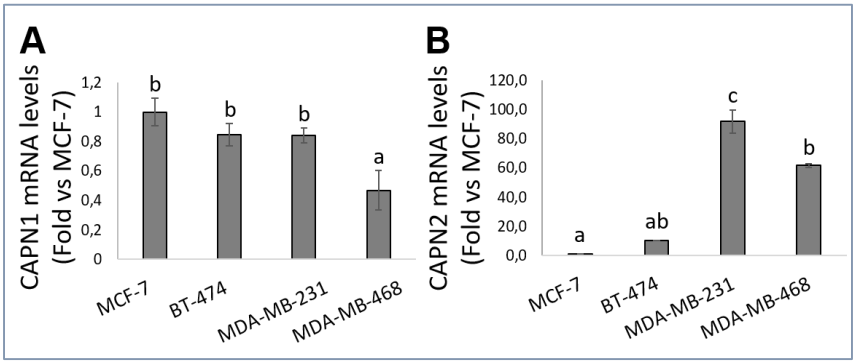

Figure 21: Isoform-specific mRNA expression in breast cancer cell lines. *(A) CAPN1 and (B) CAPN2 mRNA levels of MCF-7, BT-474, MDA-MB-231, and MDA-MB-468 cell lines were analysed by quantitative real-time PCR. Data were normalized according to 18S mRNA, analysed and quantified in the same sample reaction. Expression levels are shown as fold vs. MCF-7. Results ($n \geq 4$) are mean values ± SEM. ANOVA was performed for the statistical analysis, where different superscript letters indicate significant differences. Groups that do not share a letter are significantly different, $p \leq 0.05$. The letter 'a' always represents the lowest value within the group.*

cell lines studied. On the other hand, mRNA expression and protein levels for CAPN2 were much higher in TNBC than in luminal cells (Figures 21, 22A). This switch between both isoforms is clearly observed in Figure 22A; as CAPN1 levels decreased, CAPN2 increased. Consequently, CAPN1/CAPN2 ratio was dramatically higher in luminal than in TNBC cells (Figure 22B).

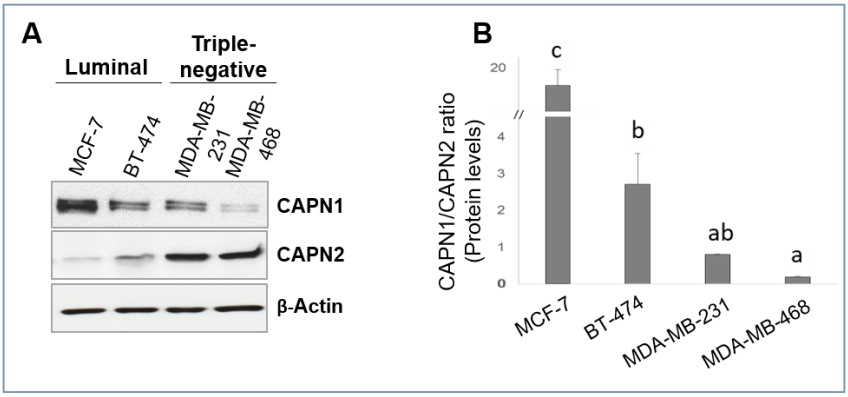

Figure 22: CAPNs protein levels in breast cancer cell lines. *(A) CAPN1 and CAPN2 total protein levels from breast cancer cell lines were analysed by western blot. β-Actin was used as loading control. (B) Expression of CAPN1 and CAPN2 was quantified and plotted as CAPN1/CAPN2 ratio. Data are represented as mean values ± SEM (n ≥ 3). ANOVA was performed for the statistical analysis, where different superscript letters indicate significant differences. Groups that do not share a letter are significantly different, p ≤ 0.05. The letter 'a' always represents the lowest value within the group.*

Regulation of the CAPN system is quite complex and several factors may influence CAPN activity. Therefore, higher levels of CAPN expression do not necessarily correlate with higher enzymatic activity. In order to elucidate CAPN activity within these cell lines, an enzymatic assay that measures the cleavage of a fluorogenic CAPN substrate was used. The results obtained are shown on Figure 23A. The proteolytic cleavage of the fluorogenic substrate was higher in luminal than in TNBC cell lines, being MDA-MB-468 the cell line with the lowest CAPN activity.

Different well-known mechanisms may regulate CAPN activation. Autolysis of CAPN1 anchor helix or dissociation from CAPNS1 are thought to overcome Ca^{2+} requirements and thus facilitate CAPN activation[58,59].

Conversely, binding of the endogenous enzymatic inhibitor (CAST) to CAPNs would limit their over-activation[20,43,62]. In order to explore the mechanisms that might be differentially controlling CAPN activation in each breast cancer cell line, the afore-mentioned molecular events were analysed by western blot (Figure 23B). In brief, the different approaches were:

(i) Autolysis of the CAPN1 anchor helix. Autolysis was determined with an antibody that recognized specifically the amino-terminal (-Nt) region of CAPN1. As seen in Figure 23B, the absence of CAPN1 amino-terminal domain in western blot analysis, indicates a complete autolysis of CAPN1 anchor helix in luminal cells.

(ii) Cleavage and dissociation of the small regulatory subunit CAPNS1. CAPNS1 protein levels were unprocessed and equally abundant in all cell lines tested, so it was excluded as a determinant in the differences of CAPN activity observed among cell lines.

(iii) CAST levels. CAST protein levels resulted to be significantly higher in TNBC cells than in luminal cells, which could be related to the lower CAPN activity determined in TNBC cell lines. Moreover, CAST was not even detected in BT-474 cell line. This result was already observed by IF; indeed,

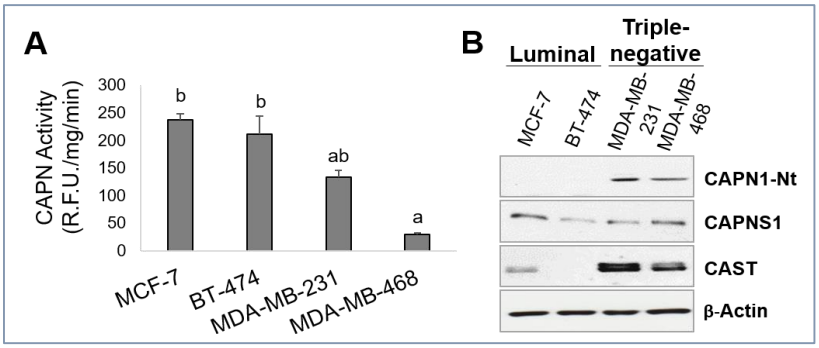

Figure 23: CAPN enzymatic activity and molecular activation mechanisms in breast cancer cell lines. *(A) CAPN activity was measured by a fluorogenic assay where Suc-LLY-AFC was used as CAPN substrate. Results shown are mean values ± SEM (n=3). ANOVA was performed for the statistical analysis, where different superscript letters indicate significant differences. Groups that do not share a letter are significantly different, p≤0.05. The letter 'a' always represents the lowest value within the group. (B) CAPN1 (N-terminal), CAPNS1, and CAST total protein levels from breast cancer cell lines were analysed by western blot. β-actin was used as loading control.*

confocal studies had showed that BT-474 cells showed the lowest CAST levels and it seemed to be restricted to the nuclear compartment (Figure 20). Most likely, CAST is confined within the nuclei or nucleoli and its levels are so low compared to the other cellular subtypes that it remains undetectable in western blots from total cell extracts.

Therefore, the N-terminal cleavage of CAPN1 in luminal cells plus the increased CAST levels in TNBC cells could explain the higher CAPN activity measured in luminal cell lines compared to TNBC cells.

1.2.3 Cleavage of adhesion proteins according to breast cancer subtype.

In order to establish a putative correlation between a specific CAPN isoform and the proteolytic processing of adhesion proteins in breast cancer cells, cleavage of adherens (E-cadherin, β-catenin, and δ-catenin (p-120)) and focal adhesion proteins (talin-1) was analysed by western blot in total extracts from all the different breast cancer cell lines under study.

Luminal cells form epithelia and are characterized for sowing cell-cell, together with cell-basement membrane interactions. All these cellular junctions have to disappear for a cancer cell to migrate and invade neighbour tissues. Both, adherens junctions and focal adhesion proteins were cleaved in luminal cells, in agreement with their metastatic potential. Nevertheless, as it has already been described, TNBC (MDA-MB-231 and MDA-MB-468 cells) do not establish adherens junctions between neighbours cells[260,273,278], and consequently, in TNBC cell lines only talin-1 was cleaved (Figure 24).

Adhesion protein levels were also verified by IF analysis. As can be seen in Figure 25, MCF-7 and BT-474 showed high levels of adherens proteins E-cadherin and β-catenin. As expected, this fluorescent signal was localized along the plasma membrane, defining the cellular limit and cell-cell junctions. In contrast, in TNBC cell lines MDA-MB-231 and MDA-MB-468, no signal was discernible for E-cadherin and only β-catenin was detected by IF. However, its location was not in the cell-cell junction as in luminal cells, but in the nucleus instead.

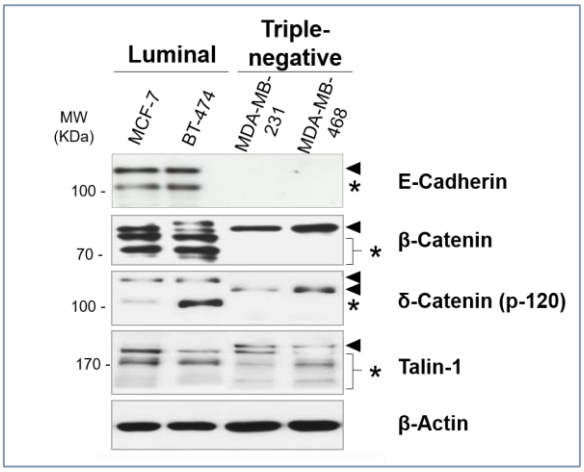

Figure 24: Cleavage of adhesion proteins in breast cancer cell lines. *Western blots show cleavage of different adhesion proteins in luminal (MCF-7 and BT-474) and TNBC (MDA-MD-231 and MDA-MD-468) breast cancer cell lines. β-Actin was used as loading control. Protein cleavage was analysed by either detection of truncated fragments (asterisks) or disappearance of full proteins (arrow heads). Representative immunoblots are shown (n ≥ 3).*

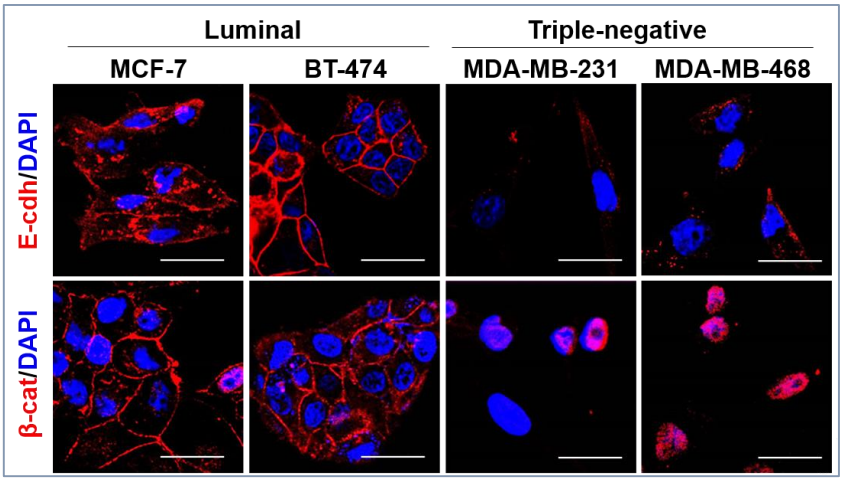

Figure 25: Confocal images of adhesion proteins in breast cancer cell lines. *Adherens junction proteins, E-cadherin and β-catenin (red) were analysed by immunofluorescence staining in luminal (MCF-7 and BT-474) and TNBC (MDA-MD-231 and MDA-MD-468) breast cancer cell lines. Nuclei were stained with DAPI (blue). Scale bars, 25μm. Representative images are shown (n ≥ 3).*

1.2.4 Isoform-specific role of CAPNs in the cleavage of adhesion proteins.

To discern the role of each CAPN isoform on the cleavage of cellular junctions in breast cancer cells, CAPN1 or CAPN2 were knocked down in the four cell lines by transient esiRNA transfections. First of all, the efficiency of the gene silencing was examined measuring CAPN1 and CAPN2 mRNA levels by RT-qPCR. As can be observed in Figures 26 and 27, mRNA levels of the silenced CAPN decreased about 80-90%, demonstrating that high efficiency was achieved in the transfection procedure. Specificity was also tested and no cross reaction between CAPN1 and CAPN2 was detected; each esiRNA only knocked down its specific isoform. Moreover, it is important to point out that there was no compensation between both isoforms as consequence of the gene silencing.

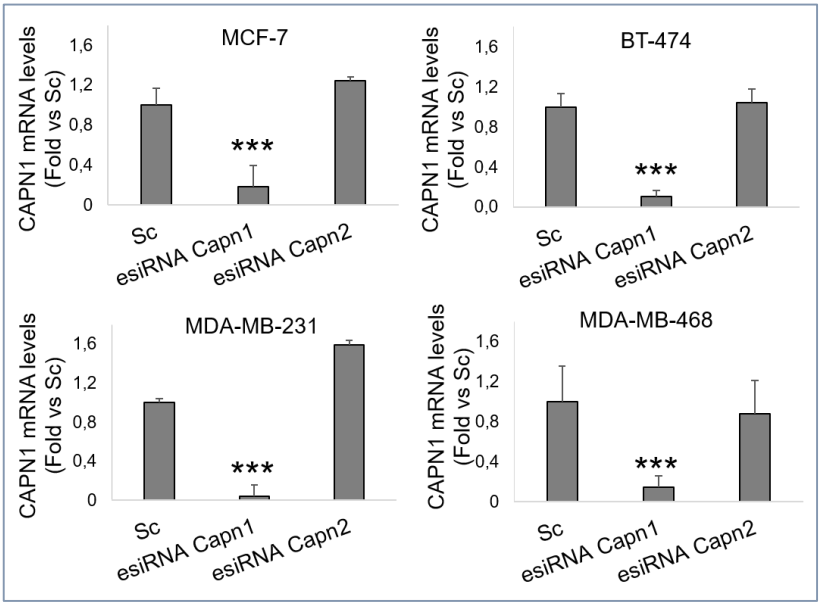

Figure 26: CAPN1 gene expression in knocked-down breast cancer cell lines. *CAPN1 mRNA levels were measured by RT-qPCR in MCF-7, BT-474, MDA-MB-231 and MDA-MB-468 breast cancer cell lines at 72 h after transfection with either Scramble control (Sc), CAPN1 or CAPN2 esiRNA. Data were normalized according to 18S mRNA in the same sample reaction. Data (n≥4) are mean values ±SEM, Student's t-test was performed for the statistical analysis ***p≤0.001 vs Sc.*

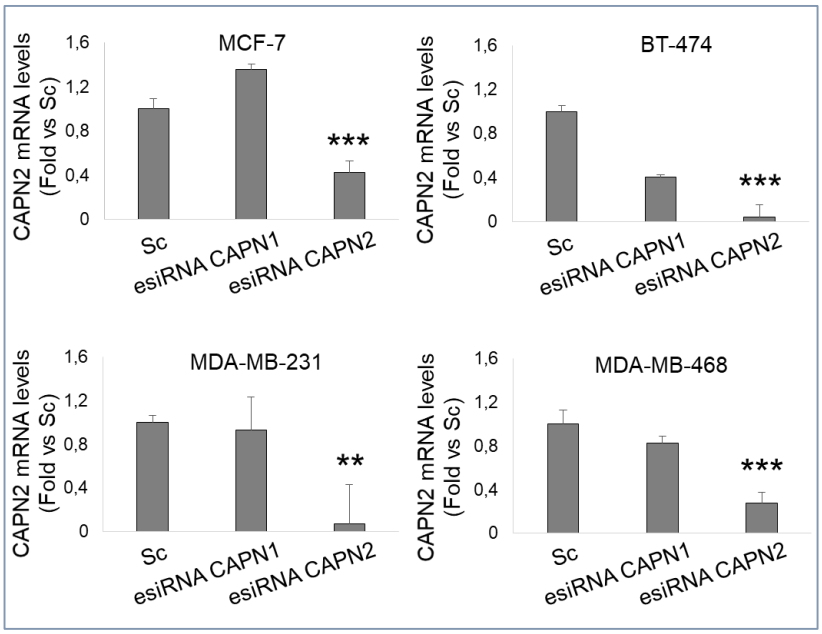

Figure 27: CAPN2 gene expression in knocked-down breast cancer cell lines. *CAPN2 mRNA levels were measured by RT-qPCR in MCF-7, BT-474, MDA-MB-231, MDA-MB-468 breast cancer cell lines after 72 h of transfection with either scramble control (Sc), CAPN1 or CAPN2 esiRNA. Data were normalized according to 18S mRNA in the same sample reaction. Data (n≥4) are mean values ±SEM, Student's t-test was performed for the statistical analysis **p≤0.01, ***p≤0.001 vs Scramble control.*

Once transfection efficiency was confirmed, the cleavage of adhesion proteins was studied by western blot in these cell lines transfected with either CAPN1 or CAPN2 esiRNA (Figure 28). In CAPN1-knockdown luminal cells the cleavage of both, focal and adherens proteins, was prevented as can be seen in Figure 28A where no truncated form is detected for E-cadherin, β-catenin and δ-catenin or talin-1. In a similar manner, in TNBC cells (MDA-MB-231 and MDA-MB-468), cleavage of focal adhesion protein talin-1 was also prevented after silencing CAPN1 expression (Figure 28B).

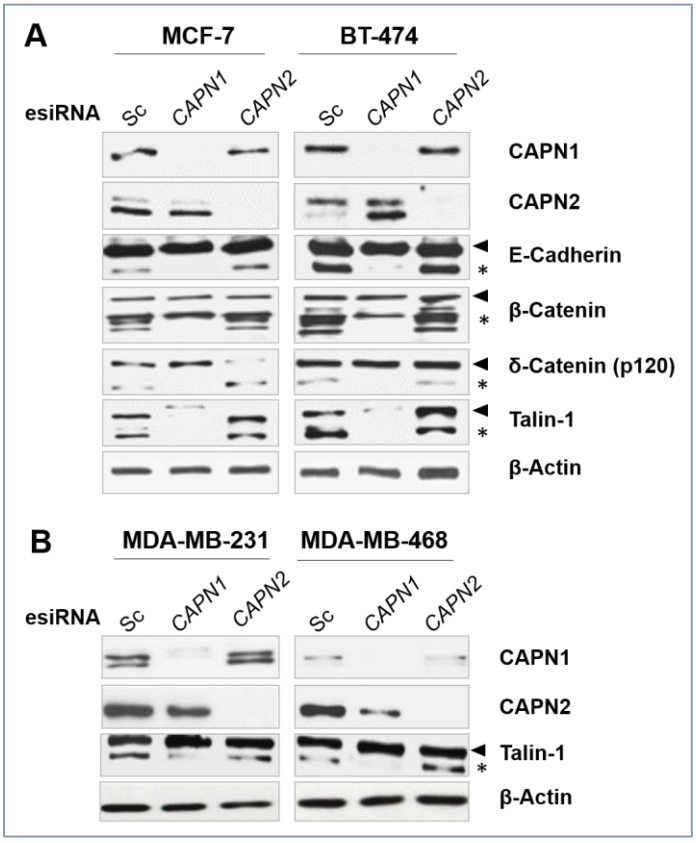

Figure 28: Study of CAPN1 and CAPN2 involvement in adhesion proteins cleavage. *(A) Luminal or (B) TNBC cell lines were transfected with Scramble control siRNA (Sc), CAPN1 or CAPN2 esiRNAs, and cleavage of E-cadherin, β-catenin, δ-catenin (p-120), and talin-1 was analysed by western blot at 72 h after transfection (n≥3). CAPN1 and CAPN2 protein levels were also analysed to confirm the efficiency of knockdown experiments. Protein cleavage was assessed by either detection of truncated fragments (asterisks) or disappearance of full length proteins (arrow heads). β-Actin levels were used as loading control.*

Surprisingly, CAPN2 knockdown showed no apparent effect on adhesion proteins proteolysis, neither in luminal nor in TNBC cell lines. These results suggest that, independently of the tumour subtype, CAPN1 is the preferential isoform involved in the regulation of cell adhesion in breast cancer cell lines.

After unveiling that CAPN1 was the isoform responsible for the cleavage of adhesion proteins, IF analysis was performed to verify that the proteolysis was a direct consequence of CAPN1 interaction with its target proteins. MCF-7 and MDA-MB-231 were selected as representative cell lines from luminal and TNBC tumours subtypes.

E-Cadherin was selected to analyse CAPN1 interaction with adhesion proteins in MCF7. Interestingly, CAPN1 and E-cadherin co-localized not only at the cellular membrane, but also in the cytosol (arrowheads in Figure 29A). Since co-localization does not necessarily mean a physical interaction between two proteins, direct interaction between CAPN1 and E-cadherin was further studied by PLA assay. As shown (Figure 29B) a direct interaction between both proteins was also detected by PLA. Furthermore, the cytosolic interaction between CAPN1/E-cadherin resembled what was previously

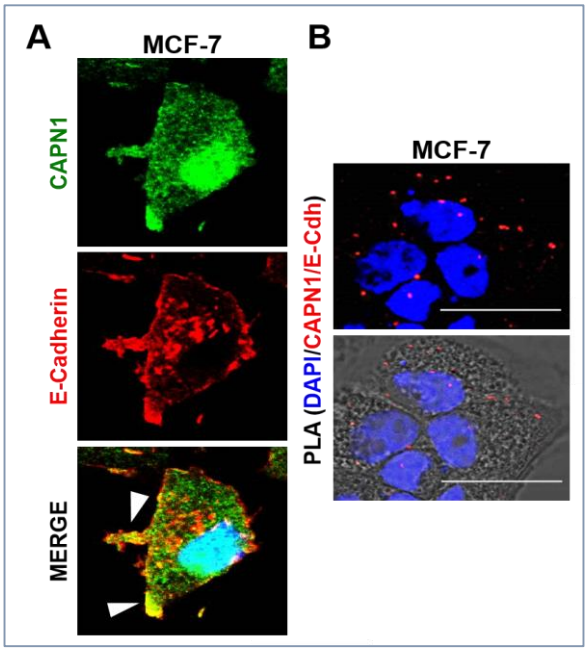

Figure 29: CAPN1/E-cadherin interaction in MCF-7 breast cancer cell line. *(A) Double immunofluorescence of CAPN1 (green) and E-cadherin (red) in MCF-7 cells. Nuclei, stained with DAPI (blue), are shown in merge image. (B) PLA analysis to study the interaction between CAPN1 and E-cadherin in MCF-7, resulting in red spots signals. Scale bars, 25µm. Representative images are shown ($n \geq 3$).*

observed in involuting mammary gland sections, which might suggest that CAPN1 remains bound to the cleaved E-cadherin products within the cytosolic compartment.

On the other hand, talin-1, was chosen as the most representative target to analyse CAPN1 interaction with adhesion proteins in MDA-MB-231 cells. Interestingly, as observed in MCF-7 cells (Figure 29) co-localization between CAPN1 and talin-1 was also detected by both, IF (Figure 30A) and PLA (Figure 30B) analysis in the plasmatic membrane and cytoplasm of MDA-MB-231 cells. Strikingly, talin-1 shows cytoplasmic distribution. It has been described that most of talin-1 is thought to accumulate in the cytosol, translocating to the plasma membrane and binding to integrins after activation[327–329]. From these results one could infer that CAPN1 proteolyzes talin-1 and remains bound to it in the cytoplasm, affecting its function in focal adhesion and, thus cellular adhesion.

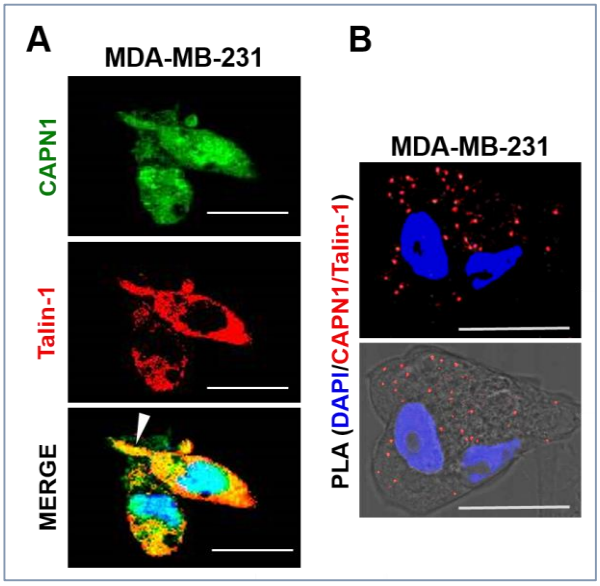

Figure 30: CAPN1/talin-1 interaction in MDA-MB-231 breast cancer cell line. *(A) Double immunofluorescence of CAPN1 (green) and talin-1 (red) in MDA-MB-231 cell line. Nuclei were stained with DAPI (blue) and are shown in merge image. Scale bars, 25µm. Representative images are shown (n ≥ 3). (B) PLA analysis to study interaction of CAPN1 and talin-1 in MDA-MB-231, resulting in red spots signals. Scale bars, 25µm. Representative images are shown (n ≥ 3).*

1.2.5 Functional role of specific CAPNs in breast tumour cells.

Correlation of each CAPN isoform activity with cell migration was studied by two different approaches: wound-healing and Transwell assays. MCF-7 and MDA-MB-231 were chosen as representative of both subtypes of breast tumours. Both cell lines were transfected with either CAPN1 or CAPN2 esiRNA for wound healing assays. The experiment was carried out in serum-starving conditions to ensure cell proliferation did not affect the result.

Wound-healing assays demonstrated that CAPN1 down-regulation decreased migration in both, MCF-7 (Figure 31A) and MDA-MB-231 (Figure 31B) cells by 50% compared with not silenced (Scramble) cells. Conversely, in agreement with previous results in which CAPN2 was not involved in

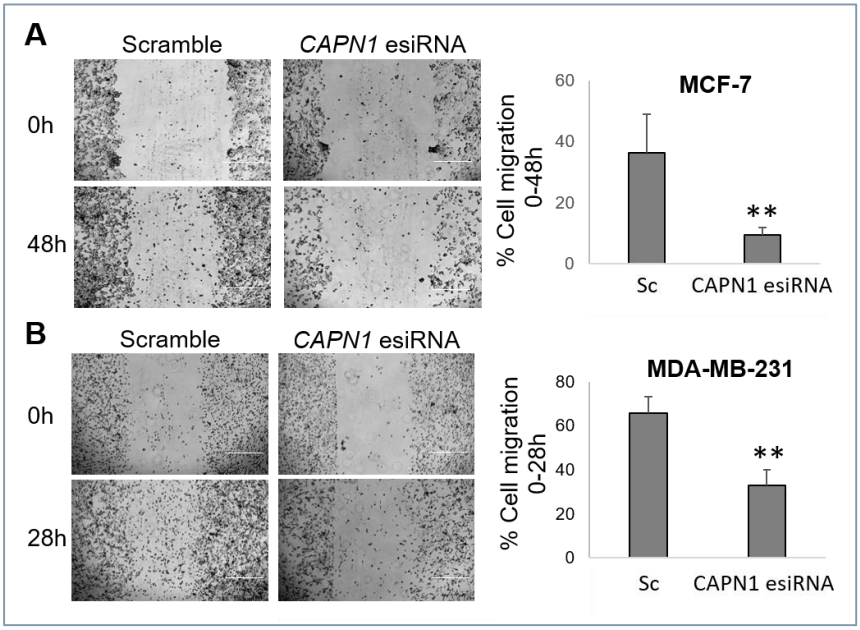

Figure 31. Functional role of CAPN1 on cell migration in breast cancer cell lines. *(A) Cell migration in MCF-7 and (B) MDA-MB-231CAPN1-knockdown cells was analysed by wound-healing assay. Graphs show the percentage of cells that migrated to the wounded area after 48 h (MCF-7) or 28h (MDA-MB-231). Data (n ≥ 3) are represented as mean values ± SEM. Student's t-test was performed for the statistical analysis, **p≤0.01 vs. scramble control (Sc). Scale bar, 500 µm.*

adhesion proteins cleavage (Figure 28), cell migration was not affected by CAPN2 knockdown in any cell type (Figure 32).

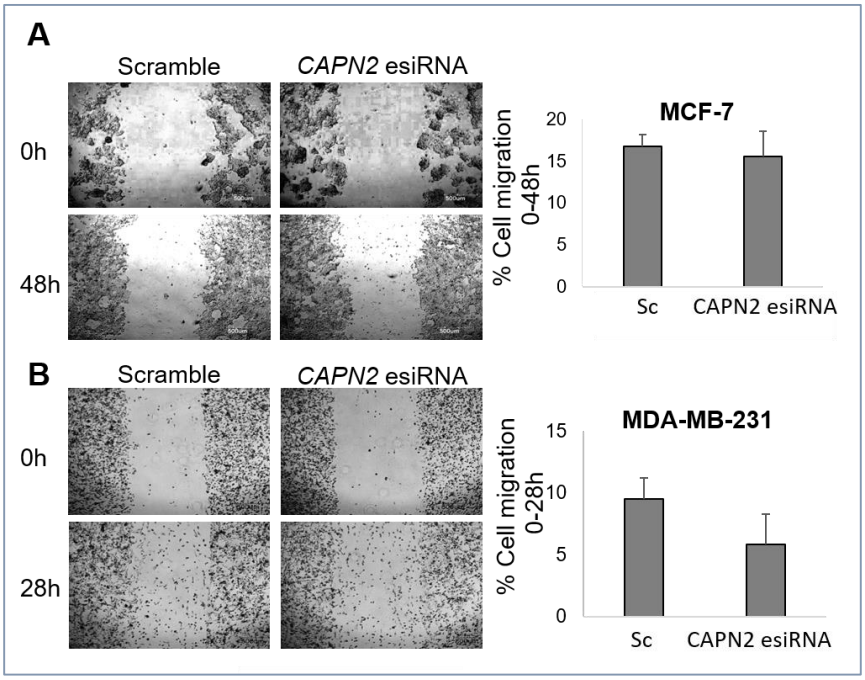

Figure 32. Functional role of CAPN2 on cell migration in breast cancer cell lines *(A) Cell migration in MCF-7 and (B) MDA-MB-231 CAPN2-knockdown cells was analysed by wound healing assay. Data (n ≥ 3) are represented as mean values ± SEM. No significant differences were found after Student's t-test analysis vs scramble controls (Sc). Scale bar, 500 µm.*

To further evaluate CAPN1 involvement in cell migration, the ability of cells to migrate through a polycarbonated membrane was evaluated by Transwell assay in control (scramble) and CAPN1-knockdown MCF-7 and MDA-MB-231 cells. As can be observed in Figure 33, CAPN1 silenced cells showed decreased migration compared to non-silenced cells. Hence, wound-healing and Transwell migration assays further confirmed that CAPN1 favours migration of breast tumour cells.

On the whole, these evidences point to CAPN1 as the major isoform involved in cell migration in breast cancer cell lines independently of the breast tumour subtype. It is important to highlight that the results presented herein show that CAPN1 and CAPN2 although ubiquous do not have

redundant roles and that their functions seem to be dependent not only on the cell type but also on the cellular conditions. In this sense, we have demonstrated a molecular switch of both CAPNs in physiological/pathological conditions. CAPN2 was the isoform responsible for cleaving adhesion proteins in a physiological model of mammary gland involution, which in turn rendered the cell more sensitive to cell death programmes. Nevertheless, in a pathological model of breast cancer it was CAPN1 the isoform essential for cellular adhesion disruption, although the final fate of these cells is nor death but migration and invasion.

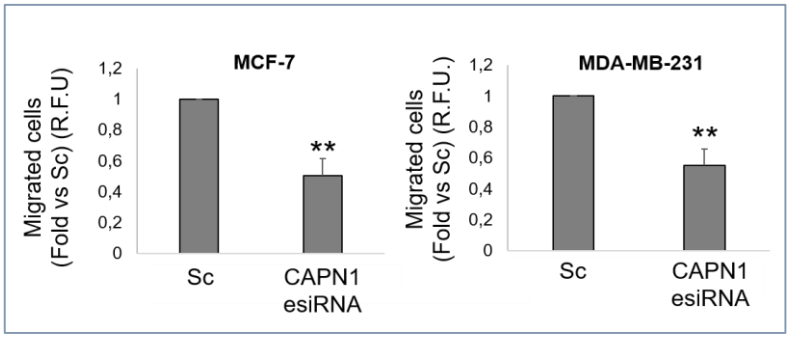

Figure 33. Functional role of CAPN1 on cell invasion in breast cancer cell lines. *(A) Cell migration was analysed by Transwell assays in control (Sc) and CAPN1 knocked-down MCF-7 and MDA-MB-231 cells. Cells migrating through the membrane were measured by fluorescence using the CyQUANT® GR Dye and plotted as fold vs Scramble controls (Sc). Data (n≥3) are represented as mean values ± SEM. Student's t-test was performed for the statistical analysis, **p≤0.01* vs. Sc.

2. ISOFORM-SPECIFIC ROLE OF CALPAINS IN NUCLEI

During the second phase of mammary gland involution, tissue remodelling occurs along with adipocyte differentiation[298]. As previously mentioned, in murine mammary gland involution CAPN1 was also found to be localized within the nucleus of adipocytes that were repopulating the fat pad during the second phase of involution. Nuclear CAPN1 was suggested to be involved in the cleavage of Nt-histone H3 tails in adipocytes. Furthermore, CAPN1 was bound to leptin and CCAAT/enhancer-binding protein alpha (C/EBP-α) promoters[88], which suggest that CAPN1 might be favouring the activation of adipogenic genes during adipocyte redifferentiation[330,331]. CAPNs are already known to be involved in this process[108,157,332]. However, the specific function of each isoform during the time course of adipocyte differentiation is still unclear.

Adipocyte differentiation is a complex process that occurs in sequential stages (Figure 34). After growth arrest at confluence, 3T3-L1 pre-adipocytes differentiation can be induced by adipogenic inducers: 1-isobutyl 3-metylxanthine, dexamethasone, insulin, rosiglitazone (MDIR). After induction of differentiation, cells undergo at least one round of replication between days 0 and 2 in a phase known as mitotic clonal expansion (MCE). By day 2-3 of differentiation, cells complete the postconfluent mitosis and enter into G_0 growth arrest[333]. During early differentiation (ED) at 2-4 days after MDIR-induction pre-adipocytes begin to adquire characteristics of mature adipocytes, which will be completed at the end of terminal differentiation (TD) by day 7-9[334,335]. These phases require the sequential and coordinated expression of different transcription factors from the family of CCAAT/enhancer binding protein (C/EBP) and peroxisome proliferator-activated receptor (PPAR), which control the induction and silencing of more than 2000 genes involved in adipocyte morphological and physiological regulation[336,337].

3T3-L1 has been used as a standardized and well established adipocyte differentiation model. In order to gain a better knowledge of the role of CAPNs in nuclei from adipocytes, murine 3T3-L1 fibroblast were used in these studies.

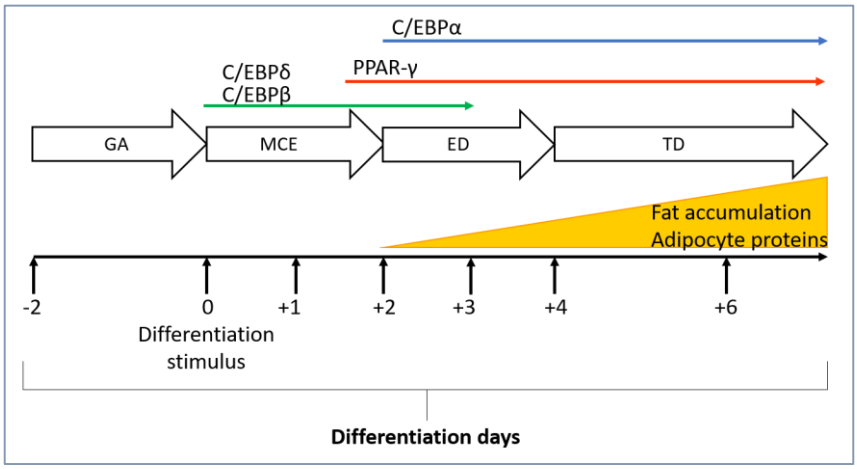

Figure 34: Representative scheme of 3T3-L1 differentiation phases. *After the stimulation of growth arrested (GA) 3T3-L1 fibroblasts with adipogenic inducers (MDIR), cells enter into mitosis in a phase known as mitotic clonal expansion phase (MCE). Then, cells go through the early differentiation (ED) phase, during which cells acquire adipocyte characteristics, completing their differentiation at the terminal differentiation (TD) phase. This complex process is controlled by the sequential expression of different transcription factors (C/EBP-β, C/EBP-δ, C/EBP-α and PPAR-γ).*

2.1 CHARACTERIZATION OF 3T3-L1 DIFFERENTIATION MODEL

Cultured 3T3-L1 cells are a well known model to study the sequential steps of adipocyte differentiation. Nevertheless, there is a high variability of data among laboratories using this model. This variability is believed to be caused by culture methods and, most importantly, the time point chosen for the induction of differentiation. Mitotic clonal expansion of growth-arrested pre-adipocytes appears to be necessary for optimal differentiation. Thus exposure of subconfluent proliferating pre-adipocytes to differentiation inducers results in poor differentiation or changes in the time frame for the molecular events leading to differentiation[338]. Consequently, a previous characterization of the model seems to be a prerequisite to accurately stablish the time-pattern of CAPNs expression and function along adipocyte differentiation.

Pre-adipocytes were cultured under stimulating conditions to differentiate into adipocytes (see material and methods section for more

details). The effective differentiation of 3T3-L1 cells was evaluated by phase contrast microscopy. Images were taken at confluent growth arrested pre-adipocytes (GA), at initial stages of early differentiation (ED) and terminal differentiation (TD) of MDIR-induced pre-adipocytes. Figure 35 (upper panels) shows a progressive morphological change from a spindle-fibroblastic shape in pre-adipocytes (GA) to a spherical shape of mature adipocytes (TD). Furthermore, along the differentiation course, cell lipid content increased, as can be observed by the accumulation of lipid droplets in the cytosolic compartment. Perilipin-1, a protein that encloses the lipid droplets and is essential for lipids mobilization[339], is a well-established marker of adipocyte differentiation. Indeed, perilipin-1 is a PPARγ-target known to be induced at ED. Therefore, changes in lipid content and differentiation were more specifically evaluated by perilipin-1 immunostaining. As observed in Figure 35 (lower panels), lipid accumulation began at initial stages of ED and greatly increased at TD, when adipocytes completed their terminal differentiation, demonstrating that an effective differentiation was being achieved.

Although perilipin-1 can be detected by IF staining at ED this initial lipid accumulation is the result of a previous increase of adipogenic genes. The mRNA levels of perilipin-1 and leptin, another PPARγ-target gene, were

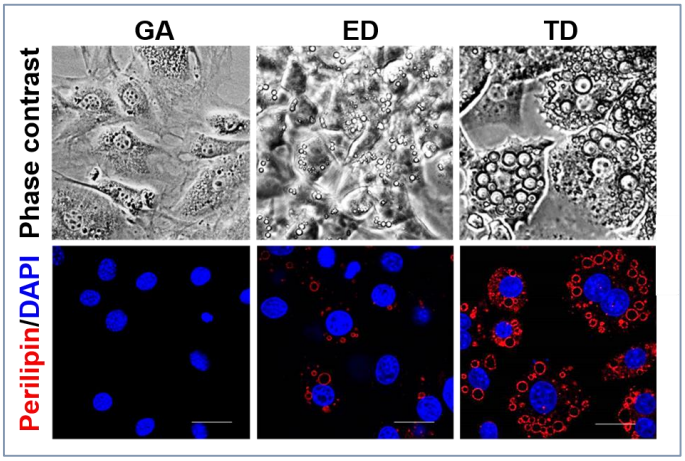

Figure 35: 3T3-L1 differentiation efficiency. *Phase contrast (upper panels) and perilipin-1 immunofluorescent staining (lower panels) of 3T3-L1 cells at growth arrest (GA), early differentiation (ED) and terminal differentiation (TD). Nuclei were stained with DAPI (blue). Scale bars, 21 µm. Representative images are shown (n ≥ 3).*

analysed by RT-qPCR to characterize the earlier events leading to the fat accumulation during differentiation of 3T3-L1. Differentiation of confluent 3T3-L1 pre-adipocytes was induced and total RNA extracted every day post-induction until TD. As can be observed in Figure 36, the expression of both adipogenic genes was triggered during transition from MCE to ED and their mRNA levels dramatically increased along the differentiation course.

Perilipin-1 protein levels are known to be accumulated at ED and along the differentiation course[340]. Total protein extracts from 3T3-L1 were obtained every day post-induction until TD to analyse perilipin-1 protein levels by western blot. As loading control, β-actin, GAPDH and α-tubulin were evaluated. However, these housekeeping proteins were also subjected to changes during differentiation. Therefore, protein levels were normalized by

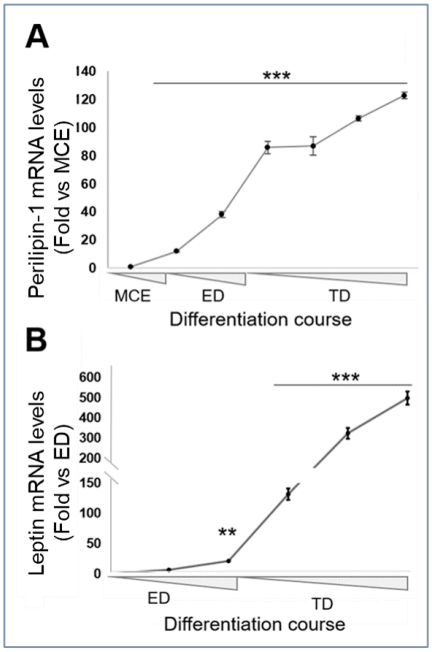

Figure 36: Adipogenic genes mRNA expression along 3T3-L1 differentiation time course. *(A) Perilipin-1 and (B) leptin mRNA levels were analysed by RT-qPCR along 3T3-L1 differentiation. Data were normalized by 18S, quantified and plotted as fold vs. MCE for (A) and initial stages of ED for (B), phases in which each gene was firstly detected, respectively. Results (n ≥ 3) are mean values ± SEM. ** p≤0.01 y ***p≤0.001. (MCE) mitotic clonal expansion, (ED) early differentiation and (TD) terminal differentiation.*

membrane-Ponceau staining. As expected, although perilipin-1 was completely absent in fibroblasts, it gradually increased from MCE until TD (Figure 37).

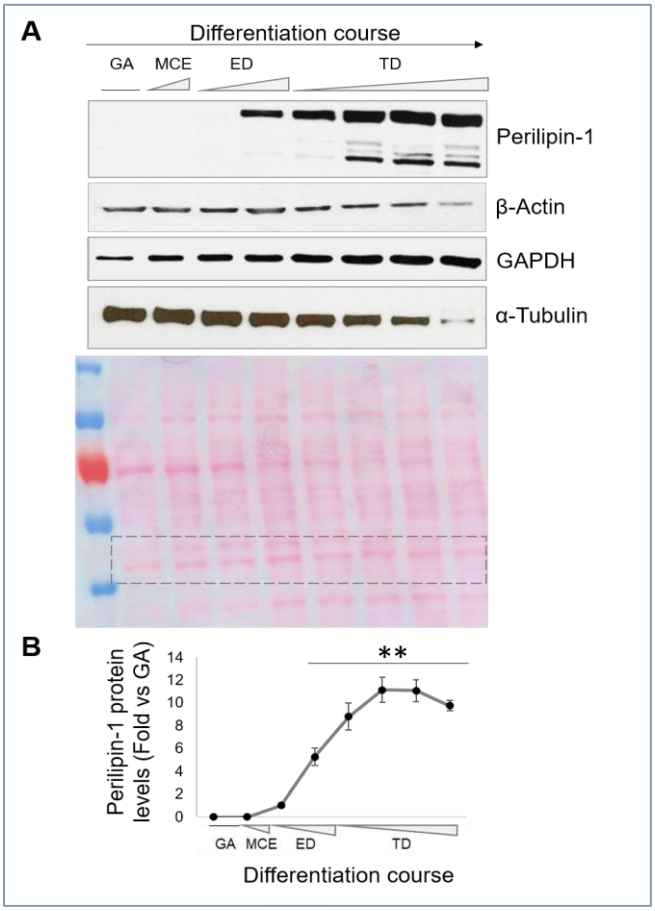

Figure 37: Changes in perilipin-1 protein levels along 3T3-L1 differentiation course. *Differentiating 3T3-L1 total protein extracts were obtained from GA to day 7 of TD. (A) Perilipin-1 protein levels were analysed by western blot. Total protein levels of β-actin, GAPDH and α-tubulin revealed that their levels also changed along differentiation, excluding them as loading controls. Ponceau staining of the membrane to ensure correct loading. (B) Perilipin-1 protein levels were quantified and normalized according to Ponceau staining (dotted rectangle), and are represented as fold vs. day 0. Results ($n \geq 3$) are mean values ± SEM. Student's t-test was performed for the statistical analysis, $**p \leq 0.01$ vs. GA.*

2.2 ROLE OF CALPAINS DURING 3T3-L1 DIFFERENTIATION TIME-COURSE

As described in the introduction section, the pleiotropic CAPN system is exposed to multiple mechanisms of regulation, including modulation of abundance, activity, location and specificity. It has been shown that this variety of mechanisms can be fine-tuned to fit the functional context of different cell types. Once 3T3-L1 differentiation model was established and characterized, CAPN1 and CAPN2 levels, as well as their activity and molecular mechanism involved in their specific activation, were evaluated along the differentiation course.

2.2.1 Phase-dependent abundance of CAPNs during induced pre-adipocyte differentiation.

To determine whether a specific phase of pre-adipocyte differentiation could be controlled by CAPN abundance, total protein extracts from confluent 3T3-L1 cells or at MCE, ED and TD after MDIR-induction were analysed by western blot. As shown in Figure 38 both, CAPN1 and CAPN2 total protein levels progressively increased along the time-course of

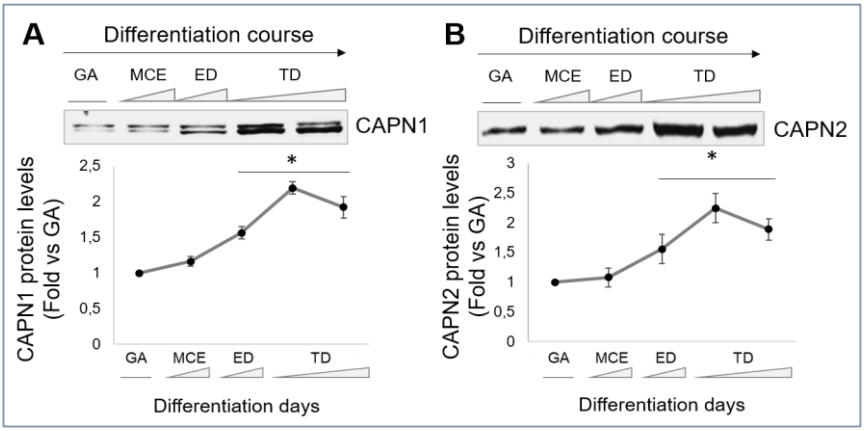

Figure 38: Analysis of CAPN1 and CAPN2 protein levels along 3T3-L1 differentiation course. *CAPN1 (A) and CAPN2 (B) analysed by western blot in total protein extracts from pre-adipocytes (GA) or MDIR-induced 3T3-L1 cells at MCE, ED and TD. Protein levels, quantified and normalized according to Ponceau-staining, were plotted as fold vs. GA. Results ($n \geq 3$) are mean values ± SEM $*p \leq 0.05$ vs GA.*

differentiation. Protein levels of both isoforms reached a peak at ED and remained constant thereafter.

In the hypothetical case that a specific phase was dependent on CAPNs abundance, these data would suggest that most likely both CAPNs are modulating early and terminal differentiation. However, as previously explained, the increase in CAPN protein levels does not necessarily mean higher CAPN activity. Therefore, different molecular evidences of CAPN activity and subcellular localization should be evaluated.

2.2.2 Modulation of the differentiation program by CAPN activity.

During MCE-ED transition, the expression of C/EBP-α and PPAR-γ is induced[341,342]. These transcription factors cooperate with each other to transactivate the expression of adipogenic genes which trigger and modulate TD[333,334,336]. Remarkably, our previous results showed a concomitant increase of adipogenic genes and CAPN levels at MCE-ED transition (Figures 36 and 38). These data suggest that CAPN activity might be involved in the modulation of early key events leading to the onset of terminal differentiation. Although the specific role of each CAPN isoform in adipocyte differentiation has not been previously recognised, the unspecific cysteine protease inhibitor ALLN has been reported to prevent MDIR-induced differentiation of 3T3-L1 cells[157]. Interestingly, ALLN blocked mitotic clonal expansion when added prior to MDIR treatment, but showed no effect when early differentiation had been already triggered.

To determine the role of CAPN activity during specific phases of the 3T3-L1 differentiation program, several experimental approaches were used:

(i) Analysis of molecular mechanisms mediating CAPN activity

Total protein extracts from 3T3-L1 cells at different phases of differentiation after MDIR-treatment were analysed by western blot. CAPN1 activity was analysed as means of **cleavage of Nt-anchor helix** by western blot using an antibody recognizing Nt-CAPN1 (Figure 39). As can be observed, Nt-CAPN1 levels followed the same pattern as CAPN1 (Figure 38A). Nevertheless, the ratio Nt-CAPN1/CAPN1 shows a dramatic drop at MCE. These results showing CAPN1 autoproteolysis, might suggest an early activation of CAPN1 during 3T3-L1 differentiation.

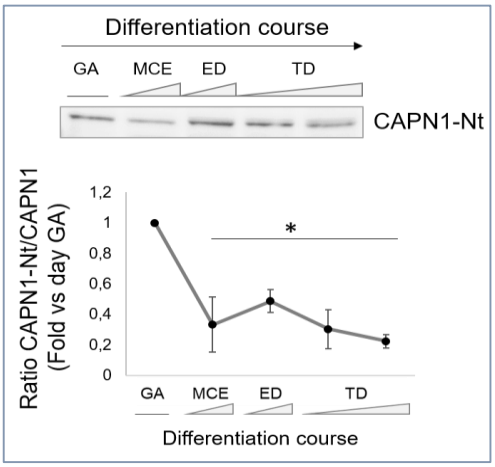

Figure 39. CAPN1 N-terminal cleavage during 3T3-L1 differentiation. *Nt-CAPN1 protein levels were analysed by western blot. Protein levels were quantified and plotted as the ratio Nt-CAPN1/CAPN1 and normalized according to Ponceau staining. Results ($n \geq 3$) are mean values ± SEM. $*p \leq 0.05$ vs GA.*

Protein levels of CAPNS1 and CAST, the regulatory elements of ubiquitous CAPNs, were also evaluated by western blot. In accordance with the upregulation observed for both catalytic subunits, CAPN1 and CAPN2, CAPNS1 levels also progressively rose during differentiation (Figure 40A). Interestingly, CAPNS1 was proteolyzed at MCE-ED transition. Cleavage and dissociation of the small regulatory subunit CAPNS1 has been considered as the result of high CAPN activity[20,62]. On the other hand, CAST, the endogenous inhibitor of both CAPN isoforms, being completely absent at initial days of differentiation (Figure 40B), also increased at MCE-ED transition. This might suggest that CAST is needed in further stages to limit an excessive CAPN activation[20,44]. These evidences suggest that not only CAPNs levels, but also CAPN activity are upregulated at the end of MCE and the onset of ED.

(ii) Specific role of CAPN activity during mitotic clonal expansion.

To determine the role of CAPN during MCE, 3T3-L1 pre-adipocytes were pre-treated with calpeptin 24 h prior MDIR-induction. ALLN was also used as a positive control of differentiation inhibition. Cells were then

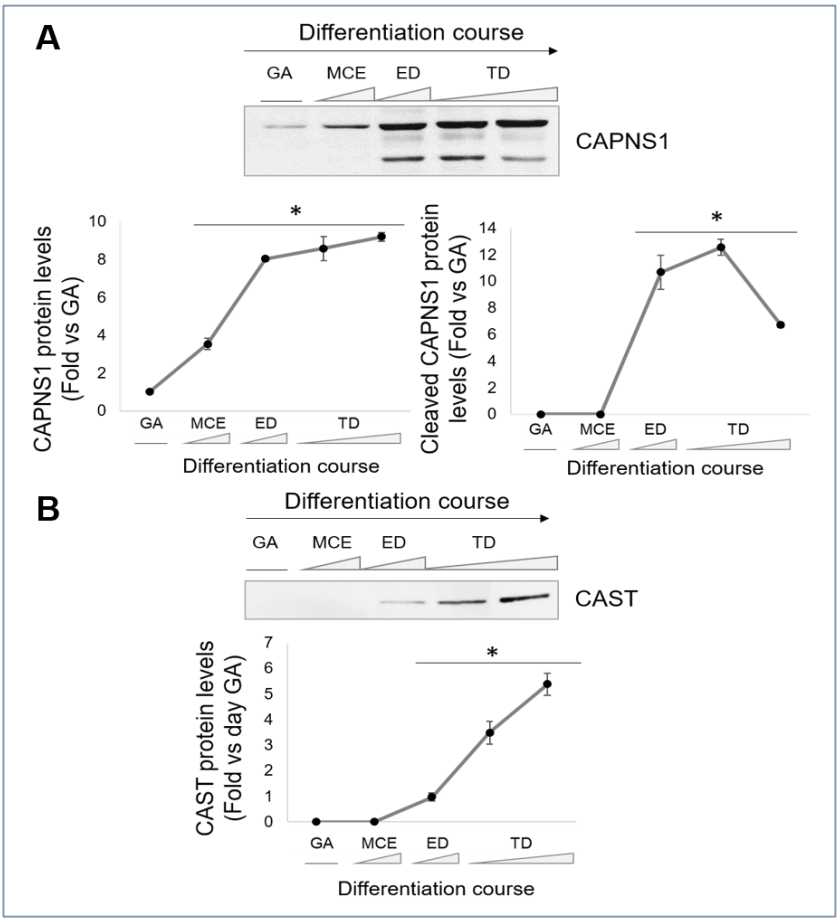

Figure 40: CAPNS1 and CAST protein levels along 3T3-L1 differentiation. *(A) CAPNS1 (left), cleaved CAPNS1 (right) and (B) CAST total protein levels from 3T3-L1 at different differentiation stages were analysed by western blot. Protein levels were quantified and normalized according to Ponceau staining. Results ($n \geq 3$) are represented as mean values ± SEM. $*p \leq 0.05$ vs GA.*

analysed by Oil Red O staining, to mark lipid droplets, and western blots at ED, when lipids and perilipin-1 accumulation begins.

As can be seen in Oil Red O stained images (Figure 41A), cell treatment with both inhibitors led to a decrease in oil droplets (red spots) compared to DMSO-treated (control) cells. It has to be taken into account that ALLN can also inhibit other cystein proteases apart from CAPNs, such as cathepsins, whose role on adipocyte differentiation has been extensively

documented[343,344]. For this reason, ALLN-treated cells revealed a complete inhibition of differentiation, maintaining the fibroblastic shape with no sign of lipid accumulation. Similarly, perilipin-1 protein levels were dramatically reduced after specific CAPN inhibition in pre-adipocytes treated with calpeptin (Figure 41B). Even more evident was the complete disappearance of perilipin-1 protein level in ALLN-treated cells, in which adipocyte differentiation was completely prevented. These results indicate that CAPN activity is involved in the modulation of early phases (MCE and ED) after MDIR-induced differentiation of 3T3-L1 cells.

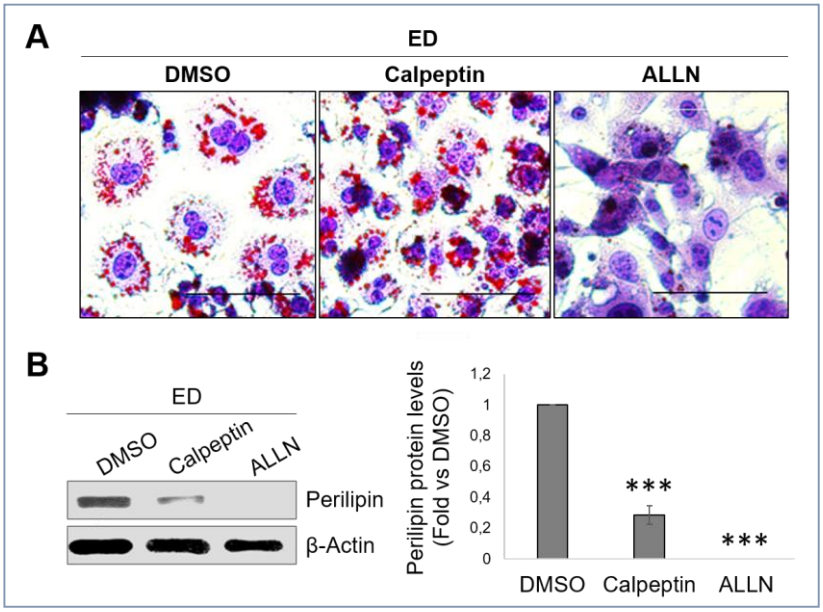

Figure 41: Involvement of CAPN activity in 3T3-L1 early differentiation. *DMSO, calpeptin and ALLN pre-treated 3T3-L1 cells at initial stages of ED. Cells were pre-treated 24 h before MDIR-induction. (A) Oil Red staining of triglycerides and lipids (in red) and cell nuclei are shown in blue, so lipid accumulation can be recognised. Representative images are shown (n ≥ 3). Scale bars, 100 µm. (B) Perilipin-1 protein levels analysed by Western blot in whole cell lysates. Protein levels were quantified and normalized according to β-actin. Protein levels are shown as fold vs. DMSO-pre-treated cells. Results (n ≥ 3) are represented as mean values ± SEM. ***p≤0.001 vs. DMSO.*

2.2.3 Functional role of nuclear CAPNs during pre-adipocyte differentiation.

Few hours after MDIR-treatment, pre-adipocytes suffer important changes in the nuclear compartment that affect adipogenic genes, such as relocation of gene positioning[345,346], interactions between adipogenic gene promoters previous to their transcription[336,347] and chromatin remodelling[348]. It is well-established that adipogenic gene promoters are marked by early changes on histone modification patterns[349,350] so that an opened chromatin structure will be accessible to transcription factors. On the other hand, histone H3 has been previously reported to be a CAPN-target[88].

(i) Histone H3 and CAPNs interaction as part of the priming events leading to adipocyte differentiation.

Changes in chromatin structure and location during MCE are thought to be part of the priming events needed to fully respond to the differentiation signals during ED. According to this fact, CAPN-mediated modification of histone H3 might have a role in these important priming events during pre-adipocyte MCE. Consequently, an early interaction between any of both ubiquitous CAPNs and histone H3-Nt tails was studied by PLA assay during pre-adipocytes differentiation. As shown in Figure 42 an interaction between histone H3/CAPN1, and to a lesser extent histone H3/CAPN2, was observed during MCE after MDIR-induction. However, quantification of PLA signals per nuclei in both experiments (Figure 42C) indicated that there were a higher number of nuclei positive for CAPN1/histone H3 interactions compared to CAPN2/H3 interactions during MCE. Interestingly, no interaction at all was detected at ED-TD transition suggesting that Nt-tails from histone H3 were already cleaved or that CAPNs did not interact with histone H3 at this time point and therefore, it was not involved in chromatin remodelling during ED-TD transition.

(ii) CAPN-mediated cleavage of histone H3-Nt tails.

The enzymes that post-translationally modify histone promoters are good candidates to regulate the local chromatin structure during pre-adipocyte differentiation[351]. Histone H3 clipping has been suggested to alter the epigenetic signature upon differentiation[352]. Therefore, histone H3-cleavage

during 3T3-L1 differentiation was examined by western blot in total protein extracts obtained at different days of differentiation.

To fulfil with this approach, an antibody directed against Ct-histone H3 was used to detect both, the non-cleaved and the cleaved histone H3 proteins (Figure 43). As can be seen in Figure 43B, concomitant with the peak of adipogenic gene expression at ED-TD transition a cleaved band of histone H3 was accumulated and detected by western blot. In order to determine whether CAPN activity was involved in this cleavage, 3T3-L1 pre-adipocytes

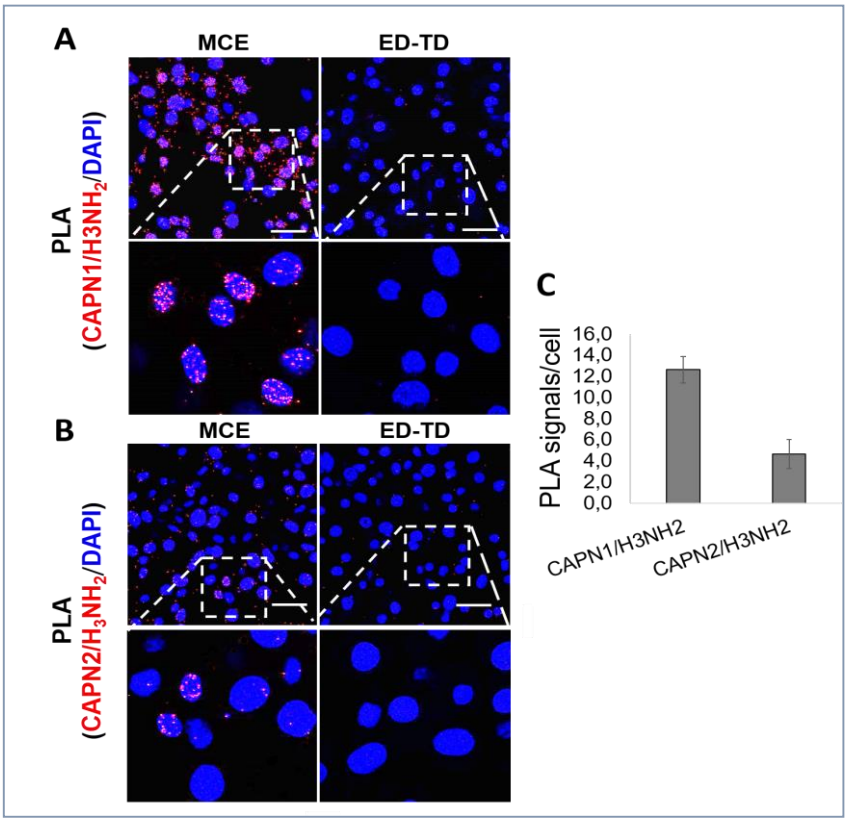

Figure 42: CAPNs interaction with the N-tail of histone H3 during 3T3-L1 differentiation. *(A) CAPN1/histone H3-NH_2 and (B) CAPN2/histone H3-NH_2 interaction was analysed by PLA in 3T3-L1 cells during MCE and ED-TD differentiation phases (red spots). Nuclei were stained with DAPI (blue). Scale bar, 21 µm. (C) Quantification with Image J software of PLA signals obtained from CAPN1/H3-NH_2 and CAPN2/H3-NH_2 interactions as the number of PLA signals/nuclei. Results ($n \geq 3$) are shown as mean values ± SEM.*

were treated with CAPN activity inhibitors (calpeptin and ALLN) prior to the induction of differentiation. Cells were collected at the beginning of TD, when the accumulation of cleaved histone H3 was enough to be detected. As observed in Figure 43C, cleavage of histone H3 was strongly and equally prevented by both CAPN inhibitors. These results explain why it wasn't detected any interaction between CAPN/Nt-histone H3 by PLA assays at ED-TD transition (Figure 42).

These data indicate that CAPNs are modulating histone H3-cleavage. Nonetheless, as seen in Figure 43B, the product of histone H3 cleavage could not be detected during MCE-ED by western blot. As mentioned, enough

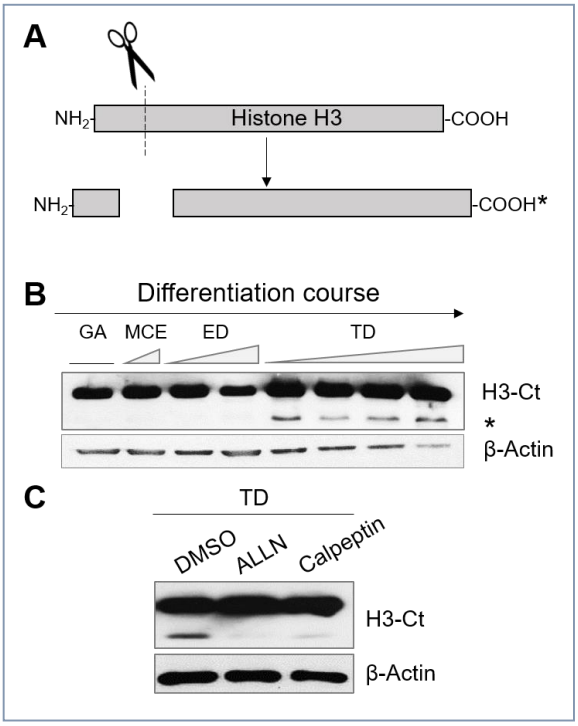

Figure 43: CAPN-mediated histone H3 cleavage along 3T3-L1 differentiation course. *(A) Scheme of histone H3 N-tail cleavage. (B) Western blot analysis of histone H3 along 3T3-L1 differentiation. The antibody used for the detection is directed against the C-terminal end of histone H3. (C) Western blot of total protein extracts of DMSO, calpeptin and ALLN-treated 3T3-L1 cells at TD in which Ct-histone H3 levels were analysed. Cells were treated with inhibitors 24 h before the induction of differentiation. β-Actin was used as loading control.*

product of cleaved histone H3 should be accumulated to be detected. Actually, it has been suggested that most likely any chromatin modification or structural changes during MCE would be reasonably stable and not subjected to a dynamic cycle of addition/removal of specific marks and/or histones[351].

Local opening of chromatin structure has been reported to take place during MCE until the induction of PPAR-γ. Consequently, to find out if CAPNs could regulate this chromatin-remodelling by cleaving histone H3, the expression of two PPAR-γ-target genes induced at MCE-ED transition was evaluated in calpeptin and ALLN-treated cells. Cells were pretreated with the inhibitors 24 h before the MDIR induction. Then, total RNA was isolated from adipocytes at the MCE-ED transition and mRNA levels of C/EBP-α and leptin genes was analysed by RT-qPCR. As shown in Figure 44, the expression of C/EBP-α and leptin was strongly prevented by both CAPN inhibitors. Although the role of other proteases in the differentiation is out of discussion, our data suggest that CAPNs are clearly involved in the modulation of the sequential steps triggered during mitotic clonal expansion leading to early differentiation.

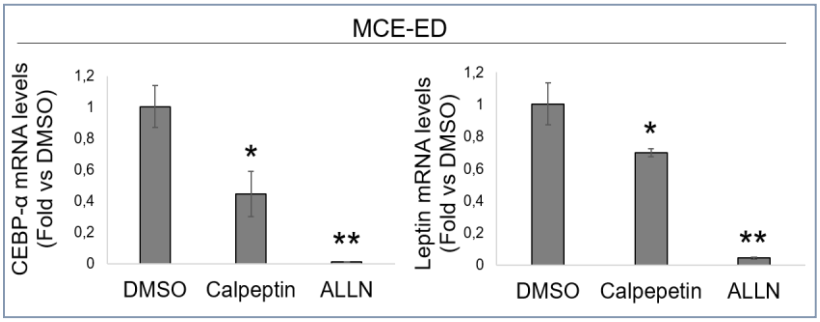

Figure 44: mRNA levels of adipogenic genes after CAPN inhibition. *C/EBP-α and leptin mRNA levels in DMSO, calpeptin and ALLN-treated 3T3-L1 cells at MCE-ED transition were analysed by qPCR. Data were normalized according to 18S mRNA, analysed and quantified in the same sample reaction. Expression levels are shown as fold vs. DMSO. Results (n ≥ 3) are shown as mean ± SEM. Student's t-test was performed for the statistical analysis, ⁎p≤0.05, ⁎⁎p≤0.01 vs DMSO.*

2.3 IDENTIFICATION OF THE NUCLEAR CAPN ISOFORM INVOLVED IN ADIPOCYTE DIFFERENTIATION

Herein it is hypothesized that the distribution of specific CAPN-isoforms is determinant for their functions. CAPN seems to be a key enzyme during the MCE to trigger early differentiation of 3T3-L1 cells after MDIR-induction. Nevertheless, since the differentiation of 3T3-L1 is a sequential process, the particular contribution of each isoform to the differentiation of 3T3-L1 cells remains unknown.

2.3.1 Isoform-specific role of CAPN1 in nuclei of differentiating pre-adipocytes

Although western blot analysis showed that CAPNs levels were mainly increased at MCE-ED transition and onwards, we wondered whether CAPNs distribution could change during the whole differentiation time-course. In addition, the isoform-specific role of CAPNs on nuclear targets needs to be addressed.

(i) Subcellular localization

CAPN1 subcellular distribution was studied by a detailed IF analysis. Perilipin-1 co-immunostaining was used to correlate more accurately CAPN1 distribution with the differentiation stage. As can be seen in Figure 45, in agreement with our previous IF analysis, cells suffered a dramatic morphological change from a fibroblastic (at GA phase) to a spherical shape (at TD). The earlier detection of perilipin-1, was at the burst of adipogenic proteins accumulation at ED; then, it gradually increased along the differentiation course, reaching a peak at TD.

Regarding CAPN1, it is important to point out that it was dramatically redistributed during the differentiation process. In growth arrested (GA) pre-adipocytes, CAPN1 was diffusely distributed in nucleus and cytoplasm. However, although also found in the cytoplasm, during MCE some cells showed unusual CAPN1 aggregates within the nucleus that were strongly detected throughout ED and the onset of TD. By the end of TD, these aggregates were not detected and CAPN1 was only found in the cytosol, in closed proximity to cell membranes and lipid droplets (Figure 45, upper panel).

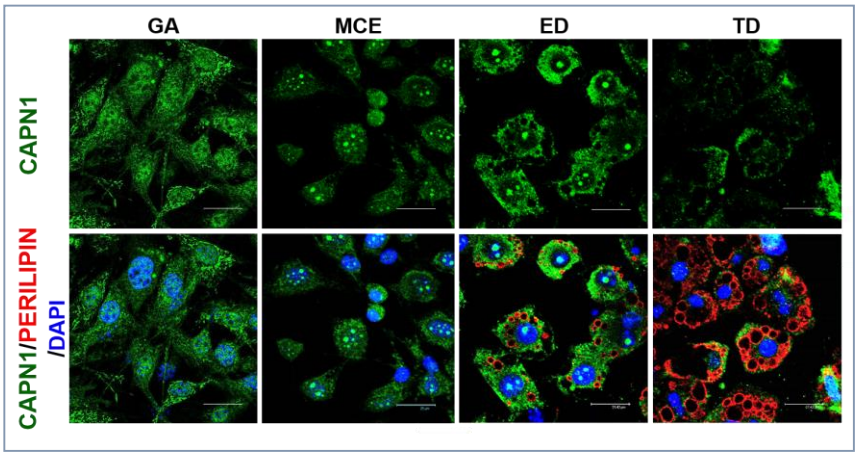

Figure 45: Subcellular localization of CAPN1 along 3T3-L1 differentiation course. *Immunostaining of CAPN1 (green) and perilipin-1 (red) in 3T3-L1 cells during GA, MCE, ED and TD differentiation phases. Nuclei were stained with DAPI. Upper panels show CAPN1 images and lower panels show merge images of CAPN1 (green), perilipin-1 (red) and DAPI (blue). Scale bars, 21 µm. Representative images are shown ($n \geq 3$).*

CAPN1 distribution during differentiating pre-adipocytes was verified by western blot. For this purpose, subcellular fractionation was performed and nuclear and cytoplasmic fractions from 3T3-L1 cells were obtained. To ensure the purity of both fractions, fibrillarin and α-tubulin were used as nuclear and cytosolic markers, respectively. Consistent with its reputation of being a cytoplasmic protein, CAPN1 protein levels were always higher in the cytosol than in the nucleus (Figure 46). Both, nuclear and cytosolic CAPN1 increased throughout the whole process of differentiation, and declined in fully differentiated adipocytes. However, in agreement with IF analysis (Figure 45), the highest CAPN1 increase in the nuclear compartment was observed at MCE and ED phases. These results demonstrate that CAPN1 is completely re-localized during the early stages of pre-adipocyte differentiation at MCE phase.

These data suggest that subcellular distribution of CAPN1 at MCE might be related to its function during adipocyte differentiation. Although synchronized 3T3-L1 cells are being used, a heterogeneous population of pre-adipocytes at different time-points during MCE could mask a differential isoform-specific distribution of CAPNs during this phase. Consequently, the

nuclear distribution of CAPN1 was carefully analysed in MDIR-induced pre-adipocytes at different stages of cell differentiation following a qualitative study in single cells.

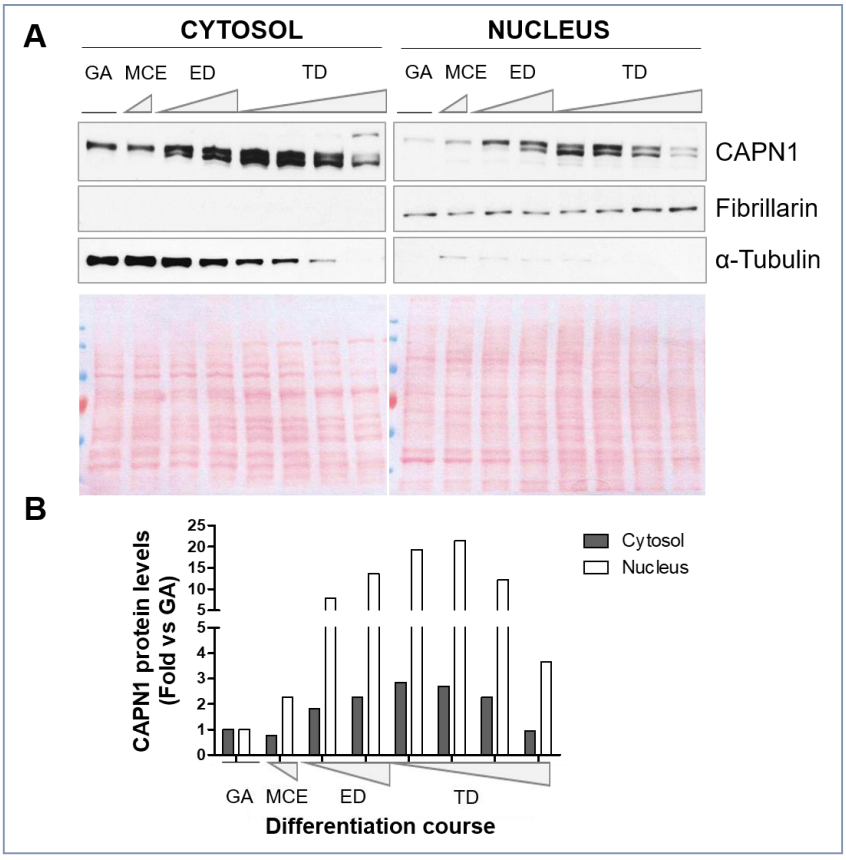

Figure 46: Subcellular distribution of CAPN1 in cytosolic and nuclear fractions along 3T3-L1 differentiation course. *(A) Changes in CAPN1 levels along 3T3-L1 differentiation course were analyzed in cytosolic and nuclear fractions by western blot. Fibrillarin and α-tubulin were analyzed as markers of fraction purity. (B) Cytosolic and nuclear CAPN1 protein levels were quantified and normalized according to Ponceau staining. Protein levels are shown as fold vs. GA phase.*

As can be observed, in dividing cells during MCE, CAPN1 was localized within the perichromatic territory, surrounding the condensed chromosomes at metaphase (Figure 47A, upper panels), but it did not

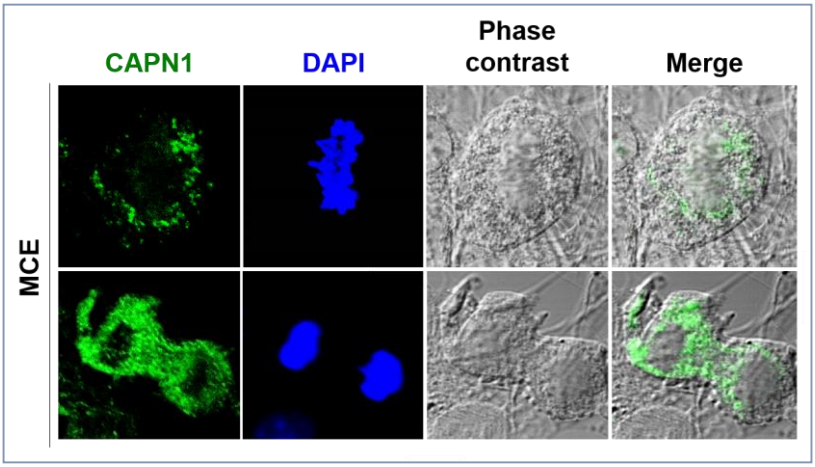

Figure 47: Subcellular distribution of CAPN1 during mitotic clonal expansion phase. *Immunostaining of CAPN1 in 3T3-L1 cells during MCE phase. Inset shows merge images of immunofluorescence staining and phase contrast. Nuclei were stained with DAPI. Representative images are shown ($n \geq 3$).*

colocalize with them. At telophase, CAPN1 was widely distributed in the cytosol (Figure 47A, lower panels). Interestingly, CAPN1 showed a particular and highly dynamic distribution, surrounding chromosomes during metaphase at MCE or gathered in specific compartments within the nuclei of differentiating pre-adipocytes starting at the end of MCE and ED (Figure 46). More detailed images of CAPN1 localization during the differentiation course of 3T3-L1 cells are shown in Figure 48.

As can be observed (Figure 48), the pattern of CAPN1 distribution changed along the differentiation course. Initially, in post-mitotic cells at MCE, CAPN1 was gathered at small and numerous dispersed aggregates within the nucleus. As long as the differentiation progressed, those aggregates seemed to rearrange and unify in bigger structures. Notoriously, at TD, when the adipocyte has achieved a complete differentiation, CAPN1 was almost restricted to the nuclear periphery. Detailed phase contrast images (Figure 48) revealed that CAPN1 congregated in dense nuclear structures that look like nucleoli. This CAPN1 distribution resembled the CAPN2 nucleolar localization previously observed in breast cancer cell lines (Figure 19).

CAPN1 nucleolar localization was further analysed by western blot in nucleolar fractions of 3T3-L1 at GA, MCE and ED. Nucleolar fractions were

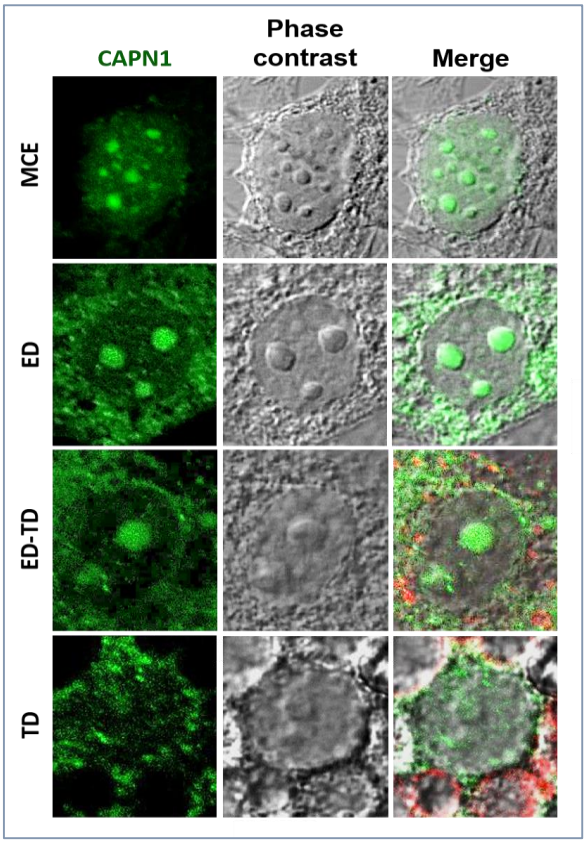

Figure 48. Detailed subcellular localization of CAPN1 in 3T3-L1 cells along the differentiation course. *Immunofluorescence CAPN1 staining (green) and phase contrast in 3T3-L1 cells during MCE, ED, ED-TD transition and TD differentiation phases. Perilipin-1 (red) was used as a marker of differentiation. Merge image of CAPN1, perilipin-1 and phase contrast were also included. A representative image is shown (n≥3).*

obtained following a standardized protocol[317] that uses the higher density of nucleoli to isolate them from the rest of the cell (nucleolar-less fraction) by means of a sucrose gradient. To ensure the purity of both fractions, fibrillarin and α-tubulin were evaluated as nucleolar and nucleolar-less fractions markers, respectively. This western blot analysis corroborated the presence of CAPN1 within the nucleolus (Figure 49). In accordance with the nuclear fractionation and IF studies, nucleolar CAPN1 increased from GA to ED during adipocyte differentiation. Conversely, CAPN2 was not detected within

nucleolar fractions, thus confirming the isoform-specificity of CAPN1 in this localization.

CAPN1 nucleolar distribution has never been described before. These observations indicate that CAPN1 could be exerting different functions in the nuclear compartment, functions that may be delimited by the specific localization within nuclear substructures at each specific time point.

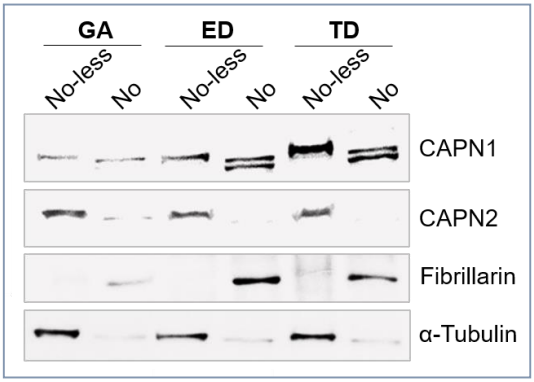

Figure 49: Distribution of CAPN1 and CAPN2 in nucleolar 3T3-L1 extracts along the differentiation course. *Western blot analysis of CAPN1 and CAPN2 in nucleolar-less (No-less) and nucleolar (No) fractions during GA, ED and TD phases of 3T3-L1 differentiation. Fibrillarin and α-tubulin were analysed as markers of fraction purity.*

(ii) Key targets of CAPN1 in the nuclear compartment

In addition to histone H3 cleavage, adipogenic gene promoters could have nucleosomal composition altered by addition or removal of histone variants[349], interact with other adipogenic gene promoters[351] or even be re-localized within nuclei[353]. Consequently, although both CAPNs interact with histone H3-Nt tails (Figure 42), each CAPN isoform could have a specific role on chromatin reorganization.

In order to decipher the implication of CAPN1 in H3-clavage, its expression was silenced by means of esiRNA transfections. 3T3-L1 cells were transfected with either scramble or CAPN1 esiRNA 48 h before the induction of differentiation. Next, cells were collected at ED-TD transition, to detect the accumulated product of cleaved-H3. As observed, high esiRNA silencing efficiency was achieved and no compensatory mechanisms were observed in CAPN1-knockdown cells (Figure 50A). CAPN1-knockdown cells showed a

decrease in histone H3 cleavage that once quantified it was around 50% less cleaved product (Figure 50B). These data show that CAPN1 is involved in the histone H3-cleavage of particular nucleosomes.

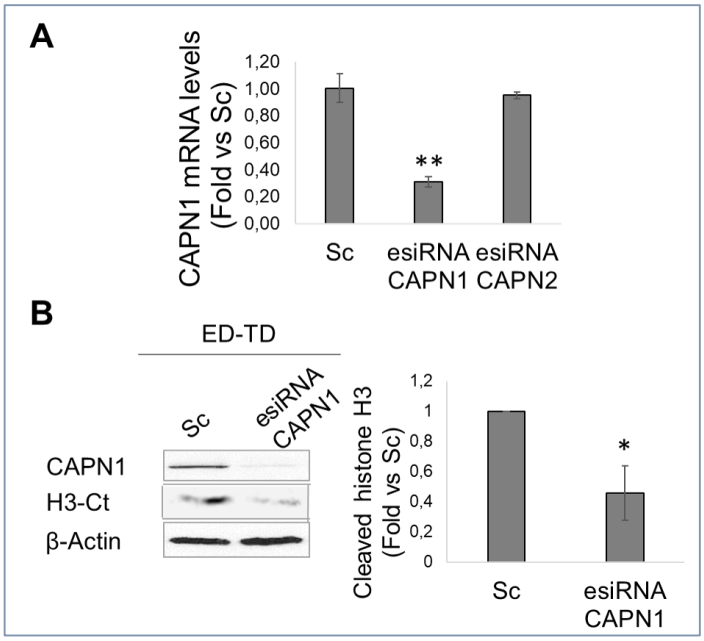

Figure 50: CAPN1-mediated cleavage of the N-tail histone H3 during 3T3-L1 differentiation. *(A) CAPN1 mRNA levels of control (Sc), CAPN1 esiRNA and CAPN2 esiRNA-transfected 3T3-L1 cells at ED-TD phase were analysed by RT-qPCR to confirm silencing efficiency. Data (n≥3) are represented as mean values ± SEM. Student's t-test was performed for the statistical analysis, ∗∗p≤0.01, vs. scramble (Sc). (B) Cleavage of histone H3 was studied in control (Sc) and esiRNA CAPN1-transfected cells at ED-TD phase with an antibody directed towards histone H3-Ct. Blot shows the accumulated cleaved product of histone H3. CAPN1 protein levels were also analysed to demonstrate knocking down efficiency. Graph shows quantification of histone H3 cleaved band. Results are expressed as fold decrease vs. Sc. Data (n≥3) are mean values ± SEM. Student's t-test was performed for the statistical analysis, ∗p≤0.05, vs. Sc.*

In previous published studies from our laboratory, it was suggested that C/EBP-α and leptin gene expression was modulated by CAPN1 in differentiating adipocytes during mammary gland involution[88]. To further explore the effect of CAPN1 on adipogenic gene expression during adipocyte differentiation, C/EBP-α and leptin steady-state mRNA levels were analysed

in CAPN1-knockdown cells at ED by RT-qPCR. As shown in Figure 51, CAPN1 down-regulation partially prevented MDIR-induction of C/EBP-α and leptin expression during ED.

All in all, these data confirm that CAPN1 is involved in the modulation of adipogenic networks triggered in pre-adipocytes during MCE. Although CAPN1 seems to be partially involved in histone H3 cleavage, other mechanism by which CAPN1 mediates local chromatin structure during MCE cannot be ruled out and should be further explored.

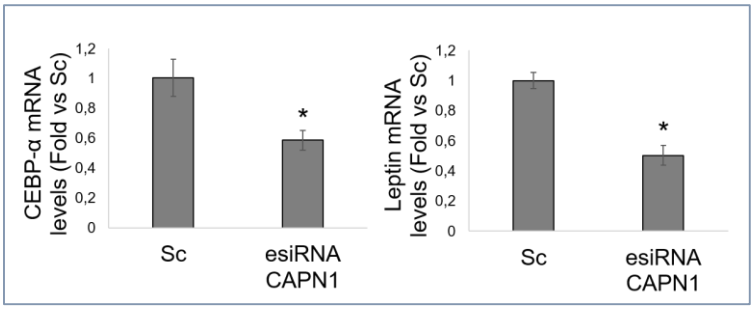

Figure 51: Adipogenic genes expression in CAPN1-knockdown differentiating 3T3-L1 cells. *C/EBP-α (left) and leptin (right) mRNA levels of control (Sc) and CAPN1 esiRNA transfected 3T3-L1 cells were analysed by RT-qPCR at ED phase. Transfection took place prior to MDIR-treatment. Data were normalized according to 18S mRNA, analysed and quantified in the same sample reaction. Expression levels are shown as fold vs. Sc. Data ($n \geq 3$) are mean values ± SEM. Student's t-test was performed for the statistical analysis, $*p \leq 0.05$ vs. Sc.*

2.3.2 Isoform-specific role of CAPN2 in nuclei of differentiating pre-adipocytes.

(i) Subcellular localization.

CAPN2 subcellular distribution during pre-adipocyte differentiation was studied using the same experimental approaches as those for CAPN1. CAPN2 IF analysis showed that this isoform was predominantly localized in the cytoplasmic compartment along the differentiation course (Figure 52). CAPN2 was also present in nuclei of adipocytes until the onset of terminal differentiation, although to a much lesser extent than in the cytoplasmic compartment. What is clear from the IF images is that CAPN2 does not form

aggregates inside the nuclei, which suggests that it does not have a nucleolar localization as it did CAPN1.

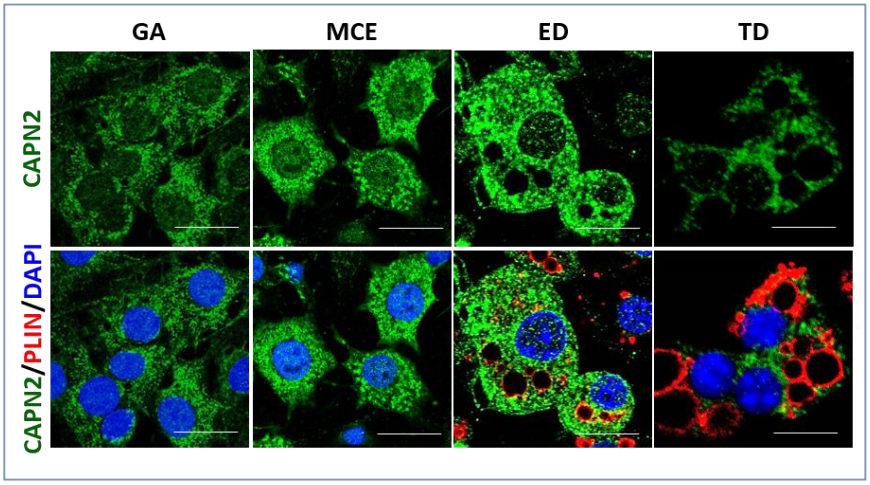

Figure 52: Subcellular localization of CAPN2 in 3T3-L1 along the differentiation course. *Immunostaining of CAPN2 (green) and perilipin-1 (red) in 3T3-L1 cells at GA, MCE, ED and TD phases. Nuclei were stained with DAPI (blue). Upper panels show CAPN2 staining images and lower panel show merge images of CAPN2, perilipin-1 and DAPI staining. Scale bars, 21 µm. Representative images are shown (n ≥ 3).*

CAPN2 subcellular distribution was further analysed in cytoplasmic and nuclear fractions from differentiating pre-adipocytes by western blot (Figure 53A). Even though it was also detected in nuclei, CAPN2 was mainly compartmentalized within the cytosolic fraction. However, while cytosolic CAPN2 barely changed throughout the whole differentiation process, nuclear CAPN2 exhibited an abrupt 4-fold nuclear increase at MCE that lasted until the onset of TD. These results are in agreement with the pattern of CAPN2 distribution detected by IF, proving that both isoforms translocate to the nuclear compartment at MCE after MDIR-induced differentiation.

Once again, the nuclear distribution of CAPN2 was analysed in MDIR-induced pre-adipocytes during MCE by a detailed study in single cells. IF staining showed that CAPN2 was co-localizing with chromosomes at different phases of mitosis. In Figure 54 (i) CAPN2 was detected co-localizing with prometaphasic chromosomes rosette and surrounding chromosomes along the metaphase plate (Figure 54, ii, iii). Finally, CAPN2 was highly

concentrated in the whole nucleus during telophase (Figure 54, iv). As mentioned, during mitotic clonal expansion, CAPN1 was found in nuclear aggregates with a preferential perinuclear and cytoplasmic distribution, while CAPN2 was highly concentrated in nuclei, co-localizing with chromosomes during mitosis. This dissimilar pattern of distribution found in CAPN1 and CAPN2 suggests that CAPN2 might also have a role in chromosome alignment and segregation and consequently, with a predictable impact on chromatin structure.

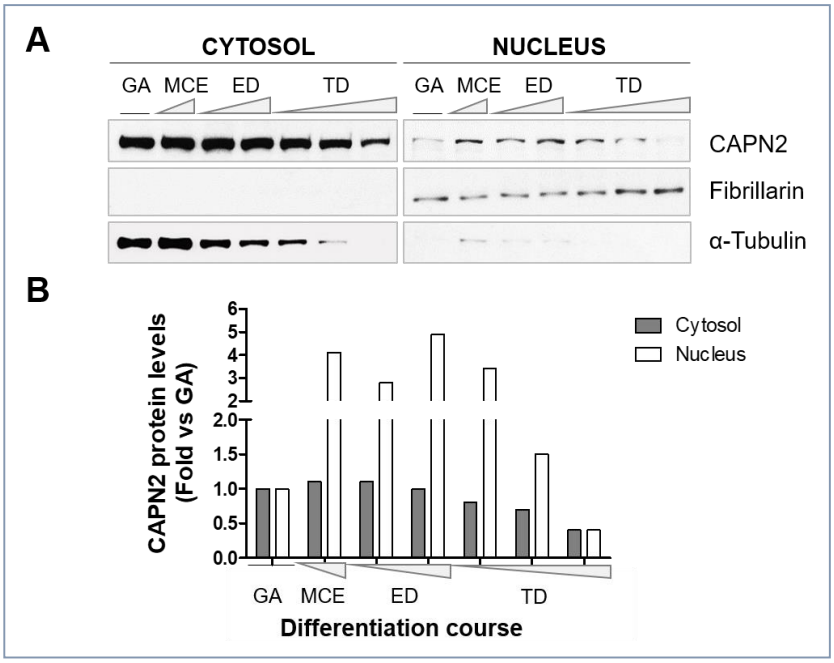

Figure 53: Subcellular distribution of CAPN2 in cytosolic and nuclear fractions along 3T3-L1 differentiation course. *(A) Changes in CAPN2 levels along 3T3-L1 differentiation course were analyzed in cytosolic and nuclear fractions by western blot. Fibrillarin and α-tubulin and were used as markers of fraction purity. (B) Cytosolic (grey bars) and nuclear (white bars) CAPN2 protein levels were quantified and normalized according to Ponceau staining. Protein levels are shown as fold vs. GA phase.*

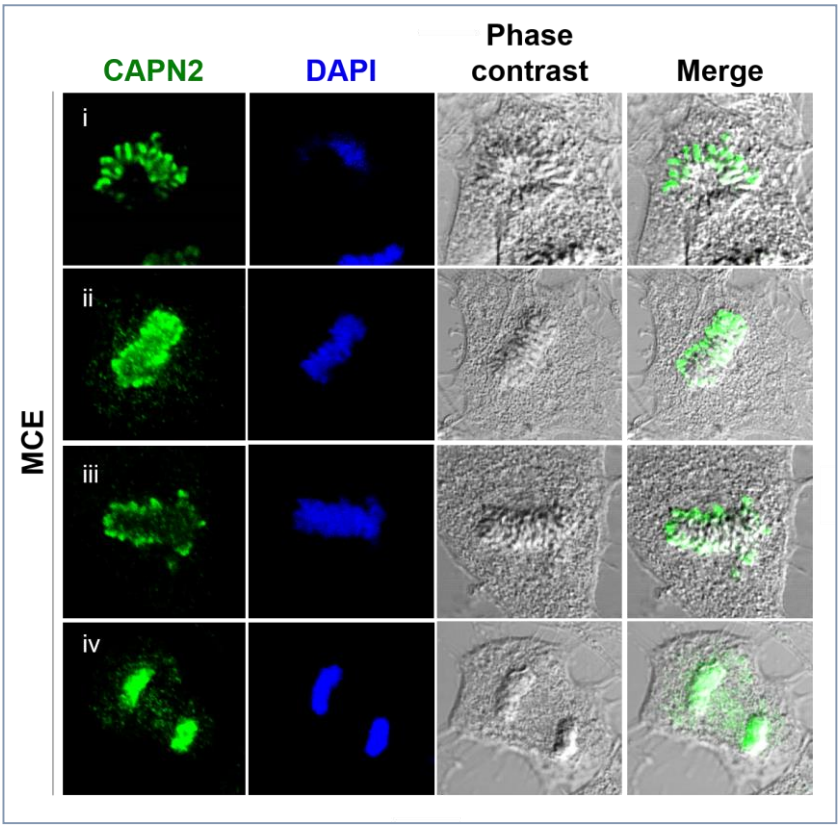

Figure 54: Subcellular distribution of CAPN2 during mitotic clonal expansion phase. *Immunostaining of CAPN2 in 3T3-L1 cells ongoing MCE phase at different mitotic stages. Inset shows merge images of immunofluorescence staining and phase contrast. Nuclei were stained with DAPI. Representative images are shown (n ≥ 3).*

(ii) Key targets of CAPN2 in the nuclear compartment.

As for CAPN1, the implication of CAPN2 in the cleavage of histone H3 was also studied. CAPN2 expression was silenced by esiRNA transfections. Transfected 3T3-L1 cells with either scramble or CAPN2 esiRNA 48 h before the induction of differentiation were collected at ED-TD transition and analysed by western blot to detect the accumulated product of cleaved-H3. CAPN2 silencing also diminished the proteolysis of histone H3

around 50% in relation to control (Figure 55B). These results indicate that CAPN2 is also involved in the cleavage of the N-tail of histone H3.

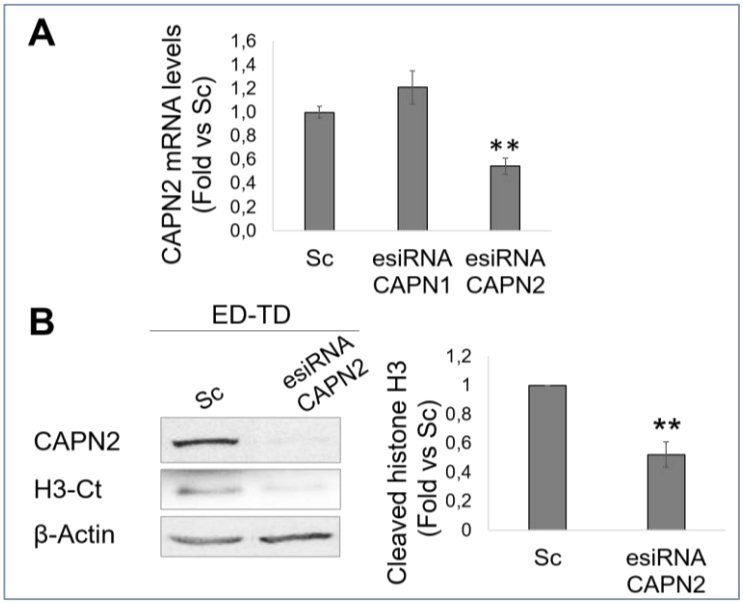

Figure 55: CAPN2-mediated cleavage of Nt-tail of histone H3 during 3T3-L1 differentiation. *(A) CAPN2 mRNA levels of control (Sc), CAPN1 esiRNA and CAPN2 esiRNA-transfected 3T3-L1 cells at ED-TD phase were analysed by RT-qPCR for silencing efficiency. Data were normalized according to 18S mRNA, analysed and quantified in the same sample reaction. CAPN2 mRNA levels are shown as fold vs. Scramble (Sc). Data (n≥3) are mean values ± SEM. Student's t-test was performed for the statistical analysis, ∗∗p<0.01, vs Sc. (B) Cleavage of histone H3 was studied in control (Scramble) and esiRNA CAPN2-transfected cells at ED-TD phase with an antibody directed towards histone H3-Ct. Blot shows the accumulated cleaved product of histone H3. CAPN2 levels were also shown. Graphs show quantification of histone H3 cleaved band. Results are expressed as fold decrease vs Sc. Data (n≥3) are mean values ± SEM. Student's t-test was performed for the statistical analysis, ∗∗p<0.01, vs Sc.*

Finally, C/EBP-α and leptin mRNA levels were also analysed in knockdown cells at ED by RT-qPCR. As can be observed in Figure 56, CAPN2-knockdown 3T3-L1 cells showed a reduced C/EBP-α and leptin expression during ED, confirming that CAPN2 is also involved in the modulation of adipogenic networks triggered in pre-adipocytes during MCE.

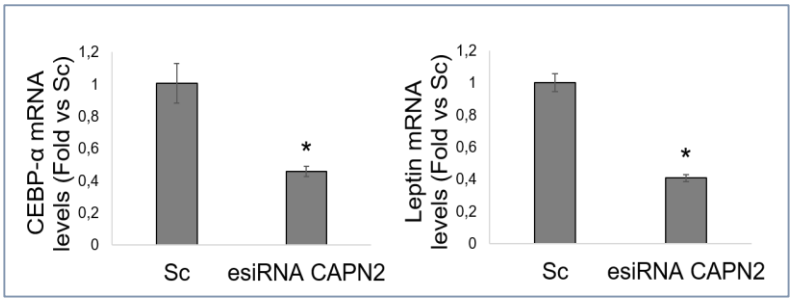

Figure 56: Adipogenic genes expression in CAPN2-knocked down 3T3-L1 cells. *C/EBP-α (left) and leptin (right) mRNA levels of control (Sc) and CAPN2 esiRNA transfected 3T3-L1 cells were analysed by RT-qPCR at ED phase. Data were normalized according to 18S mRNA, analysed and quantified in the same sample reaction. Expression levels are shown as fold vs. Sc. Results ($n \geq 3$) are represented as mean values ± SEM. Student's t-test was performed for the statistical analysis, $*p \leq 0.05$ vs Sc.*

Taking together, these data may suggest that both CAPN isoforms could be contributing to the modulation of chromatin structure by cleaving the N-tails of histone H3 in particular nucleosomes. Nevertheless, further experiments are needed to clarify the specific cleavage pattern in which each CAPN isoform is involved or to study whether CAPNs follow other mechanisms to support adipogenic genes expression.

3. STUDY OF CAPN2 NUCLEOLAR LOCALIZATION

Previous immunofluorescence studies in breast cancer cell lines and in differentiating 3T3-L1 (Figure 19 and 45), revealed that CAPN1 and CAPN2, respectively, were highly concentrated in a subnuclear structure resembling the nucleolus. Although the nucleolus is known to be responsible of different important cell functions like rRNA synthesis, ribosome and ribonucleoproteins assembly and protein sequestration, new unexpected nucleolar functions are being discovered, revealing how complex the nucleolus system is. Furthermore, nucleolar functions are deregulated in cancer, which has been linked to cancer progression[176,178,354].

The nucleolus, contrary to cell compartments, is not delimited by any membrane. Protein trafficking to membrane-systems is driven by recognition of specific and well characterized protein motifs. Although nucleolar internalization seems not to be regulated by a particular motif, Nucleolar Localization Signals (NoLS) have been propose to mediate the nucleolar internalization of proteins.

3.1 STUDY OF SUBCELLULAR DISTRIBUTION OF CAPNS IN BREAST CANCER CELL LINES

Given the relevance of nucleoli in tumour progression, we focused on the study of CAPN2 within this nuclear substructure. The nucleolar localization of isoform-specific CAPNs in breast cancer cell lines was analysed by IF staining of CAPN2 or CAPN1 and fibrillarin, a specific nucleolar protein involved in pre-ribosomal RNA (pre-rRNA) biogenesis[355].

Figure 57 shows that CAPN2 follows the same distribution as fibrillarin, proving that certainly it accumulates into the nucleolus. MDA-MB-231 and MDA-MB-468 showed higher levels of CAPN2 than luminal cells. Accordingly, a higher co-localization between CAPN2 and fibrillarin was also observed in these cell lines compared to luminal cells.

Based on these IF studies, it seems that independently of the breast cancer subtype CAPN2 is gathered within the nucleolus. But importantly, the abundance of nucleolar CAPN2 is directly related to total CAPN2 protein levels in the cell.

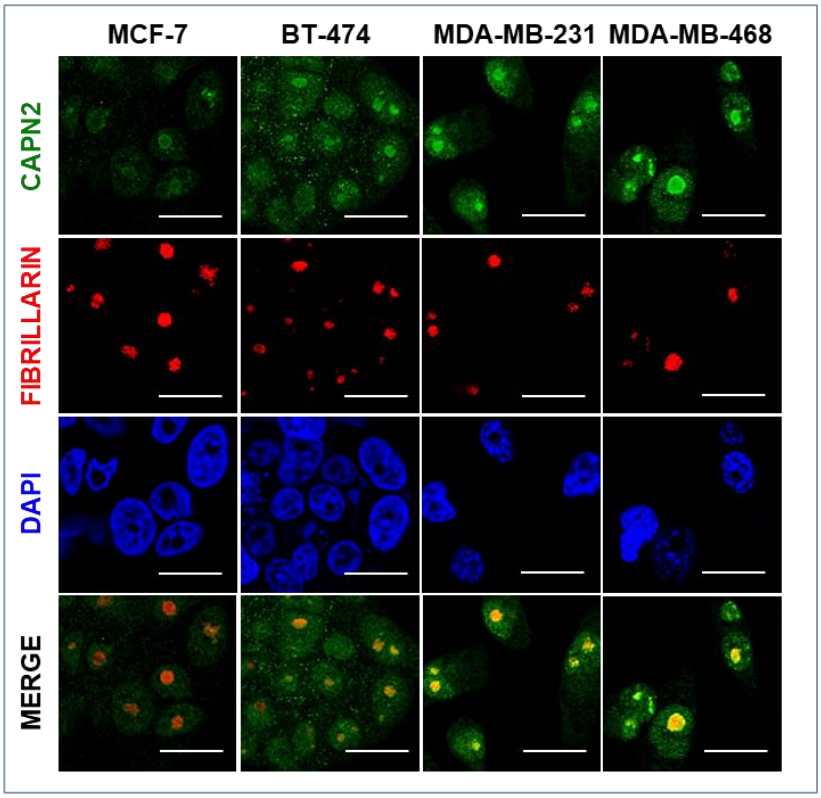

Figure 57: Subcellular localization of CAPN2 in breast cancer cell lines. *Immunofluorescence staining of CAPN2 (green), fibrillarin (red), and merge in luminal (MCF-7 and BT-474) and TNBC-negative (MDA-MB-231 and MDA-MB-468). Nuclei were stained with DAPI (blue). Scale bar 25µm. Data n≥3.*

In our previous analysis of CAPN1 in breast cancer cells we could not detect CAPN1 in nuclear aggregates that could suggest its nucleolar localization. However, CAPN1/fibrillarin co-localization was not specifically studied. In order to further confirm the absence of CAPN1 from nucleoli, its subcellular co-location with fibrillarin was also analysed by IF staining. As can be observed in Figure 58, no CAPN1 was found to co-localize with fibrillarin in any cell type, further confirming that CAPN2 nucleolar localization is isoform-specific.

It is worth to mention that cell distribution of CAPNS1 and CAST, the regulatory components of the ubiquitous CAPNS, was already studied in

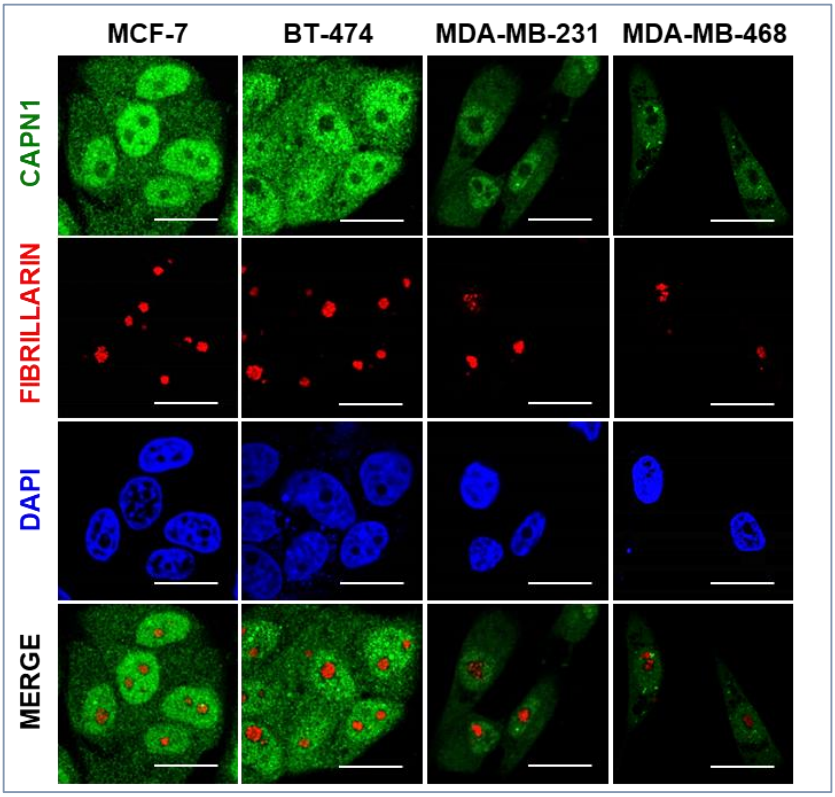

Figure 58: Subcellular localization of CAPN1 in breast cancer cell lines. *Immunofluorescence staining of CAPN1 (green), fibrillarin (red), and merge in luminal (MCF-7 and BT-474) and TNBC (MDA-MB-231 and MDA-MB-468). Nuclei were stained with DAPI (blue). Scale bar 25µm. Data n≥3.*

in breast cancer cell lines by IF analysis (Figure 20). In those experiments, no nucleolar CAPNS1 could be detected in any of the tested cell lines. On the other hand, nucleolar CAST was detected only in BT-474 cells.

CAPN2 nucleolar localization was first described by our group in colorectal cancer cell lines[93]. In short, these data suggest an isoform-specific role of CAPN2 in nucleoli of cancer cells that was not cancer-type specific. However, the abundance of nucleolar CAPN2 seems to be dependent on the cancer-subtype. The presence and abundance of CAPN2 in nucleoli of breast cancer cells was analyzed by western blot (Figure 59) in nucleolar and nucleolar-less fractions. To ensure the purity of fractions, fibrillarin and α-tubulin were evaluated as nucleolar and nucleolar-less fractions markers,

respectively. As seen in Figure 59, these analyses confirmed that CAPN2 was present within the nucleolus.

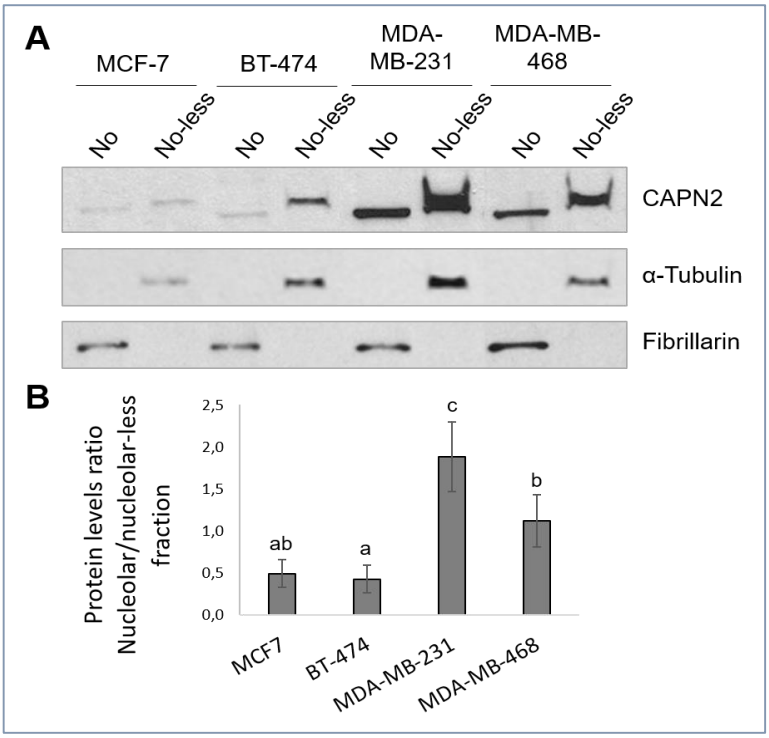

Figure 59: CAPN2 levels in subcellular fractions from breast cancer cell lines. *(A) Western blot analysis of CAPN2 in nucleolar (No) and nucleolar-less (No-less) fractions from MCF-7, BT-474, MDA-MB-231, MDA-MB-468. α-Tubulin and fibrillarin were analyzed as marker of fraction purity. (B) CAPN2 levels were quantified and normalized by their respective markers. Bar chart represents the CAPN2 nucleolar/nucleolar-less ratio, represented as mean values ± SEM. Data (n≥3). ANOVA was performed for the statistical analysis, where different superscript letters indicate significant differences, p≤0.05; the letter 'a' always represents the lowest value within the group.*

In agreement with previous data about CAPN2 expression in breast cancer cell lines (Figures 19, 21 and 22), CAPN2 protein levels from both nucleolar and nucleolar-less fractions were higher in TNBC than in the luminal subtype (Figure 59B). These results reinforce the previous statement, that despite breast cancer cell lines do not present differences regarding the

overall pattern of CAPN2 distribution, nucleolar CAPN2 abundance is dependent on the differential total CAPN2 levels found in luminal and TNBC cell lines.

In addition to these observations, a striking difference in the electrophoretic mobility of CAPN2 was found among fractions; the mobility of the band recognized by CAPN2 antibody was faster in nucleolar than in nucleolar-less fractions in all cell lines tested. Nucleoli are aggregates of proteins which could easily cross-react with antibodies resulting in unspecific immunodetection of nucleolar proteins. Therefore, in order to ensure that the detected protein was certainly CAPN2 and not a consequence of the antibody cross-reaction, the specificity of this recognition was assessed by different approaches:

3.1.1 Specificity of antibody recognition *in vitro*.

The specificity of CAPN2 antibody was verified as means of antibody incubation with a blocking peptide prior to western blot analysis. As can be seen in Figure 60, the blocking peptide prevented the detection of CAPN2 observed in control. This analysis confirmed that the band recognized by the antibody was indeed CAPN2 and not the result of an unspecific artifact.

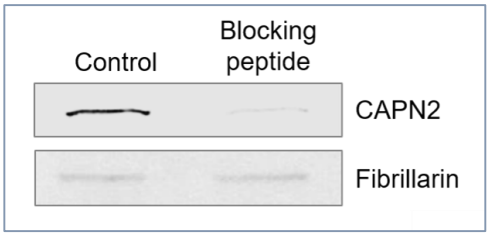

Figure 60: Specific nucleolar CAPN2 recognition by western blot. *Western blot analysis of CAPN2 in MDA-MB-231 nucleolar extracts in the absence or presence of a blocking peptide. Fibrillarin was used to assess purity of fractions and equal loading.*

Finally, in order to definitively confirm CAPN2 nucleolar localization, MCF-7 and MDA-MB-231 breast cancer cell lines were transfected with an expression vector codifying for full 700aa CAPN2 variant 1 (NM_001748.4). The protein was tagged with an N-terminal DYKDDDDK epitope that generates a DYK-CAPN2 product (Figure 61A).

Whole cell lysates from 48 h transfected cells were analysed by western blot with anti-DYK antibodies. Figure 61B (left panels) shows that DYK is only detected in CAPN2 overexpressing MCF-7 and MDA-MB-231 cells, being absent in empty vector-transfected cells. As expected, the same cell lysates incubated with anti-CAPN2 antibody (Figure 61B, right panels), showed an increased CAPN2 output. Moreover, anti-CAPN2 detection demonstrated that overexpressed DYK-CAPN2 had the same size as the endogenous CAPN2 since DYK tag did not alter the protein electrophoretic mobility.

DYK tag is an artificial amino acidic sequence that is not found in nature, so anti-DYK antibody only detects the overexpressed protein not cross-reacting with any endogenous protein. As can be observed in Figure 61B, no DYK signal was detected in control MCF-7 and MDA-MB-231 cells. As expected, the overall CAPN2 levels were dramatically increased in DYK-CAPN2 overexpressing cells. No differences between cell lines were found.

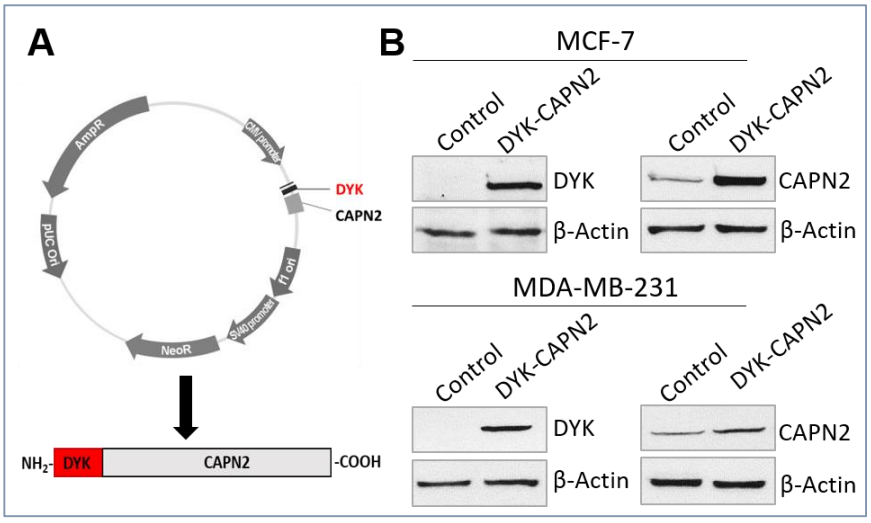

Figure 61: DYK-CAPN2 overexpression in MCF-7 and MDA-MB-231 cells. *(A) DYK-CAPN2 overexpression vector. The 700 amino acids tagged product is shown. (B) MCF-7 and MDA-MB-231 breast cancer cell lines were transfected with the empty (Control) or DYK-CAPN2 vectors, and total protein extracts were analysed by western blot with anti-DYK (Left panels) or anti-CAPN2 (right panels) antibodies. α-Actin was used as loading control. Data (n≥3).*

3.1.2 Specificity of antibody recognition *in vivo.*

The specific recognition of CAPN2 in the nucleolar compartment was also tested *in vivo* by IF analysis in either CAPN2-knockdown or epitope-tagged CAPN2-overexpressing cells.

CAPN2 nucleolar localization was analysed in control (Scramble siRNA-transfected) and CAPN2-knockdown cells. As may be noted in Figure 62, CAPN2-knockdown cells exhibited an overall decreased of CAPN2 signal (cytosol, nucleus and nucleoli), proving that the nucleolar recognition of CAPN2 by IF was also specific.

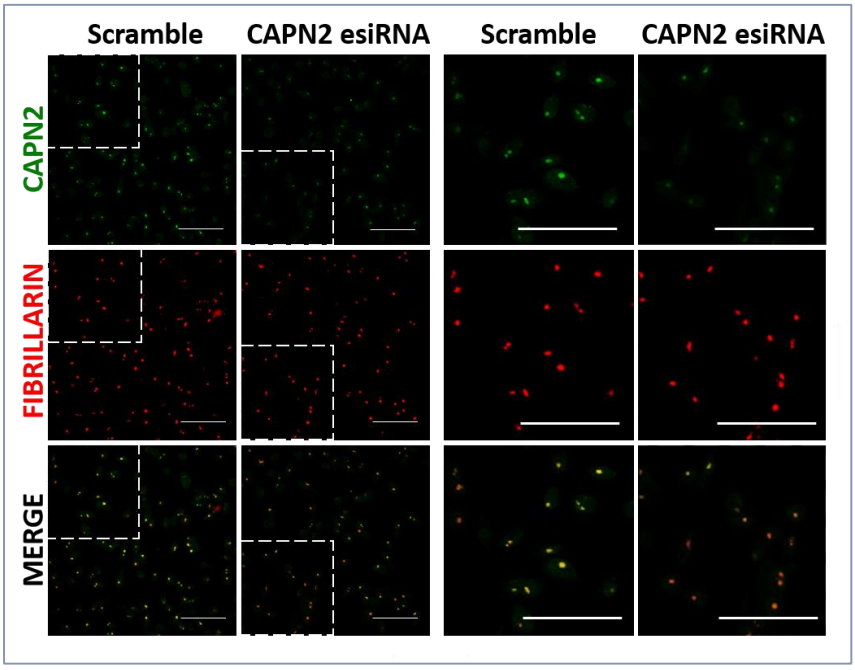

Figure 62: Subcellular distribution of CAPN2 in control and knockdown cells. *Immunofluorescence analysis of CAPN2 (green) and fibrillarin (red) in control (Scramble) and 72 h CAPN2 esiRNA transfected MDA-MB-231 cells. Nuclei were stained with DAPI (blue). Scale bar 75µm. Data n≥3.*

Confocal analysis was also performed for the study of CAPN2 distribution in DYK-CAPN2 overexpressing cells. IF DYK-CAPN2 signal could be detected within the nucleoli of breast cancer cell lines. Figure 63 shows detailed Z-stack series images of CAPN2 localization in DYK-CAPN2

overexpressing MCF-7 cells. Interestingly, this localization seems to be at the fibrillary center known to be at the central part of nucleoli.

Taking into account all these data, it can be concluded that CAPN2 is specifically localized in nucleoli of breast cancer cells and although this distribution was not dependent on the cancer subtype, the nucleolar abundance of CAPN2 is in agreement with the differential expression levels previously observed in each subtype.

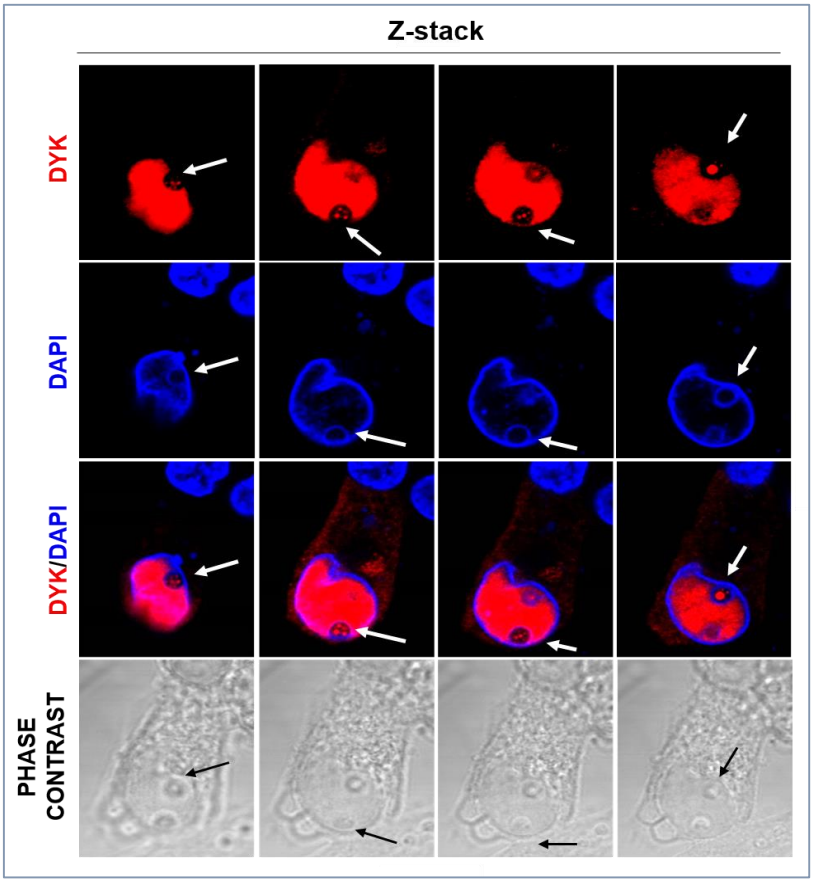

Figure 63: Immunofluorescence detection of DYK-CAPN2 distribution. *MCF-7 DYK-CAPN2 overexpressing cells were analysed by immunofluorescence with anti-DYK antibody (red). DAPI (blue) was used for nuclei detection. Immunofluorescence Z-stack images are shown. White and black arrows indicate nucleoli.*

3.2 STRUCTURAL DETERMINANTS OF NUCLEOLAR CAPN2 DISTRIBUTION: BIOINFORMATICS ANALYSIS

Due to the relevance of CAPNs localization in the regulation of their functions, it would be of interest to understand how CAPN2 translocate to nucleoli. As has been thoroughly explained, CAPNs localization could in part be defined by some features found in their structure. Although the rules mediating nucleolar localization are not completely understood different structural characteristics might favor protein nucleolar retention. Therefore, an exhaustive bioinformatics analysis was carried out to define those structural characteristics that could be determining CAPN2 nucleolar internalization.

In our analysis, common features found in nucleolar proteins, known to contribute to selective retention of proteins in the nucleolus, were assessed: (i) Nucleolar localization Signals (NOLS)[356] (ii) Positively charged regions rich in lysine and arginine residues[357,358]; (iii) Nuclear Localization Sequences (NLS) within the protein sequence[359]; (iv) Structurally disordered regions that allow interactions with nucleolar proteins[360]; (v) Protein sequences or a domains that specifically can bind to nucleolar proteins or nucleolar nucleic acids (rDNA, rRNAs))[177,360].

3.2.1 Nucleolar Localization Signals.

The presence of potential NoLS motifs in CAPN2 sequence was analysed by the "Nucleolar localization sequence detector" platform (NoD, http://www.compbio.dundee.ac.uk/nod[319]. NoD is based on an algorithm created from the high number of different NoLs sequences that have already been identified considering only the primary and secondary structure of proteins.

Strikingly, although a strong peak of NOLS prediction was found around residue 400, it did not reach the minimum score to be considered as a NOLS (Figure 64A). In order to discard whether the DYK-tag might be influencing CAPN2 nucleolar internalization, the DYK-CAPN2 sequence was also analysed by the same bioinformatics tool (Figure 64B). NoD platform did not predict NoLS sequence in DIK-CAPN2.

3.2.2 Positively charged regions.

Positively charged sequences allow proteins to accumulate in the nucleolus by interacting electrostatically with negatively charged molecules,

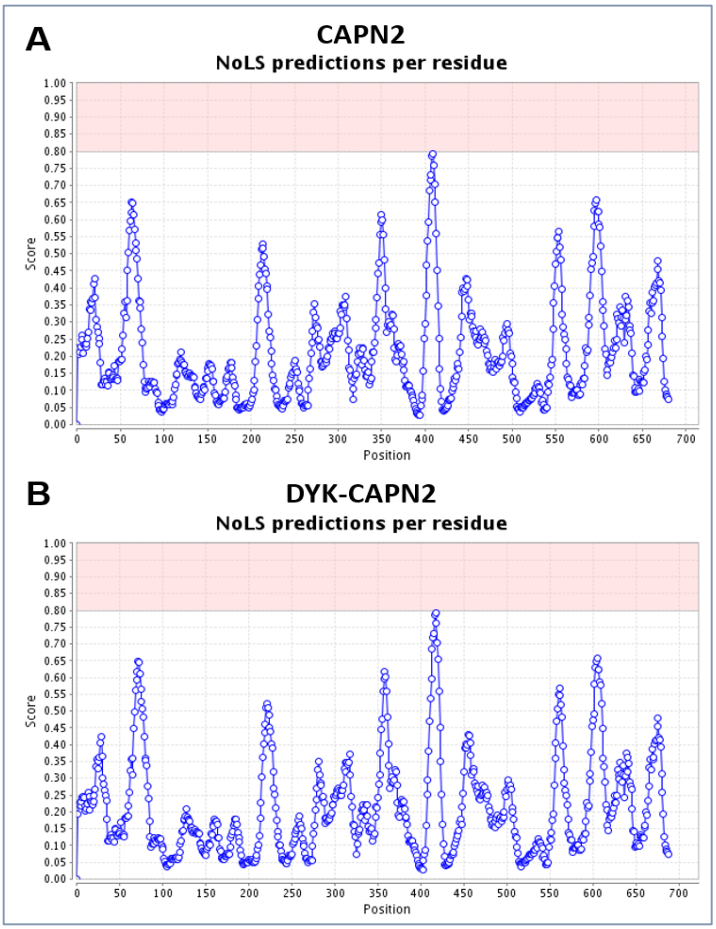

Figure 64: Prediction of NoLS in CAPN2 and DYK-CAPN2. *NoD software analysis for NoLS detection in CAPN2 (A) and DYK-CAPN2 (B) sequences. Graphs represent the score per residue. Threshold score ≥ 0.8 to be recognized as NoLS.*

like rDNA or rRNAs[357]. Repeated lysine (K) and arginine (R) motifs have been recognized to be necessary an even enough for nucleolus internalization[279]. CAPN2 amino acidic sequence charge was analysed by "EMBOSS: charge platform" (www.bioinformatics.nl/cgi-bin/emboss/charge). Figure 65A, (left panel) shows a graph with the charge values per residue found in CAPN2 sequence. A region GLIQKHRRRQR (410 to 420) was found to contain the highest positive charge (encircled in green). The charge values corresponding to each residue are listed in the

Figure 65A, right table (green).

NoLSs are known to be lysine or arginine-enriched sequences; however, the NoLS primary structure is usually heterogeneous. In agreement with this, although not recognized as a consensus NOLS we found a lysine and arginine–rich sequence in CAPN2 (Figure 65B) that could be a putative NOLS.

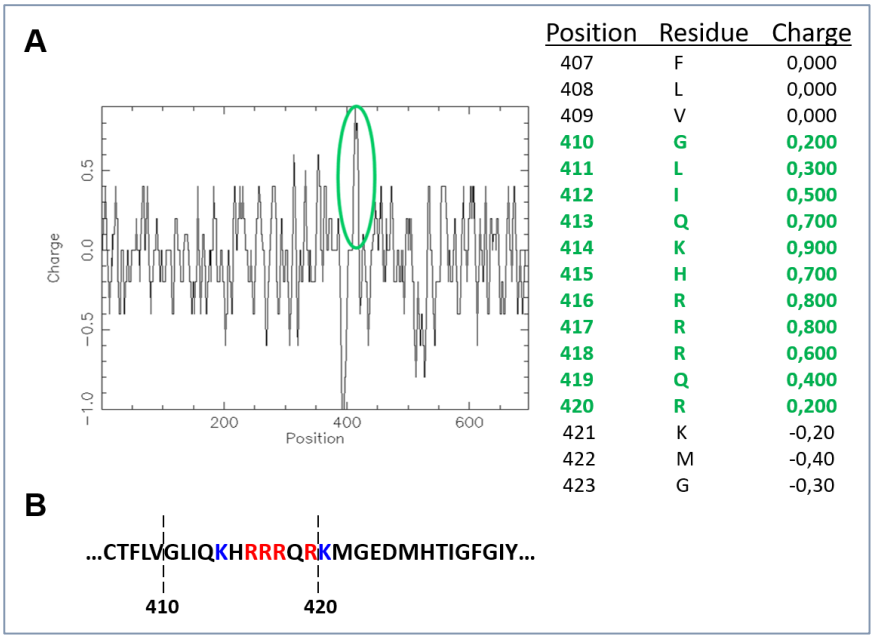

Position	Residue	Charge
407	F	0,000
408	L	0,000
409	V	0,000
410	**G**	**0,200**
411	**L**	**0,300**
412	**I**	**0,500**
413	**Q**	**0,700**
414	**K**	**0,900**
415	**H**	**0,700**
416	**R**	**0,800**
417	**R**	**0,800**
418	**R**	**0,600**
419	**Q**	**0,400**
420	**R**	**0,200**
421	K	-0,20
422	M	-0,40
423	G	-0,30

Figure 65: Amino acidic charge of CAPN2 sequence. *(A) Amino acids charge in CAPN2 sequence. Residues with the higher charge score are encircled in green. The table shows the amino acid residues and corresponding charge. The highest positive charge values are highlighted in green. (B) The positively charged region was rich in lysine (K) (blue) and arginine (R) (red) residues.*

3.2.3 Nuclear Localization Signals (NLSs).

Different studies have reported that NLSs can overlap with NoLSs or even be part of NoLS sequences[361]. In order to find overlapping regions for NLSs and identified putative NOLS (aminoacids 410-420) in CAPN2, its amino acidic sequence was analysed by PSORTII[320], a prediction tool designed for detection of protein subcellular localization signals.

Two pat4 motifs were identified as possible NLSs[321], both of them overlapping with putative non-consensus NOLS: KHRR (NLS1) and HRRR (NLS2), at positions 414-418 and 415-419, respectively (Figure 66).

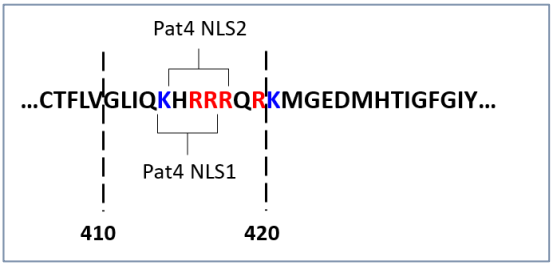

Figure 66. Prediction of Nucleolar Localization Signals in CAPN2. *Two potential Pat4 NLSs are indicated at positions 414 and 415, respectively.*

3.2.4 Disordered regions.

Non-nucleolar proteins are thought to translocate to nucleoli through direct interaction with nucleolar macromolecules such as rDNA, rRNA or nucleolar proteins. Indeed, NoLS motifs are being assumed to regulate those

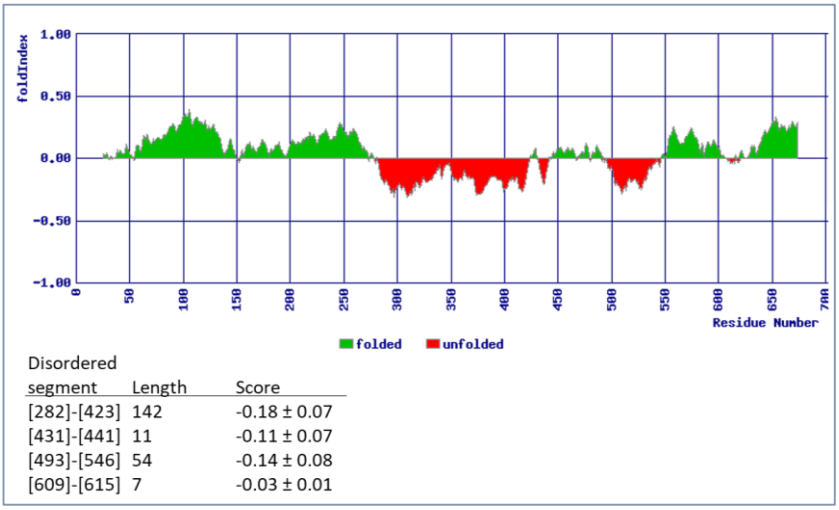

Figure 67: Prediction of folding regions in CAPN2 *Positive values (folded protein) and negative values (unfolded protein) are represented in green and red, respectively. Disordered score for the corresponding region is shown.*

interactions rather than the protein nucleolar distribution *per se*. Disordered regions have been described to be more prone to this interaction[360]. Structure disorder regions in CAPN2 were analyzed by Foldindex[323] (*https://fold.weizmann.ac.il/fldbin/findex)* which predicts disordered and flexible sequences in proteins. As can be seen in Figure 67, four regions were detected as unfolded regions followed by a folded structure towards the C-terminal end. It is interesting to note that the longest disorganized region extended from position 282 to 423 contained the NLSs, the R/K-rich sequence and the highest score for NOLS prediction.

3.2.5 Protein-protein and protein-nucleic acid interaction motifs.

In order to examine whether CAPN2 has potential interaction sites with either nucleic acid or proteins, its sequence was analysed by https://www.predictprotein.org/ database. No protein-nucleic acid interaction motif was predicted on CAPN2 sequence.

Protein-protein interaction sites were also explored. The prediction network *ISIS*[324] (https://www.predictprotein.org/ database), analyses possible interface residues involved in such interactions. Several protein-protein interaction sites were predicted in the whole CAPN2 sequence (data not shown). Interestingly, one of the protein-protein interaction predicted sites was located within our previously identified non-consensus NOLS (position 414-415) (Figure 68). Remarkably, the positively charged region rich in K-R

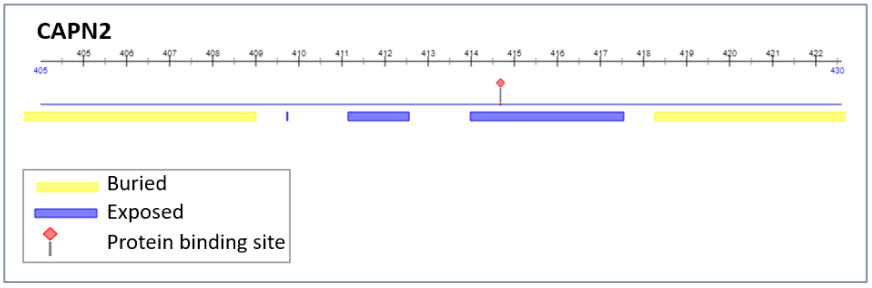

Figure 68: Prediction of protein-protein interaction sites on CAPN2 sequence. *Exposed regions and protein-protein interaction sites in CAPN2. Blue and yellow regions indicate exposed and buried regions, respectively. Red rhombus indicates protein-protein interaction sites. Graph shows protein-protein interaction sites in the sequence contained within residues 405 and 430.*

residues and the NLSs sequences were also contained within this disorganized region in the C2L domain (residues 356-514).

Despite CAPN2 sequence was not predicted as a consensus NOLS, it contains several sequence and structural factors typical of nucleolar proteins. All in all, from these data we can conclude that C2L domain seems to play an important role in nucleolar CAPN2 distribution.

3.3 ROLE OF C2L-DOMAIN IN NUCLEOLAR CALPAIN-2 DISTRIBUTION

The prediction methods use in our analysis take into account the primary and secondary structure of the protein but not the 3D structure, or importantly those conformational changes affecting CAPN2 structure. Therefore, we wondered whether CAPN2 translocation into the nucleolus was being determined by its conformational structure. Conformational changes known to affect CAPN2 structure could mask the non-consensus NoLS region within domain C2L. Actually, it seems that the interactions between anchor helix and the basic loop (residues 413–426) in domain C2L are important for CAPN1 stability and activity[35].

Consequently, to study the role of particular regions of C2L in CAPN2 nucleolar localization, we analysed nucleolar CAPN2 in breast cancer cell lines by IF using antibodies specifically recognizing Ct-C2L from CAPN2. Interestingly, anti-(Ct-C2L)-CAPN2 could recognize CAPN2 in its native conformation in all cell compartments but the nucleolus (data not shown). The same antibody recognized nucleolar CAPN2 by western blot in denaturing conditions. This result could suggest a conformational change of nucleolar CAPN2 involving the Ct-end from C2L. This region could be masked in the native conformation of nucleolar CAPN2.

A common approach to study the structural determinants of CAPNs regulation has been to express individual domains or combinations of domains. The protease core of CAPN1 or "mini-calpain" has been widely used as tool for those studies[20].

3.3.1 Bioinformatics analysis of mini-CAPN2.

To explore the role of Nt-C2L as a structural determinant of CAPN2 nucleolar localization, we first analyzed the effect of (Ct)C2L-PEF removal from CAPN2 (ΔCAPN2) on several parameters by the same bioinformatics tools as described for full length CAPN2.

As Figures 69A and B shows, positive charge or the Foldindex score were unaffected by (Ct)C2L-PEF removal in the ΔCAPN2, extending from residue 1 to 447.

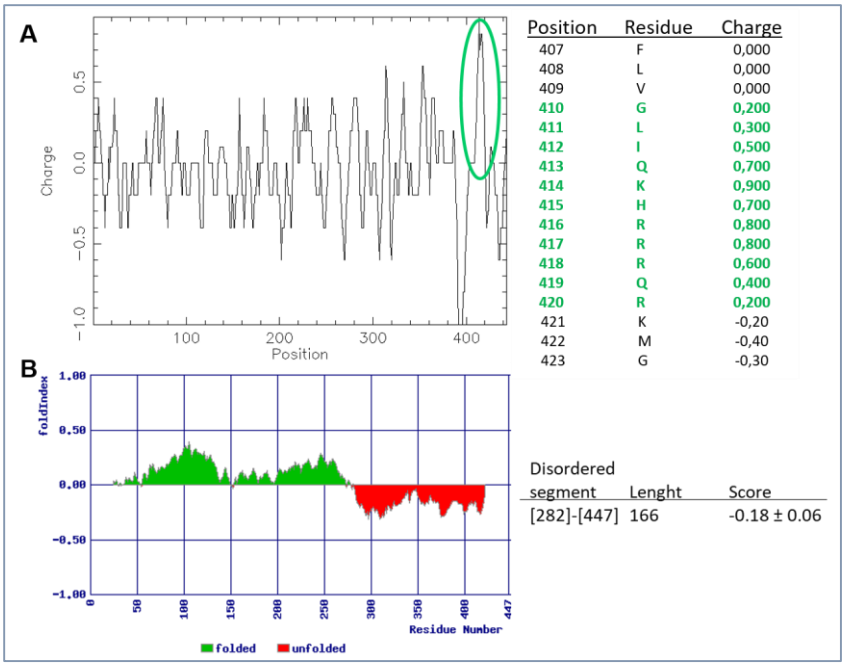

Figure 69: Prediction of charge and Foldindex score of mini-CAPN2. *(A) Amino acids charge analysis of ΔCAPN2 sequence. Residues with the higher charge score are encircled in green. The table shows the amino acid residues and corresponding charge. The highest positive charge values are highlighted in green. (B) Prediction of ΔCAPN2 folding. Positive values (folded protein) and negative values (unfolded protein) are represented in green and red, respectively. Disordered score for the corresponding region is shown.*

Interestingly, after analysis of ΔCAPN2 sequence by the NoD software, a NoLS sequence was predicted between positions 405 and 430: CTFLVGLIQKHRRRQRKMGEDMHTIG (Figure 70A). This sequence was also present in CAPN2, as can be seen in full length CAPN2 and ΔCAPN2 sequence alignment of Figure 70B (the complete sequences alignment can be found in Appendix 1). Interestingly, this NoLS sequence was included within the disordered structural region and also overlapped with the positively charged area rich in K-R residues and the NLS signal detected in CAPN2 sequence (Figure 70C).

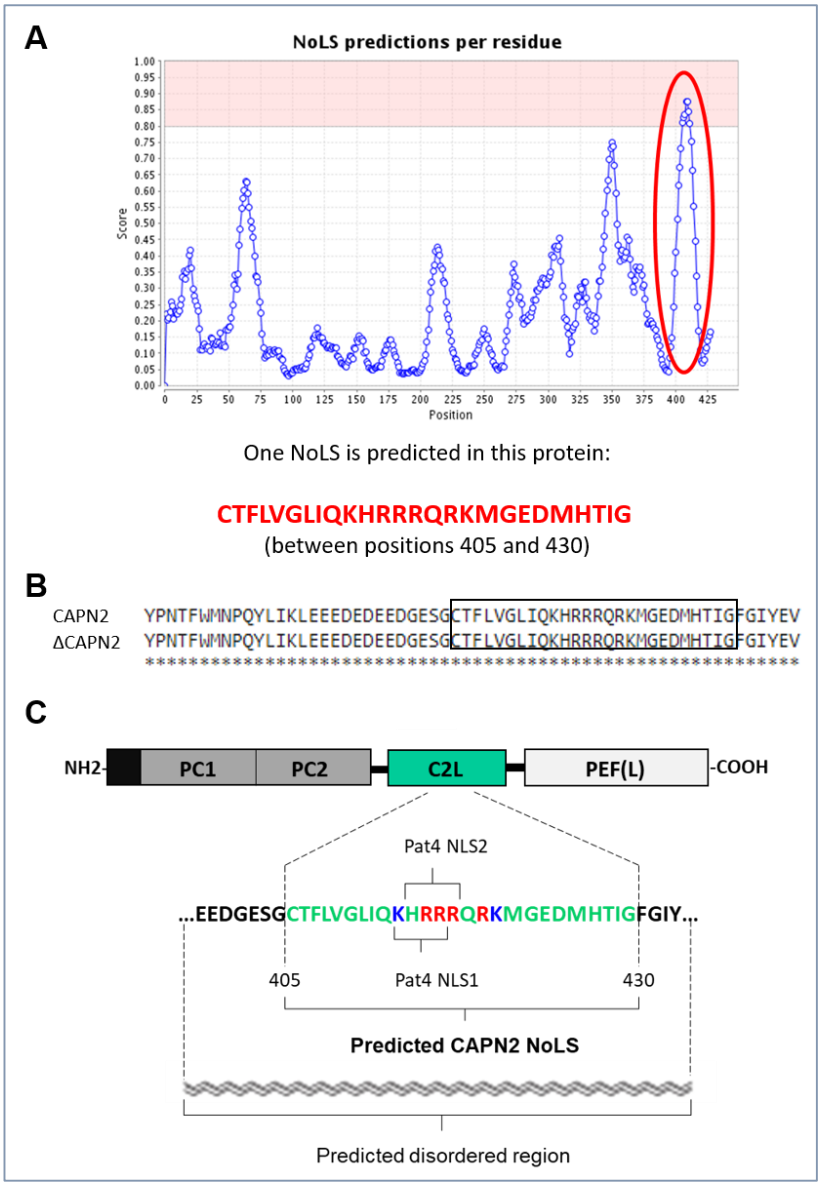

Figure 70: Prediction of NoLS signals in mini-CAPN2. *(A) NoLS prediction of ΔCAPN2. The red circle indicates the predicted NoLS region by NoD software. Predicted NoLS sequence is written in red. (B) CAPN2 and ΔCAPN2 sequences alignment. (C) Sequence and structural features of CAPN2 predicted to be involved in protein nucleolar localization.*

The tri-dimensional structure of CAPN2 (https://swissmodel.expasy.org/), (Figure 71A), and analysis of exposed sequences (https://www.predictprotein.org/) in CAPN2 revealed that the non-consensus NoLS was within an exposed region of CAPN2 structure. Surprisingly, the same analysis of ΔCAPN2 sequence, predicted a new protein-protein interaction site at the exposed region that was buried in full length CAPN2.

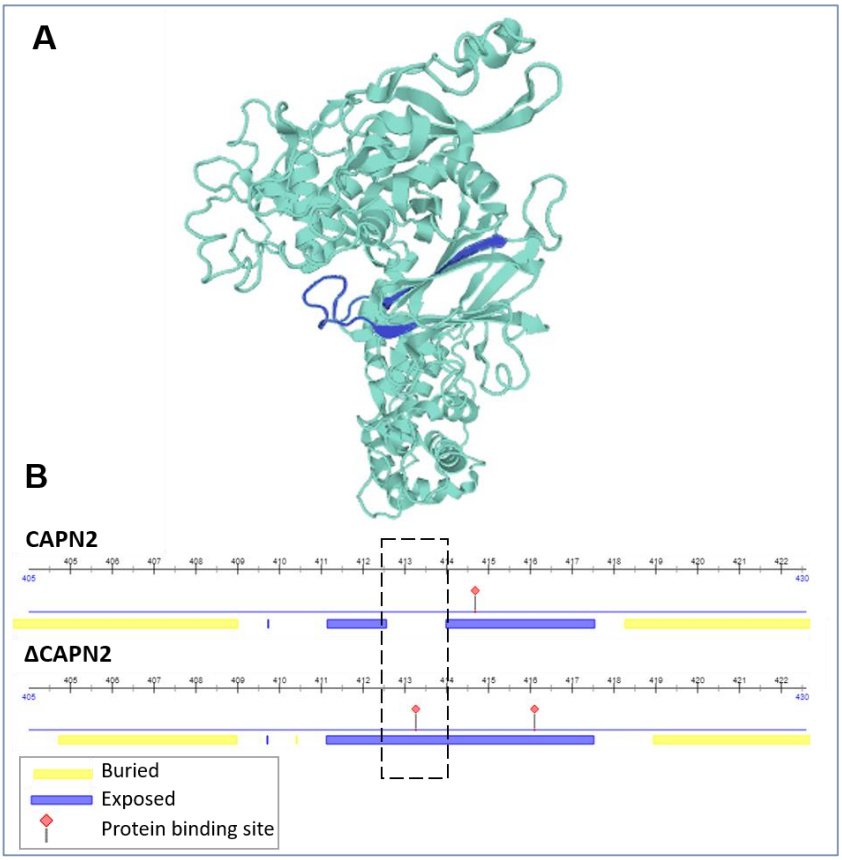

Figure 71: Study of exposed regions and protein-protein interaction sites in the CAPN2 sequence. *(A) 3D structure of CAPN2 (NoLS labelled dark blue). (B) Exposed regions and protein-protein interaction sites in the CAPN2 (upper panel) and ΔCAPN2 sequence (lower panel). Blue and yellow regions indicate exposed and buried regions, respectively. Red rhombuses indicate protein-protein interaction sites. Graph shows protein-protein interaction sites contained within residues 405 and 430 of both CAPN2 and ΔCAPN2 sequences.*

All these data sustain the possible role of NoLS as an interaction motif that could be guiding CAPN2 nucleolar internalization. Furthermore, recognition of non-consensus NoLS in CAPN2 sequence seems to be determined by its structural conformation; a conformational change might expose or bury those protein-protein interaction sites and lead to CAPN2 nucleolar or nucleoplasm localization.

3.3.2 Subcellular distribution of mini-CAPN2 in breast cancer cells.

To explore the hypothesis of C2L-PEF as a structural determinant for CAPN2 nucleolar localization, we used an DYK-epitope tagged expression vector of mini-CAPN2. The mini-CAPN2 expression vector rendered a product extending from the start of anchor helix to residue 447 in C2L-domain (Figure 72A).

The Ct-end of C2L domain was removed together with PEF domain. Truncated CAPN2 had also the DYK tag on its N-terminal end to prevent putative disturbances of protein interactions with other proteins. The DYK-ΔCAPN2 sequence was analysed by the previously described bioinformatics tool. The bioinformatics analysis did not predict any change in the structural parameters of DYK tagged-ΔCAPN2 compared to ΔCAPN2 (data not shown).

MCF-7 and MDA-MB-231 breast cancer cell lines were transfected with empty vector, full length DYK-CAPN2 or DYK-ΔCAPN2 expression vectors and analysed by western blot (Figure 72B). DYK-ΔCAPN2 product was detected by both anti-DYK antibody (Figure 72B, left panels) and anti-CAPN2 antibody (Figure 72B, right panels) as a 50 KDa protein, in agreement with the expected size based on its nucleotide sequence.

We hypothesize here that removal of structural restrictions imposed by Ct-C2L-PEF domains could condition the nucleolar localization of CAPN2. Consequently, subcellular distribution of truncated CAPN2 was analyzed in DYK-ΔCAPN2-overexpressing MCF-7 cells by IF staining with anti-DYK antibodies.

As shown in Figure 73 truncated CAPN2 was completely absent from nuclei and strongly accumulated in nucleoli of MCF7. Moreover, when compared to cells overexpressing full length DYK-CAPN2 (Figure 63) it can be observed that nucleolar concentration of truncated CAPN2 was higher than full length CAPN2.

Interestingly, as shown in Z-stack images (Figure 73), ΔCAPN2 was not only strongly found into the nucleolus but also at cell membranes.

Actually, truncated CAPN2 includes the acidic loop (E^{390}-E^{400}) in C2L domain known to facilitate interaction with membrane phospholipids[18]. These results lead us to question whether related mechanisms are driving the localization of CAPN2 at nucleoli and cell membranes.

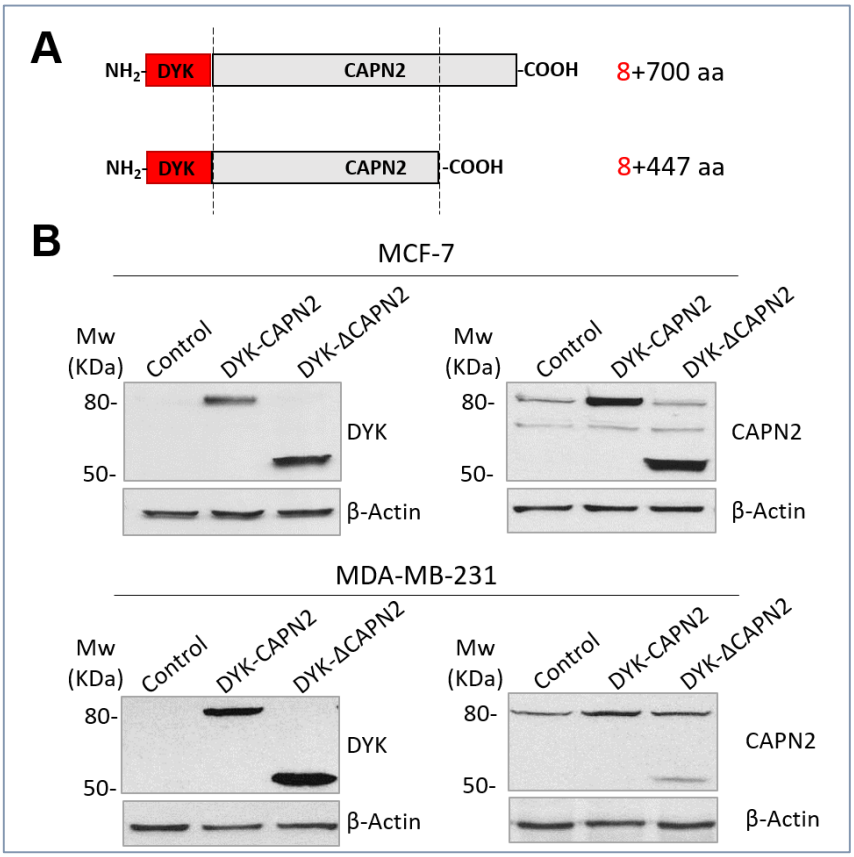

Figure 72: Full length and truncated CAPN2 overexpression in breast cancer cells. *(A) Diagram showing the products of (DYK) epitope-tagged full length and truncated CAPN2 expression vectors. (B) MCF-7 and MDA-MB-231 cells were transfected with empty (Control), DYK-CAPN2 or DYK-ΔCAPN2 expression vectors and total protein extracts analysed by western blot with either, anti-DYK (Left panels) or anti-CAPN2 (right panels) antibodies. α-Actin was used to assess equal loading. Data (n≥3).*

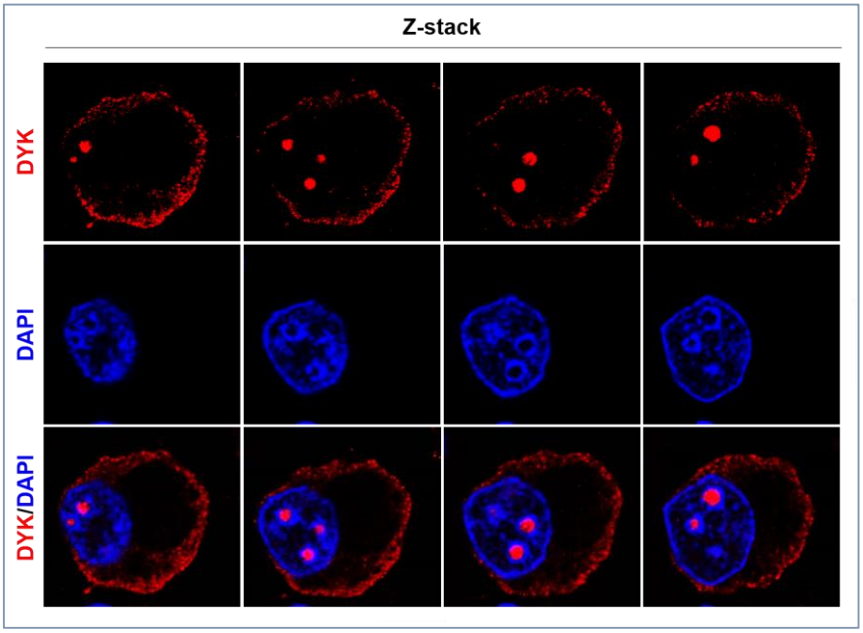

Figure 73: Detailed analysis of ΔCAPN2 distribution. *MCF-7 DYK-ΔCAPN2 overexpressing cells were analysed by immunofluorescence with anti-DYK antibody (red) counterstained with DAPI (blue) for nuclei detection. Immunofluorescence Z-stack images are shown.*

On the whole, these experimental data further reinforce our hypothesis that releasing restrictions imposed by C2L-PEF domains upon CAPN2 conformational change, might be part of the mechanisms driving CAPN2 nucleolar localization.

DISCUSSION

DISCUSSION

1. CALPAIN-1 AND CALPAIN-2 ARE NOT REDUNDANT ENZYMES

Literature regarding the involvement of each CAPN isoform in a specific cell function has always been confusing, attributing particular functions to both isoforms indistinctively. The idea of an interchangeable role for CAPN1 and CAPN2 is most probably the result of a very heterogeneous number of experimental models reported in the literature and inaccurate technical approaches. Moreover, CAPN1 and CAPN2 isoforms have the ability of recognising *in vitro* the same proteins as substrates, leading to the misconception of redundant roles for both CAPNs *in vivo*. Following that rational, most of the information regarding CAPN functions is derived from the use of unspecific chemical inhibitors of CAPN activity or substrate cleavage by recombinant CAPNs. Furthermore, since ablation of CAPN2 *in vivo* was embryonically lethal[362], experimental models to abrogate CAPN activity use CAPNS1-knockdown cells or CAST overexpression.

Nevertheless, *in vivo* each CAPN is involved in the recognition of specific proteins as substrates, and thus, of particular functions. Herein we have shown in different experimental models the isoform-specific role of CAPN1 and CAPN2. Interestingly, although in biochemical terms they would be able to recognize the same substrates, both CAPNs seem to be so tightly regulated *in vivo* by the cell microenvironment that actually do not cleave the same targets. In agreement with this, as it will be discussed later, we have shown that in post-lactating mammary gland tissue CAPN2 is the only isoform directly interacting with E-cadherin. Conversely, in breast cancer cell lines CAPN1 was the isoform mediating the cleavage of adhesion proteins and cell migration. Interestingly, our group previously showed in a cell-free assay with recombinant CAPNs and extracts from lactating mammary acini that *in vitro* both CAPNs were able to cleave LAMP2A, nucleoporins Mab414 and NUP62 or E-cadherin[88,147,325]. Moreover, the latter *in vitro* studies clearly showed that both, focal and adherens-junctions from lactating samples were cleaved when extracts were incubated with increasing concentrations of recombinant CAPN1 or -2 in the presence of Ca^{2+}. In the absence of CAPN and/or Ca^{2+}, no cleavage was observed. CAPN inhibitors blocked cleavage of adhesion

proteins induced by recombinant CAPNs, further demonstrating that *in vitro* both CAPNs were able to specifically recognize and cleave adhesion proteins from mammary gland epithelia.

All these data highlight the relevance of choosing an adequate approach for the study of CAPNs which by no means could be considered as redundant enzymes. In this sense, it could be argued that in differentiating adipocytes we observed a parallel increase of both CAPN1 and CAPN2 mRNA and protein levels, translocation to the nucleus, binding to Nt-histone H3 tails and direct or indirect modulation of adipogenic gene expression.

Adipocyte differentiation is a multifactorial process in which several signalling pathways will converge to specifically modulate each step in a sequential manner. Confluence of signalling pathways in a biological process does not mean redundancy; on the contrary, it reflects an accurate regulation of the process. Indeed, following that wrong conception we would consider redundant all the Ser/Thr-kinases triggered by a growth factor upon binding to its receptor. As it will be discussed later, even though we were not able to precisely dissect the role of isoform-specific CAPNs in adipocyte differentiation, the dramatically different distribution of both isoforms suggests that actually they do not have redundant roles in this process.

2. SUBCELLULAR DISTRIBUTION OF CALPAINS IS DEPENDENT ON THE SPECIFIC ISOFORM, CELL TYPE AND BIOLOGICAL CONTEXT

It has been suggested that specific substrate recognition is determined by the subcellular localization of each CAPN isoform within the cell. This compartmentalization would limit the substrates that could possibly be recognized by a particular CAPN isoform. CAPNs have been traditionally considered as cytoplasmic proteins. Nevertheless, now it is well known that CAPNs can translocate to different cell compartments, such as endoplasmic reticulum, Golgi apparatus, mitochondria, lysosome, nucleus and plasmatic membrane[88,90,95,125,132,147,152,155,166,235,325,363]. This translocation seems to be isoform-specific, and it is different depending on the cell type, biological context or activating stimulus.

In this work we have used different physiological and pathological models to study the localization of CAPNs as a key determinant of their

functions. We have observed here that depending on the cell type or biological context, each CAPN can translocate to specific cell compartments, such as plasmatic membrane, nucleus or nucleolus, where they exert specific functions.

2.1 THE SAME CELL TYPE, THE SAME BIOLOGICAL CONTEXT, DIFFERENT CALPAIN 1 AND CALPAIN 2 SUBCELLULAR DISTRIBUTION

Cleavage of adhesion-protein complexes plays an important role in the regulation of epithelial homeostasis that encompasses the effective clearance of undesired cells[364,365]. The role played by CAPNs and their importance in cell adhesion disruption, has been extensively reported. Furthermore, many reports have linked CAPN activity to the cleavage of adhesion complexes[111,221,238,250,366]. Nevertheless, most studies do not identify the specific CAPN isoform involved. In addition, tissue organization is not an issue to be overlooked when studying the physiological disruption of cell contacts[254]. It is important to highlight that most of the studies of cell migration and CAPNs, were carried out on two-dimensional cell culture. However, these models do no recapitulate neither the tissue environment, nor the complexity of polarized tissue structure or cross-talk between different cell types.

In this work we have used an excellent physiological model that allows the study of cell detachment processes within the tissue context. Post-lactational involution of the mammary gland is one of the best physiological models to study *in vivo* the molecular events leading to the effective clearance of secretory epithelial cells that are no longer needed.

Herein it has been shown that adhesion proteins were cleaved at 72 h of involution and that this cleavage was mediated by CAPN activity. Our data suggest that CAPN2 has a prominent role in the proteolytic cleavage of adhesion proteins in weaning-induced mammary gland involution. By mean of PLA technique, we have demonstrated that only CAPN2 co-localizes with E-cadherin at the peak of lactation. Moreover, as can be deduced from the experiments in calpeptin-treated mice analysed by PLA, E-cadherin was specifically bound to and cleaved by CAPN2 during involution. This indicates that CAPN2-mediated cleavage of E-cadherin is dependent on the specific localization of CAPN2 in the plasmatic membrane.

In addition to E-cadherin, we observed the proteolytic processing of other adhesion proteins during mammary gland involution. The cleavage of

these proteins was also dependent on CAPN activity, as demonstrated in calpeptin-treated mice. The cytoplasmic cleavage of E-cadherin, β-catenin, or talin-1 by CAPN has been already described in other tissues[111,250,284,366]. Although most likely these proteins are also CAPN2-targets, we did not demonstrate the direct role of this isoform in their cleavage. Consequently, we cannot rule out the possibility of a proteolytic destabilization of the adhesion complex as a consequence of E-cadherin cleavage[249,367,368], or the indirect effect of another target of CAPN.

Previous studies from our research group reported that CAPN1 favoured epithelial cell death during mammary gland involution. CAPN1 was mediating cell death induced by lysosomal membrane permeabilization through the proteolysis of LAMP2A[147]. In addition, CAPN1 caused nuclear envelope destabilization by cleaving different nuclear pore complex components such as NUP98 or NUP153[88] and also the release of cytochrome c from mitochondria[147]. Conversely, in those studies a completely different distribution of CAPNs was observed in adipocytes repopulating the fat pad from involuting mammary gland[88]. Now, we propose a specific role for CAPN2 in epithelial cell detachment as another mechanism of clearance of undesired cells during mammary gland involution. But importantly, in addition our data further confirm that isoform-specific distribution of CAPNs to different compartments is dependent on the cell type; in those compartments they would recognize different substrates and play specific functions which coordinated will render the final output, such as epithelial cell death and clearance after weaning.

2.2 THE SAME CELL TYPE, DIFFERENT BIOLOGICAL CONTEXT, DIFFERENT CALPAIN 1 AND CALPAIN 2 SUBCELLULAR DISTRIBUTION

Cell death induced by detachment from ECM and cell-to-cell contacts is part of a luminal clearing mechanism during mammary gland involution. But, the proteolytic cleavage of adhesion proteins by proteases can be not only the response to physiological stimuli, but also the pathological consequence of cell transformation. Therefore, having only physiological data into consideration, it might be concluded that both CAPN isoforms are involved in the epithelial cell clearance in mammary gland; each CAPN isoform following specific mechanisms and cleaving particular proteins. Nevertheless, our data

suggest that isoform-specific functions of CAPNs are not only depending on the cell type but also on the biological context.

Disruption of cell adhesions is the initial step for cell migration and epithelial-to-mesenchymal transition during breast tumour progression[247,248]. Thus, detachment of cells and luminal filling is a hallmark of breast cancer. Deregulated expression or activity of proteases involved in the proteolytic processing of adhesion proteins is known to lead to metastatic events[256,365,369].

The role of CAPNs in cancer cell migration has been extensively explored. Nevertheless, data about the isoform-specific role of CAPNs in tumour progression has been controversial[45,210,217,240,282,370]. While low levels of CAPN expression are associated with poor survival in gastric carcinomas[183,216,371], high levels of CAPN expression have been associated with breast cancer[45,201,210,280]. Nevertheless, studies of the CAPN system in breast cancer show different implications of this system depending on the breast cancer type, treatment or CAPN isoform. On the one hand, in non-inflammatory breast cancer patients, high CAST and low CAPN2 expression has been associated with improved breast cancer-specific survival. Conversely, in inflammatory cases, high CAPN1 and high CAST expression have been related with improved breast cancer-specific survival[237]. In other studies, high levels of CAPN1 were related to poor prognosis or even resistance to trastuzumab treatment in breast cancer[201,282,372]. Conversely, low CAPN9 expression has been associated with adverse-disease specific survival following endocrine therapy[217]. In studies in which CAPN levels were related to lymphovascular invasion opposing conclusions were obtained. In one of them, high CAPN2 expression was correlated with lymphovascular invasion in TNBC[210]. Conversely, in other study, high levels of CAPN1 were correlated with lymphovascular invasion in TNBC[280].

It has been argued that discrepancies among reports are most probably caused by the type of analysis performed in these clinical studies and to the different classification of breast tumour subtypes. It is important to point out that most of the former clinical studies mentioned are based just on correlations. Besides, in these studies the possible mechanism by which each CAPN isoform could be favouring lymphovascular invasion have not been studied. CAPNs have been determined to be involved in different tumorigenic processes such as cell invasion, cell transformation and cell survival[13,200]. Therefore, a merely observation of CAPN1 or CAPN2 levels with an outcome, is not sufficient to establish a functional relationship. Studies to determine the

involvement of CAPN isoforms in specific tumorigenic process could be important for the identification of CAPNs isoforms as disease prognostic factors.

Besides, understanding the deregulation of CAPNs in cell detachment during breast tumour progression requires the exhaustive study of their normal counterparts under physiological conditions. In this sense, many studies use as experimental model of 'normal cells' the human cell line MCF10A, which has recently been classified as basal subtype[373,374]. Breast cancer has been revealed as a heterogeneous disease and choosing the right cancer cell line for breast cancer research is not a minor point[273,274,278]. For that reason, we selected cell lines including the most common luminal A and luminal B subtypes (MCF-7 and BT-474, respectively) and the more aggressive triple-negative A (Basal A) and triple negative B (claudin-low) subtypes (MDA-MB-468 and MDA-MB-231, respectively).

Here, we could demonstrate in CAPN1 and CAPN2 knockdown experiments that although there were important differences in mRNA, protein levels and enzymatic activity of both CAPN isoforms among cell lines, CAPN1 was the only isoform involved in the proteolytic cleavage of adhesion proteins of breast cancer cells. It is interesting to point out that the CAPN1-mediated cleavage of adhesion protein complex was not dependent on the breast cancer subtype. Furthermore, we could co-relate CAPN1-mediated cleavage of adhesion proteins with migration processes. In agreement with this, CAPN1 had been previously identified as the major isoform involved in MCF-7 breast cancer cell line migration. Nevertheless, the selection of CAPN1 as the only isoform regulating this process was explained by the low expression of CAPN2 in MCF-7[375]. Importantly, our results showed that CAPN1 is the isoform regulating migration regardless of CAPN2 levels. Indeed, even though TNBC express high CAPN2 levels, still CAPN1 is the isoform involved in cell migration. Therefore, the regulation of this process might be due to something different than just CAPNs levels, an important statement for its obvious clinical implications.

Even though during mammary gland involution CAPN2 was the isoform found in the plasmatic membrane cleaving cell adhesion complexes, here we showed that in breast cancer cell lines CAPN1 is the isoform regulating this process. Despite cancer cell lines are originally epithelial cells, the isoform found localized in the plasmatic membrane and the one responsible of proteolyzing adhesion protein complexes is different depending

on the biological context. Although we are not unaware of possible interspecies differences, these data indicate a switch in the CAPN isoform responsible of the cleavage of adhesion complexes depending on whether it is a physiologic or a pathologic context.

2.3 DIFFERENT CELL TYPE, THE SAME BIOLOGICAL CONTEXT, DIFFERENT CALPAIN 1 AND CALPAIN 2 SUBCELLULAR DISTRIBUTION

Several studies have detected the presence of CAPNs in the nuclear compartment[154,376,377]. This CAPN compartmentalization would restrict CAPNs access to nuclear substrates. Nuclear CAPNs have been related to different cell processes, like DNA replication, cell cycle, cell death and cell differentiation[10,108,155,376]. Here we have also obtained clear data demonstrating that CAPNs translocate to the nuclear compartment, but interestingly, we have observed that CAPN isoforms show a particular subnuclear distribution pattern depending on the cell type.

As mentioned, in previous studies from our group it was shown a differential role of CAPN1 in the nuclei of mammary gland cells after weaning: while CAPN1, upon nuclear membrane translocation and NUP degradation participates in epithelial cell death, it also seems to have an important role in adipocyte differentiation and fat-pad repopulation. CAPN1 was present in the nuclei of stromal cells that were also perilipin-1-stained in weaned glands. However, in these cells, CAPN1 was not merely restricted to the peripheral nuclear membrane but it seemed internalized within the nuclei. Nevertheless, in this case, this protease was not degrading NUPs as in epithelial cells undergoing cell death, but bound to adipogenic genes.

But remarkably, apart from their unquestionable role in adipocyte differentiation, we observed a completely different subcellular distribution of CAPN1 and CAPN2 which was dependent on the cell type. Indeed, CAPN1 was preferentially localized in the periphery of nuclei and nucleoplasm of fibroblastic 3T3-L1 cells. No obvious CAPN1 was detected at fibroblastic cell membranes. However, CAPN1 was almost absent from the rest of the cell and strongly gathered at cell membranes of fully differentiated adipocytes. On the other hand, CAPN2 although also detected in nuclei, it was preferentially found in the cytosolic compartment of fibroblastic cells. At the end of TD CAPN2 was found exclusively at the cytosolic compartment of adipocytes.

This data further highlights the cell type-dependent subcellular distribution of both CAPNs.

2.4 THE CELL TYPE AND BIOLOGICAL CONTEXT AS DYNAMIC DRIVERS OF CAPN1 AND CAPN2 DISTRIBUTION

The dynamic changes taking place during pre-adipocytes differentiation could represent an excellent model to study the isoform-specific distribution of CAPNs in a progressively changing biological context within a gradually changing cell type.

In differentiating 3T3-L1 adipocytes we have seen by IF and WB analysis that both, CAPN1 and CAPN2 translocate to the nuclear compartment, where they are involved in the regulation of the differentiation course. CAPNs are known to actively participate in the differentiation processes of different cell types; It has been widely studied the involvement of CAPNs in differentiation of neural stem cell[10] and mesenchymal stem cell, chondrocytes, osteoblasts or even adipocytes[332]. However, little is known about the implication of specific isoforms in this process. This is because most of these studies are based on unspecific approaches, such as treatment with ALLN. In addition to CAPNs, ALLN can also inhibit other proteases like cathepsins, neutral cysteine proteases or the proteasome. Therefore, conclusions obtained from these studies should be carefully interpreted. In many of these studies, their conclusions are also supported by CAST overexpression experiments. Although these data reinforce CAPN involvement in adipocyte differentiation, since CAST can inhibit different CAPNs, information regarding the implication of each CAPN isoform in this process is still missing.

Here we have presented data showing that both CAPN isoforms participate in 3T3-L1 differentiation into adipocytes, and that each CAPN isoform is differently involved in this process. CAPN1 and CAPN2 expression analysis indicated that both isoforms were induced after the differentiation stimulus and progressively increased during ED-TD transition, being downregulated once 3T3-L1 achieved complete differentiation.

2.4.1 CAPNs in the modulation of MCE during pre-adipocyte differentiation.

Although this temporal pattern of CAPNs expression might lead to the conclusion that both CAPNs are modulating ED-TD transition, our results indicate that again, the pattern of CAPN expression do not necessarily reflects the time point for CAPN activation and the earlier effects of its activity.

Indeed, our analysis of MCE-ED transition in calpeptin pre-treated 3T3-L1 fibroblasts, showed decreased perilipin-1 levels and lipid droplets content, supporting that CAPN activity is important during the early events of 3T3-L1 differentiation. Furthermore, we could observe a dramatic increase of CAST levels after MCE. CAST levels have been suggested to increase to limit an excessive CAPN activity. Consequently, our data indicate that CAPN activity was upregulated during MCE. However, a role for CAPN activity at very earlier time points cannot be ruled out. Indeed, the approaches followed in these experiments would not allow the detection of a low but functionally significant increase of CAPN activity soon after MDI-treatment. Actually we could observe CAPN1 and CAPN2 interaction with Nt-histone H3 tails soon after MDIR-treatment (data not shown) suggesting that both CAPNs are participating in the very early events of adipocyte differentiation.

All in all, this temporal expression pattern of CAPNs indicates that both isoforms are important regulators of the MCE, either by triggering or modulating this phase. In agreement with this, a role for unidentified CAPNs in the modulation of MCE has been already suggested. Although the mechanisms and targets of those CAPNs remain elusive, several hypotheses have been raised:

(i) *Mechanisms of MCE modulation by CAPN-mediated cleavage of p27*

CAPNs might regulate the entry into mitotic clonal expansion by cleaving p27, a CDKs inhibitor. Degradation of p27 allows cells to re-enter the cell cycle and start the MCE phase. In this study, authors concluded that the degradation of p27 was mediated by CAPN activity.

Nevertheless, the experimental procedure in this study was not accurate enough. Conclusions were obtained based just on experiments performed with ALLN, a non-specific CAPN activity inhibitor, or digestions with recombinant CAPNs[108].

(ii) *Mechanisms of MCE modulation by CAPN-mediated modulation of transcription factors*

This hypothesis postulates that CAPNs will modulate the early phases of adipocyte differentiation by regulating the expression of different transcription factors. Pre-adipocytes treated with ALLN showed an impaired adipocyte differentiation and reduced adipose specific gene expression, such as C/EBP-α, aP2/422 or SCD-2[157].

However, in these studies, the involvement of specific CAPNs was not clear. Our results in knockdown pre-adipocytes indicate that both, CAPN1 and CAPN2 might be directly or indirectly involved in the modulation of C/EBPα and leptin expression. C/EBP-β is the transcriptional activator of C/EBP-α. In pre-adipocytes, C/EBP-β has been shown to dimerize with CHOP-10, a dominant-negative isoform of C/EBP-β. It has been suggested that CAPN activity was involved in the suppression of CHOP-10, as ALLN treated pre-adipocytes showed increased CHOP-10 mRNA levels[156]. We cannot discard a role for both CAPNs in the modulation of transcription factors activity during the time-course of adipocyte differentiation, but since both, CAPN1 and CAPN2 silencing have the same effect on C/EBP-α and leptin gene expression we should conclude that most probably CAPNs are modulating previous steps. Since adipocyte differentiation is a sequential process, blocking a key step of MCE would result in inhibition of any of the following steps in the process.

(iii) *Mechanisms of MCE modulation by isoform-specific CAPNs: Putative role on chromatin rearrangements*

Previous experimental data obtained in our laboratory suggested that CAPN1 was participating in the epigenetic program of adipocyte differentiation during mammary gland involution. CAPN1 was suggested to be involved in the cleavage of the N-terminal (N-t) tail of histone H3, and it was found to be associated with the promoters of some adipogenic genes, such as CEPB-α and leptin[88].

In this work, we have obtained data supporting that CAPN activity might be involved in histone H3-cleavage during MCE of 3T3-L1 differentiating pre-adipocytes: (i) In calpeptin pre-treated fibroblasts the accumulation of cleaved-histone H3 at ED-TD was prevented. (ii) In CAPN1 and CAPN2 knocking down experiments we observed that in both cases

cleavage of N-t histone H3 was prevented. (iii) Finally, during MCE a direct interaction between CAPN1 and CAPN2 with Nt-histone H3 tails was detected *in vivo* by PLA assay.

Despite the significance of histone cleavage is not completely understood, it has been postulated that such cleavage alters the epigenetic signature and chromatin compaction, and could be involved in transcriptional regulation[352]. In particular, it has been observed that the N-t of histone H3 is cleaved during cell differentiation[88,378,379]. Histone H3 contains numerous sites that are susceptible to proteolytic processing. Indeed, several proteases have been observed to be involved in such proteolysis[380]. For example, cathepsin L is responsible of the cleavage histone H3 N-t during mouse embryonic stem cell differentiation[379]. Nevertheless, other studies have claimed that histone H3 proteolysis could be a consequence of histone degradation or an artefact during the extraction procedure[381]. In spite of this, we have been able to demonstrate *in vivo* for the first time the direct interaction of CAPN1 and CAPN2 with the N-t end of histone H3 by the sensitive PLA technique. However, the apparently redundant effect of both CAPNs on H3-cleavage further complicates its interpretation:

- Data from PLA assays shows that both CAPNs are in direct contact with histone H3, but not that they are both processing histone Nt-tails at the same residue. It has been published previously that the promoters of genes playing key functions in development and differentiation have the bivalent signal H3K4me3/ H3K27me3[382–384]. The nuclear localization of these 'bivalent' genes was found along the nuclear border of immature cells and dramatically rearranged towards the central nucleoplasm in differentiated cells[353,385,386]. Therefore, CAPNs could differentially mediate the relocation and expression of different genes through the isoform-dependent cleavage of Nt-tails at specific residues.
- Although, CAPN-histone H3 interaction *in vivo* is undoubtedly an important finding, analysing objectively our data it does not fully demonstrate a direct cause-effect relationship between CAPNs and histone H3-cleavage. As previously mentioned, blocking one step within a sequence of events would also block the next series of events. Therefore, we cannot be sure whether calpeptin or CAPNs silencing prevented a step prior to histone H3-cleavage by other protease. Actually, PLA data shows CAPN/histone H3 interaction, but not necessarily histone H3 cleavage by

both enzymes. In this sense, it is noteworthy to mention that while recombinant CAPN1 cleaves histone H3 *in vitro*, CAPN2 was not able to process histone H3[88]. CAPN2 could be part of a protein complex including histone H3.

Specific rearrangements of chromatin in the nucleoplasm are known to be the result of the interaction of nucleosomes with proteins from the inner nuclear membrane, nucleoskeleton and nucleocitoplasm[387]. Moreover, during mitosis, to accomplish chromosome segregation, the interactions between all these proteins and chromatin are broken[388]. In this sense, it is important to mention that, despite both CAPNs interact with histone H3, PLA experiments showed higher CAPN1 interaction with the N-t of histone H3 than CAPN2 at a particular time-point of MCE. This could mean that despite both CAPNs could interact with N-tail of histone H3, each one could have different functions during MCE of differentiating 3T3-L1 cells.

Indeed, in agreement with this, we have observed that CAPN1 and CAPN2 were differentially distributed during 3T3-L1 differentiation into adipocytes. IF analysis of mitotic cells showed that during prophase and metaphase CAPN2 localized to foci on condensed chromosomes. As cells progressed from metaphase to anaphase CAPN2 was spread along chromosomes. At late anaphase and telophase, CAPN2 was intensely covering condensed chromosomes. Despite we could not identify the targets of CAPN2 during MCE, its localization would indicate that CAPN2 might be regulating some specific process involved in chromosome alignment or segregation. In support of this, it has been previously reported that CAPN2 is involved in chromosome alignment and segregation during mitosis of HeLa cells by regulating polar ejection forces[167].

Conversely, CAPN1 seemed to localize closed to the mitotic spindle during metaphase and at the spindle midzone and cleaved furrow in cells progressing from anaphase to telophase. The NE acts as a peripheral scaffold to spatially organize chromatin. Once mitosis is completed, the dispersed NE proteins are assembled to organize the interphase nuclear architecture. NE re-assembly requires the coordinated action of many cellular activities such as, nucleocytoplasmic transport, membrane fusion as well as the action of cytoskeleton motor-proteins[388]. CAPN1 has been extensively documented to be involved in cytoskeleton remodelling[6,139]. It could be possible that CAPN1 might be additionally controlling mitosis by regulating these processes.

Nevertheless, this possible role of CAPN1 prior and during mitosis would need further exploration.

On the whole, although we were not able to decipher the isoform-specific role of CAPNs on histone H3, our observations of CAPN1 and CAPN2 localizing at different subcellular structures during MCE strongly indicate that they are bound to diffcerent subsets of targets which are involved in the modulation of unique functions. Identifying target proteins and how they are selectively and temporally modulated by CAPN1 and CAPN2 throughout the cell cycle are important questions which remain to be answered.

2.4.2 CAPNs in the modulation of ED-TD transition during pre-adipocyte differentiation.

As shown in our IF studies, upon MCE exit at the early G1 and during ED-TD transition, the signal from CAPN1 was progressively fading away from the nucleoplasm and concentrated in nuclear substructures. Nuclear CAPN1 re-location was accompanied by a dramatic increase of the enzyme in the cytosolic fraction. Importantly, upon 3T3L1 TD into adipocytes, CAPN1 was detected mostly surrounding perilipin-1 droplets and at cell membranes. These results suggest a cytosolic-independent role for CAPN1 in the remodelling of the nuclear architecture upon mitosis exit and/or the reassembly of nucleoli.

During mitosis, rRNA is shut down and nucleoli dissembled. Upon mitosis exit the transcriptional machinery is reactivated at the nucleolar organiser regions where nucleoli are reassembled. Some pre-nucleolar bodies thought to be intermediates of nucleoli reconstitution are fused to reformed nucleoli. After the analysis of phase contrast images, we could observe that nuclear CAPN1 aggregates were strongly overlapping with highly dense nucleolar regions. Importantly, CAPN1 nucleolar localization has never been described before.

In agreement with a role for CAPNs in this subnuclear structure the localization of other CAPNs such as the tissue-specific CAPN3[102,103], CAPN single isoform from *Plasmodium falciparum*[389] or CAPN2 have been reported to be localized in the nucleolar compartment[93]. Interestingly, we recently reported the role of nucleolar CAPN2 as a transcriptional repressor of 47S pre-rRNA transcription in CRC cells under growth limiting conditions. Moreover, we suggested a putative role for CAPN2 as a sensor for external cues,

repressing rRNA synthesis under stress conditions such as serum or growth factor deprivation[93]. Nevertheless, since CAPN2 showed a completely different pattern of subcellular distribution during ED-TD transition, CAPN1 location in differentiating pre-adipocytes seems to be related to the isoform-specific role of CAPN1 at this stage of adipocyte differentiation, Consequently, as described for CAPN2 in other biological context, CAPN1 might have a role as a suppressor of rDNA transcription during the early burst of adipogenic gene expression.

In line with this, it is known that during cell differentiation rRNA transcription is downregulated[390,391]. After 3T3L1 MCE and when adipogenic gene expression is triggered, the rRNA expression is suppressed[392]. Most importantly, would our hypothesis be confirmed, the consequences of rRNA shutdown in this biological context could involve important genomic rearrangements within the nuclear compartment. Indeed, it has been recently shown that rRNA genes are not only involved in rRNA synthesis[393].

During MCE we observed multiple nucleoli that were progressively fusing during ED-TD transition. In fully differentiated adipocytes a single nucleolus was observed. Large-scale reorganization of the genome is indicated by the formation of a single nucleolus from multiple nucleoli upon differentiation[394]. Heterochromatin condensation of ribosomal RNA genes has been recently reported to attract highly condensed chromatin structures outside of the nucleolus. The formation of such transcriptionally repressed heterochromatin promotes transcriptional activation of differentiation genes[385].

Interestingly, this specific subnuclear localization was also observed in breast cancer cell lines. However, in this case was CAPN2 and not CAPN1 the isoform that was internalized/retained within the nucleolus. Again, as we showed for the CAPN-dependent cleavage of adhesion proteins, we observed a molecular switch between CAPN1 and CAPN2 that was dependent on both, the cell type and the biological context. Despite here we have not explored a possible function of CAPN1 or CAPN2 in the nucleolus, is tempting to think that in breast cancer cell lines and in 3T3-L1 differentiation, CAPN2 and CAPN1, respectively, might be involved in the regulation of rRNA expression.

Nevertheless, many different functions take place in the nucleolar compartment, and therefore the role of CAPNs in this compartment should be further studied. Indeed, the nucleolus is the biggest subnuclear compartment,

being the ribosomal biogenesis, rDNA transcription, pre-rRNA processing and finally ribosomes assembly the main process that takes place there[168,172]. Nonetheless, now it is known that the nucleolus regulates many other cellular functions, such as cell stress, cell cycle, cell replication, DNA repair, apoptosis induction and biogenesis of non-ribosomal nucleoproteins[169]. In the near future, it would be interesting to perform proteomic analysis to identify possible CAPN substrates within nucleoli which might shed some light about the role of these proteases in the nucleolus.

3. REGULATION OF CALPAINS SUBCELLULAR LOCALIZATION

An important question regarding the mechanisms driving the specific CAPN isoform to a given subcellular localization remains to be answered. Ca^{2+}- binding has been widely studied to unveil the mechanisms of CAPN activation. Ca^{2+} influx is known to locally increase in response to several stimuli, but it does not seem to be the driving force for isoform-specific CAPN localization.

CAPN2 binding to membrane lipids seems to be an important mechanism for both, its activation[40,97] and membrane localization. Phosphorylation of specific amino acids of CAPN2 by PKA or extracellular regulated kinase (ERK) has been suggested to prevent or induce its stable binding to phosphoinositides, respectively[40,73,97]. Moreover, it has been proposed that CAPN2 needs to be bound to membrane PIP_2 to be activated by stimuli triggered by EGFR pathway. Indeed, CAPN2 activation can be prevented by internalization of EGFR or ERK[91], indicating that the EGFR pathway from the cytosolic compartment cannot reach or affect membrane-bound CAPN2. MAPK/ERK pathway is one of the most important pathways known to be triggered during mammary gland involution. CAPN2 activation by ERK during involution is most likely supporting its localization at plasma membranes during involution.

Nevertheless, our data from breast cancer cell lines showed that CAPN1 and not CAPN2 was the isoform involved in the cleavage of adhesion proteins at the plasma membrane. It is noteworthy to mention that CAPN1 and CAPN2 have been found to be redistributed to the sites of locomotion in cultured cells forced to migrate[111,395]. In breast cancer cell lines both isoforms were found in the cytoplasmic compartment to a greater or lesser extent. EGFR pathway is one of the major deregulated pathways in breast cancer[396];

whether the mutational state of this pathway could drive the isoform fate of CAPN2/CAPN1 in breast cancer remains to be elucidated.

On the other hand, we cannot rule out the possibility that culture conditions might affect the switch of the specific CAPN isoform involved in cell adhesion of breast cancer cells that were grown on plastic plates. Therefore, in the future, an *in vivo* study analysing not just CAPN1/CAPN2 expression, but rather the direct interaction of specific isoforms with E-cadherin in breast cancer samples, would help to elucidate this important question.

However, not resting importance to the mechanisms so far described for the specific distribution of CAPNs to cell membranes, our data add relevant information regarding a new localization for both CAPNs in nucleoli of adipocytes or breast cancer cells. Since this is the first description, there is no data in the literature regarding the mechanism behind this new localization of CAPNs. Although aware of the limitations of this preliminary study, our first experimental observations and bioinformatics analysis may lead to speculate with several hypotheses derived from CAPNs structure.

3.1 CONFORMATIONAL CHANGES MEDIATING CALPAIN DISTRIBUTION

It has been suggested that the non-core domains of CAPNs have ancillary roles in their enzymatic activity. It is thought that C2L and PEF domains from large and small subunits would provide an additional regulation but still, the core enzyme can be active in the absence of these domains[20]. In agreement with this, we observed that both CAPNS1 and CAST were absent from nucleoli of breast cancer cells.

Under some pathological conditions CAST is eventually proteolyzed[1]. In addition, the C2L domain is known to be very susceptible to proteolysis. When the native enzyme containing the catalytic and regulatory subunits is proteolyzed, the C2L domain is cleaved, releasing the PEF domains of the two subunits as a stable heterodimer[20]. As a consequence, the restraint movement of PC1 and PC2 core domains will be release resulting in active enzyme.

Interestingly, our analysis in nucleolar fractions from adipocytes and breast cancer cells showed a higher electrophoretic mobility for CAPN1 and CAPN2, than the matching CAPN in nucleolar-less fractions. However, although nucleolar CAPNs could be partially cleaved, the difference between the expected and the observed sizes was not in agreement with a complete

removal of C2L-PEF domains from nucleolar CAPNs. Our results in breast cancer cells rather suggest that most likely C2L-PEF domains suffered a post-translational modification in the nucleoplasm that is removed in the nucleolus. This modification could mediate the conformation of CAPNs. In the case this hypothesis would be confirmed, it would explain CAPNS1 or CAST release from CAPNs catalytic subunit in nucleoli.

In agreement with a conformational change affecting C2L domain, we have observed that native CAPN2 was not detected by IF in nucleoli from breast cancer cells when using antibodies recognizing Ct-CAPN2 (not shown). It could be argued that the antibodies used in our studies were not specifically recognizing CAPN2 but an artefact. Nevertheless, herein we present evidences demonstrating the specificity of antibody-recognition: A specific blocking peptide prevented antibody recognition of endogenous CAPN2 by western blot and, anti-DYK antibody recognized overexpressed DYK epitope-tagged-CAPN2 in the nucleolar compartment of MCF-7 cells. These results and our bioinformatics analysis of CAPN2 led us to hypothesize that a post-translational modification affecting CAPN2 Ct-domain would not only induce a conformational change of the enzyme, but could release the constraints of the protease core. This conformational change could expose functional residues previously masked in the structure of CAPN2.

In support of this notion, conformational changes of CAPNs are the basis of CAPNs activity. Ca^{2+}-binding to CBSs at the PC1 and PC2 domains rearranges the structure and activates CAPNs[18,20,32,33]. In addition, phospholipid binding and phosphorylation also modify CAPNs structure, which are determinant for their activation and distribution. For example, PIP_2-binding and ERK phosphorylation mediate CAPN2 activation and translocation to plasma membrane[40]. Besides, the internalization of CAPN2 into RE and GA lumen seems to be a consequence of CAPN2 intramolecular conformation change[90]. Therefore, as happens with other motifs that are exposed after protein conformational changes, it would be reasonable to think that a structural change might be behind this new subcellular localization of CAPN1 and CAPN2. Nevertheless, the leading cause of this CAPNs structural change is still unknown.

3.2 PUTATIVE ROLE OF C2L DOMAIN IN SUBCELLULAR DISTRIBUTION OF CALPAINS

A common approach to gain some structural information about CAPN isoforms has been to express individual domains or combinations of domains

from different isoforms, particularly the protease core. Indeed, the protease core of CAPN1 or "mini-calpain" has been a useful tool to study target sequence preferences, stability, inhibitors design, etc[20]. Following the same approach, we overexpressed mini-CAPN2 as a tool to study the role of C2L domain as part of the mechanisms of CAPN2 distribution in breast cancer cells.

The mini-CAPN2 has been reported to have very little proteolytic activity compared to mini-CAPN1. The low activity of CAPN2 is explained by a Gly^{203} instead of Ala^{203} found in CAPN1. The glycine-containing isoforms have an increased sensitivity to autoproteolysis after removal of C2L domain[35]. However, it seems that the interactions between the anchor helix and the basic loop (residues 413–426) in domain C2L can prevent the collapse of core domains. Therefore, our construct for truncated CAPN2 extends from the anchor helix to residue 447 in domain C2L.

Interestingly, removal of part of C2L and PEF domains from CAPN2 rendered a dramatic change in its subcellular distribution. Although higher levels of CAPN2 were detected, overexpression of full length-CAPN2 followed the same subcellular distribution as endogenous CAPN2 detected in control cells. Conversely, truncated CAPN2 was strikingly accumulated in nucleoli and cell membranes of MCF-7 cells.

For technical reasons we were not able to measure CAPN activity in nucleolar fractions from transfected cells. Therefore, we cannot discard that a low protease activity of truncated CAPN2 could be conditioning its subcellular fate. However, even after films over-exposure we could not detect any sign of additional mini-CAPN2 cleavage in our analysis of truncated CAPN2 by western blot.

These results most likely suggest the presence of regulatory sites within the first 447 amino acids important for the subcellular distribution of CAPN2. This is in agreement with our bioinformatics analysis and previously reported data. A post-translational modification in the C2L could induce a conformational change of CAPN2 exposing previously buried residues involved in nucleolar localization. Actually, the acidic loop in C2L domain also present in truncated CAPN2 is known to mediate CAPN2 binding to cell membranes. Accordingly, we observed that truncated CAPN2 was strongly accumulated in nucleoli and cell membranes from DYK-ΔCAPN2-overexpressing MCF-7 cells.

Previous reports in the literature already linked CAPN distribution at cell membranes and nucleoli. The single CAPN version of *Plasmodium falciparum* on its palmitoylated form is bound to cell membrane, while on its de-palmitoyated form it enters the nucleolus[389]. Despite sequence analysis of CAPN1 and CAPN2 do not predict any phenylation, myristolation, palmitoylation or glycophosphatidylinositol fatty acid modification sites that could anchor the protease to cell membranes[99] CAPNs are known to bind to membranes. Thus, although these modifications seem not to be determinant for CAPN1 or CAPN2 nucleolar entrance, following the same mechanism as CAPN from *Plasmodium falciparum*, a post-translational modification could release CAPNs from membranes and induce the nucleolar translocation.

3.3 CALPAINS DIMERIZATION

Intact CAPN2 large subunits are known to be also subjected to inhibition by C2L-proteolysis, which can be prevented through assembly of the heterodimers. We might speculate with the idea of CAPN2 dimerization than upon activation, could drive CAPN2 to different cell compartments.

3.3.1 CAPNs dimerization with CAPNs end-products.

Conversely to many other proteases, CAPNs are known to exert limited proteolysis on their substrates in such a way that alter their original functions. However, in order to fully comprehend the mechanisms behind CAPNs cellular fate, it would be mandatory to have knowledge of all their substrates, as well as the functions derived from their specific processing events. This is currently far from the case, as most of CAPN substrates or the implication of such processing have not been fully understood.

It has been reported that CAPNs can dimerize with their processed substrates[48,49,397,398]. That dimerization could have a number of consequences not only for the end-products of CAPNs, but also for CAPN itself which could experience a conformational change, a different subcellular localization or a limited enzymatic activity.

In this work we have observed in mammary gland tissue samples that the fragments of E-cadherin remained bound to CAPN2 and accumulated in the cytosol at 72 h of involution. In this sense, it is known that the fate of cytoplasmic fragments of E-cadherin can be the proteasomal degradation or alternatively, the acquisition of a different biological function related to cell

proliferation or cell death through the activation of signalling pathways[222,365,399,400]. CAPN-mediated cleavage of E-cadherin has been reported to result in a stable 100 KDa molecular weight protein. This E-cadherin fragment has been linked to apoptotic processes in mammary and prostate cancer cells[250,401]. This new acquired function of the truncated E-cadherin would be consistent with the apoptotic context of epithelial cells during involution. Therefore, CAPN2 could be involved in the epithelial cell death program by a dual mechanism: by promoting epithelial cell detachment and by rendering pro-apoptotic E-cadherin fragments or even E-cadherin/CAPN2 dimers.

Interestingly, in the cytosol of MCF-7 cells cleaved E-cadherin was also observed by IF and PLA assays to remain bounded to CAPN1. Nevertheless, in this case the cell context is different, and therefore we cannot assume that in both situations the implication or meaning of this cytosolic E-cadherin-CAPN1 interaction would be the same. In line with this, other studies have reported an apoptotic suppressive role of nuclear E-cadherin in staurosporine stimulated cells. It was observed that nuclear E-cadherin formed a complex with DNA through the interaction with p120 and regulated gene transcription from Kaiso-regulated promoters[367].

Moreover, CAPN1/talin-1 PLA in MDA-MB-231 breast cancer cell line indicated that this interaction was taking place in the cytosol in addition to cell membranes. Inactive talin-1 is abundant in the cytosol compartment and after activation it translocates to plasma membrane to bind to integrins and the actin cytoskeleton[327]. Talin-1 cleavage by CAPNs increases affinity of talin-1 for β3-integrin, and also modulates integrin activation and clustering[124]. Therefore, deciphering whether talin-1 cleavage by CAPNs is favouring either focal adhesion formation or disassembly could be important for understanding the specific regulation by CAPNs of this process.

Nevertheless, if the functions of the cytosolic fragments of E-cadherin or Talin-1 are not completely understood, the effects of their dimerization with calpain on the protease distribution have not been even explored[402].

3.3.2 NoLS-mediated dimerization of CAPNs with nucleolar chaperone-like proteins.

Unlike other cellular membrane-delimited compartments, whose protein-trafficking is mediated by specific targeting systems that recognize common consensus sequences, the precise mechanism by which proteins are

retained within the nucleolus is currently unknown. Nevertheless, nucleolar proteins share some sequence features and in many of them have been identified different NoLS[356,361]. Those NoLS are not recruiting signals but rather they are thought to mediate the interaction with nucleolar proteins or nucleic acids, which favours non-nucleolar proteins internalization into the nucleolus. Several nucleolar proteins can interact with many non-nucleolar proteins, which would explain the great diversity among NoLS sequences[360]. In this sense, CAPN3 which is known to contain two NoLS, translocate to nucleoli of melanoma cell lines by interaction with the nucleolar protein Def (Digestive organ expansion factor)[101-103].

Based on different bioinformatics analysis, we have identified a non-consensus NoLS in the CAPN2 sequence that might be involved in this nucleolar internalization. These motifs are characterized by R/K rich sequences[361], positively charged residues[357], overlapping NLS signals[359] and disorganized structures[360]. We found that CAPN2 contains a sequence which fulfilled all the features to be recognize as a NoLS.

Here we have presented evidences that seem to indicate that a change of CAPN2 structural conformation might expose this sequence to be recognized as a NoLS. The study of CAPN2 sequence by different bioinformatics tools showed that the non-consensus NoLS could be masked and that only after removing the C-terminal folded region, this sequence would be exposed. In agreement with this, overexpression of truncated CAPN2 lacking the C-terminal end (DYK-ΔCAPN2) suggest that a structural change is determinant for CAPN2 localization.

DYK-ΔCAPN2 construct renders a protein 250 amino acids smaller than the endogenous one. This could lead to the idea that big structural changes are needed for CAPN2 nucleolar targeting. However, bioinformatics analysis predicted that 30 amino acids were the minimum C-terminal fragment that had to be removed for the CAPN2 NoLS sequence to be detected by the NOD predictor. This might indicate that a small conformational change would be sufficient to uncover CAPN2 NoLS. Although we have not proved that a structural change would favour the recognition of NoLS in CAPN1, data obtained from the bioinformatics analysis points also to this.

Interestingly, this region showed also protein-protein interaction sites, which could be involved in CAPNs-nucleolar protein interaction, supporting the hypothesis that these sequences might be involved in CAPNs nucleolar targeting. However, in order to further confirm that this motif is actually

responsible for CAPNs nucleolar internalization, it would be necessary to analyse subcellular distribution of overexpressed CAPN2 with mutated non-consensus NoLS.

3.3.3 Post-translational modifications mediating CAPN dimerization.

Different factors have been reported to modify NoLS recognition, like post-translational modifications or ligand binding, which alters protein structure and enables the interaction with the anchoring protein. The most common post-translational modifications that influence nucleolar targeting are phosphorylation[403–406] and sumoylation[407,408]. For example, nucleophosmin is a nucleolar protein that is involved in nucleolar protein import. This protein binding is determined by phosphorylation. Phosphorylation of nucleophosmin, weakens nucleophosmin interaction with nucleic acids, and thus allows its binding to proteins[404]. CAPN1 and CAPN2 have nine and eight different phosphorylation sites, respectively[1]. As previously explained, phosphorylation is involved in CAPN activation and modulation of their distribution[40,73,92]. However, the physiological meaning or the functional implication of all phosphorylation sites are not completely understood. Therefore, it would be interesting to explore whether the phosphorylation pattern of CAPNs might be involved in NoLS recognition or nucleolar targeting.

Sumoylation is a kind of posttranslational protein modification by which a protein is conjugated with a SUMO(Small ubiquitin-like modifier) protein[409]. This modification regulates several protein functions, especially in the cell nucleus, and is also involved in protein targeting into the nucleolus[410,411]. CAPN2 has been reported to be sumoylated at K360[412]. It was determined that sumoylation positively regulated CAPN2 activity and had influence on cell motility. Nevertheless, in that study the localization of SUMO-CAPN2 was not evaluated. In this sense, CAPN5 is abundant in the nuclear compartment of cells in the central nervous system, and in particular in promyelocytic leukemia (PML) nuclear bodies. This CAPN5 nuclear and PML internalization is mediated by two NLS, containing one of these a SUMO-interacting motif involved in this distribution[413].

In addition to phosphorylation and sumoylation, other posttranslational modifications such as methylation, acylation or palmitoylation could also mediate protein nucleolar localization.

CONCLUSIONS

CONCLUSIONS

In the present study we have explored the relationship between CAPN1 and CAPN2 isoforms subcellular localization with their involvement in different cell functions, such as cell adhesions cleavage and cell differentiation. Based on the results presented herein we have concluded that:

1. CAPN1 and CAPN2 isoforms do not have redundant functions since the substrate recognition is isoform-specific in both, physiological and pathological conditions.

2. Depending on the cell type or cell context, each CAPN isoform shows a specific subcellular distribution, which ranges from plasma membrane to nuclei or nucleoli.

3. The subcellular distribution of each CAPN isoform seems to determine their functions within a specific biological process. CAPNs in plasma membrane cleave cell adhesion complexes, being involved in either cell death in involuting mammary gland, or cell migration in breast cancer cells. Whereas, nuclear CAPNs may control differentiation processes as in 3T3-L1 adipocyte differentiation.

4. CAPN deregulation observed in cancer, not only occurs in terms of higher expression, but also affects their subcellular localization. Changes in this localization will affect substrate recognition and thus, CAPNs functions. In breast cancer cell lines there is a switch between both isoforms with respect to the physiological context: CAPN1 is the isoform found in plasma membrane, while in mammary gland involution is CAPN2. Moreover, in breast cancer cell lines CAPN2 is the isoform found in nucleoli, contrary to differentiating 3T3-L1 cells, in which is CAPN1.

5. Bioinformatics analysis of CAPN2 sequence and the ΔCAPN2 overexpression experiments suggest that CAPN2 nucleolar internalization could be mediated by a non-consensus NoLS sequence, whose recognition seems to be dependent on a CAPN2 conformational change.

RESUMEN

RESUMEN

INTRODUCCIÓN

Las calpainas (CAPNs) son una familia de proteasas intracelulares cuya actividad es dependiente de Ca^{2+} y se caracterizan por tener en su estructura un motivo cisteína-proteasa llamado CysPc[1]. Estas proteasas intracelulares se encuentran en casi todos los organismos eucariotas y en algunas bacterias y hongos[4]. De entre los quince miembros identificados que componen la familia de las CAPNs, las isoformas calpaina-1 (CAPN1) y calpaina-2 (CAPN2), las cuales tienen una expresión ubicua en mamíferos, son las mejor caracterizadas. Estas dos isoformas actúan como heterodímeros compuestos por una subunidad catalítica de 80 KDa (codificada por los genes CAPN1 y CAPN2), y una pequeña subunidad reguladora, CAPNS1, de 28 KDa que es común a ambas subunidades catalíticas[1]. Otro de los principales componentes reguladores del sistema CAPN es la calpastatina (CAST), el único inhibidor fisiológico especifico de las CAPNs que se conoce hasta ahora[1,24].

La peculiaridad de estas enzimas radica en que no son unas proteasas meramente degradativas, sino que producen cortes específicos y limitados en sus sustratos, de tal manera que los modifica de manera irreversible. Estos cortes precisos producen alteraciones en las propiedades originales de dichos sustratos, lo cual puede modificar la función, actividad, especificidad, regulación y localización de éstos. Más de 100 sustratos de las CAPNs han sido identificados en estudios *in vitro*, incluyendo: proteínas de membrana, proteínas del citoesqueleto, factores de transcripción y quinasas. Debido a la gran variedad de sustratos que pueden ser procesados por las CAPNs, están involucradas en un gran número de funciones celulares, como el remodelado del citoesqueleto, señalización celular, migración celular, control del ciclo celular, regulación de la expresión génica, diferenciación celular, apoptosis, etc[5–12].

Dado el gran número de procesos fisiológicos en los que las CAPNs están involucradas, es importante una correcta regulación de este sistema para asegurar la homeostasis celular. De hecho, desregulaciones en el sistema CAPN se han visto relacionadas con varios procesos patológicos, como diabetes mellitus tipo 2, enfermedad de Alzheimer y otras enfermedades

neurodegenerativas, infarto de miocardio, algunos tipos de distrofia muscular y en cáncer[1,13–15].

A pesar de que las CAPNs están implicadas en varios procesos fisiológicos y patológicos, ni las funciones precisas de las CAPNs ni el mecanismo de reconocimiento de sus sustratos han sido esclarecidos completamente. Además, la información disponible en la literatura al respecto es confusa. Muchos estudios no disciernen entre las implicaciones específicas de las isoformas CAPN1 y CAPN2, relacionándolas indistintamente con las mismas funciones[112]. Esto se debe, principalmente, a la falta de precisión en los estudios de las funciones de CAPNs. Dichos estudios se basan mayoritariamente en la utilización de inhibidores de actividad CAPN, los cuales son inespecíficos y actúan sobre diferentes isoformas de CAPN, e incluso sobre otras proteasas[113]. Otra aproximación frecuentemente utilizada es el silenciamiento de la expresión de CAPNS1 o la sobreexpresión de CAST, reguladores comunes de CAPN1 y CAPN2[114–116]. Asimismo, varios sustratos de las CAPNs se han identificado mediante digestiones *in vitro* con CAPNs recombinantes. *In vitro* ambas proteasas tienen la capacidad de reconocer a las mismas proteínas como sustratos, lo cual no refleja su especificidad de reconocimiento *in vivo*. Por todos estos motivos, los resultados y conclusiones obtenidos a partir de este tipo de estudios deben ser interpretados con cautela.

Es importante destacar que, aunque ambas CAPNs tienen la misma capacidad de reconocer *in vitro* a los mismos sustratos, *in vivo* cada isoforma es responsable de la proteólisis de ciertas dianas y, por lo tanto, regulan funciones específicas[119]. Resultados obtenidos en estudios con ratones *knockout* sustentan la hipótesis de que las CAPNs no tienen funciones intercambiables *in vivo*. Los ratones *knockout* de *CapnS1,* la subunidad reguladora de ambas isoformas, no son viables, y mueren durante el desarrollo embrionario[57]. Por otro lado, mientras que los ratones *knockout* de *Capn1* generan ratones viables y fértiles[120], los ratones *knockout* de *Capn2* no son viables[28]. Esto demuestra que *in vivo* las isoformas de CAPN tienen implicaciones biológicas diferentes y, por consiguiente, son responsables de funciones particulares.

Al igual que en el caso de otros sistemas proteasa intracelulares, como el proteasoma, las peptidasas lisosomales o las caspasas[74–77], el reconocimiento de sustratos por las CAPNs está estrictamente regulado. No obstante, a diferencia de los otros sistemas, el mecanismo de reconocimiento de sustratos por las CAPNs es más complejo. Las CAPNs no utilizan ningún

sistema externo para identificar a sus sustratos, como ubiquitinación o formación de autofagosoma, sino que son ellas mismas las que participan en dicho reconocimiento. Además, a diferencia de las caspasas, las CAPNs no reconocen secuencias aminoacídicas consenso en sus sustratos. Debido a que ambas isoformas tienen potencialmente la misma capacidad de proteolizar a los mismos sustratos, se ha propuesto que la especificidad de reconocimiento *in vivo* de sustratos por las CAPNs está mediada por su localización subcelular. Tras ciertos estímulos, las CAPNs pueden trasladarse de un compartimento celular a otro, como el retículo endoplasmatico, el aparato de Golgi, caveolas, membrana plasmática, núcleo o nucléolo[87–93,102]. Esta compartimentalización restringiría a las CAPNs a estar en contacto con limitados sustratos y, por lo tanto, supondría una regulación más precisa de sus funciones.

OBJETIVOS

Las desregulaciones en el sistema CAPN están consideradas como un factor agravante de diferentes enfermedades, entre las que se encuentra el cáncer[13,14,200]. Sin embargo, no existen datos claros acerca de la participación de cada isoforma de CAPN en las diferentes funciones fisiológicas que regulan, ni de cómo estas isoformas están desreguladas en condiciones patológicas. *In vivo*, cada isoforma de CAPN reconoce proteínas específicas como sustrato. Se ha propuesto que la localización subcelular de las CAPNs puede determinar la especificidad de dicho reconocimiento, y consecuentemente, sus funciones.

Por ello, el objetivo global de este proyecto de tesis es evaluar la relación entre la localización de las isoformas de CAPN con la participación de éstas en determinados procesos biológicos y si dicha localización varía dependiendo del contexto celular. En base a ello, se propusieron los siguientes objetivos específicos:

1. EVALUAR SI LAS FUNCIONES Y LA LOCALIZACIÓN DE LAS ISOFORMAS DE CALPAÍNA ES DIFERENTE DEPENDIENDO DEL CONTEXTO BIOLÓGICO

Para la consecución de este objetivo, se seleccionaron como modelos de estudio fisiológicos y patológicos a la glándula mamaria en involución y diferentes líneas de cáncer de mama, respectivamente. Es bien conocido que

la proteólisis de proteínas de adhesión es el primer paso que se produce en el proceso de involución post-lactancia de la glándula mamaria para la eliminación fisiológica de células que ya no son necesarias tras el cese de la lactancia[288,298]. Nuestro grupo estableció previamente mediante estudios *in vitro*, que la proteólisis de diferentes proteínas de adhesión está mediada por CAPNs[325]. De manera similar, las proteínas de adhesión también son diana de las CAPNs en modelos de cáncer de mama[45,279,281]. No obstante, en este proceso patológico, las células no mueren, sino que migran tras la disrupción de las uniones celulares. Por lo tanto, nuestro primer objetivo es identificar la isoforma de CAPN que específicamente está involucrada en la proteólisis de complejos de adhesión en ambos modelos.

2. EVALUAR SI LAS FUNCIONES Y LOCALIZACIÓN DE LAS ISOFORMAS DE CALPAÍNA SON DEPENDIENTES DEL CONTEXTO CELULAR

En estudios previos, se observó que la CAPN1 estaba localizada en el compartimento nuclear de adipocitos en diferenciación durante la segunda fase de involución de la glándula mamaria, en la que se producía una repoblación del estroma mamario por adipocitos[88]. El segundo objetivo es explorar el posible papel específico de cada isoforma de CAPN en diferentes tipos celulares, ya que se ha postulado que la CAPN1 podría tener diferentes funciones dependiendo del nicho celular. Como modelo experimental se empleó la línea celular de fibroblastos de ratón 3T3-L1. Los cambios dinámicos que tienen lugar durante la diferenciación de pre-adipocitos a adipocitos podrían representar un modelo excelente para estudiar la distribución de las CAPNs en un contexto biológico cambiante dentro de un tipo celular que también está cambiado gradualmente.

3. ESTUDIAR LOS DETERMINANTES ESTRUCTURALES Y DE SECUENCIA QUE PODRÍAN FAVORECER LA INTERNALIZACIÓN DE LA CALPAÍNA 2 NUCLEOLAR

Diferentes estudios de microscopía confocal revelaron que las CAPNs estaban particularmente concentradas en unos agregados específicos dentro del núcleo, los cuales resultaron ser nucléolos. Esta nueva localización de CAPNs fue observada tanto en adipocitos en diferenciación como en líneas celulares de cáncer de colon y mama[93]. El último objetivo de esta tesis es

elucidar aquellas señales específicas dentro de la secuencia y estructura de las CAPNs que podrían estar determinando la internalización nucleolar de éstas.

RESULTADOS

1. PAPEL DE LAS ISOFORMAS DE CALPAÍNA EN MEMBRANAS CELULARES

1.1 ESTUDIO DE LAS ISOFORMAS DE CALPAÍNA EN UN MODELO FISIOLÓGICO DE GLÁNDULA MAMARIA: INVOLUCIÓN DE LA GLÁNDULA MAMARIA

Durante cada ciclo de embarazo/lactancia, la glándula mamaria sufre un proceso de regresión conocido como involución, en el cual se produce tanto la muerte celular del epitelio secretor como el remodelado tisular, con el objetivo de devolver a la glándula mamaria a un estado similar al que tenía previo al embarazo[289,299]. En organismos multicelulares, las diferentes vías apoptóticas y no apoptóticas de muerte celular proporcionan importantes mecanismos que aseguran, por un lado, la eliminación de células innecesarias o células defectuosas no deseadas, y por otro, el remodelado tisular durante el crecimiento y desarrollo. El desprendimiento de las células de la matriz extracelular y de la capa epitelial desencadena la muerte celular tanto en el desarrollo como en la involución de la glándula mamaria postlactancia[288,292,297,298,303].

Estudios previos realizados en el laboratorio a partir de extractos de glándula mamaria de ratón, mostraron que proteínas implicadas en uniones adherentes y focales, como E-cadherina, β-catenina, δ-catenina (p-120) y talina-1, se proteolizaban a lo largo de la curva de involución[325]. Digestiones *in vitro* de muestras de glándula mamaria lactante con CAPN1 y CAPN2 recombinantes indicaron que dichas proteínas eran proteolizadas indistintamente por ambas isoformas. Estos resultados demostraron que, efectivamente, tanto la CAPN1 como la CAPN2 son capaces de reconocer *in vitro* a las mismas proteínas de adhesión como sustratos[325]. No obstante, las funciones específicas de cada isoforma de CAPN en la proteólisis de uniones celulares nunca han sido elucidadas en un modelo fisiológico *in vivo*.

Para poder determinar si la actividad CAPN estaba implicada *in vivo* en la proteólisis de proteínas de adhesión, se analizaron por western blot niveles de E-cadherina, β-catenina, δ-catenina (p-120) y talina-1, en extractos de glándula mamaria a 72 h de involución de ratones control y ratones tratados con calpeptin, inhibidor específico de actividad CAPN (Figura 15). Tras estos estudios, se observó que la proteólisis de dichas proteínas se prevenía tras la inhibición de la actividad CAPN. Este resultado muestra que el procesamiento de estas proteínas de adhesión a lo largo de la involución de glándula mamaria está mediado por actividad CAPN.

A continuación, para poder identificar la isoforma de CAPN responsable *in vivo* del procesamiento proteolítico de dichas proteínas de adhesión durante la involución, se realizaron estudios de interacción entre CAPN1 y CAPN2 con E-cadherina en cortes de tejido de glándula mamaria de ratón a distintos tiempos de involución (0 h, 24 h y 72 h tras el destete) (Figura 16). Dicha interacción se estudió mediante la técnica de PLA (Proximity Ligation Assay). Estos experimentos mostraron que era la isoforma CAPN2, y no la CAPN1, la cual interaccionaba con la E-cadherina a lo largo de la involución. Además, en muestras de glándula mamaria de ratones que habían sido tratados con un inhibidor específico de actividad CAPN, calpeptin, dicha interacción se prevenía, apoyando la especificidad de dicha interacción (Figura 17).

1.2 ESTUDIO DE LAS ISOFORMAS DE CALPAÍNA EN UN MODELO PATOLÓGICO DE GLÁNDULA MAMARIA: LÍNEAS DE CÁNCER DE MAMA

La disrupción de uniones celulares no sólo es importante para la eliminación de células en procesos fisiológicos, sino que también supone el paso inicial en procesos de migración celular y de transición epitelio-mesénquima que acontecen en la progresión tumoral[247,248]. De hecho, la actividad proteolítica de las proteasas favorece el desarrollo de dichos procesos metastásicos[256,365,369]. Respecto a las CAPNs, varios estudios han destacado su implicación en procesos fundamentales para el desarrollo y progresión del cáncer de mama[13,14,200]. En concreto, el papel de las CAPNs en procesos de migración celular y metástasis ha sido extensamente documentado[70,92,97,206,250].

No obstante, al igual que en el caso de las funciones fisiológicas, no se conoce con claridad el papel específico de cada isoforma de CAPN en la progresión tumoral[45,210,217,240,282,370]. Como se ha comentado previamente, el patrón de expresión y localización subcelular de las CAPNs es determinante para delimitar sus funciones. Sin embargo, esta compartimentalización es variable dependiendo del contexto celular. En este sentido, las diferencias de localización y actividad de ambas isoformas de CAPN no se han estudiado en tumores de cáncer de mama.

En un primer lugar se caracterizaron los niveles de CAPN1 y CAPN2 en diferentes líneas celulares de cáncer de mama. Para dicho estudio, se emplearon líneas celulares representantes de distintos subtipos de cáncer de mama: MCF-7 (luminal A), BT-474 (luminal B), MDA-MB-468 (triple negativo A o Basal A), y MDA-MB-231 (triple negativo B o claudin-low). Dichos análisis mostraron que las líneas luminales tenían mayores niveles de CAPN1, y bajos los de CAPN2, mientras que las triple negativas tenían mayores niveles de CAPN2 que de CAPN1 (Figura 21, 22 y 23). A posteriori, mediante estudios de IF (Figura 19 y 20), se analizó la distribución de las CAPN1 y CAPN2 en dichas líneas celulares. Las IFs mostraron que, en los cuatro tipos celulares, la CAPN1 estaba distribuida en la membrana plasmática, citosol y núcleo, mientras que la CAPN2 estaba concentrada principalmente en el núcleo.

Para estudiar la relación específica de cada isoforma de CAPN con el procesamiento de proteínas de adhesión, se realizaron silenciamientos de expresión de cada isoforma mediante transfecciones con esiRNA. Se analizaron los niveles de E-cadherina, β-catenina, δ-catenina (p-120) y talina-1 en líneas de cáncer de mama luminales, y talina-1 en líneas triple negativas, por western blot (Figura 28). Los resultados obtenidos mostraron que tras el silenciamiento de la expresión de CAPN1, se prevenía la proteólisis de dichas proteínas, independientemente del subtipo de cáncer de mama.

Finalmente, para correlacionar la proteólisis de proteínas de adhesión celular con procesos de migración celular, se realizaron dos tipos de aproximaciones: estudios de *wound-healing* (Figura 31 y 32) y estudios con dispositivos *Transwell* (Figura 33). Dichos análisis se realizaron con las líneas de cáncer de mama MCF-7 y MDA-MB-231. Ambos estudios demostraron que tras el silenciamiento de la expresión de CAPN1, y no de CAPN2, la migración celular disminuía respecto al control en ambos tipos celulares.

Por lo tanto, se pudo concluir que, contrariamente a lo que ocurría en el caso fisiológico de la involución de glándula mamaria, en el contexto patológico de cáncer de mama, es la CAPN1 y no la CAPN2 la implicada en el procesamiento de proteínas de adhesión y en fenómenos de migración celular, independientemente de los niveles de CAPN y del subtipo ce cáncer de mama.

2. PAPEL DE LAS ISOFORMAS DE CALPAÍNA EN EL NÚCLEO

Durante la segunda fase de involución de la glándula mamaria, además de la muerte celular y remodelado tisular, se produce la proliferación de adipocitos con el objetivo de repoblar el tejido que está siendo eliminado[298]. En estudios previos realizados en el laboratorio, se observó que la CAPN1 se localizaba en el núcleo de los adipocitos que estaban repoblando la glándula mamaria de ratón en involución. Diferentes experimentos sugerían que la CAPN1 estaba implicada en el corte de la histona H3 y que, además, estaba asociada a los promotores de genes adipogénicos (leptina y CEBP-α), lo cual apuntaba a que la CAPN1 podría estar favoreciendo la activación de dichos genes durante la diferenciación de adipocitos[88].

Varios estudios han descrito la importancia de las CAPNs en la diferenciación de adipocitos[108,109,157]. Sin embargo, la implicación de cada isoforma en la regulación de dicho proceso se desconoce. Para poder estudiar el papel específico de las isoformas 1 y 2 de CAPN en el núcleo, se seleccionó un modelo de diferenciación celular: la línea celular de fibroblastos 3T3-L1, el cual es un modelo bien conocido y estandarizado de diferenciación celular a adipocitos.

La diferenciación de 3T3-L1 a adipocitos es un proceso complejo que ocurre en diferentes etapas secuenciales y que se puede inducir de manera coordinada mediante el tratamiento con un coctel de inductores adipogénicos (insulina, 3-isobutil-1-metilxantina, dexametasona y rosiglitazona)[315]. Una vez las células alcanza la confluencia y ya no se produce proliferación (GA), se estimulan y entran en una fase conocida como expansión mitótica clonal (MCE), que abarca aproximadamente los primeros dos días tras el estímulo, y durante la cual las células pasan, al menos, por una ronda de mitosis[333]. A continuación, comienza la fase de diferenciación temprana (ED) (días 2-4), durante la cual las células comienzan a adquirir características propias de adipocitos, culminando su diferenciación tras la fase de diferenciación

terminal (TD) (días 7-9)[334,335]. Estas fases están controladas de forma coordinada y secuencial por diferentes factores de transcripción de la familia C/EBP y PPAR, los cuales controlan la expresión y silenciamiento de más de 2000 genes implicados en la regulación morfológica y fisiológica de adipocitos[336,337].

2.1 PAPEL DE LAS CALPAÍNAS DURANTE EL CURSO DE DIFERENCIACIÓN DE 3T3-L1

Inicialmente, se caracterizó la expresión de CAPN1 y CAPN2 a lo largo de la curva de diferenciación de 3T3-L1 (Figura 37). Estudios por western blot mostraron que los niveles proteicos de ambas isoformas sufren un incremento durante la fase de ED, llegando a niveles máximos en las primeras fases de TD. Tras alcanzar la diferenciación completa, los niveles de ambas CAPNs comienzan a descender. Debido a que el incremento de los niveles de CAPNs se producía en las primeras fases de ED, se estudió si la actividad CAPN era importante en las fases iniciales del proceso de diferenciación. Para ello, las células fueron tratadas con dos inhibidores de actividad CAPN (calpeptin y ALLN) (Figura 41). Dicho tratamiento se realizó 24 h antes de la inducción de diferenciación. Mediante tinciones con Oil red O, que tiñe los núcleos de azul y los lípidos y triglicéridos en rojo, se observó que tras la inhibición de la actividad CAPN, los niveles de lípidos eran menores respecto al control. Además, mediante western blot se evaluaron los niveles de perilipina-1, proteína específica de adipocitos cuya acumulación se produce en las primeras fases de ED. Tras este estudio, se observó que en las células tratadas con inhibidores de actividad CAPN, los niveles de perilipina-1 eran menores respecto al control. Ambos experimentos permitieron concluir que la actividad CAPN es importante durante las primeras fases (MCE-ED) de diferenciación de adipocitos.

Los cambios en la estructura de la cromatina en las primeras fases de diferenciación son clave para desencadenar los procesos de diferenciación celular. En este sentido, se ha establecido que las modificaciones de histonas están involucradas en la regulación epigenética durante la adipogénesis. Por lo tanto, se estudió si las CAPNs podrían estar interaccionando con la histona H3 durante las primeras fases de diferenciación.

Mediante la técnica PLA, se analizó la interacción entre CAPN1 y CAPN2 con la cola N-terminal de la histona H3 en células 3T3-L1 durante la

transición MCD-ED y ED-TD (Figura 42). Estos estudios mostraron que, durante las fases iniciales de diferenciación (transición MCD-ED), ambas isoformas interaccionaban con la cola N-terminal de la histona H3. No obstante, dicha interacción se perdía en fases posteriores (transición ED-TD). Tras la cuantificación de las señales de PLA, se determinó que la CAPN1 tenía una interacción mayor que la CAPN2 con la cola N-terminal de la histona H3.

Se ha sugerido que las modificaciones de histonas como el 'histone clipping' podrían alterar las marcas epigenéticas y favorecer la apertura de la cromatina durante al diferenciación, lo cual facilitaría el acceso de los factores de transcripción a los promotores de genes adipogénicos[349,352]. Como previamente se ha comentado, la histona H3 ha sido descrita como posible diana de las CAPNs[88]. En base a esto, se estudió si a lo largo de la curva de diferenciación se producía proteólisis de la histona H3. Mediante el uso de un anticuerpo que reconoce tanto la histona H3 total como el producto de proteólisis, se observó mediante western blot que la histona H3 sufría proteólisis a partir de la transición ED-TD (Figura 43B). Para determinar si la actividad CAPN estaba implicada en dicho corte, las células 3T3-L1 se trataron con inhibidores de actividad CAPN (calpeptin y ALLN) antes de la inducción de diferenciación. Mediante western blot se observó que en el caso de las células tratadas con inhibidores de actividad CAPN, el corte de la histona H3 se prevenía, estableciendo así que la actividad CAPN estaba implicada en el procesamiento de la histona H3 (Figura 43C). Además, en dichas células se estudió la expresión de dos genes adipogénicos, C/EBP-α y leptina. Tras el tratamiento con inhibidores, los niveles de ambos genes eran menores respecto al control, lo cual reafirma la importancia de la actividad CAPN en las primeras fases de diferenciación de adipocitos (MCE-ED) (Figura 44).

2.2 IDENTIFICACIÓN DE LA ISOFORMA DE CALPAÍNA NUCLEAR IMPLICADA EN LA DIFERENCIACIÓN DE ADIPOCITOS

Como previamente se ha comentado, la distribución específica de las isoformas de CAPN es determinante para sus funciones. Debido a que la actividad CAPN es importante para las primeras fases de diferenciación de 3T3-L1, se estudió la posible contribución de cada isoforma en dicho proceso.

2.2.1 Estudio del papel específico de la CAPN1 en la diferenciación de adipocitos.

Primeramente, se estudió la distribución de la CAPN1 durante todo el proceso de diferenciación de 3T3-L1 (Figura 45). Estudios por IF indicaron que la CAPN1 sufre una redistribución desde la fase GA hasta la culminación de la fase TD. En pre-adipocitos en fase GA, la CAPN1 se distribuía de manera difusa en núcleo y citoplasma. Durante la fase MCE, la CAPN1 se localizaba rodeando a los cromosomas condensados en la metafase, pero no colocalizando con ellos (Figura 47). Además, durante la telofase, la CAPN1 se observó distribuida por el citosol. Por último, en células post-mitóticas, la CAPN1 se acumulaba en pequeños y numerosos agregados dentro del núcleo (Figura 48). Dichos agregados parecían unificarse a lo largo de la fase ED y transición ED-TD en estructuras de mayor tamaño, que fueron identificadas como nucléolos. Finalmente, cuando los adipocitos completaban su diferenciación, la localización nuclear de CAPN1 era prácticamente indetectable, acumulándose principalmente en el citosol y periferia nuclear. Estos cambios de localización de la CAPN1 fueron corroborados mediante el análisis por WB de fracciones nucleares y citosólicas (Figura 46) y fracciones nucleolares (Figura 49).

Debido a que la CAPN1 mostraba una localización nuclear, se estudió específicamente si dicha isoforma estaba implicada en la proteólisis de la histona H3. Para ello, se silenció la expresión de CAPN1 en células 3T3-L1 48h antes de la inducción de diferenciación (Figura 50). Seguidamente, se estudiaron los niveles de histona H3 en células control y células silenciadas durante la transición ED-TD, que es cuando se producía la acumulación del producto de proteólisis de la histona. Los estudios por western blot mostraron que el silenciamiento de CAPN1 prevenía el corte de la histona H3 en un 50% respecto al control. Además, tras analizar mediante RT-qPCR la expresión de los genes adipogénicos previamente estudiados (C/EBP-α y leptina), se observó una disminución en la expresión de dichos genes (Figura 51). Estos datos confirman que la CAPN1 está implicada en la modulación de las primeras fases del proceso de diferenciación de 3T3-L1.

2.2.2 Estudio del papel específico de la CAPN2 en la diferenciación de adipocitos.

Para estudiar la implicación de la CAPN2 en el proceso de diferenciación de adipocitos, se siguió el mismo procedimiento que en el caso de la CAPN1. Las imágenes de IF de CAPN2 mostraron que esta isoforma se

localizaba preferentemente en el compartimento citosólico a lo largo de todo el proceso de diferenciación (Figura 52). La CAPN2 también se detectó en el núcleo de adipocitos hasta la TD, aunque en niveles mucho menores que en el compartimento citosólico. Además, a diferencia de la CAPN1, la CAPN2 no se acumulaba en ninguna subestructura nuclear, sino que mostraba una distribución más difusa por todo el núcleo.

Tras el análisis por western blot de los niveles de CAPN2 en fracciones nucleares y citosólicas, se observó un incremento en los niveles nucleares de esta isoforma durante la fase MCE (Figura 53). Un análisis más exhaustivo de la localización de la CAPN2 durante el proceso de mitosis, mostró que la CAPN2 colocalizaba con los cromosomas condensados durante diferentes fases de mitosis (prometafase y metafase), y a posteriori, durante la telofase, se encontraba altamente concentrada en el núcleo (Figura 54). Esta distribución diferente entre la CAPN1 y CAPN2 durante la MCE podría sugerir un papel específico de la CAPN2 en la alineación y segregación de los cromosomas.

Al igual que en el caso de la CAPN1, se estudió la posible implicación de la CAPN2 en el corte de la histona H3. Tras el silenciamiento de la expresión de CAPN2 también se observó una disminución del 50% en el corte de la histona H3 (Figura 55). Además, en estudios de expresión de genes adipogénicos por RT-qPCR, la expresión de C/EBP-α y leptina también se prevenía (figura 56). Estos estudios demostraron que, al igual que la CAPN1, la CAPN2 también estaba implicada en la regulación de las primeras fases de diferenciación de 3T3-L1 a adipocitos. Por lo tanto, parece que ambas isoformas podrían estar contribuyendo a la modulación de la estructura de la cromatina mediante el corte de la cola N-terminal de la histona H3 en nucleosomas determinados.

3. ESTUDIO DE LA LOCALIZACIÓN NUCLEOLAR DE LA CALPAÍNA 2

Los experimentos anteriormente explicados, en los que se analizó la localización de las CAPN1 y CAPN2 tanto en las líneas de cáncer de mama como en las células 3T3-L1, revelaron que ambas CAPNs estaban concentradas en un compartimento nuclear, el nucléolo (CAPN1 en 3T3-L1 y CAPN2 en células de cáncer de mama). Aunque el nucléolo es conocido

principalmente por ser responsable de diferentes funciones celulares importantes como la biosíntesis del rRNA, el ensamblaje de ribosomas y ribonucleoproteínas, y secuestro de proteínas[168], se están descubriendo otras funciones inesperadas del nucléolo, mostrando cuan complejo es el sistema nucleolar[169–172]. Además, se ha demostrado que las funciones nucleolares están desreguladas en muchas enfermedades, entre las cuales se encuentra el cáncer[174,176–178].

El nucleolo, al contrario que otros compartimentos celulares, no está delimitado por ninguna membrana. El tráfico de proteínas a través de membranas está mediado por el reconocimiento de motivos de proteínas determinados. A pesar de que la retención nucleolar de proteínas parece no estar regulada por un motivo consenso, se ha propuesto que las señales de localización nucleolar (NoLS), podrían estar mediando dicha internalización.

3.1 ESTUDIO DE LA DISTRIBUCIÓN SUBCELULAR DE LAS CALPAÍNAS EN LÍNEAS DE CÁNCER DE MAMA

Debido a la importancia del nucléolo en la progresión tumoral, nos centramos en el estudio de la CAPN2 en esta subestructura nuclear. Mediante estudios de IF en diferentes líneas celulares representativas de diferentes subtipos de cáncer de mama, se observó que la CAPN2 (Figura 57), y no la CAPN1 (Figura 58), seguía la misma distribución que la fibrillarina, proteína involucrada en la biogénesis del RNA pre-ribosomal[355]. A pesar de que no se apreciaron diferencias en cuanto a la distribución nucleolar de la CAPN2 entre las distintas líneas de cáncer de mama, sí que se observaron diferencias en cuanto a niveles de CAPN2 nucleolares entre los subtipos de cáncer de mama. Estos niveles de CAPN2 nucleolares eran mayores en líneas celulares triple negativas (MDA-MB-231 y MDA-MB-468) que en luminales (MCF-7 y BT-474), en concordancia con los niveles totales de CAPN2 determinados en dichas líneas celulares.

Tanto la distribución como los niveles nucleolares de CAPN2 fueron corroborados por estudios de western blot de fracciones nucleolares de las diferentes líneas de cáncer de mama (Figura 59). En dichos estudios, se observó una pequeña diferencia en la movilidad electroforética de la CAPN2 de las fracciones nucleolares respecto a la CAPN2 de la fracción no nucleolar (resto celular). Por lo tanto, en un primer lugar quisimos descartar que dicha

detección de un tamaño ligeramente diferente fuese un producto de reacción cruzada del anticuerpo con otra proteína nucleolar.

3.1.1 Estudio de la especificidad de reconocimiento del anticuerpo *in vitro* e *in vivo*.

Inicialmente, se estudió la especificidad del reconocimiento del anticuerpo mediante incubaciones con un péptido bloqueante, el cual previno la detección de la CAPN2 por western blot en extractos nucleolares, corroborando que la banda detectada inicialmente era CAPN2 (Figura 60).

A continuación, para comprobar que el reconocimiento de CAPN2 *in vivo* era específico, se realizaron silenciamientos con esiRNA de CAPN2. Mediante análisis por IF se observó una disminución en el reconocimiento de la CAPN2 en toda la célula, incluido el nucléolo, tras el silenciamiento (Figura 62). Finalmente, se realizó otra aproximación para corroborar la especificidad de reconocimiento de la CAPN2 nucleolar *in vivo*. En las líneas MCF-7 y MDA-MB-231, se sobreexpresó la variante 1 de CAPN2 (NM_001748.4) mediante transfecciones con un vector de expresión. La proteína estaba marcada con un tag DYK en la región N-terminal de la CAPN2, generando el producto DYK-CAPN2 (Figura 61). Tras el análisis por IF de las células transfectadas con dicho vector, y usando un anticuerpo anti DYK, se observó que el producto DYK-CAPN2 se localizaba en el nucléolo de dichas células (Figura 63). Estos experimentos permitieron concluir que la CAPN2 está mayoritariamente localizada en el núcleo y nucléolo, aunque también en el citosol, de líneas de cáncer de mama, independientemente del subtipo.

3.2 ESTUDIO DE LOS DETERMINANTES ESTRUCTURALES DE LA DISTRIBUCIÓN NUCLEOLAR DE LA CALPAÍNA 2. ANÁLISIS BIOINFORMÁTICOS

Debido a la importancia de la localización de las CAPNs en la regulación de sus funciones, se decidió estudiar aquellas características estructurales que pudiesen estar determinando la localización nucleolar de la CAPN2. Para cumplir dicho objetivo, se realizó un análisis de la estructura de la CAPN2 mediante análisis bioinformáticos. Esas plataformas bioinformáticas permitieron el estudio de diferentes características recurrentes en proteínas nucleolares y que se sabe que contribuyen a la retención selectiva de dichas proteínas en el nucléolo: (i) señales de localización nucleolar

(NoLS)[356]; (ii) regiones con carga positiva ricas en residuos de lisina y arginina[357,358]; (iii) señales de localización nuclear (NLS) dentro de la secuencia proteica[359]; (iv) regiones estructuralmente desordenadas que permiten la interacción con proteínas nucleolares[360]; (v) secuencias proteicas o dominios que específicamente puedan unirse a proteínas nucleolares o ácidos nucleicos (rDNA, rRNAs)[177,360].

(i) Tras el análisis de la secuencia de aminoácidos de la CAPN2 mediante la plataforma "Nucleolar localization sequence detector" (NoD) (http://www.compbio.dundee.ac.uk/nod)[319], se observó un pico alrededor del residuo 400. No obstante, la señal no llegó al umbral mínimo para que fuese considerada o reconocida como una secuencia NoLS (Figura 64).

(ii) Las secuencias con carga positiva permiten interaccionar electrostáticamente con moléculas con carga negativa (como rDNA o rRNAs), lo cual favorece su acumulación en el nucléolo. Tras analizar la secuencia de CAPN2 mediante la plataforma 'EMBOSS: charge platform'(www.bioinformatics.nl/cgi-bin/emboss/charge), se detectó que la región comprendida entre los residuos 410 y 420 tenía una alta carga positiva (Figura 65).

(iii) Varios estudios han descrito que las secuencias NLS pueden solaparse con secuencias NoLS, o incluso ser parte de éstas[361]. La secuencia de CAPN2 fue analizada mediante el programa PSORTII[320], herramienta que permite la detección de señales de localización subcelular, y se determinó que la CAPN2 tenía dos motivos pat4 como posibles señales NLS[321]. Dichos motivos pat4 se solapaban con las regiones ricas en lisina y arginina positivamente cargadas, en las posiciones 414-418 y 415-419, respectivamente (Figura 66).

(iv) Las proteínas nucleolares pueden entrar en el nucléolo mediante la interacción directa con macromoléculas nucleolares tales como rDNA, rRNA o proteínas nucleolares. De hecho, se piensa que los motivos NoLS pueden mediar dichas interacciones en vez de la distribución de la proteína *per se*. Además, se ha visto que las regiones desestructuradas son más propensas a establecer dichas interacciones[360]. Por esta razón, las regiones desestructuradas de la CAPN2 fueron analizadas mediante la plataforma Foldindex (https://fold.weizmann.ac.il/fldbin/findex)[323], la cual predice secuencias desordenadas y flexibles dentro de la secuencia de una

proteína. Tras el análisis, se obtuvo que la CAPN2 tenía cuatro regiones desestructuradas cerca del extremo C-terminal de la proteína. Cabría destacar que la región desestructurada de mayor tamaño se extendía desde los residuos 282 al 423, región que contenía las secuencias NLSs, rica en lisinas y argininas y que además era la secuencia con mayor puntuación en la predicción de secuencias NoLS (Figura 67).

(v) Para analizar si la CAPN2 contenía en su secuencia residuos implicados en interacciones proteína-proteína, se analizó la secuencia en la base de datos http://www.predictoprotein.org/. Se identificaron varios sitios posibles de interacción proteína-proteína, uno de los cuales estaba localizado en la región desestructurada rica en lisinas y argininas (Figura 68).

A pesar de que en la secuencia de la CAPN2 no se predijo ninguna posible secuencia NoLS, ésta contiene varios factores estructurales y de secuencia típicos de proteínas nucleolares, localizados en el dominio C2L de la CAPN2.

3.3 ESTUDIO DEL PAPEL DEL DOMINIO C2L EN LA DISTRIBUCIÓN NUCLEOLAR DE LA CALPAÍNA 2

En base a que las herramientas bioinformáticas anteriormente descritas no tienen en cuenta la estructura tridimensional de la proteína ni los cambios conformacionales que ésta pueda sufrir, decidimos analizar si la internalización nucleolar de la CAPN2 pudiese estar determinada por cambios conformacionales. Estos cambios conformacionales podrían enmascarar o desenmascarar las secuencias NoLS dentro del dominio C2L.

Para estudiar el posible papel de la región C2L, se adquirió un plásmido de sobreexpresión que contenía la secuencia de una versión de CAPN2 que carecía de toda la región C-terminal de la CAPN2 hasta el residuo 447, de tal manera que se eliminaba la región C-terminal del dominio C2L y el dominio PEF. Dicha CAPN2 (ΔCAPN2) también estaba marcada con un tag DYK en la región N-terminal.

En un primer lugar, al igual que en el caso de la CAPN2, se realizó el mismo análisis bioinformático de la secuencia de la proteína ΔCAPN2. Tras el análisis de posibles secuencias NoLS en la secuencia de ΔCAPN2, la plataforma NoD detectó una posible secuencia de NoLS entre los residuos

405-430: CTFLVGLIQKHRRRQRKMGEDMHTIG (Figura 70). Dicha secuencia también estaba presente en la secuencia de la CAPN2. Además, estaba incluida en la región desestructurada, positivamente cargada rica en lisinas y argininas y que contenía las dos secuencias NLS detectadas en la secuencia de la CAPN2.

El estudio de posibles sitios de interacción proteína-proteína de la secuencia de la ΔCAPN2, reveló un posible sitio de interacción que no había sido identificado como tal en el análisis que se realizó previamente de la secuencia de la CAPN2 completa. Además, dicho sitio de interacción estaba localizado en una región expuesta de la secuencia de ΔCAPN2 (mientras que en la secuencia de la CAPN2 aparecía como una región no expuesta) (Figura 71).

Finalmente, se sobreexpresó en las líneas MCF-7 y MDA-MB-231 la proteína DYK-ΔCAPN2 y se exploró la localización subcelular de ésta mediante IF. Tras este análisis, se observó que DYK-ΔCAPN2 se localizaba en membranas y nucléolo de las líneas de cáncer de mama (Figura 73).

Todos los datos obtenidos, apuntan a que la liberación de las restricciones estructurales ejercidas por el dominio C2L-PEF tras un cambio conformacional, podrían estar mediando la internalización de la CAPN2 en el compartimento nucleolar.

CONCLUSIONES

En el presente trabajo se ha explorado la relación que existe entre la localización subcelular de las isoformas CAPN1 y CAPN2 con su implicación en determinadas funciones celulares, como proteólisis de adhesiones celulares y diferenciación celular. En base a estos estudios se ha podido concluir:

1. Las isoformas CAPN1 y CAPN2 no tienen funciones redundantes ya que, tanto en condiciones fisiológicas como patológicas, cada isoforma es responsable del reconocimiento específico de distintos sustratos.
2. Dependiendo del tipo celular y contexto celular, cada isoforma de CAPN muestra una distribución subcelular específica, que puede variar desde membrana plasmática a núcleo o nucléolo.
3. La distribución subcelular de cada isoforma de CAPN parece determinar sus funciones dentro de un proceso biológico concreto. Las CAPNs en la

membrana plasmática proteolizan los complejos de adhesión celular, favoreciendo tanto la muerte celular en la glándula mamaria durante la involución, como la migración celular en líneas de cáncer de mama. Por otro lado, las CAPNs nucleares parecen regular procesos de diferenciación celular, como en el caso de diferenciación de fibroblastos 3T3-L1 a adipocitos.

4. Las desregulaciones de CAPNs observadas en cáncer, no ocurren solo en términos de mayor expresión, sino que también afectan a la localización subcelular. Cambios en su localización afectarían al reconocimiento de sustrato y, por lo tanto, a las funciones de CAPNs. En líneas de cáncer de mama se produce un cambio de localización de isoformas respecto al contexto fisiológico: en líneas de cáncer de mama, la CAPN1 es la isoforma localizada en la membrana plasmática, mientras que durante la involución de la glándula mamaria es la CAPN2 la que se encuentra en dicho compartimento. Además, contrariamente a las líneas de cáncer de mama, en las cuales es la CAPN2, en células 3T3-L1 en diferenciación es la CAPN1 la isoforma que se encuentra localizada en el compartimento nucleolar.
5. Análisis bioinformaticos de la secuencia de CAPN2 y experimentos de sobreexpresión de ΔCAPN2 sugieren que la internalización nucleolar de la CAPN2 puede estar mediada por una secuencia NoLS no consenso, cuyo reconocimiento parecer depender de un cambio conformacional de la CAPN2.

BIBLIOGRAPHY

BIBLIOGRAPHY

1. Goll, D. E. *et al.* The calpain system. *Physiological Reviews*, **1990**, 731–801 (2003).
2. Guroff, G. A neutral, calcium-activated proteinase fraction from the soluble of rat brain. *Journal of Biological Chemistry*, **239**, 149–155 (1964).
3. Murachi, T. *et al.* Intracellular Ca^{2+}-dependent protease (CALPAIN) and its high-molecular-weight endogenous inhibitor (CALPASTATIN). *Advances in Enzyme Regulation*, **19**, 407–424 (1981).
4. Croall, D. E. & Ersfeld, K. The calpains: modular designs and functional diversity. *Genome Biology*, **8**, 1–11 (2007).
5. Sorimachi, H. *et al.* Structure and physiological function of calpains. *The Biochemical Journal*, **328**, 721–32 (1997).
6. Lebart, M. C. & Benyamin, Y. Calpain involvement in the remodeling of cytoskeletal anchorage complexes. *FEBS Journal*, **273**, 3415–3426 (2006).
7. Glading, A. *et al.* Cutting to the chase: calpain proteases in cell motility. *Trends in Cell Biology*, **12**, 46–54 (2002).
8. Jánossy, J. *et al.* Calpain as a multi-site regulator of cell cycle. *Biochemical Pharmacology*, **67**, 1513–1521 (2004).
9. Gomes, M. D. *et al.* Atrogin-1, a muscle-specific F-box protein highly expressed during muscle atrophy. *Proceedings of the National Academy of Sciences of the United States of America*, **98**, 14440–5 (2001).
10. Santos, D. M. *et al.* Distinct regulatory functions of calpain 1 and 2 during neural stem cell self-renewal and differentiation. *PLoS ONE*, **7**, (2012).
11. Moyen, C. *et al.* Involvement of μ-calpain (CAPN 1) in muscle cell differentiation. *International Journal of Biochemistry and Cell Biology*, **36**, 728–743 (2004).
12. Kulkarni, S. *et al.* Calpain mediates integrin-induced signaling at a point upstream of Rho family members. *Journal of Biological Chemistry*, **274**, 21265–21275 (1999).
13. Leloup, L. & Wells, A. Calpains as potential anti-cancer targets. *Expert Opinion on Therapeutic Targets*, **15**, 309–323 (2011).
14. Ono, Y. *et al.* Calpain research for drug discovery: challenges and potential. *Nature Reviews Drug Discovery*, **15**, 854–876 (2016).
15. Huang, Y. & Wang, K. K. The calpain family and human disease. *Trends in Molecular Medicine*, **7**, 355–362 (2001).
16. Sorimachi, H. *et al.* Impact of genetic insights into calpain biology.

Journal of Biochemistry, **150**, 23–37 (2011).

17. Dutt, P. *et al.* Origins of the difference in Ca^{2+} requirement for activation of μ-and m-calpain. *Biochemical Journal*, **367**, 263–269 (2002).
18. Strobl, S. *et al.* The crystal structure of calcium-free human m-calpain suggests an electrostatic switch mechanism for activation by calcium. *Proceedings of the National Academy of Sciences of the United States of America*, **97**, 588–592 (2000).
19. Nalefski, E. A. *et al.* The C2 domain calcium-binding motif: structural and functional diversity. *Protein Science*, **5**, 2375–2390 (1996).
20. Campbell, R. L. & Davies, P. L. Structure–function relationships in calpains. *Biochemical Journal*, **447**, 335–351 (2012).
21. Takano, J. *et al.* Structure of mouse calpastatin isoforms: implications of species-common and species-specific alternative splicing. *Biochemical and Biophysical Research Communications*, **260**, 339–345 (1999).
22. Woon Joo Lee *et al.* Molecular diversity in amino-terminal domains of human calpastatin by exon skipping. *Journal of Biological Chemistry*, **267**, 8437–8442 (1992).
23. Hanna, R. A. *et al.* Calpastatin simultaneously binds four calpains with different kinetic constants. *FEBS Letters*, **581**, 2894–2898 (2007).
24. Wendt, A. *et al.* Interaction of calpastatin with calpain: A review. *Biological Chemistry*, **385**, 465–472 (2004).
25. Ma, H. *et al.* Requirement inhibition of different subdomains of calpastatin for and for binding to calmodulin-like calpain. *Journal of Biochemistry*, **113**, 591–599 (1993).
26. Moldoveanu, T. *et al.* Concerted multi-pronged attack by calpastatin to occlude the catalytic cleft of heterodimeric calpains. *Nature*, **456**, 404–408 (2008).
27. Arthur, J. S. *et al.* Disruption of the murine calpain small subunit gene, Capn4: calpain is essential for embryonic development but not for cell growth and division. *Molecular and cellular biology*, **20**, 4474–4481 (2000).
28. Dutt, P. *et al.* m-Calpain is required for preimplantation embryonic development in mice. *BMC Developmental Biology*, **6**, 3 (2006).
29. Carragher, N. Calpain Inhibition: a therapeutic strategy targeting multiple disease states. *Current Pharmaceutical Design*, **12**, 615–638 (2006).
30. Saez, M. E. *et al.* The therapeutic potential of the calpain family: new aspects. *Drug Discovery Today*, **11**, 917–923 (2006).
31. Hosfield, C. M. *et al.* Crystal structure of calpain reveals the structural basis for Ca^{2+}-dependent protease activity and a novel mode of enzyme

activation. *The EMBO Journal*, **18**, 6880–6889 (1999).
32. Suzuki, K. *et al.* Structure, activation, and biology of calpain. *Diabetes*, **53**, (2004).
33. Khorchid, A. & Ikura, M. How calpain is activated by calcium. *Nature Structural Biology*, **9**, 239–241 (2002).
34. Moldoveanu, T. *et al.* A Ca^{2+} switch aligns the active site of calpain. *Cell*, **108**, 649–660 (2002).
35. Moldoveanu, T. *et al.* Calpain silencing by a reversible intrinsic mechanism. *Nature Structural Biology*, **10**, 371–378 (2003).
36. Suzuki, K. *et al.* Structure and function of the small (30K) subunit of calcium-activated neutral protease (CANP). *Biomedica Biochimica Acta*, **45**, 1487–91 (1986).
37. Friedrich, P. The intriguing Ca^{2+} requirement of calpain activation. *Biochemical and Biophysical Research Communications*, **323**, 1131–1133 (2004).
38. Cong, J. *et al.* The role of autolysis in activity of the Ca(2+)-dependent proteinases (μ-calpain and m-calpain). *Journal of Biological Chemistry*, **264**, 10096–10103 (1989).
39. Saido, T. C. *et al.* Positive regulation of μ-calpain action by polyphosphoinositides. *The Journal of Biological Chemistry*, **267**, 24585–90 (1992).
40. Leloup, L. *et al.* M-calpain activation is regulated by its membrane localization and by its binding to phosphatidylinositol 4,5-bisphosphate. *Journal of Biological Chemistry*, **285**, 33549–33566 (2010).
41. Kiss, R. *et al.* Local structural preferences of calpastatin, the intrinsically unstructured protein inhibitor of calpain. *Biochemistry*, **47**, 6936–6945 (2008).
42. Hata, S. *et al.* Stomach-specific calpain, nCL-2/calpain 8, is active without calpain regulatory subunit and oligomerizes through C2-like domains. *Journal of Biological Chemistry*, **282**, 27847–27856 (2007).
43. Hanna, R. A. *et al.* Calcium-bound structure of calpain and its mechanism of inhibition by calpastatin. *Nature*, **456**, 409–412 (2008).
44. Takano, J. *et al.* Calpain mediates excitotoxic DNA fragmentation via mitochondrial pathways in adult brains: evidence from calpastatin mutant mice. *Journal of Biological Chemistry*, **280**, 16175–16184 (2005).
45. Storr, S. J. *et al.* Calpastatin is associated with lymphovascular invasion in breast cancer. *Breast*, **20**, 413–418 (2011).
46. Niapour, M. *et al.* Regulation of calpain activity by c-Myc through calpastatin and promotion of transformation in c-Myc-negative cells by calpastatin suppression. *Journal of Biological Chemistry*, **283**,

21371–21381 (2008).
47. Higuchi, M. *et al.* Mechanistic involvement of the calpain-calpastatin system in Alzheimer neuropathology. *The FASEB Journal*, **26**, 1204–1217 (2012).
48. Stifanese, R. *et al.* Adaptive modifications in the calpain/calpastatin system in brain cells after persistent alteration in Ca^{2+} homeostasis. *Journal of Biological Chemistry*, **285**, 631–643 (2010).
49. De Tullio, R. *et al.* Differential degradation of calpastatin by μ- and m-calpain in Ca^{2+}-enriched human neuroblastoma LAN-5 cells. *FEBS Letters*, **475**, 17–21 (2000).
50. Averna, M. *et al.* Changes in calpastatin localization and expression during calpain activation: A new mechanism for the regulation of intracellular Ca^{2+}-dependent proteolysis. *Cellular and Molecular Life Sciences*, **60**, 2669–2678 (2003).
51. Averna, M. *et al.* Changes in intracellular calpastatin localization are mediated by reversible phosphorylation. *The Biochemical Journal*, **354**, 25–30 (2001).
52. Salamino, F. *et al.* Modulation of rat brain calpastatin efficiency by post-translational modifications. *FEBS Letters*, **412**, 433–438 (1997).
53. Averna, M. *et al.* Phosphorylation of rat brain calpastatins by protein kinase C. *FEBS Letters*, **450**, 13–16 (1999).
54. Meyer, S. L. *et al.* Biologically active monomeric and heterodimeric recombinant human calpain I produced using the baculovirus expression system. *Biochemical Journal*, **314 (Pt-2)**, 511–519 (1996).
55. Vilei, E. M. *et al.* Functional properties of recombinant calpain I and of mutants lacking domains III and IV of the catalytic subunit. *Journal of Biological Chemistry*, **272**, 25802–25808 (1997).
56. Yoshizawa, T. *et al. A* catalytic subunit of calpain possesses full proteolytic activity. *FEBS Letters*, **358**, 9–11 (1995).
57. Zimmerman, U. J. *et al.* The calpain small subunit gene is essential: its inactivation results in embryonic lethality. *IUBMB life*, **50**, 63–68 (2000).
58. Yoshizawa, T. *et al.* Calpain dissociates into subunits in the presence of calcium ions. *Biochemical and Biophysical Research Communications*, **208**, 76-83 (1995).
59. Pal, G. P. *et al.* Dissociation and aggregation of calpain in the presence of calcium. *Journal of Biological Chemistry*, **276**, 47233–47238 (2001).
60. Dutt, P. *et al.* m-Calpain subunits remain associated in the presence of calcium. *FEBS Letters*, **436**, 367–371 (1998).
61. Zhang, W. & Mellgren, R. L. Calpain subunits remain associated during catalysis. *Biochemical and Biophysical Research*

Communications, **227**, 891–896 (1996).

62. Chou, J. S. *et al.* M-calpain activation in vitro does not require autolysis or subunit dissociation. *Biochimica et Biophysica Acta - Proteins and Proteomics*, **1814**, 864–872 (2011).
63. Wiederanders, B. Structure-function relationships in class CA1 cysteine peptidase propeptides. in *Acta Biochimica Polonica*, **50**, 691–713 (2003).
64. Baki, A. *et al.* Autolysis parallels activation of mu-calpain. *The Biochemical Journal*, **318 (Pt 3**, 897–901 (1996).
65. Brown, N. & Crawford, C. Structural modifications associated with the change in Ca^{2+} sensitivity on activation of m-calpain. *FEBS Letters*, **322**, 65–68 (1993).
66. Elce, J. S. *et al.* Autolysis, Ca^{2+} requirement, and heterodimer stability in m-calpain. *Journal of Biological Chemistry*, **272**, 11268–11275 (1997).
67. Hosfield, C. M. *et al.* Crystal structure of calpain reveals the structural basis for Ca^{2+}-dependent protease activity and a novel mode of enzyme activation. *The EMBO Journal*, **18**, 6880–6889 (1999).
68. Kitagaki, H. *et al.* Autolysis of calpain large subunit inducing irreversible dissociation of stoichiometric heterodimer of calpain. *Bioscience, Biotechnology, and Biochemistry*, **64**, 689–695 (2000).
69. Glading, A. *et al.* Epidermal growth factor activates m-calpain (calpain II), at least in part , by extracellular signal-regulated kinase-mediated phosphorylation. *Molecular and Cellular Biology*, **24**, 2499–2512 (2004).
70. Xu, L. & Deng, X. Protein kinase Ciota promotes nicotine-induced migration and invasion of cancer cells via phosphorylation of micro- and m-calpains. *The Journal of Biological Chemistry*, **281**, 4457–4466 (2006).
71. Smolock, A. R. *et al.* Protein kinase C upregulates intercellular adhesion molecule-1 and leukocyte-endothelium interactions in hyperglycemia via activation of endothelial expressed calpain. *Arteriosclerosis, Thrombosis, and Vascular Biology*, **31**, 289–296 (2011).
72. Smith, S. D. *et al.* Glutamate substitutions at a PKA consensus site are consistent with inactivation of calpain by phosphorylation. *FEBS Letters*, **542**, 115–118 (2003).
73. Shiraha, H. *et al.* Activation of m-calpain (Calpain II) by epidermal growth factor is limited by protein kinase A phosphorylation of m-calpain. *Molecular and Cellular Biology*, **22**, 2716–2727 (2002).
74. Ciechanover, A. & Stanhill, A. The complexity of recognition of ubiquitinated substrates by the 26S proteasome. *Biochimica et*

Biophysica Acta - Molecular Cell Research, **1843**, 86–96 (2014).
75. Schreiber, A. & Peter, M. Substrate recognition in selective autophagy and the ubiquitin-proteasome system. *Biochimica et Biophysica Acta - Molecular Cell Research*, **1843**, 163–181 (2014).
76. Kraft, C. *et al.* Selective autophagy: ubiquitin-mediated recognition and beyond. *Nature Cell Biology*, **12**, 836–841 (2010).
77. Fischer, U. *et al.* Many cuts to ruin: a comprehensive update of caspase substrates. *Cell Death and Differentiation*, **10**, 76–100 (2003).
78. Barnes, J. A. & Gomes, A. V. PEST sequences in calmodulin-binding proteins. *Molecular and Cellular Biochemistry*, **149**–**150**, 17–27 (1995).
79. Carillo, S. *et al.* PEST motifs are not required for rapid calpain-mediated proteolysis of c-fos protein. *The Biochemical Journal*, **313**, 245–251 (1996).
80. Molinari, M. *et al.* PEST sequences do not influence substrate susceptibility to calpain proteolysis. *Journal of Biological Chemistry*, **270**, 2032–2035 (1995).
81. Tompa, P. *et al.* On the sequential determinants of calpain cleavage. *Journal of Biological Chemistry*, **279**, 20775–20785 (2004).
82. Cuerrier, D. *et al.* Determination of peptide substrate specificity for μ-calpain by a peptide library-based approach: the importance of primed side interactions. *Journal of Biological Chemistry*, **280**, 40632–40641 (2005).
83. Moldoveanu, T. *et al.* Crystal structures of calpain-E64 and -leupeptin inhibitor complexes reveal mobile loops gating the active site. *Journal of Molecular Biology*, **343**, 1313–1326 (2004).
84. Sorimachi, H. & Ono, Y. Regulation and physiological roles of the calpain system in muscular disorders. *Cardiovascular Research*, **96**, 11–22 (2012).
85. Pariat, M. *et al.* The sensitivity of c-Jun and c-Fos proteins to calpains depends on conformational determinants of the monomers and not on formation of dimers. *Biochem Journal*, **345**, 129–138 (2000).
86. Dunphy, K. A. *et al.* Oncogenic transformation of mammary epithelial cells by transforming growth factor beta independent of mammary stem cell regulation. *Cancer Cell International*, **13**, 1–12 (2013).
87. Yoneda, T. *et al.* Activation of caspase-12, an endoplastic reticulum (ER) resident caspase, through tumor necrosis factor receptor-associated factor 2-dependent mechanism in response to the ER stress. *Journal of Biological Chemistry*, **276**, 13935–13940 (2001).
88. Arnandis, T. *et al.* Differential functions of calpain 1 during epithelial cell death and adipocyte differentiation in mammary gland involution. *Biochemical Journal*, **459**, 355–368 (2014).

89. Shaikh, S. *et al.* m-Calpain-mediated cleavage of Na^+/Ca^{2+} exchanger-1 in caveolae vesicles isolated from pulmonary artery smooth muscle. *Molecular and Cellular Biochemistry*, **341**, 167–180 (2010).
90. Hood, J. L. *et al.* Differential compartmentalization of the calpain/calpastatin network with the endoplasmic reticulum and Golgi apparatus. *Journal of Biological Chemistry*, **279**, 43126–43135 (2004).
91. Glading, A. *et al.* Membrane proximal ERK signaling is required for m-calpain activation downstream of epidermal growth factor receptor signaling. *The Journal of Biological Chemistry*, **276**, 23341–23348 (2001).
92. Leloup, L. *et al.* Involvement of the ERK/MAP kinase signalling pathway in milli-calpain activation and myogenic cell migration. *International Journal of Biochemistry and Cell Biology*, **39**, 1177–1189 (2007).
93. Telechea-Fernández, M. *et al.* New localization and function of calpain-2 in nucleoli of colorectal cancer cells in ribosomal biogenesis: effect of KRAS status. *Oncotarget*, **9**, 9100–9113 (2018).
94. Tompa, P. *et al.* Domain III of calpain is a Ca^{2+}-regulated phospholipid-binding domain. *Biochemical and Biophysical Research Communications*, **280**, 1333–1339 (2001).
95. Hood, J. L. *et al.* Association of the calpain/calpastatin network with subcellular organelles. *Biochemical and Biophysical Research Communications*, **310**, 1200–1212 (2003).
96. Chou, J. *et al.* Distribution of gelsolin and phosphoinositol 4,5-bisphosphate in lamellipodia during EGF-induced motility. *International Journal of Biochemistry and Cell Biology*, **34**, 776–790 (2002).
97. Shao, H. *et al.* Spatial localization of m-calpain to the plasma membrane by phosphoinositide biphosphate binding during epidermal growth factor receptor-mediated Activation. *Molecular and Cellular Biology*, **26**, 5481–5496 (2006).
98. Badugu, R. K. *et al.* N terminus of calpain 1 is a mitochondrial targeting sequence. *Journal of Biological Chemistry*, **283**, 3409–3417 (2008).
99. Hood, J. L. *et al.* Subcellular mobility of the calpain/calpastatin network: An organelle transient. *BioEssays*, **28**, 850–859 (2006).
100. Averna, M. *et al.* Interaction between calpain-1 and HSP90: New insights into the regulation of localization and activity of the protease. *PLoS ONE*, **10**, 1–19 (2015).
101. Guan, Y. *et al.* Phosphorylation of Def regulates nucleolar p53 turnover and cell cycle progression through Def recruitment of calpain3. *PLoS Biology*, **14**, 1–31 (2016).

102. Tao, T. *et al.* Def defines a conserved nucleolar pathway that leads p53 to proteasome-independent degradation. *Cell Research*, **23**, 620–634 (2013).
103. Moretti, D. *et al.* Novel variants of muscle calpain 3 identified in human melanoma cells: Cisplatin-induced changes in vitro and differential expression in melanocytic lesions. *Carcinogenesis*, **30**, 960–967 (2009).
104. Tanaka, K. The proteasome: from basic mechanisms to emerging roles. *Keio Journal of Medicine*, **62**, 1–12 (2013).
105. Reinheckel, T. *et al.* Towards specific functions of lysosomal cysteine peptidases: phenotypes of mice deficient for cathepsin B or cathepsin L. *Biological Chemistry*, **382**, 735–741 (2001).
106. Shalini, S. *et al.* Old, new and emerging functions of caspases. *Cell Death and Differentiation*, **22**, 526–539 (2015).
107. Branca, D. Calpain-related diseases. *Biochemical and Biophysical Research Communications*, **322**, 1098–1104 (2004).
108. Patel, Y. M. & Lane, M. D. Mitotic clonal expansion during preadipocyte differentiation: calpain- mediated turnover of p27. *Journal of Biological Chemistry*, **275**, 17653–17660 (2000).
109. Yajima, Y. *et al.* Calpain system regulates the differentiation of adult primitive mesenchymal ST-13 adipocytes. *Endocrinology*, **147**, 4811–4819 (2006).
110. Lebart, M. C. & Benyamin, Y. Calpain involvement in the remodeling of cytoskeletal anchorage complexes. *FEBS Journal*, **273**, 3415–3426 (2006).
111. Franco, S. J. & Huttenlocher, A. Regulating cell migration: calpains make the cut. *Journal of Cell Science*, **118**, 3829–3838 (2005).
112. Siklos, M. *et al.* Cysteine proteases as therapeutic targets: does selectivity matter? A systematic review of calpain and cathepsin inhibitors. *Acta Pharmaceutica Sinica B*, **5**, 506–519 (2015).
113. Donkor, I. O. An updated patent review of calpain inhibitors (2012 – 2014). *Expert Opinion on Therapeutic Patents*, **25**, 17–31 (2014).
114. Raimondi, M. *et al.* Calpain restrains the stem cells compartment in breast cancer. *Cell Cycle*, **15**, 106–116 (2016).
115. Cataldo, F. *et al.* CAPNS1 regulates USP1 stability and maintenance of genome integrity. *Molecular and Cellular Biology*, **33**, 2485–2496 (2013).
116. Shimada, M. Overview of calpain-mediated regulation of bone and fat mass in osteoblasts. *Cell Biochemistry and Biophysics*, **66**, 23–28 (2013).
117. Wang, C.-F. & Huang, Y.-S. Calpain 2 activated through N-methyl-D-aspartic acid receptor signaling cleaves CPEB3 and abrogates CPEB3-

repressed translation in neurons. *Molecular and Cellular Biology*, **32**, 3321–3332 (2012).

118. Chen, M. *et al.* Bid is cleaved by calpain to an active fragment in vitro and during myocardial ischemia/reperfusion. *Journal of Biological Chemistry*, **276**, 30724–30728 (2001).
119. Wang, Y. *et al.* Roles for μ-calpain and m-calpain in synaptic NMDAR-mediated neuroprotection and extrasynaptic NMDAR-mediated neurodegeneration. *Journal of Neuroscience*, **33**, 18880–18892 (2013).
120. Azam, M. *et al.* Disruption of the mouse mu-calpain gene reveals an essential role in platelet function. *Molecular and Cellular Biology*, **21**, 2213–20 (2001).
121. Bialkowska, K. *et al.* Evidence that β3-integrin-induced Rac activation involves the calpain-dependent formation of integrin clusters that are distinct from the focal complexes and focal adhesions that form as Rac and RhoA become active. *The Journal of Cell Biology*, **151**, 685–695 (2000).
122. Yao, X. *et al.* Ezrin-calpain I interactions in gastric parietal cells. *The American Journal of Physiology*, **265**, C36-46 (1993).
123. Pfaff, M. *et al.* Calpain cleavage of integrin beta cytoplasmic domains. *FEBS letters*, **460**, 17–22 (1999).
124. Yan, B. *et al.* Calpain Cleavage Promotes Talin Binding to the β3 Integrin Cytoplasmic Domain. *Journal of Biological Chemistry*, **276**, 28164–28170 (2001).
125. Carragher, N. O. *et al.* Cleavage of focal adhesion kinase by different proteases during Src-regulated transformation and apoptosis. Distinct roles for calpain and caspases. *Journal of Biological Chemistry*, **276**, 4270–4275 (2001).
126. Satish, L. *et al.* Interferon-inducible protein 9 (CXCL11)-induced cell motility in keratinocytes requires calcium flux-dependent activation of μ-calpain. *Molecular and Cellular Biology*, **25**, 1922–1941 (2005).
127. Kim, S. G. *et al.* A novel anti-cancer agent, FPDHP, induces anoikis in various human cancer cells through activation of calpain, and downregulation of anoikis-related molecules. *Journal of Cellular Biochemistry*, **119,** 5620–5631 (2018).
128. Wei, L. *et al.* Cleavage of p130Cas in anoikis. *Journal of Cellular Biochemistry*, **91**, 325–335 (2004).
129. Kim, J. Y. *et al.* Disulfiram induces anoikis and suppresses lung colonization in triple-negative breast cancer via calpain activation. *Cancer Letters*, **386**, 151–160 (2017).
130. Harwood, S. M. *et al.* Caspase and calpain function in cell death: bridging the gap between apoptosis and necrosis. *Annals of Clinical*

Biochemistry, **42**, 415–431 (2005).
131. Orrenius, S. *et al.* Regulation of cell death: the calcium-apoptosis link. *Nature Reviews. Molecular Cell Biology*, **4**, 552–565 (2003).
132. Yousefi, S. *et al.* Calpain-mediated cleavage of Atg5 switches autophagy to apoptosis. *Nature Cell Biology*, **8**, 1124–1132 (2006).
133. Menzies, F. M. *et al.* Calpain inhibition mediates autophagy-dependent protection against polyglutamine toxicity. *Cell Death and Differentiation*, **22**, 433–444 (2015).
134. Conacci-Sorrell, M. *et al.* Myc-nick: A cytoplasmic cleavage product of Myc that promotes α-tubulin acetylation and cell differentiation. *Cell*, **142**, 480–493 (2010).
135. Schoonbroodt, S. *et al.* Crucial role of the amino-terminal tyrosine residue 42 and the carboxyl-terminal PEST domain of IκBαI in NF-κB Activation by an Oxidative Stress. *The Journal of Immunology*, **164**, 4292–4300 (2000).
136. Li, X. *et al.* Cleavage of IκBα by calpain induces myocardial NF- B activation, TNF- expression, and cardiac dysfunction in septic mice. *AJP: Heart and Circulatory Physiology* **306**, H833–H843 (2014).
137. Shen, J. *et al.* Phosphorylation by the protein kinase CK2 promotes calpain-mediated degradation of IκBα. *The Journal of Immunology*, **167**, 4919–4925 (2001).
138. Demarchi, F. *et al.* Ceramide triggers an NF-κB-dependent survival pathway through calpain. *Cell Death and Differentiation*, **12**, 512–522 (2005).
139. Potter, D. A. *et al.* Calpain regulates actin remodeling during cell spreading. *Journal of Cell Biology*, **141**, 647–662 (1998).
140. Spira, M. E. *et al.* Calcium, protease activation, and cytoskeleton remodeling underlie growth cone formation and neuronal regeneration. *Cellular and Molecular Neurobiology*, **21**, 591–604 (2001).
141. Dho, S. H. *et al.* Control of cellular Bcl-xL levels by deamidation-regulated degradation. *PLoS Biology*, **11**, (2013).
142. Mandic, A. *et al.* Calpain-mediated Bid cleavage and calpain-independent Bak modulation: two separate pathways in cisplatin-induced apoptosis. *Molecular and Cellular Biology*, **22**, 3003–3013 (2002).
143. Gao, G. & Dou, Q. P. N-terminal cleavage of Bax by calpain generates a potent proapoptotic 18-kDa fragment that promotes Bcl-2-independent cytochrome C release and apoptotic cell death. *Journal of Cellular Biochemistry*, **80**, 53–72 (2000).
144. Panaretakis, T. *et al.* Activation of Bak, Bax, and BH3-only proteins in the apoptotic response to doxorubicin. *Journal of Biological Chemistry*, **277**, 44317–44326 (2002).

145. Łopatniuk, P. & Witkowski, J. M. Conventional calpains and programmed cell death. *Acta Biochimica Polonica*, **58**, 287–296 (2011).
146. Garcia, M. *et al.* Mitochondrial localization of μ-calpain. *Biochemical and Biophysical Research Communications*, **338**, 1241–1247 (2005).
147. Arnandis, T. *et al.* Calpains mediate epithelial-cell death during mammary gland involution: Mitochondria and lysosomal destabilization. *Cell Death and Differentiation*, **19**, 1536–1548 (2012).
148. Polster, B. M. *et al.* Calpain I induces cleavage and release of apoptosis-inducing factor from isolated mitochondria. *Journal of Biological Chemistry*, **280**, 6447–6454 (2005).
149. Cao, G. *et al.* Critical role of calpain I in mitochondrial release of apoptosis-inducing factor in ischemic neuronal injury. *Journal of Neuroscience*, **27**, 9278–9293 (2007).
150. Aits, S. & Jaattela, M. Lysosomal cell death at a glance. *Journal of Cell Science*, **126**, 1905–1912 (2013).
151. Villalpando Rodriguez, G. E. & Torriglia, A. Calpain 1 induce lysosomal permeabilization by cleavage of lysosomal associated membrane protein 2. *Biochimica et Biophysica Acta - Molecular Cell Research*, **1833**, 2244–2253 (2013).
152. Marcassa, E. *et al.* Calpain mobilizes Atg9/Bif-1 vesicles from Golgi stacks upon autophagy induction by thapsigargin. *Biology Open*, **6**, 551–562 (2017).
153. Demarchi, F. *et al.* Calpain as a novel regulator of autophagosome formation. *Autophagy*, **3**, 235–237 (2007).
154. Chang, H. *et al.* ROS-induced nuclear translocation of calpain-2 facilitates cardiomyocyte apoptosis in tail-suspended rats. *Journal of Cellular Biochemistry*, **116**, 2258–2269 (2015).
155. Chou, S. M. *et al.* Calcium-induced cleavage of DNA topoisomerase I involves the cytoplasmic-nuclear shuttling of calpain 2. *Cellular and Molecular Life Sciences*, **68**, 2769–2784 (2011).
156. Tang, Q. Q. & Lane, M. D. Role of C/EBP homologous protein (CHOP-10) in the programmed activation of CCAAT/enhancer-binding protein-beta during adipogenesis. *Proceedings of the National Academy of Sciences*, **97**, 12446–12450 (2000).
157. Patel, Y. M. & Lane, M. D. Role of calpain in adipocyte differentiation. *Proceedings of the National Academy of Sciences*, **96**, 1279–1284 (1999).
158. Libertini, S. J. *et al.* Cyclin E both regulates and is regulated by calpain 2, a protease associated with metastatic breast cancer phenotype. *Cancer Research*, **65**, 10700–10708 (2005).
159. Wang, X. D. *et al.* Cyclin E in breast tumors is cleaved into its low

molecular weight forms by calpain. *Oncogene*, **22**, 769–774 (2003).
160. Choi, Y. H. *et al.* Regulation of cyclin D1 by calpain protease. *Journal of Biological Chemistry*, **272**, 28479–28484 (1997).
161. Kubbutat, M. H. & Vousden, K. H. Proteolytic cleavage of human p53 by calpain: a potential regulator of protein stability. *Molecular and Cellular Biology*, **17**, 460–468 (1997).
162. Jariel-Encontre, I. *et al.* Complex mechanisms for c-fos and c-jun degradation. *Molecular Biology Reports*, **24**, 51–56 (1997).
163. Hirai, S. I. *et al.* Degradation of transcription factors, c-Jun and c-Fos, by calpain. *FEBS Letters*, **287**, 57–61 (1991).
164. Brockly, F. D. *et al.* The sensitivity of c-Jun and c-Fos proteins to calpains depends on conformational determinants of the monomers and not on formation of dimers. *Society*, **138**, 129–138 (2000).
165. Bano, D. *et al.* Alteration of the nuclear pore complex in Ca^{2+}-mediated cell death. *Cell Death and Differentiation*, **17**, 119–133 (2010).
166. Yamashita, T. *et al.* Calpain-dependent disruption of nucleo-cytoplasmic transport in ALS motor neurons. *Scientific Reports*, **7**, 1–11 (2017).
167. Honda, S. *et al.* Activation of m-calpain is required for chromosome alignment on the metaphase plate during mitosis. *Journal of Biological Chemistr,y* **279**, 10615–10623 (2004).
168. Sirri, V. *et al.* Nucleolus: the fascinating nuclear body. *Histochemistry and Cell Biology*, **129**, 13–31 (2008).
169. Boisvert, F. M. *et al.* The multifunctional nucleolus. *Nature Reviews. Molecular Cell Biology*, **8**, 574–585 (2007).
170. Tsai, R. Y. L. & Pederson, T. Connecting the nucleolus to the cell cycle and human disease. *The FASEB Journal*, **28**, 3290–3296 (2014).
171. Pederson, T. & Tsai, R. Y. L. In search of nonribosomal nucleolar protein function and regulation. *Journal of Cell Biology*, **184**, 771–776 (2009).
172. Hernandez-Verdun, D. Nucleolus in the spotlight. *Cell Cycle*, **4**, 106–108 (2005).
173. Andersen, J. S. *et al.* Nucleolar proteome dynamics. *Nature*, **433**, 77–83 (2005).
174. Hein, N. *et al.* The nucleolus: An emerging target for cancer therapy. *Trends in Molecular Medicine*, **19**, 643–654 (2013).
175. Ahmad, Y. *et al.* NOPdb: Nucleolar proteome database - 2008 Update. *Nucleic Acids Research*, **37**, 181–184 (2009).
176. Quin, J. E. *et al.* Targeting the nucleolus for cancer intervention. *Biochimica et Biophysica Acta- Molecular Basis of Disease*, **1842**, 802–816 (2014).
177. Berger, C. M. *et al.* The roles of nucleolin subcellular localization in

cancer. *Biochimie*, **113**, 78–85 (2015).
178. Bacalini, M. G. *et al.* The nucleolar size is associated to the methylation status of ribosomal DNA in breast carcinomas. *BMC Cancer*, **14**, 361 (2014).
179. Gan-Or, Z. *et al.* Mutations in CAPN1 cause autosomal-recessive hereditary spastic paraplegia. *American Journal of Human Genetics*, **98**, 1038–1046 (2016).
180. Richard, I. *et al.* Mutations in the proteolytic enzyme calpain 3 cause limb-girdle muscular dystrophy type 2A. *Cel,l* **81**, 27–40 (1995).
181. Mahajan, V. B. *et al.* Calpain-5 mutations cause autoimmune uveitis, retinal neovascularization, and photoreceptor degeneration. *PLoS Genetics*, **8**, 2–10 (2012).
182. Rosenbaum, J. T. *et al.* Retinal vasculitis. *Current Opinion in Rheumatology*, **28**, 228–235 (2016).
183. Hata, S. *et al.* Calpain 8/nCL-2 and Calpain 9/nCL-4 constitute an active protease complex, G-Calpain, involved in gastric mucosal defense. *PLoS Genetics*, **6**, 1–14 (2010).
184. Horikawa, Y. *et al.* Genetic variation in the gene encoding calpain-10 is associated with type 2 diabetes mellitus. *Nature genetics*, **26**, 163–175 (2000).
185. Pánico, P. *et al.* Role of calpain-10 in the development of diabetes mellitus and its complications. *Archives of Medical Research*, **45**, 103–115 (2014).
186. Bochner, R. *et al.* Calpain 12 function revealed through the study of an atypical case of autosomal recessive congenital ichthyosis. *Journal of Investigative Dermatology*, **137**, 385–393 (2017).
187. Litosh, V. A. *et al.* Calpain-14 and its association with eosinophilic esophagitis. *Journal of Allergy and Clinical Immunology*, **139**, 1762–1771.e7 (2017).
188. Tidball, J. G. & Spencer, M. J. Calpains and muscular dystrophies. *International Journal of Biochemistry and Cell Biology*, **32**, 1–5 (2000).
189. Samantaray, S. *et al.* Calpain as a potential therapeutic target in Parkinson's disease. *CNS & neurological disorders drug targets*, **7**, 305–312 (2008).
190. Yamashita, T. *et al.* A role for calpain-dependent cleavage of TDP-43 in amyotrophic lateral sclerosis pathology. *Nature Communications*, **3**, (2012).
191. Hübener, J. *et al.* Calpain-mediated ataxin-3 cleavage in the molecular pathogenesis of spinocerebellar ataxia type 3 (SCA3). *Human Molecular Genetics*, **22**, 508–518 (2013).
192. Yamada, M. *et al.* Inhibition of calpain increases LIS1 expression and

partially rescues in vivo phenotypes in a mouse model of lissencephaly. *Nature Medicine*, **15**, 1202–1207 (2009).
193. Bevers, M. B. & Neumar, R. W. Mechanistic role of calpains in postischemic neurodegeneration. *Journal of Cerebral Blood Flow and Metabolism*, **28**, 655–673 (2008).
194. Chen, M. *et al.* Calpain and mitochondria in ischemia/reperfusion injury. *The Journal of Biological Chemistry*, **277**, 29181–29186 (2002).
195. Nishida, K. *et al.* Degradation systems in heart failure. *Journal of Molecular and Cellular Cardiology*, **84**, 212–222 (2015).
196. Thompson, J. *et al.* Activation of mitochondrial calpain and increased cardiac injury: beyond AIF release. *American Journal of Physiology - Heart and Circulatory Physiology*, **310**, H376–H384 (2016).
197. Saito, T. *et al.* Calpain activation in Alzheimer's model mice is an artifact of APP and presenilin overexpression. *Journal of Neuroscience*, **36**, 9933–9936 (2016).
198. Goñi-Oliver, P. *et al.* N-terminal cleavage of GSK-3 by calpain: a new form of GSK-3 regulation. *Journal of Biological Chemistry*, **282**, 22406–22413 (2007).
199. Yiu, E. M. & Kornberg, A. J. Duchenne muscular dystrophy. *Journal of Paediatrics and Child Health*, **51**, 759–764 (2015).
200. Storr, S. J. *et al.* The calpain system and cancer. *Nature Reviews Cancer*, **11**, 364–374 (2011).
201. Pu, X. *et al.* Calpain-1 is associated with adverse relapse free survival in breast cancer: a confirmatory study. *Histopathology*, **68**, 1021–1029 (2016).
202. Ma, D. A. *et al.* High level of calpain1 promotes cancer cell invasion and migration in oral squamous cell carcinoma. *Oncology Letters*, **13**, 4017–4026 (2017).
203. Reichrath, J. *et al.* Different expression patterns of calpain isozymes 1 and 2 (CAPN1 and 2) in squamous cell carcinomas (SCC) and basal cell carcinomas (BCC) of human skin. *Journal of Pathology*, **199**, 509–516 (2003).
204. Lakshmikuttyamma, A., Selvakumar, P., Kanthan, R., Kanthan, S. C. & Sharma, R. K. Overexpression of m-Calpain in human colorectal adenocarcinomas. *Cancer Epidemiol. Biomarkers Prev.* **13**, 1604–1609 (2004).
205. Marciel, M. P. *et al.* Calpain-2 inhibitor treatment preferentially reduces tumor progression for human colon cancer cells expressing highest levels of this enzyme. *Cancer Medicine*, **7**, 175–183 (2018).
206. Sundaramoorthy, P. *et al.* Modulation of intracellular calcium levels by calcium lactate affects colon cancer cell motility through calcium-

dependent calpain. *PLoS ONE*, **10**, 1–15 (2015).
207. Liu, T. *et al.* Prolonged androgen deprivation leads to overexpression of calpain 2: Implications for prostate cancer progression. *International Journal of Oncology*, **44**, 467–472 (2014).
208. Mamoune, A. *et al.* Calpain-2 as a target for limiting prostate cancer invasion. *Cancer Research*, **63**, 4632–4640 (2003).
209. Roumes, H. *et al.* Calpains: markers of tumor aggressiveness? *Experimental Cell Research*, **316**, 1587–1599 (2010).
210. Storr, S. J. *et al.* Calpain system protein expression in basal-like and triple-negative invasive breast cancer. *Annals of Oncology*, **23**, 2289–2296 (2012).
211. Bai, D. S. *et al.* Capn4 overexpression underlies tumor invasion and metastasis after liver transplantation for hepatocellular carcinoma. *Hepatology*, **49**, 460–470 (2009).
212. Yang, M. *et al.* Capn4 overexpression indicates poor prognosis of ovarian cancer patients. *Journal of Cancer*, **9**, (2018).
213. Cai, J. J. *et al.* Increased expression of Capn4 is associated with the malignancy of human glioma. *CNS Neuroscience and Therapeutics*, **20**, 521–527 (2014).
214. Wang, E. *et al.* Melanoma-restricted genes. *Journal of Translational Medicine*, **2**, (2004).
215. Lee, S. J. *et al.* Increased expression of calpain 6 during the progression of uterine cervical neoplasia: immunohistochemical analysis. *International Journal of Gynecological Cancer*, **19**, 859–863 (2008).
216. Peng, P. *et al.* Decreased expression of Calpain-9 predicts unfavorable prognosis in patients with gastric cancer. *Scientific Reports*, **6**, 1–11 (2016).
217. Davis, J. *et al.* Low calpain-9 is associated with adverse disease-specific survival following endocrine therapy in breast cancer. *BMC Cancer*, **14**, 1–8 (2014).
218. Moreno-Luna, R. *et al.* Calpain 10 gene and laryngeal cancer: a survival analysis. *Head and Neck*, **33**, 72–76 (2011).
219. Esteban, F. *et al.* CAPN10 alleles modify laryngeal cancer risk in the Spanish population. *European Journal of Surgical Oncology*, **34**, 94–99 (2008).
220. Frances, C. P. *et al.* Identification of a protective haplogenotype within CAPN10 gene influencing colorectal cancer susceptibility. *Journal of Gastroenterology and Hepatology (Australia)*, **22**, 2298–2302 (2007).
221. Moretti, D. *et al.* Calpains and cancer: friends or enemies? *Archives of Biochemistry and Biophysics*, **564**, 26–36 (2014).
222. Carragher, N. O. & Frame, M. C. Calpain: a role in cell transformation

and migration. *International Journal of Biochemistry and Cell Biology*, **34**, 1539–1543 (2002).

223. Carragher, N. O. *et al.* Calpain activity is generally elevated during transformation but has oncogene-specific biological functions. *Neoplasia (New York, N.Y.)*, **6**, 53–73 (2004).
224. Small, G. W. *et al.* Evidence for involvement of calpain in c-Myc proteolysis in vivo. *Archives of Biochemistry and Biophysics*, **400**, 151–161 (2002).
225. Conacci-Sorrell, M. *et al.* Stress-induced cleavage of Myc promotes cancer cell survival. *Genes and Development*, **28**, 689–707 (2014).
226. Pianetti, S. *et al.* Her-2/neu overexpression induces NF-κB via a PI3-kinase/Akt pathway involving calpain-mediated degradation of IκB-α that can be inhibited by the tumor suppressor PTEN. *Oncogene*, **20**, 1287–1299 (2001).
227. Han, Y. *et al.* Tumor necrosis factor-α-inducible IκBα proteolysis mediated by cytosolic m-calpain. *Biochemistry*, **274**, 787–794 (1999).
228. Atencio, I. A. *et al.* Calpain inhibitor 1 activates p53-dependent apoptosis in tumor cell lines. *Cell growth & differentiation: the molecular biology journal of the American Association for Cancer Research*, **11**, 247–53 (2000).
229. Zhang, Y. *et al.* Endothelial cell calpain as a critical modulator of angiogenesis. *Biochimica et Biophysica Acta - Molecular Basis of Disease*, **1863**, 1326–1335 (2017).
230. Su, Y. *et al.* Calpain-2 regulation of VEGF-mediated angiogenesis. *FASEB journal : official publication of the Federation of American Societies for Experimental Biology*, **20**, 1443–51 (2006).
231. Sergeev, I. N. Genistein induces Ca(2+)-mediated, calpain/caspase-12-dependent apoptosis in breast cancer cells. *Biochemical and Biophysical Research Communications* **321**, 462–7 (2004).
232. Shim, H. Y. *et al.* Genistein-induced apoptosis of human breast cancer MCF-7 cells involves calpain-caspase and apoptosis signaling kinase 1-p38 mitogen-activated protein kinase activation cascades. *Anti-cancer drugs*, **18**, 649–57 (2007).
233. Yeh, T. C. *et al.* Genistein induces apoptosis in human hepatocellular carcinomas via interaction of endoplasmic reticulum stress and mitochondrial insult. *Biochemical Pharmacology*, **73**, 782–792 (2007).
234. Liu, L. *et al.* Calpain-mediated pathway dominates cisplatin-induced apoptosis in human lung adenocarcinoma cells as determined by real-time single cell analysis. *International Journal of Cancer*, **122**, 2210–2222 (2008).
235. Liu, L. *et al.* μ-Calpain regulates caspase-dependent and apoptosis inducing factor-mediated caspase-independent apoptotic pathways in

cisplatin-induced apoptosis. *International Journal of Cancer*, **125**, 2757–2766 (2009).

236. Anguissola, S. *et al.* Bid and calpains cooperate to trigger oxaliplatin-induced apoptosis of cervical carcinoma HeLa cells. *Molecular Pharmacology*, **76**, 998–1010 (2009).
237. Storr, S. J. *et al.* The calpain system is associated with survival of breast cancer patients with large but operable inflammatory and non-inflammatory tumours treated with neoadjuvant chemotherapy. *Oncotarget*, **7**, 47927–47937 (2016).
238. Cortesio, C. L. *et al.* Calpain 2 and PTP1B function in a novel pathway with Src to regulate invadopodia dynamics and breast cancer cell invasion. *Journal of Cell Biology*, **180**, 957–971 (2008).
239. Wells, a, Kassis, J., Solava, J., Turner, T. & Lauffenburger, D. a. Growth factor-induced cell motility in tumor invasion. *Acta Oncologica*, **41**, 124–130 (2002).
240. Chen, B. *et al.* Calpains are required for invasive and metastatic potentials of human hcc cells. *Cell Biology International*, **37**, 643–652 (2013).
241. Kassis, J. *et al.* Motility is rate-limiting for invasion of bladder carcinoma cell lines. *International Journal of Biochemistry and Cell Biology*, **34**, 762–775 (2002).
242. Braun, C. *et al.* Expression of calpain I messenger RNA in human renal cell carcinoma: correlation with lymph node metastasis and histological type. *International Journal of Cancer*, **84**, 6–9 (1999).
243. Popp, O. *et al.* The calpastatin-derived calpain inhibitor CP1B reduces mRNA expression of matrix metalloproteinase-2 and -9 and invasion by leukemic THP-1 cells. *Biological Chemistry*, **384**, 951–958 (2003).
244. Fan, D. G. *et al.* Silencing of calpain expression reduces the metastatic potential of human osteosarcoma cells. *Cell biology international*, **33**, 1263–7 (2009).
245. Gu, J. *et al.* Capn4 promotes non-small cell lung cancer progression via upregulation of matrix metalloproteinase 2. *Medical Oncology*, **32**, 51 (2015).
246. Jang, H. S. *et al.* Calpain 2 is required for glioblastoma cell invasion: Regulation of matrix metalloproteinase 2. *Neurochemical Research*, **35**, 1796–1804 (2010).
247. Gonzalez, D. M. & Medici, D. Signaling mechanisms of the epithelial-mesenchymal transition. *Science Signaling*, *7*, *re8* (2014).
248. Kalluri, R. & Weinberg, R. A. The basics of epithelial-mesenchymal transition. *Journal of Clinical Investigation*, **119**, 1420–1428 (2009).
249. Tian, X. *et al.* E-Cadherin/β-catenin complex and the epithelial barrier. *Journal of Biomedicine and Biotechnology*, **2011**, (2011).

250. Rios-Doria, J. *et al.* The role of calpain in the proteolytic cleavage of E-cadherin in prostate and mammary epithelial cells. *Journal of Biological Chemistry*, **278**, 1372–1379 (2003).
251. Sawhney, R. S. *et al.* Integrin α2-mediated ERK and calpain activation play a critical role in cell adhesion and motility via focal adhesion kinase signaling: Identification of a novel signaling pathway. *Journal of Biological Chemistry*, **281**, 8497–8510 (2006).
252. Xu, Y. *et al.* Filamin A regulates focal adhesion disassembly and suppresses breast cancer cell migration and invasion. *The Journal of Experimental Medicine*, **207**, 2421–2437 (2010).
253. Franco, S. J. *et al.* Calpain-mediated proteolysis of talin regulates adhesion dynamics. *Nature Cell Biology*, **6**, 977–983 (2004).
254. Carter, E. P. *et al.* A 3D in vitro model of the human breast duct: a method to unravel myoepithelial-luminal interactions in the progression of breast cancer. *Breast Cancer Research*, **19**, 1–10 (2017).
255. Clark, A. G. & Vignjevic, D. M. Modes of cancer cell invasion and the role of the microenvironment. *Current Opinion in Cell Biology*, **36**, 13–22 (2015).
256. Krakhmal, N. V *et al.* Cancer invasion: patterns and mechanisms. *Acta Naturae*, **7**, 17–28 (2015).
257. Carragher, N. O. *et al.* Calpain 2 and Src dependence distinguishes mesenchymal and amoeboid modes of tumour cell invasion: a link to integrin function. *Oncogene*, **25**, 5726–5740 (2006).
258. Yates, L. R. *et al.* Subclonal diversification of primary breast cancer revealed by multiregion sequencing. *Nature Medicine*, **21**, 751–9 (2015).
259. Sorlie, T. *et al.* Repeated observation of breast tumor subtypes in independent gene expression data sets. *Proceedings of the National Academy of Sciences*, **100**, 8418–8423 (2003).
260. Koboldt, D. C. *et al.* Comprehensive molecular portraits of human breast tumours. *Nature* **490**, 61–70 (2012).
261. Perou, C. M. *et al.* Molecular portraits of human breast tumours. *Nature*, **406**, 747–752 (2000).
262. Prat, A. *et al.* Phenotypic and molecular characterization of the claudin-low intrinsic subtype of breast cancer. *Breast Cancer Research*, **12**, (2010).
263. Sorlie, T. *et al.* Gene expression patterns of breast carcinomas distinguish tumor subclasses with clinical implications. *Proceedings of the National Academy of Sciences of the United States of America*, **98**, 10869–10874 (2001).
264. Brenton, J. D. *et al.* Molecular classification and molecular forecasting

of breast cancer: ready for clinical application? *Journal of Clinical Oncology*, **23**, 7350–7360 (2005).
265. Hennigs, A. *et al.* Prognosis of breast cancer molecular subtypes in routine clinical care: a large prospective cohort study. *BMC Cancer*, **16**, 1–9 (2016).
266. Schneider, B. P. *et al.* Triple-negative breast cancer: risk factors to potential targets. *Clinical Cancer Research*, **14**, 8010–8018 (2008).
267. Kreike, B. *et al.* Gene expression profiling and histopathological characterization of triple-negative/basal-like breast carcinomas. *Breast Cancer Research*, **9**, 1–14 (2007).
268. Prat, A. & Perou, C. M. Deconstructing the molecular portraits of breast cancer. *Molecular Oncology*, **5**, 5–23 (2011).
269. Lehmann, B. D. *et al.* Identification of human triple-negative breast cancer subtypes and preclinical models for selection of targeted therapies. *The Journal of Clinical Investigation*, **121**, 2750–2767 (2011).
270. Sotiriou, C. *et al.* Breast cancer classification and prognosis based on gene expression profiles from a population-based study. *Proceedings of the National Academy of Sciences of the United States of America*, **100**, 10393–10398 (2003).
271. Eroles, P. *et al.* Molecular biology in breast cancer: intrinsic subtypes and signaling pathways. *Cancer Treatment Reviews*, **38**, 698–707 (2012).
272. Li, Z. *et al.* The differences in ultrasound and clinicopathological features between basal-like and normal-like subtypes of triple negative breast cancer. *PLoS ONE*, **10**, 1–13 (2015).
273. Dai, X. *et al.* Breast cancer cell line classification and Its relevance with breast tumor subtyping. *Journal of Cancer*, **8**, 3131–3141 (2017).
274. Neve, R. M. *et al.* A collection of breast cancer cell lines for the study of functionally distinct cancer subtypes. *Cancer Cell*, **10**, 515–527 (2006).
275. Prat, A. & Perou, C. M. Mammary development meets cancer genomics. *Nature Medicine*, **15**, 842–844 (2009).
276. Lim, E. *et al.* Aberrant luminal progenitors as the candidate target population for basal tumor development in BRCA1 mutation carriers. *Nature Medicine*, **15**, 907–913 (2009).
277. Lacroix, M. *et al.* Gene regulation by phorbol 12-myristate 13-acetate in MCF-7 and MDA-MB-231, two breast cancer cell lines exhibiting highly different phenotypes. *Oncology Reports*, **12**, 701–707 (2004).
278. Holliday, D. L. & Speirs, V. Choosing the right cell line for breast cancer research. *Breast cancer research : BCR*, **13**, 215 (2011).
279. Storr, S. J. *et al.* Calpain in breast cancer: role in disease progression

and treatment response. *Pathobiology*, **82**, 133–141 (2015).
280. Al-bahlani, S. M. *et al.* Calpain-1 expression in Triple-Negative Breast Cancer: A Potential Prognostic Factor Independent of the Proliferative /Apoptotic Index. *BioMed Research International*, **2017**, 11–13 (2017).
281. Ye, Y. *et al.* The genesis and unique properties of the lymphovascular tumor embolus are because of calpain-regulated proteolysis of E-cadherin. *Oncogene*, **32**, 1702–1713 (2013).
282. Storr, S. J. *et al.* Calpain-1 expression is associated with relapse-free survival in breast cancer patients treated with trastuzumab following adjuvant chemotherapy. *International Journal of Cancer*, **129**, 1773–1780 (2011).
283. Ho, W. C. *et al.* Calpain 2 regulates the Akt-FoxO-p27Kip1 signaling pathway in mammary carcinoma. *Journal of Biological Chemistry*, **287**, 15458–15465 (2012).
284. Benetti, R. *et al.* The calpain system is involved in the constitutive regulation of β-catenin signaling functions. *Journal of Biological Chemistry*, **280**, 22070–22080 (2005).
285. Kouros-Mehr, H. & Werb, Z. Candidate regulators of mammary branching morphogenesis identified by genome-wide transcript analysis. *Developmental Dynamics*, **235**, 3404–3412 (2006).
286. Nelson, C. M. *et al.* Tissue geometry determines sites of mammary branching morphogenesis in organotypic cultures. *Science*, **314**, 298–300 (2006).
287. Watanabe, K. *et al.* Mammary morphogenesis and regeneration require the inhibition of EMT at terminal end buds by ovol2 transcriptional repressor. *Developmental Cell*, **29**, 59–74 (2014).
288. Watson, C. J. Post-lactational mammary gland regression: molecular basis and implications for breast cancer. *Expert Reviews in Molecular Medicine*, **8**, 1–15 (2006).
289. Zaragozá, R. *et al.* Involvement of different networks in mammary gland involution after the pregnancy/lactation cycle: Implications in breast cancer. *IUBMB Life*, **67**, 227–238 (2015).
290. Radisky, D. C. & Hartmann, L. C. Mammary involution and breast cancer risk: transgenic models and clinical studies. *Journal of Mammary Gland Biology and Neoplasia*, **14**, 181–191 (2009).
291. Fornetti, J. *et al.* Mammary gland involution as an immunotherapeutic target for postpartum breast cancer. *Journal of Mammary Gland Biology and Neoplasia*, **19**, 213–228 (2014).
292. Macias, H. & Hinck, L. Mammary gland development. *Wiley Interdisciplinary Reviews: Developmental Biology*, **1**, 533–557 (2012).

293. Musumeci, G. *et al.* Mammary gland: from embryogenesis to adult life. *Acta Histochemica,* **117**, 379–385 (2015).
294. Lanigan, F. *et al.* Molecular links between mammary gland development and breast cancer. *Cellular and Molecular Life Sciences* **64**, 3159–84 (2007).
295. Van Keymeulen, A. *et al.* Distinct stem cells contribute to mammary gland development and maintenance. *Nature,* **479**, 189–193 (2011).
296. Yang, X. *et al.* Mammary gland stem cells and their application in breast cancer. *Oncotarget,* **8**, 10675–10691 (2017).
297. Inman, J. L. *et al.* Mammary gland development: cell fate specification, stem cells and the microenvironment. *Developmen,t* **142**, 1028–1042 (2015).
298. Watson, C. J. & Kreuzaler, P. A. Remodeling mechanisms of the mammary gland during involution. *International Journal of Developmental Biology,* **55**, 757–762 (2011).
299. Jena, M. K. *et al.* Molecular mechanism of mammary gland involution: An update. *Developmental Biology,* **1606**, 30267-7 (2018).
300. Schedin, P. *et al.* Microenvironment of the involuting mammary gland mediates mammary cancer progression. *Journal of Mammary Gland Biology and Neoplasia*, **12**, 71–82 (2007).
301. Sakakura, T. *et al.* Mammary stroma in development and carcinogenesis. *Journal of Mammary Gland Biology and Neoplasia*, **18**, 189–197 (2013).
302. Almholt, K. *et al.* Extracellular proteolysis in transgenic mouse models of breast cancer. *Journal of Mammary Gland Biology and Neoplasia*, **12**, 83–97 (2007).
303. McDaniel, S. M. *et al.* Remodeling of the mammary microenvironment after lactation promotes breast tumor cell metastasis. *American Journal of Pathology*, **168**, 608–620 (2006).
304. Clarkson, R. W. *et al.* Gene expression profiling of mammary gland development reveals putative roles for death receptors and immune mediators in post-lactational regression. *Breast Cancer Research,* **6**, R92-109 (2004).
305. Clarkson, R. W. & Watson, C. J. Microarray analysis of the involution switch. *Journal of Mammary Gland Biology and Neoplasia*, **8**, 309–319 (2003).
306. Meier-Abt, F. & Bentires-Alj, M. How pregnancy at early age protects against breast cancer. *Trends in Molecular Medicine,* **20**, 143–153 (2014).
307. Schedin, P. Pregnancy-associated breast cancer and metastasis. *Nature Reviews Cancer,* **6**, 281–291 (2006).
308. O'Brien, J. & Schedin, P. Macrophages in breast cancer: do involution

macrophages account for the poor prognosis of pregnancy-associated breast cancer? *Journal of Mammary Gland Biology and Neoplasia*, **14**, 145–157 (2009).
309. Baud, V. & Karin, M. Is NF-κB a good target for cancer therapy? Hopes and pitfalls. *Nature Reviews Drug Discovery*, **8**, 33–40 (2009).
310. Xia, Y. *et al.* NF-κB, an Active Player in Human Cancers. *Cancer Immunology Research*, **2**, 823–830 (2014).
311. Didonato, J. A. *et al.* NF-kB and the link between inflammation and cancer. *Immunological Reviews*, **246**, 379–400 (2012).
312. Torres, L. *et al.* NF-κB as node for signal amplification during weaning. *Cell Physiol. Biochem*, **28**, 833–846 (2011).
313. Serrano-Puebla, A. & Boya, P. Lysosomal membrane permeabilization as a cell death mechanism in cancer cells. *Biochemical Society Transactions*, **46**, 207-215 (2018).
314. Kreuzaler, P. A. *et al.* Stat3 controls lysosomal-mediated cell death in vivo. *Nature Cell Biology* **13**, 303–309 (2011).
315. Zebisch, K. *et al.* Protocol for effective differentiation of 3T3-L1 cells to adipocytes. *Analytical Biochemistry*, **425**, 88–90 (2012).
316. Heninger, A. K. & Buchholz, F. Production of endoribonuclease-prepared short interfering RNAs (esiRNAs) for specific and effective gene silencing in mammalian cells. *CSH protocols* (2007).
317. Liang, Y. M. *et al.* Novel nucleolar isolation method reveals rapid response of human nucleolar proteomes to serum stimulation. *Journal of Proteomics*, **77**, 521–530 (2012).
318. Akoumianaki, T. *et al.* Nucleocytoplasmic shuttling of soluble tubulin in mammalian cells. *Journal of Cell Science*, **122**, 1111–1118 (2009).
319. Scott, M. S. *et al.* NoD: a nucleolar localization sequence detector for eukaryotic and viral proteins. *BMC Bioinformatics*, **12**, (2011).
320. Nakai, K. & Horton, P. PSORT: A program for detecting sorting signals in proteins and predicting their subcellular localization. *Trends in Biochemical Sciences*, **24**, 34–35 (1999).
321. Macara, I. G. Transport into and out of the cell nucleus. *Microbiology and Molecular Biology Reviews*, **65**, 570–594 (2001).
322. Uversky, V. N., Gillespie, J. R. & Fink, A. L. Why are 'natively unfolded' proteins unstructured under physiologic conditions? *Proteins: Structure, Function and Genetics*, **41**, 415–427 (2000).
323. Prilusky, J. *et al.* FoldIndex©: A simple tool to predict whether a given protein sequence is intrinsically unfolded. *Bioinformatics*, **21**, 3435–3438 (2005).
324. Ofran, Y. & Rost, B. ISIS: Interaction sites identified from sequence. *Bioinformatics*, **23**, 21–24 (2007).
325. Rodriguez-Fernandez, L. *et al.* Isoform-specific function of calpains in

cell adhesion disruption: studies in postlactational mammary gland and breast cancer. *Biochemical Journal*, **473**, 2893–2909 (2016).
326. Söderberg, O. *et al.* Direct observation of individual endogenous protein complexes in situ by proximity ligation. *Nature Methods*, **3**, 995–1000 (2006).
327. Banno, A. *et al.* Subcellular localization of talin is regulated by inter-domain interactions. *Journal of Biological Chemistry*, **287**, 13799–13812 (2012).
328. Lee, H. S. *et al.* RIAM activates integrins by linking talin to Ras GTPase membrane-targeting sequences. *Journal of Biological Chemistry*, **284**, 5119–5122 (2009).
329. Calderwood, D. A. *et al.* Talins and kindlins: partners in integrin-mediated adhesion. *Nature reviews. Molecular Cell Biology*, **14**, 503–517 (2013).
330. Wang, Q. A. *et al.* Reversible de-differentiation of mature white adipocytes into preadipocyte-like precursors during lactation. *Cell Metabolism*, **28**, 282–288 (2018).
331. Corsa, C. A. S. & MacDougald, O. A. Cyclical dedifferentiation and redifferentiation of mammary adipocytes. *Cell Metabolism*, **28**, 187–189 (2018).
332. Yajima, Y. & Kawashima, S. Calpain function in the differentiation of mesenchymal stem cells. *Biological Chemistry*, **383**, 757–764 (2002).
333. Ntambi, J. M. & Young-Cheul, K. Adipocyte differentiation and gene expression. *The Journal of Nutrition*, **130**, 3122–3126 (2000).
334. Gregoire, F. M. *et al.* Understanding adipocyte differentiation. *Physiological Reviews*, **78**, 783–809 (1998).
335. Ali, A. T., Hochfeld, W. E., Myburgh, R. & Pepper, M. S. Adipocyte and adipogenesis. *European Journal of Cell Biology*, **92**, 229–236 (2013).
336. Farmer, S. R. Transcriptional control of adipocyte formation. *Cell Metabolism*, **4**, 263–273 (2006).
337. Guo, L. *et al.* Transcriptional regulation of adipocyte differentiation: A central role for CCAAT/ enhancer-binding protein (C/EBP) β. *Journal of Biological Chemistry*, **290**, 755–761 (2015).
338. Student, A. K. *et al.* Induction of fatty acid synthetase synthesis in differentiating 3T3-L1 preadipocytes. *Journal of Biological Chemistry*, **255**, 4745–4750 (1980).
339. Sztalryd, C. & Kimmel, A. R. Perilipins: lipid droplet coat proteins adapted for tissue-specific energy storage and utilization, and lipid cytoprotection. *Biochimie*, **96**, 96–101 (2014).
340. Brasaemle, D. L. *et al.* Adipose differentiation-related protein is an ubiquitously expressed lipid storage droplet-associated protein.

Journal of Lipid Research, **38**, 2249–2263 (1997).
341. Lane, M. D. *et al.* Role of the CCAAT enhancer binding proteins (C/EBPs) in adipocyte differentiation. *Biochemical and Biophysical Research Communications*, **266**, 677–83 (1999).
342. Cowherd, R. M. *et al.* Molecular regulation of adipocyte differentiation. *Seminars in Cell & Developmental Biology*, **10**, 3–10 (1999).
343. Xiao, Y. *et al.* Cathepsin K in adipocyte differentiation and its potential role in the pathogenesis of obesity. *The Journal of Clinical Endocrinology and Metabolism*, **91**, 4520–7 (2006).
344. Rauner, M. *et al.* Cathepsin S controls adipocytic and osteoblastic differentiation, bone turnover, and bone microarchitecture. *Bone*, **64**, 281–287 (2014).
345. Kuroda, M. Alteration of chromosome positioning during adipocyte differentiation. *Journal of Cell Science*, **117**, 5897–5903 (2004).
346. Charó, N. L. *et al.* Organization of nuclear architecture during adipocyte differentiation. *Nucleus*, **7**, 249–269 (2016).
347. Rosen, E. D. & MacDougald, O. A. Adipocyte differentiation from the inside out. *Nature Reviews Molecular Cell Biology*, **7**, 885–896 (2006).
348. Salma, N. *et al.* Temporal recruitment of transcription factors and SWI/SNF chromatin-remodeling rnzymes during adipogenic induction of the peroxisome proliferator-activated receptor nuclear hormone receptor. *Society*, **24**, 4651–4663 (2004).
349. Zhang, Q. *et al.* Dynamic and distinct histone modifications modulate the expression of key adipogenesis regulatory genes. *Cell Cycle*, **11**, 4310–4322 (2012).
350. Zhou, Y. *et al.* Role of histone acetyltransferases and histone deacetylases in adipocyte differentiation and adipogenesis. *European Journal of Cell Biology*, **93**, 170–177 (2014).
351. LeBlanc, S. E. *et al.* The PPARγ locus makes long-range chromatin interactions with selected tissue-specific gene loci during adipocyte differentiation in a protein kinase a dependent manner. *PLoS ONE*, **9**, (2014).
352. Zhou, P. *et al.* Histone Cleavage as a mechanism for epigenetic regulation: current insights and perspectives. *Current Molecular Medicine*, **14**, 1164–1172 (2014).
353. Musri, M. M. *et al.* A chromatin perspective of adipogenesis. *Organogenesis*, **6**, 15–23 (2010).
354. Montanaro, L. *et al.* Nucleolus, Ribosomes, and Cancer. *The American Journal of Pathology*, **173**, 301–310 (2008).
355. Shubina, M. Y. *et al.* Nucleolar methyltransferase fibrillarin: evolution

of structure and functions N terminal domain. *Biochemistry*, **81**, 941–950 (2016).
356. Scott, M. S. *et al.* Characterization and prediction of protein nucleolar localization sequences. *Nucleic Acids Research*, **38**, 7388–7399 (2010).
357. Musinova, Y. R. *et al.* A charge-dependent mechanism is responsible for the dynamic accumulation of proteins inside nucleoli. *Biochimica et Biophysica Acta - Molecular Cell Research*, **1853**, 101–110 (2015).
358. Musinova, Y. R. *et al.* Nucleolar localization/retention signal is responsible for transient accumulation of histone H2B in the nucleolus through electrostatic interactions. *Biochimica et Biophysica Acta - Molecular Cell Research*, **1813**, 27–38 (2011).
359. Reed, M. L. *et al.* Delineation and modelling of a nucleolar retention signal in the coronavirus nucleocapsid protein. *Traffic*, **7**, 833–848 (2006).
360. Emmott, E. & Hiscox, J. A. Nucleolar targeting: The hub of the matter. *EMBO Reports*, **10**, 231–238 (2009).
361. Martin, R. M. *et al.* Principles of protein targeting to the nucleolus. *Nucleus*, **6**, 314–325 (2015).
362. Takano, J. *et al.* Vital role of the calpain-calpastatin system for placental-integrity-dependent embryonic survival. *Molecular and Cellular Biology*, **31**, 4097–4106 (2011).
363. Gil-Parrado, S. *et al.* Ionomycin-activated calpain triggers apoptosis. A probable role for Bcl-2 family members. *Journal of Biological Chemistry*, **277**, 27217–27226 (2002).
364. Stelwagen, K. & Singh, K. The role of tight junctions in mammary gland function. *Journal of Mammary Gland Biology and Neoplasia*, **19**, 131–138 (2014).
365. Nava, P. *et al.* Cleavage of transmembrane junction proteins and their role in regulating epithelial homeostasis. *Tissue Barriers*, **1**, (2013).
366. Rios-Doria, J. *et al.* Cleavage of beta-catenin by calpain in prostate and mammary tumor cells. *Cancer Research*, **64**, 7237–7240 (2004).
367. Ferber, E. C. *et al.* A role for the cleaved cytoplasmic domain of E-cadherin in the nucleus. *Journal of Biological Chemistry* **283**, 12691–12700 (2008).
368. Ito, K. *et al.* Calcium influx triggers the sequential proteolysis of extracellular and cytoplasmic domains of E-cadherin, leading to loss of beta-catenin from cell-cell contacts. *Oncogene*, **18**, 7080–7090 (1999).
369. Willis, A. L. *et al.* Extracellular matrix determinants and the regulation of cancer cell invasion stratagems. *Journal of Microscopy*, **251**, 250–260 (2013).

370. Storr, S. J. *et al.* Expression of the calpain system is associated with poor clinical outcome in gastro-oesophageal adenocarcinomas. *Journal of Gastroenterology*, **48**, 1213–1221 (2013).
371. Liu, B. *et al.* Comparison of the protein expression of calpain-1, calpain-2, calpastatin and calmodulin between gastric cancer and normal gastric mucosa. *Oncology Letters*, **14**, 3705–3710 (2017).
372. Kulkarni, S. *et al.* Calpain regulates sensitivity to trastuzumab and survival in HER2-positive breast cancer. *Oncogene*, **29**, 1339–1350 (2010).
373. Qu, Y. *et al.* Evaluation of MCF10A as a reliable model for normal human mammary epithelial cells. *PLoS ONE*, **10**, 1–16 (2015).
374. Imbalzano, K. M. *et al.* Increasingly transformed MCF-10A cells have a progressively tumor-like phenotype in three-dimensional basement membrane culture. *Cancer Cell International*, **9**, 1–11 (2009).
375. Wu, M. *et al.* Functional dissection of human protease μ-calpain in cell migration using RNAi. *FEBS Letters*, **580**, 3246–3256 (2006).
376. Tremper-Wells, B. & Vallano, M. Lou. Nuclear calpain regulates Ca^{2+}-dependent signaling via proteolysis of nuclear Ca^{2+}/calmodulin-dependent protein kinase type IV in cultured neurons. *Journal of Biological Chemistry*, **280**, 2165–2175 (2005).
377. Tao, X. *et al.* Protective functions of PJ34, a Poly(ADP-ribose) Polymerase inhibitor, are related to down-regulation of calpain and NF-κB in a mouse model of traumatic brain injury. *World Neurosurgery*, **107**, 888–899 (2017).
378. Vossaert, L. *et al.* Identification of histone H3 clipping activity in human embryonic stem cells. *Stem Cell Research*, **13**, 123–134 (2014).
379. Duncan, E. M. *et al.* Cathepsin L proteolytically processes histone H3 during mouse embryonic stem cell differentiation. *Cell*, **135**, 284–294 (2008).
380. Yi, S. J. & Kim, K. Histone tail cleavage as a novel epigenetic regulatory mechanism for gene expression. *BMB Reports*, **51**, 211–218 (2018).
381. Dhaenens, M. *et al.* Histone proteolysis: a proposal for categorization into 'clipping' and 'degradation'. *BioEssays*, **37**, 70–79 (2015).
382. Mikkelsen, T. S. *et al.* Genome-wide maps of chromatin state in pluripotent and lineage-committed cells. *Nature*, **448**, 553-560 (2007).
383. Voigt, P., Tee, W. W. & Reinberg, D. A double take on bivalent promoters. *Genes & Development*, **27**, 1318–1338 (2013).
384. Verrier, L., Vandromme, M. & Trouche, D. Histone demethylases in chromatin cross-talks. *Biology of the Cell*, **103**, 381-401 (2011).
385. Szczerbal, I. *et al.* The spatial repositioning of adipogenesis genes is correlated with their expression status in a porcine mesenchymal stem

cell adipogenesis model system. *Chromosoma*, **118**, 647-663 (2009).
386. Musri, M. M. *et al.* Histone H3 lysine 4 dimethylation signals the transcriptional competence of the adiponectin promoter in preadipocytes. *Journal of Biological Chemistry*, **281**, 17180-17188 (2006).
387. Baarlink, C. *et al.* A transient pool of nuclear F-actin at mitotic exit controls chromatin organization. *Nature Cell Biology*, **19**, 1389–1399 (2017).
388. Ellenberg, J. Dynamics of nuclear envelope proteins during the cell cycle in mammalian cells. *Madame Curie Bioscience Database*
389. Russo, I. *et al.* Fatty acid acylation regulates trafficking of the unusual Plasmodium falciparum calpain to the nucleolus. *Molecular Microbiology*, **72**, 229–245 (2009).
390. Hayashi, Y. *et al.* Downregulation of rRNA transcription triggers cell differentiation. *PLoS ONE*, **9**, (2014).
391. Woolnough, J. L *et al.* The regulation of rRNA gene transcription during directed differentiation of human embryonic stem cells. *PLoS ONE*, **11**, 1–18 (2016).
392. Ali, S. A. *et al.* Phenotypic transcription factors epigenetically mediate cell growth control. *Proceedings of the National Academy of Sciences of the United States of America*, **105**, 6632–7 (2008).
393. Feinberg, A. P. The nucleolus gets the silent treatment. *Cell Stem Cell*, **15**, 675–676 (2014).
394. Kumaran, R. I. & Spector, D. L. A genetic locus targeted to the nuclear periphery in living cells maintains its transcriptional competence. *Journal of Cell Biology*, **180**, 51–65 (2008).
395. Glading, A. *et al.* Epidermal growth factor receptor activation of calpain is required for fibroblast motility and occurs via an ERK/MAP kinase signaling pathway. *Journal of Biological Chemistry*, **275**, 2390–2398 (2000).
396. Masuda, H. *et al.* Role of epidermal growth factor receptor in breast cancer. *Breast Cancer Research and Treatment*, **136**, 331–345 (2012).
397. Averna, M. *et al.* Physiological roles of calpain 1 associated to multiprotein NMDA receptor complex. *PLoS ONE*, **10**, 1–20 (2015).
398. Ono, Y. *et al.* The N- and C-terminal autolytic fragments of CAPN3/p94/calpain-3 restore proteolytic activity by intermolecular complementation. *Proceedings of the National Academy of Sciences*, **111**, 5527–5536 (2014).
399. Grabowska, M. M. & Day, M. L. Soluble E-cadherin: more than a symptom of disease. *Frontiers in Bioscience* **17**, 1948–1964 (2012).
400. Konze, S. A. *et al.* Cleavage of E-cadherin and β-catenin by calpain affects Wnt signaling and spheroid formation in suspension cultures of

human pluripotent stem cells. *Molecular & Cellular Proteomics*, **13**, 990–1007 (2014).
401. Rios-Doria, J. & Day, M. L. Truncated E-cadherin potentiates cell death in prostate epithelial cells. *Prostate*, **63**, 259–268 (2005).
402. David, J. M. & Rajasekaran, A. K. Dishonorable discharge: the oncogenic roles of cleaved E-cadherin fragments. *Cancer Research* **72**, 2917–2923 (2012).
403. Becherel, O. J. *et al.* Nucleolar localization of aprataxin is dependent on interaction with nucleolin and on active ribosomal DNA transcription. *Human Molecular Genetics*, **15**, 2239–2249 (2006).
404. Negi, S. S. & Olson, M. O. J. Effects of interphase and mitotic phosphorylation on the mobility and location of nucleolar protein B23. *Journal of Cell Science*, **119**, 3676–3685 (2006).
405. Matragkou, C. *et al.* On the intracellular trafficking of mouse S5 ribosomal protein from cytoplasm to nucleoli. *Journal of Molecular Biology*, **392**, 1192–1204 (2009).
406. Mayer, C. & Grummt, I. Cellular stress and nucleolar function. *Cell Cycle* **4**, 1036–1038 (2005).
407. Matafora, V. *et al.* Proteomics Analysis of nucleolar SUMO-1 target proteins upon proteasome inhibition. *Molecular & Cellular Proteomics*, **8**, 2243–2255 (2009).
408. Westman, B. J. *et al.* A proteomic screen for nucleolar SUMO targets shows SUMOylation modulates the function of Nop5/Nop58. *Molecular Cell*, **39**, 618–631 (2010).
409. Eifler, K. & Vertegaal, A. C. SUMOylation-mediated regulation of cell cycle progression and cancer. *Trends in Biochemical Sciences*, **40**, 779–793 (2015).
410. Woods, Y. L. *et al.* P14 Arf Promotes Small Ubiquitin-Like Modifier Conjugation of Werners Helicase. *Journal of Biological Chemistry*, **279**, 50157–50166 (2004).
411. Mo, Y. Y. *et al.* Nucleolar delocalization of human topoisomerase I in response to topotecan correlates with sumoylation of the protein. *Journal of Biological Chemistry*, **277**, 2958–2964 (2002).
412. Wang, H. C. *et al.* SUMO modification modulates the activity of calpain-2. *Biochemical and Biophysical Research Communications*, **384**, 444–449 (2009).
413. Singh, R. *et al.* Calpain 5 is highly expressed in the central nervous system (CNS), carries dual nuclear localization signals, and is associated with nuclear promyelocytic leukemia protein bodies. *Journal of Biological Chemistry*, **289**, 19383–19394 (2014).

APPENDIX

APPENDIX

Appendix 1. CAPN2 and ΔCAPN2 sequence alignment*. Human CAPN2 (NP_001739.2) and shorter version of CAPN2 amino acidic sequences were align by means of Protein BLAST platform of NCBI (Nation Centre for Biotechnology Information*

Biochemical Journal (2016) **473** 2893–2909
DOI: 10.1042/BCJ20160198

PORTLAND PRESS

Research Article

Isoform-specific function of calpains in cell adhesion disruption: studies in postlactational mammary gland and breast cancer

Lucía Rodríguez-Fernández[1,2], Iván Ferrer-Vicens[1], Concha García[1], Sara S. Oltra[2], Rosa Zaragozá[2,3], Juan R. Viña[1,2] and Elena R. García-Trevijano[1,2]

[1]Departamento de Bioquímica y Biología Molecular, Facultad de Medicina, Universidad de Valencia, Avda. Blasco Ibañez, 15, Valencia 46010, Spain; [2]Fundación Investigación Hospital Clínico — INCLIVA, Avda. Blasco Ibañez, 15, Valencia 46010, Spain; and [3]Departamento de Anatomia y Embriologia Humana, Facultad de Medicina, Universidad de Valencia, Valencia, Spain

Correspondence: Juan R. Viña (vinaj@uv.es)

Cleavage of adhesion proteins is the first step for physiological clearance of undesired cells during postlactational regression of the mammary gland, but also for cell migration in pathological states such as breast cancer. The intracellular Ca^{2+}-dependent proteases, calpains (CAPNs), are known to cleave adhesion proteins. The isoform-specific function of CAPN1 and CAPN2 was explored and compared in two models of cell adhesion disruption: mice mammary gland during weaning-induced involution and breast cancer cell lines according to tumor subtype classification. In both models, E-cadherin, β-catenin, p-120, and talin-1 were cleaved as assessed by western blot analysis. Both CAPNs were able to cleave adhesion proteins from lactating mammary gland *in vitro*. Nevertheless, CAPN2 was the only isoform found to co-localize with E-cadherin in cell junctions at the peak of lactation. CAPN2/E-cadherin *in vivo* interaction, analyzed by proximity ligation assay, was dramatically increased during involution. Calpain inhibitor administration prevented the cytosolic accumulation of truncated E-cadherin cleaved by CAPN2. Conversely, in breast cancer cells, CAPN2 was restricted to the nuclear compartment. The isoform-specific expression of CAPNs and CAPN activity was dependent on the breast cancer subtype. However, CAPN1 and CAPN2 knockdown cells showed that cleavage of adhesion proteins and cell migration was mediated by CAPN1, independently of the breast cancer cell line used. Data presented here suggest that the subcellular distribution of CAPN1 and CAPN2 is a major issue in target-substrate recognition; therefore, it determines the isoform-specific role of CAPNs during disruption of cell adhesion in either a physiological or a pathological context.

Introduction

During each pregnancy/lactation cycle, the mammary gland suffers a process of regression known as involution, where epithelial cell death is coupled to tissue remodeling [1,2]. In multicellular organisms, the different ways of apoptotic and nonapoptotic cell death provide important mechanisms to assure removal of undesired defective cells or tissue remodeling during growth and development. Cell detachment from extracellular matrix (ECM) is a key event triggering cell death during both development and postlactational regression of mammary gland. Importantly, disruption of cell adhesion is the initiating step not only for apoptotic and nonapoptotic cell removal [2–4], but also for cell migration and epithelial-to-mesenchymal transition during breast tumor progression [4–6].

The prominent role of calpains in the proteolytic processing of adhesion proteins to promote cell migration and metastasis has been extensively documented [7–13]. Calpains (EC 3.4.22.18; clan CA; family C2) are neutral Ca^{2+}-dependent cysteine proteases involved in the limited processing of

Received: 8 March 2016
Revised: 24 June 2016
Accepted: 11 July 2016

Accepted Manuscript online: 11 July 2016
Version of Record published: 12 September 2016

PORTLAND PRESS

Biochemical Journal (2016) **473** 2893–2909
DOI: 10.1042/BCJ20160198

proteins. Among the calpain family members, calpain-1 (CAPN1) and calpain-2 (CAPN2) are the most ubiquitously expressed isoforms. Both calpains are heterodimers, composed of a different catalytic subunit (80 kDa), and a common regulatory subunit (30 kDa), known as calpain-4 (CAPN4) [14,15]. Although they are highly specific for the recognition of substrates, the basis for this recognition is not completely understood, and redundant functions are usually described for both calpains [14]. However, the pattern of gene expression and subcellular localization of CAPNs is highly dependent on cell context [15–20]. Differences in the localization or activity of both CAPNs have not been studied in breast tumors, and although CAPNs are good targets for cancer therapy, there is no evidence for the role of a particular CAPN isoform. Reports about the isoform-specific function of CAPNs in cell migration use cultured cells that do not resemble the polarized structure of mammary epithelium [8,10,13,17,21].

The mammary gland during the pregnancy/lactation cycle has been used as a unique approach to investigate the early events during breast tumor progression [1,22]. During the early and reversible phase of involution, luminal cells detach from the ECM and are shed into the lumen of alveoli where they are cleared by different mechanisms. In the second irreversible phase of involution, the remaining epithelial cells massively die, mammary tissue is extensively remodeled, and the fat pad is repopulated with adipocytes [1,2].

We recently showed that CAPN localization/functions are subjected to the dynamic changes suffered by mammary epithelia during involution. CAPN1 was found to mediate mitochondrial and lysosomal cell death of mammary epithelia at sequential time points of early involution [18]. Its later nuclear localization in epithelial cells and adipocytes promoted both nuclei destabilization of epithelial cells and adipocyte differentiation during the second stage of involution [17]. These data suggest that although both CAPNs show almost indistinguishable substrate specificity, their differential localization at a subcellular compartment, or cell type might govern the rules for substrate recognition.

Here, we explored the isoform-specific role of CAPNs in a physiological and pathological model of cell detachment. Combining analysis in both models, such as mammary gland involution and cultured breast cancer cells, we obtained evidence supporting the notion that the subcellular distribution of isoform-specific CAPNs is dependent on the biological context. In addition, this distribution seems to condition the targets of CAPN1 or CAPN2 and therefore, their specific functions. We identified CAPN2 as the membrane-associated isoform involved in cell detachment of epithelial cells during the early phase of involution. Conversely, CAPN2 was restricted to the nuclear compartment in breast cancer cells and CAPN1 was found to be the main isoform mediating migration of these cells independently of the cancer subtype.

Experimental

Materials

Primary antibodies against CAPN1 (–COOH terminal domain, rabbit; ab39170), CAPN1 (–NH_2 terminal domain; ab28257), CAPN1 (mouse; ab3589), δ-catenin p-120 (ab11508), and β-Catenin (ab6301) were purchased from Abcam. Other antibodies used were α-Tubulin (sc-5286; Santa Cruz), α-CAPN2 for western blot (3372-100; BioVision), α-CAPN2 for immunofluorescence (2539; Cell signaling), α-Talin-1 (T3287; Sigma-Aldrich), and α-E-Cadherin (610182; BD Biosciences). Recombinant proteins and calpain inhibitors were all from Calbiochem: recombinant CAPN2 (208718), Calpain Inhibitor VI (208745), Calpeptin (03-34-0051), and ALLN (*N*-acetyl-L-leucyl-L-leucyl-norleucinal; 208719), except recombinant CAPN1 (C-6108) that was obtained from Sigma.

Animals and tissue extraction

C57BL/6 mice were obtained from Taconic (Ejby, Denmark). Virgin female (10 weeks old) were mated and males were subsequently removed at mid-gestation. Following parturition, litters were maintained with at least seven pups. Then, at the peak of lactation (days 9–11), mice were divided into different groups: control lactating mice and weaned mice whose pups were removed 10 days after delivery to initiate involution. Weaning took place for 6, 24, 48, and 72 h before sacrifice.

Calpeptin inhibitor (i.p. 40 mg/kg) was administered to 10-day lactating mice right after weaning of the pups. Mice received calpeptin or vehicle every 12 h during 3 days. Mice were killed by a single dose of sodium pentobarbital (i.p. 60 mg/kg). Inguinal mammary glands were removed and quickly freeze-clamped in liquid nitrogen or fixed in formaldehyde for histological studies. All the animals were given food and water *ad libitum* and housed in a controlled environment (12 h light/12 h dark cycle). Experimental protocols were approved by

the Research Committee of the School of Medicine (University of Valencia, Valencia, Spain). Mice were cared for and handled attending to the National Institutes of Health guidelines and the Guiding Principles for Research Involving Animals and Humans approved by the Council of the American Physiological Society.

Cell culture

Human breast cancer cell lines were purchased from American Type Culture Collection. Cell lines from luminal, basal, or the recently classified claudin-low subtypes were used in the present study as representative models of breast cancer heterogeneity [23]. Two different luminal cell lines were chosen according to their human epidermal growth factor receptor2 (HER2) status: MCF-7 (estrogen receptor (ER)+; progesterone receptor (PgR)+; HER2−) and BT474 (ER+; PgR+; HER2+). Two triple-negative cell lines, either basal or claudin-low, were also studied: MDA-MB468 (ER−; PgR−; HER2−) and MDA-MB-231 (ER−, PgR−, HER2−).

Cell lines were maintained in DMEM (Gibco) supplemented with 10% FBS, 1% penicillin/streptomycin (K952, Amresco), and L-glutamine (G7513, Sigma). Cells were maintained in a humidified atmosphere at 37°C and 5% CO_2.

CAPN knockdown by small interfering RNA

Cells were transiently transfected with 30 nM *Capn1*small interfering RNA (esiRNA) (EHU032581-50UG), CAPN2 (EHU025391-50UG), or Universal Negative Control #1 siRNA (SIC001), all of them purchased from Sigma. MDA-MD-231 and MDA-MB-468 were transfected following the forward transfection protocol and using Lipofectamine 3000 (L3000008, Life Technologies) as Transfection reagent, whereas MCF-7 and BT-474 were reverse-transfected with Lipofectamine RNAiMAX (13778075, Life Technologies). The transfection reaction was carried out for 24 h. Dilutions of esiRNA and Lipofectamine were performed in Opti-MEM following the manufacturer's instructions. esiRNA transfection efficiency was analyzed by real-time quantitative PCR (RT-qPCR) at 48 and 72 h after transfection and by western blot at 72 h after transfection.

Wound-healing assay

MB-231 cells (16×10^4) were plated in six-well plates, cultured under standard conditions for further 24 h, and transfected as described above. MCF-7 cells (6×10^5) were simultaneously plated and reverse-transfected in six-well plates. Twenty-four hours after transfection, both cell lines were starved and 24 h later, confluent monolayers were scratched with a 1 ml pipette tip to induce a wound. The wounded edges were imaged using an inverted microscope Nikon Eclipse Ti (×10 magnification). Images were collected at 48 h (MCF-7) or 28 h (MB-231) after scratch. The areas of five representative wounds for each condition were analyzed and quantified as the percentage of cells that migrated to the wound area after scratch.

Transwell migration assay

Cell migration was analyzed by transwell assay, using 'Fluorimetric QCM 24-well (8 μm) Chemotaxis Cell Migration Assay' (ECM509, Millipore) and following the manufacturer's instructions. In brief, MCF-7 and MB-231 cells were transfected as described for wound-healing experiments. Before starting transwell assays, transfected cells were cultured for 48 h under standard conditions and then starved for 24 h. Cells were suspended in serum-free medium (DMEM 5% BSA) and placed in the upper chambers of Transwell plates (12×10^4 cells/well). DMEM 10% FBS was used as a chemoattractant in the lower chambers. Cell migration was measured by fluorescence using the CyQUANT® GR Dye after 8 and 24 h incubation for MCF-7 and MB-231, respectively.

Immunofluorescence analysis

For immunohistochemistry, 5 μm sections from control and involuting mammary gland were analyzed as previously described [18]. Sections were incubated overnight at 4°C with primary antibodies (CAPN1, CAPN2, or E-cadherin). Secondary fluorescent antibodies Alexa Fluor 488 anti-rabbit IgG (A11008, Thermo Fisher) or Cy3 anti-mouse IgG (C2181, Sigma-Aldrich) were used for detection.

Breast cancer cells were cultured onto 13 mm Ø borosilicate coverglass (VWR 631-0149) and immunostained as described. In brief, cells were incubated with CAPN1 (ab3589, Abcam) or CAPN2 (#2539, Cell Signaling) overnight at 4°C. Cy3 anti-mouse IgG (CAPN1) or Alexa Fluor 488 anti-rabbit IgG (CAPN2) secondary antibodies were used for detection. Nuclei were counterstained with Hoechst 33342 (Invitrogen). Pictures were acquired on an Leica TCS-SP 2 confocal microscope.

Biochemical Journal (2016) 473 2893–2909
DOI: 10.1042/BCJ20160198

Duolink proximity ligation assay

In situ CAPN1/E-cadherin or CAPN2/E-cadherin interaction in mammary gland was detected using the Duolink® *In Situ* based on proximity ligation assay (PLA) from Sigma-Aldrich. Mammary gland tissue sections from lactating (0 h) and weaning mice (24 and 72 h involution) were fixed and permeabilized in antigen-blocking solution as described previously [24]. The calpain-mediated cleavage of E-cadherin was also analyzed in 72 h weaning samples from mice treated with calpeptin or vehicle (DMSO). Following permeabilization, tissue sections were incubated with CAPN1 or CAPN2 and E-cadherin-specific antibodies (each from different host species). PLA probe ligation and amplification were performed following the manufacturer's instructions. Finally, samples were covered with Duolink *In Situ* Mounting Medium with DAPI (for nuclei staining) and analyzed in a confocal microscope Leica TCS-SP 2.

Protein extraction and immunoblotting

Total protein was extracted in the presence of protease inhibitors as described recently [17]. Equal amounts of protein (15 μg for mammary gland extracts and 20 μg for breast cancer extracts) were separated, subjected to SDS–PAGE, and electroblotted onto nitrocellulose membranes (Protran®, Whatman). The specific proteins were detected using the indicated primary antibodies and HRP-conjugated secondary antibody (DAKO). Blots were developed by enhanced chemiluminescence reaction (ECL Detection Kit, GE Healthcare, Uppsala, Sweden). Equal loading was confirmed by reprobing the blot against α-tubulin or β-actin and by Ponceau Red staining.

Calpain activity

CAPN activity was measured as described previously using a calpain activity assay kit (QIA-120, Calbiochem, Billerica, MA, USA) and according to the manufacturer's instructions [17,18]. In brief, total protein extracts from human breast cancer cell lines were solubilized in cell lysis buffer (CytoBuster™ Protein Extraction Reagent). Samples (in the presence or absence of inhibition buffer containing BAPTA) and standards were then incubated during 15 min in a 96-well plate with activation buffer (containing Ca^{2+} and TCEP reducing agent) and the substrate (Suc Leu-Leu-Val-Tyr-AMC) provided in the kit. Fluorescence was measured using a fluorescence plate reader at an excitation wavelength of ∼360–380 nm and an emission wavelength of ∼440–460 nm. CAPN activity was determined as the difference between the activity obtained using the CAPN-inhibition buffer (BAPTA) and that detected with the activation buffer.

RT-qPCR analysis

Total RNA from breast cancer cell lines was extracted by TRIzol® (Invitrogen) followed by additional column purification (RNeasy, Qiagen, Hilden, Germany). RNA quantity and purity were determined using the NanoDrop ND-2000 (NanoDrop Technologies). RNA (1 μg) was reverse-transcribed to cDNA using a high-capacity RNA-to-cDNA kit (Applied Biosystems, Foster City, California, USA). cDNA products were amplified by qPCR using the GeneAmp Fast PCR Master Mix (Applied Biosystems). All reactions were carried out in triplicate. RT-qPCR was run in the 7900HT Fast Real-Time PCR System. Pre-developed TaqMan primers specific for *Capn1*, *Capn2*, and 18S were purchased from Applied Biosystems. Results were normalized according to 18S quantification in the same sample reaction. The threshold cycle (C_t) was determined, and the relative gene expression was expressed as follows:

$$\text{Relative amount} = 2^{-\Delta(\Delta C_t)},$$

where $C_t = C_t(\text{target}) - C_t(18S)$ and $\Delta(\Delta C_t) = \Delta C_t$ (breast cancer cell line) $- \Delta C_t$(MCF-7).

Statistics

Statistical significance was estimated with one-sample Student's *t*-test. Experiments described in Figure 5, a one-way ANOVA was used for statistical analysis. Significant differences were determined by a Tukey–Kramer test. Different superscript letters indicate significant differences. The letter 'a' always represents the lowest value within the group. Differences were considered significant at least at $P < 0.05$. Independent experiments were conducted with a minimum of three replicates per condition to allow for statistical comparison.

Biochemical Journal (2016) **473** 2893–2909
DOI: 10.1042/BCJ20160198

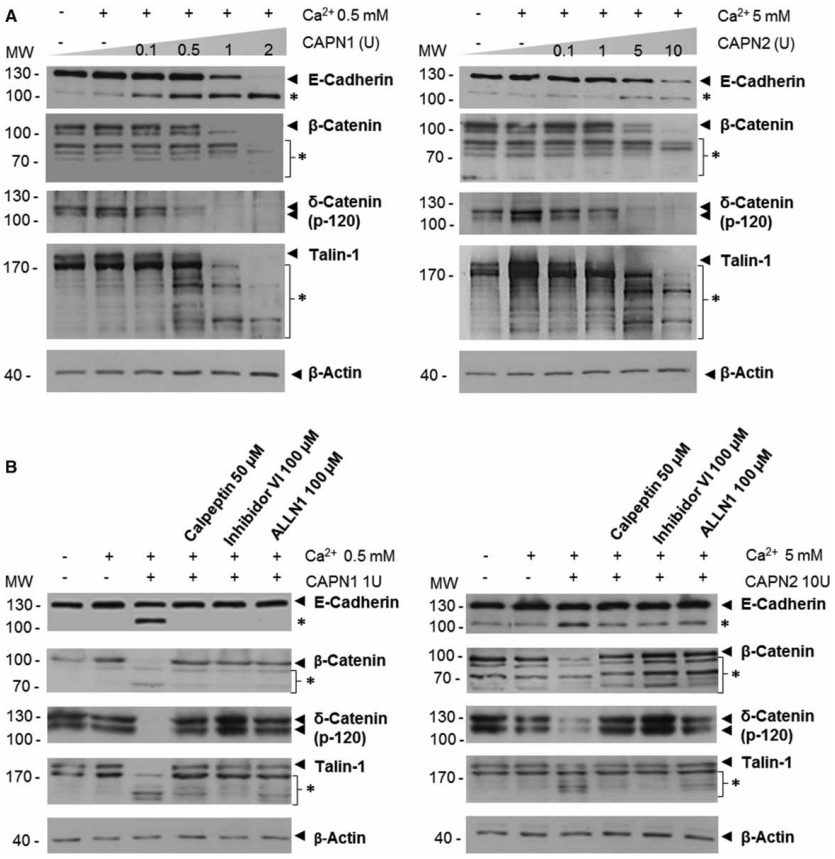

Figure 1. Adhesion proteins from lactating mammary gland as targets of CAPN1 and CAPN2 *in vitro*.
(**A**) Calpain-mediated cleavage of E-cadherin, β-catenin, δ-catenin (p-120), and talin-1 was analyzed by western blot in protein extracts from lactating mammary gland. Protein samples were incubated with increasing concentrations of either recombinant CAPN1 (left panel) or CAPN2 (right panel) in the presence of calcium. (**B**) Cleavage of adhesion proteins by recombinant CAPN1 (left) and CAPN2 (right) in the presence of specific protease inhibitors, calpeptin, calpain inhibitor VI, and ALLN, was analyzed by western blot in proteins extracts from lactating mammary gland. Protein cleavage was analyzed by either detection of truncated fragments (asterisks) or disappearance of full proteins (arrow heads). Equal loading was assessed by the analysis of β-actin expression. Representative blots are shown ($n \geq 3$). Predicted cleavage sites are shown in Supplementary Figure S1.

Results

Adhesion proteins as physiological targets of CAPN1 and CAPN2

A cell-free assay with recombinant CAPNs and extracts from lactating mammary acini was conducted to understand which of these ubiquitously expressed proteases, CAPN1 or CAPN2, is involved in cell detachment of physiological mammary epithelia *in vivo*. Proteolysis of E-cadherin, catenin p-120 and β-catenin was analyzed by western blot as a measure of adherens junction disruption, whereas loss of focal adhesion was analyzed by means of talin cleavage. These *in vitro* studies clearly showed that both focal and adherens junctions from lactating samples were cleaved when extracts were incubated with increasing concentrations of recombinant CAPN1 or CAPN2 in the presence of calcium (Figure 1A). In the absence of CAPN and/or Ca^{2+}, no

Biochemical Journal (2016) **473** 2893–2909
DOI: 10.1042/BCJ20160198

cleavage was observed. Furthermore, calpain inhibitors blocked cleavage of adhesion proteins induced by recombinant CAPNs (Figure 1B), demonstrating that both CAPNs are able to specifically recognize and cleave adhesion proteins from mammary gland epithelia.

Subcellular distribution of specific CAPN isoforms in mammary epithelial cells

The context-dependent subcellular distribution of a CAPN isoform might specify its target-substrate to undertake a given biological function. Consequently, the subcellular distribution of both CAPNs was analyzed in lactating mammary gland tissue sections and breast cancer cells. To detect possible differences among breast cancer subtypes according to their HER2 status and basal/luminal origin, a cell line from each subtype was used.

As shown in Figure 2A, CAPN1 immunostaining was diffusely detected in epithelial cells from lactating mammary tissue. CAPN2 was mainly localized at the cell-to-cell adhesion interface of basal cells. CAPN1 resulted distributed in the cytosol and nuclei of breast cancer cells (Figure 2B). CAPN2, barely detected in the cytosolic compartment, was found to be mainly localized in nuclei of all the cell lines tested. Importantly, no membrane-associated CAPN2 was identified in breast cancer cells. Although apparently expressing different CAPN levels, no difference in CAPN distribution was observed among the cell lines.

These data suggest that although the breast cancer subtype does not condition the subcellular localization of these CAPNs, CAPN2 subcellular distribution in mammary epithelial cells is dependent on cell context.

Isoform-specific colocalization of CAPN with E-cadherin during mammary gland involution

CAPN2 seemed to have a polarized basal distribution in mammary acini at the peak of lactation. Nevertheless, epithelial cells are shed into the lumen only during the time course of involution. To explore the role of CAPN2 on cell adhesion in a physiological model of cell–cell disruption, tissue sections from postlactation mammary gland were immunostained with antibodies against CAPN1 or CAPN2 and E-cadherin and their subcellular distribution was analyzed.

Co-localization of CAPN2 and E-cadherin was detected at the peak of lactation and during the time course of involution (Figure 3A). As described previously [25] at 72 h involution, E-cadherin seemed to be re-localized to the cytoplasmic fraction of epithelial cells. Interestingly, we did not observe an increased co-localization of CAPN2/E-cadherin during involution but instead, a clear redistribution of CAPN2 to the apical side of luminal cells (24 h) and thereafter to the cytosolic compartment (72 h), co-localizing at both time points with E-cadherin. On the other hand, no redistribution of CAPN1 was observed at lactation or 72 h involution (Figure 3B).

These results point out to CAPN2 as the most probable CAPN involved in cell detachment in the physiological model of mammary gland involution.

Cleavage of adhesion proteins in physiological and tumoral models of cell adhesion disruption

To examine the functional role of CAPN2 under physiological conditions, cleavage of adherens and focal adhesion proteins was studied by western blot in extracts from mammary gland during the time course of involution. In agreement with immunohistochemical data, E-cadherin was disrupted during the first phase of involution (Figure 4A). Indeed, although starting at 6 h after weaning, the proteolytic processing of E-cadherin was not completed until the next 48–72 h of involution. The same proteolytic pattern was observed for other proteins from the cell–cell interaction (catenin p-120 and β-catenin) or focal adhesion complexes (talin-1). Our *in vivo* data strongly support a correlation between the proteolytic processing of adhesion proteins and the expression and membrane localization of CAPN2 in mammary gland after weaning [17,18].

Breast cancer cell lines in agreement with their metastatic potential both adherens junctions and focal adhesion proteins were cleaved in luminal cells (Figure 4B). As described recently, triple-negative MB-231 and MB-468 cells do not establish adherens junctions [23,26] and consequently, in triple-negative cell lines only talin-1, a focal adhesion protein, was cleaved.

Biochemical Journal (2016) **473** 2893–2909
DOI: 10.1042/BCJ20160198

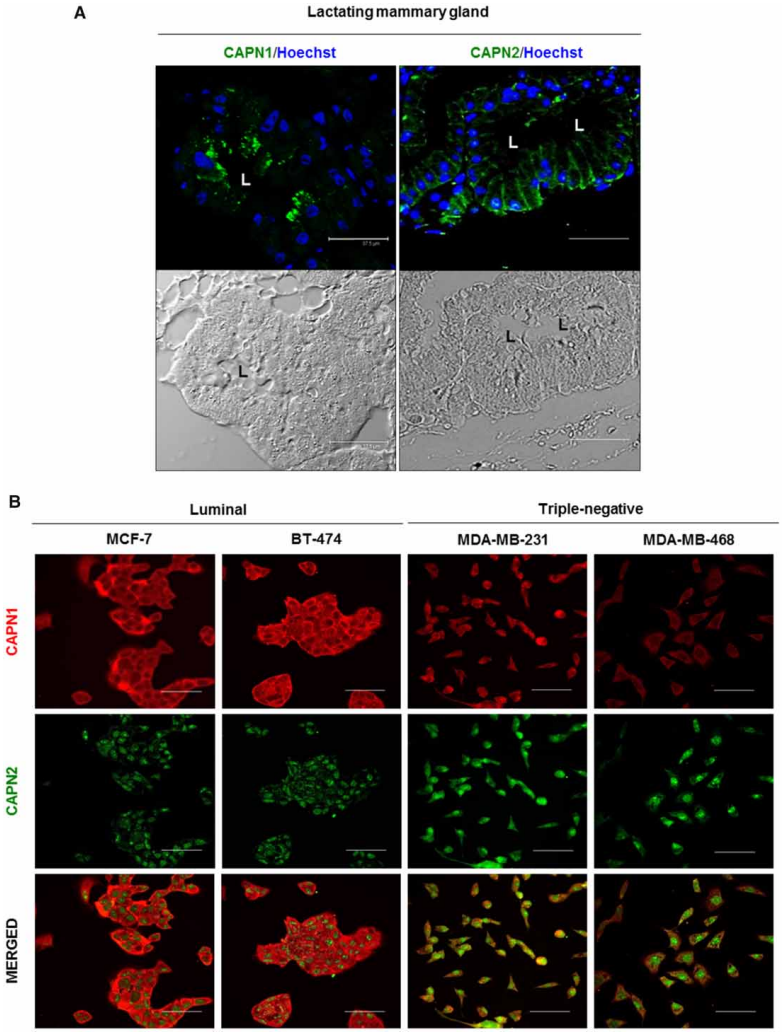

Figure 2. Subcellular distribution of CAPN1 and CAPN2 in lactating mammary gland and breast cancer cell lines.
(**A**) Representative immunofluorescence staining of CAPN1 and CAPN2 (green) in tissue sections from mice mammary gland at the peak of lactation. Cell nuclei were counterstained by Hoechst 33342 (blue). Bright field images were included simultaneously to visualize the exactly localization of immunofluorescence in mammary gland structure. L, lumen. Scale bars, 37.5 μm. (**B**) Immunostaining of CAPN1 (red) and CAPN2 (green) in MCF-7, BT-474, MDA-MB-231, and MDA-MB-468 breast cancer cell lines. Scale bars, 70 μm. Representative images are shown ($n \geq 3$).

Identification of the CAPN isoform catalytically active in different subtypes of breast cancer cells

To establish a putative correlation between a specific CAPN isoform and the proteolytic processing of adhesion proteins in breast cancer cells, an exhaustive analysis of CAPN expression and enzymatic activity was performed in all cell lines.

Biochemical Journal (2016) **473** 2893–2909
DOI: 10.1042/BCJ20160198

Expression of CAPN1 and CAPN2 was measured by RT-qPCR and western blot in cell lines cultured under standard conditions. As shown in Figure 5A,B, CAPN1 and CAPN2 were differentially expressed in the four cell lines according to either HER2 status or the triple-negative subtype. MCF-7 expressed higher CAPN1 mRNA and protein levels than the other cell lines studied. On the other hand, CAPN2 expression was much higher in triple-negative than in luminal cells (Figure 5A,B). Consequently, CAPN1/CAPN2 ratio was dramatically higher in luminal than in triple-negative cells (Figure 5B, right panel).

However, higher levels of CAPN expression do not necessarily mean higher enzymatic activity. We analyzed enzymatic activity in the different cell lines by molecular analysis of well-known mechanisms thought to overcome Ca^{2+} requirements and to facilitate calpain activation [27,28]: (i) autolysis of the anchor helix of CAPN1, but not of CAPN2; (ii) cleavage and dissociation of the small regulatory subunit CAPN4; and (iii) binding to calpastatin, the endogenous enzymatic inhibitor of both CAPNs.

As seen in Figure 5B, the absence of CAPN1 amino-terminal (Nt) domain analyzed by western blot indicates a complete autolysis of CAPN1 anchor helix in luminal cells indicating its activation. CAPN4 protein levels were equally abundant in all the cell lines tested. Calpastatin protein levels resulted to be significantly higher in triple-negative cells than in luminal cells. Moreover, calpastatin was not even detected in the more aggressive luminal phenotype HER2 cells (BT-474).

These results suggest that luminal cells show not only higher CAPN1/CAPN2 expression ratio, but also increased CAPN1 activity when compared with triple-negative cells. Calpain activity analyzed by enzymatic assay further confirmed the higher calpain activity in luminal than in triple-negative cell lines (Figure 5C), a pattern that strongly resembled CAPN1 expression.

Functional role of isoform-specific CAPNs in breast tumor cells

To dissect the role of each calpain isoform on cell adhesion of breast tumors, CAPN1 or CAPN2 was knocked down in the four cell lines and cleavage of adhesion proteins was studied by western blot (Figure 6A). In addition, CAPN1 and CAPN2 mRNA levels were analyzed by RT-qPCR to confirm the specificity of siRNA knockdown experiments (Supplementary Figure S2)

Transfection of luminal cells with CAPN1 siRNA prevented cleavage of both focal and adherens junction proteins. Although adherens junctions are known to be disrupted in MB-231 and MB-468 cells [26], cleavage of focal adhesion in these triple-negative cell lines was also prevented by CAPN1 knockdown. Conversely, knockdown of CAPN2 showed no apparent effect on adhesion proteins in either luminal or triple-negative cell lines. These results suggest that independently of the tumor subtype, CAPN1 is the preferential calpain involved in the regulation of cell adhesion of breast cancer cell lines.

The biological role of calpains was also investigated in CAPN1 and CAPN2 knocked down breast tumor cell lines. MCF-7 and MB-231 were selected as representative cell lines from both subtypes of breast tumors, and cell migration was analyzed by wound-healing assay. Wound-healing assays (Figure 6B) indicate that CAPN1 down-regulation decreased the migration of MCF-7 or MB-231 cells by 50% compared with control cells. Conversely, cell migration was not affected by CAPN2 knockdown (Supplementary Figure S3A). Transwell migration assays (Supplementary Figure S3B) further confirmed the conclusion that independently of the breast tumor subtype, CAPN1 enhances migration of tumor cells.

Interaction of CAPN2/E-cadherin in physiological mammary gland involution

Once discerned the isoform-specific role of CAPN in breast cancer migration, we sought to elucidate the functional role of CAPN2 in the proteolytic processing of adhesion proteins *in vivo*. To examine whether CAPN2 disrupts membrane localization of E-cadherin in physiological conditions, the interaction between both proteins was analyzed by the sensitive *in situ* Duolink PLA in tissue sections from mammary gland after weaning. As shown in Figure 7A, CAPN2/E-cadherin interaction was barely detected at the peak of lactation, but dramatically increased as the involution progressed (quantification of PLA data shown in Supplementary FigureS4A). Conversely, no CAPN1/E-cadherin interaction was detected (Supplementary Figure S4B).

The diffuse and punctate fluorescence staining in the cytosolic compartment during involution seems to be the product from CAPN2-mediated cleavage of E-cadherin, which was gradually accumulated in the cytoplasm. In PLA assays, a fluorescent signal is generated only when the plus and minus probes attached to each antibody are bound together [24]. This proximity could be achieved when E-cadherin is bound to the active center of CAPN2; therefore, calpain-mediated cleavage of E-cadherin would result in fluorescence increase along the

Biochemical Journal (2016) **473** 2893–2909
DOI: 10.1042/BCJ20160198

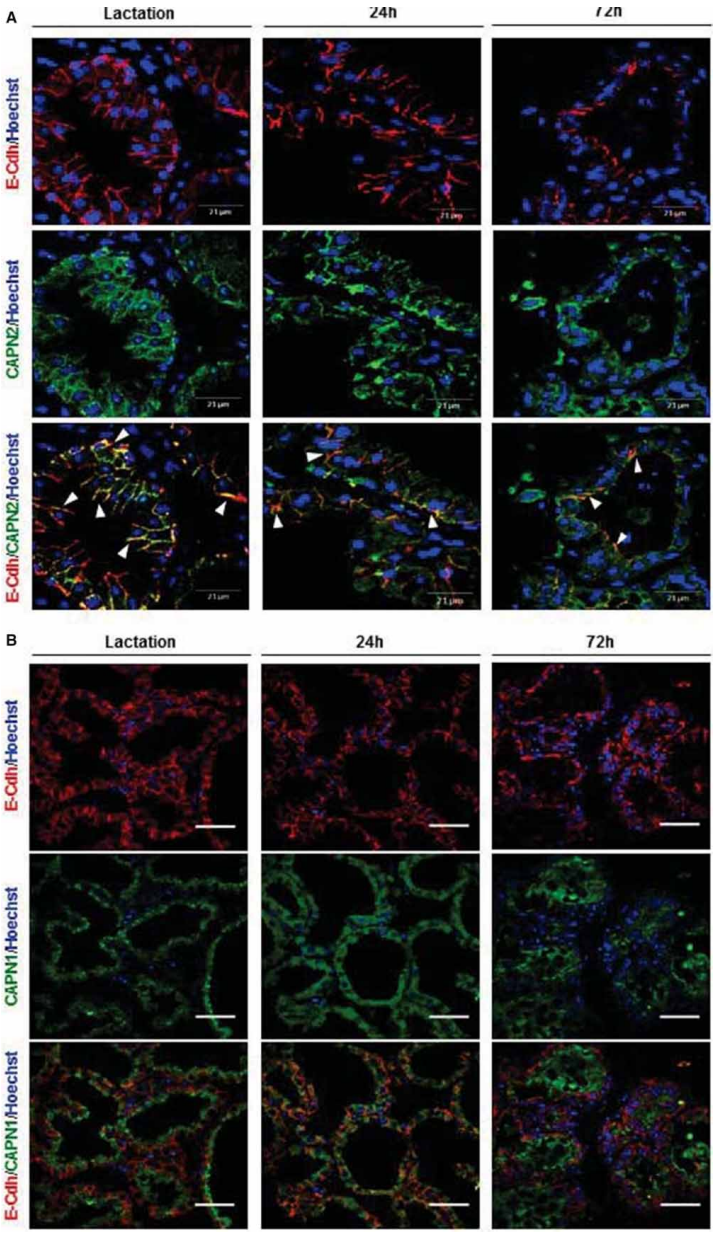

Figure 3. CAPN/E-cadherin co-localization during the time course of mammary gland involution.

(**A**) Tissue sections from mammary gland at the peak of lactation and after 24 and 72 h of involution were immunostained with antibodies against E-cadherin (red) or CAPN2 (green). Nuclei were counterstained with Hoechst 33342 (blue). Arrowheads in the merged images show CAPN2/E-cadherin co-localization (orange). Scale bar, 21 μm. (**B**) The same analysis as above was carried out for E-cadherin (red) and CAPN1 (green). No CAPN1/E-cadherin co-localization was found. Scale bar, 78 μm. Colored words in the artwork define the color staining for each protein.

Biochemical Journal (2016) **473** 2893–2909
DOI: 10.1042/BCJ20160198

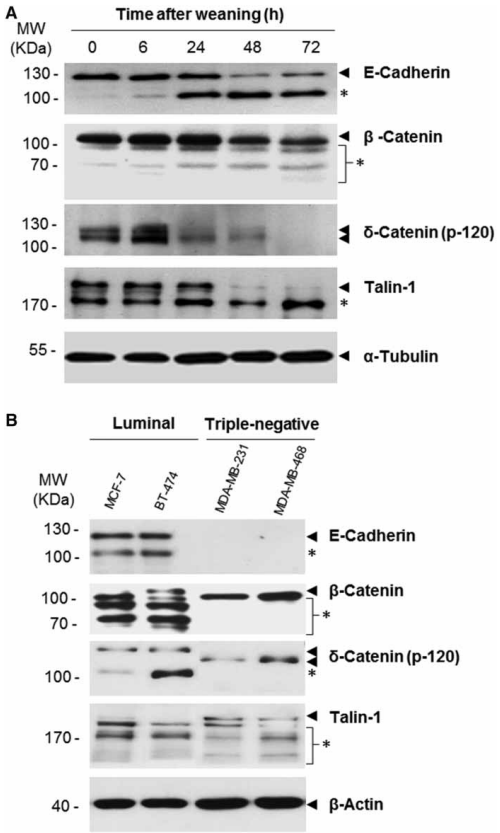

Figure 4. Cleavage of adhesion proteins in physiological and pathological mammary cells.

(**A**) Cleavage of E-cadherin, β-catenin, δ-catenin (p-120), and talin-1 was analyzed by western blot in protein samples from mammary gland at the peak of lactation (0 h), and during the time course of involution (6, 24, 48, and 72 h). α-Tubulin was used as a loading control. (**B**) Cleavage of adhesion proteins was analyzed by western blot in luminal (MCF-7 and BT-474) and triple-negative (MDA-MD-231 and MDA-MD-468) breast cancer cell lines as above. β-Actin was used as a loading control. Protein cleavage was analyzed by either detection of truncated fragments (asterisks) or disappearance of full proteins (arrow heads). Representative immunoblots are shown ($n \geq 3$).

time course of mammary gland involution. In agreement with this, CAPN2/E-cadherin interaction at 72 h after weaning was prevented by calpeptin, the specific competitive inhibitor of calpain (Figure 7B, upper panels and Supplementary Figure S4C). CAPN1/E-cadherin interaction was not detected by PLA assay at 72 h involution, in either DMSO or calpetin-treated mice (Figure 7B, middle panel).

According to the calpain-mediated cleavage of E-cadherin, mislocalization and loss of E-cadherin at cell–cell junctions were observed at 72 h weaning by immunofluorescence, and prevented in calpeptin-treated mice (Figure 7B, lower panels). In addition, proteolysis of other adhesion proteins was also prevented by calpeptin as shown by western blot analysis (Figure 7C).

Altogether these results suggest that although CAPN2 is the critical isoform involved in the disruption of cell adhesion during mammary gland involution, during tumor progression there is a molecular switch from CAPN2 to CAPN1 that is essential for the cleavage of adhesion proteins and cell migration.

Biochemical Journal (2016) **473** 2893–2909
DOI: 10.1042/BCJ20160198

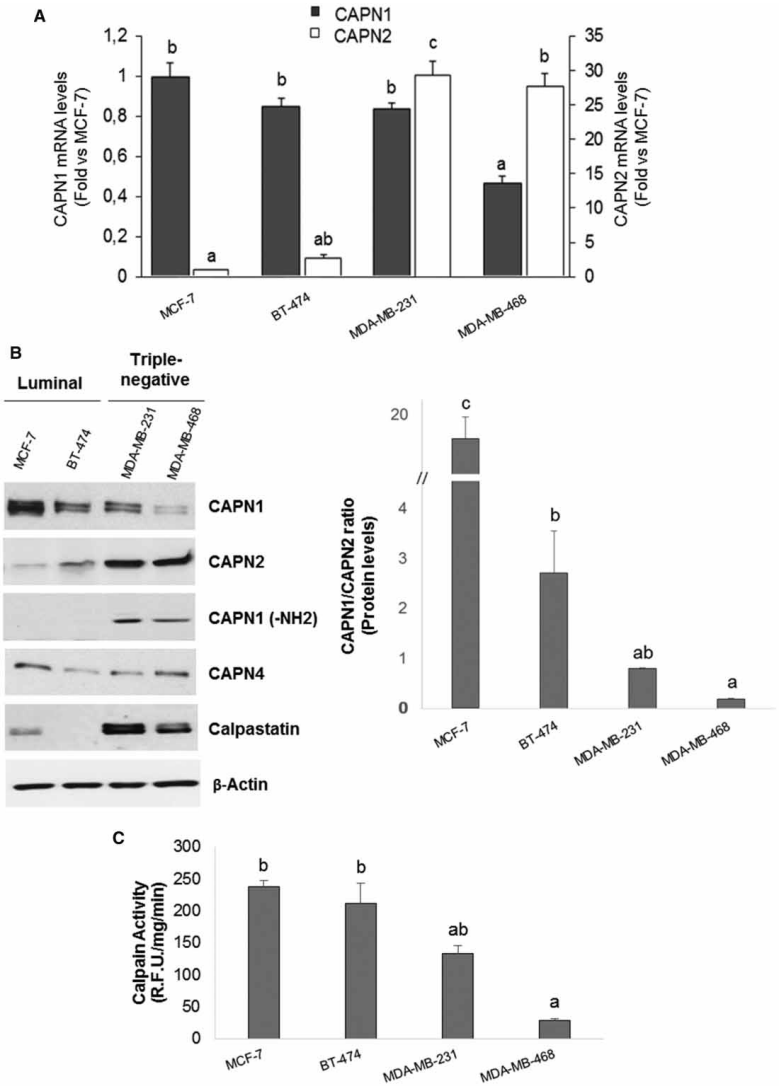

Figure 5. Isoform-specific expression and activity of calpains in breast cancer cells.

(**A**) CAPN1 (black bars) and CAPN2 (white bars) mRNA levels in MCF-7, BT-474, MDA-MB-231, and MDA-MB-468 cell lines were analyzed by quantitative real-time PCR. Data were normalized according to 18S mRNA, analyzed and quantified in the same sample reaction. Expression levels are shown as fold vs. MCF-7. Results ($n \geq 4$) are means ± SEM. (**B**) CAPN1, CAPN2, Nt-CAPN1, CAPN4, and calpastatin total protein levels from breast cancer cell lines were analyzed by western blot (left panel). β-Actin was used as a loading control. Expression of CAPN1 and CAPN2 was quantified and plotted as the ratio of CAPN1/CAPN2. Data are represented as means ± SEM ($n \geq 3$) (right panel). (**C**) Calpain enzymatic activity in breast cancer cell lines was measured by a fluorogenic assay where Suc-LLY-AFC was used as a calpain substrate. Results are shown as mean ± SEM ($n = 3$). ANOVA was performed for the statistical analysis, where different superscript letters indicate significant differences, $P < 0.05$; the letter 'a' always represents the lowest value within the group.

Biochemical Journal (2016) **473** 2893–2909
DOI: 10.1042/BCJ20160198

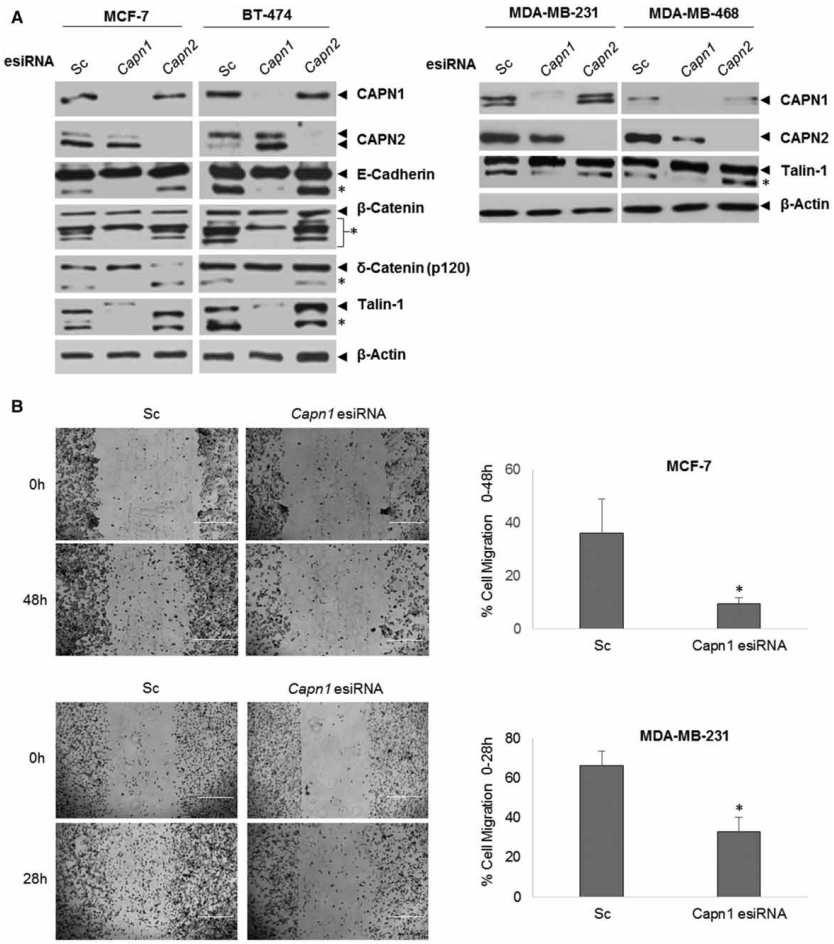

Figure 6. Functional role of CAPN1 and CAPN2 on disruption of adhesion proteins and migration of breast cancer cells.
(**A**) Breast cancer cell lines were transfected with Scramble (Sc), Capn1 or Capn2 siRNAs, and cleavage of E-cadherin, β-catenin, δ-catenin (p-120), and talin-1 in knockdown cells was analyzed by western blot. CAPN1 and CAPN2 protein levels were analyzed to confirm the efficiency of knockdown experiments. Protein cleavage was analyzed by either detection of truncated fragments (asterisks) or disappearance of full proteins (arrow heads). (**B**) Cell migration in Capn1-knockdown cells (MCF-7 and MDA-MB-231) was analyzed by wound-healing assay (left panels). Graphs show the percentage of cells that migrated to the wound area after 48 h (MCF-7) or 28 h (MDA-MB-231). Data ($n \geq 3$) are means ± SEM. Student's *t*-test was performed for the statistical analysis, $^{*}P < 0.01$ vs. scramble (Sc). Scale bar, 500 μm.

Discussion

Postlactational regression, or involution, of the mammary gland is one of the best physiological models to study *in vivo* the molecular events leading to the effective clearance of secretory epithelial cells that are no longer needed. Upon cessation of lactation, 80% of the mammary epithelium is removed. Epithelial cell death and tissue remodeling will return the gland to a pre-pregnant state for the next pregnancy/lactation cycle [1,2,17,18,22].

Biochemical Journal (2016) **473** 2893–2909
DOI: 10.1042/BCJ20160198

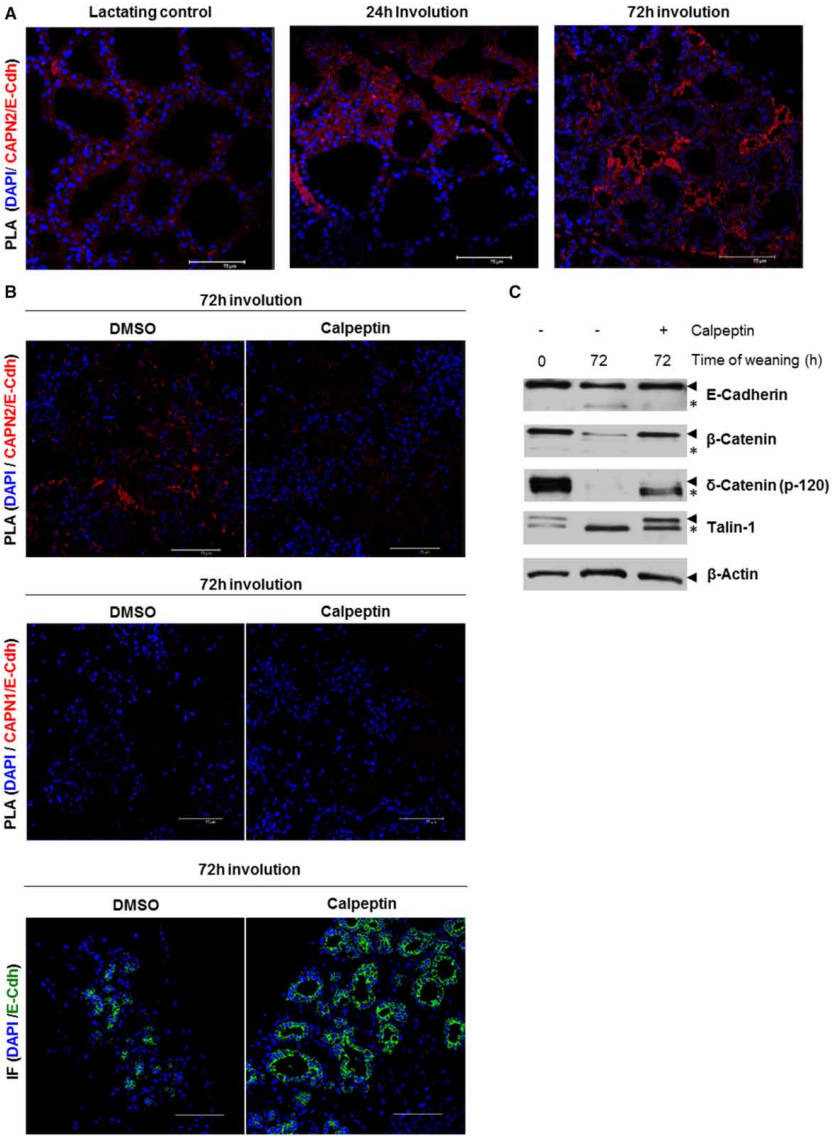

Figure 7. *In vivo* CAPN2-mediated cleavage of E-cadherin during mammary gland involution.
(**A**) CAPN2/E-cadherin *in vivo* interaction (red) was analyzed by PLA in tissue sections from mammary gland during the time course of involution (0, 24, and 72 h). (**B**) CAPN2/E-cadherin interaction (red) analyzed by PLA in tissue sections from DMSO (vehicle) or calpeptin-treated mammary gland at 72 h weaning (upper panel). No interaction was observed for CAPN1/ E-cadherin by PLA (middle panel). Lower panel shows the immunofluorescence staining of E-cadherin in the same experiments (green). Scale bar, 75 μm. Nuclei were stained with DAPI (blue). (**C**) Cleavage of E-cadherin, β-catenin, δ-catenin (p-120), and talin-1 at 0 and 72 h weaning in DMSO or calpeptin-treated mice was assessed by western blot. β-Actin was used as a loading control. Representative immunoblots are shown ($n \geq 3$).

Biochemical Journal (2016) **473** 2893–2909
DOI: 10.1042/BCJ20160198

Cleavage of adhesion-protein complexes plays an important role in the regulation of epithelial homeostasis that encompasses the effective clearance of undesired cells [3,4]. Here, we show the time-dependent cleavage of adhesion proteins during the time course of involution, all of the substrates that can be equally recognized *in vitro* by CAPN1 and CAPN2. Nevertheless, our data suggest that CAPN2 has a prominent role in the proteolytic cleavage of adhesion proteins in weaning-induced mammary gland involution. In agreement with the important role played by calpains in cell adhesion disruption, many reports have linked calpain activity to cleavage of adhesion complexes [7–13,21,29]. We have previously reported the dual role of CAPN1: inducing mitochondrial, lysosomal and nuclear membrane destabilization of epithelial cells and participating in the epigenetic program of adipocyte differentiation during mammary gland involution [17,18]. Now, we propose a role for CAPN2 in epithelial cell detachment during mammary gland involution. We have demonstrated that only CAPN2 co-localizes with E-cadherin at the peak of lactation. Moreover, as can be deduced from the experiments in calpeptin-treated mice analyzed by PLA, E-cadherin was specifically bound to and cleaved by CAPN2 during involution.

In addition to E-cadherin, we observed the proteolytic processing of other adhesion proteins during mammary gland involution. The cleavage of these proteins was also dependent on calpain activity, as demonstrated in calpeptin-treated mice. The cytoplasmic cleavage of E-cadherin, β-catenin, or Talin1 by calpain has been already described in other tissues [9,11,13,17,21]. Although most likely these proteins are also the targets of CAPN2, we did not demonstrate the direct role of this isoform in their cleavage. Therefore, we cannot rule out the possibility of a proteolytic destabilization of the adhesion complex as a consequence of E-cadherin cleavage [9,30], or the indirect effect of another target of CAPN.

It is noteworthy to mention that the fragments of E-cadherin remained bound to CAPN2 and accumulated in the cytosol at 72 h of involution. In this sense, it is known that the fate of cytoplasmic fragments of E-cadherin can be the proteasomal degradation or alternatively, the acquisition of a different biological function related to cell proliferation or cell death through the activation of signaling pathways [4,5,30,31]. In the near future, it would be of interest to explore the possible biological activity of E-cadherin fragments associated with CAPN2 in the cytoplasm of epithelial cells during involution.

Altogether these data suggest that although the expression and activity of both CAPN isoforms is increased during involution [17,18], their subcellular localization and proteolytic targets are not the same. In agreement with this, it has been recently reported that CAPN1 and CAPN2 are recruited to different compartments where they play different functions [19,20]. In addition, the idea of 'an interchangeable role for CAPN1 and CAPN2' in cell adhesion is most probably the result of a very heterogeneous number of experimental models reported in the literature. Most of studies do not identify the specific isoform of CAPN involved in cell detachment or use cultured cells from carcinoma origin or even different cell types as experimental models to be compared. Understanding the deregulation of calpains involved in cell detachment during breast tumor progression requires the exhaustive study of their normal counterparts under physiological conditions. Many studies use as experimental model of 'normal cells' the human cell line MCF10A, a predominantly myoepithelial cell line classified as basal subtype [32,33]. In addition, tissue organization is not an issue to be overlooked when studying the physiological disruption of cell contacts, and cultured cells do not resemble the polarized acinar structure of mammary gland.

Cell death induced by detachment from ECM and cell-to-cell contacts functions as a luminal clearing mechanism during mammary gland involution. But, the proteolytic cleavage of adhesion proteins by many proteases is not only the response to physiological stimuli, but also the pathological consequence of cell transformation. Detachment of cells and luminal filling is a hallmark of breast cancer. Deregulated expression or activity of proteases involved in the proteolytic processing of adhesion proteins is known to facilitate metastasis [4,6]. However, data about the isoform-specific role of CAPNs in tumor progression are confusing [34–37]. While low levels of CAPN expression are associated with poor survival in gastric carcinomas [34], high levels of CAPN expression have been associated with breast cancer [35]. A correlation between CAPN1 expression and poor prognosis or even resistance to trastuzumab treatment in breast cancer has been described, but no correlation has been found with the expression of calpastatin, the endogenous inhibitor of both calpains, or with CAPN2 levels [35,36]. It has been argued that discrepancies among reports are most probably caused by the type of analysis performed in these clinical studies and to the different classification of breast tumor subtypes. Breast cancer has been revealed as a heterogeneous disease and choosing the right cancer cell line for breast cancer research is not a minor point [23,32,33]. For that reason, although we are not unaware of possible interspecies differences, we selected cell lines including the most common luminal HER-negative and -positive

subtypes (MCF-7 and BT-474, respectively) and the more aggressive triple-negative basal and claudin-low subtypes (MB-468 and MB-231, respectively).

Interestingly, although there were important differences in mRNA, protein levels, and enzymatic activity of both CAPN isoforms among cell lines, we could demonstrate in CAPN1 and CAPN2 knockdown experiments that CAPN1 was the only isoform involved in the proteolytic cleavage of adhesion proteins of breast cancer, independently of the breast cancer subtype.

An important question regarding the mechanism driving the specific CAPN isoform to the plasma membrane remains to be answered. One could speculate with several hypotheses such as CAPN binding to other proteins that would act as chaperones, or CAPN posttranslational modifications that would favor the protease direct- or indirect-anchoring to plasma membranes. In this sense, CAPN2 binding to membrane lipids seems to be crucial for its activation [38,39]. In addition, phosphorylation of specific amino acids of CAPN2 by protein kinase (PKA) or extracellular regulated kinase (ERK) has been suggested to prevent or induce its stable binding to phosphoinositides, respectively [38–40]. Moreover, it has been proposed that CAPN2 needs to be localized at the plasma membrane to be activated by stimuli triggering the EGFR pathway. Indeed, CAPN2 activation can be prevented by internalization of EGFR or ERK [40], indicating that the EGFR pathway from the cytosolic compartment cannot reach or affect membrane-bound CAPN2. EGFR pathway is one of the most important pathways known to be triggered during mammary gland involution. In addition, it is also the major deregulated pathway in breast cancer. Whether the mutational state of this pathway could drive the isoform fate of CAPN2/CAPN1 in breast cancer remains to be elucidated. However, in the absence of EGF stimulation, inhibition of ERK activation by PD98059 prevents CAPN2 binding to the plasma membrane [38], suggesting that there is an additional substrate-driven ERK-mediated localization of CAPN2. It is noteworthy to mention that CAPN2 is unequally redistributed to the sites of locomotion in cultured cells forced to migrate [21,41]. In this sense, the ECM from postlactational mammary gland is profoundly remodeled; therefore, the redistribution of CAPN2 during mammary gland involution to the luminal side of cells could be the result of an ECM-driven mechanism. On the other hand, we cannot rule out the possibility that culture conditions might affect the switch of the specific CAPN isoform involved in cell adhesion of breast cancer cells that were grown on plastic plates. In the future, a clinical study analyzing not just CAPN1/CAPN2 expression, but rather the isoform direct interaction with E-cadherin in samples from breast cancer patients, would help to elucidate this important question.

In summary, our data point out to an isoform-specific role of calpains in physiological and pathological conditions. While CAPN2 seems to be the isoform involved in the proteolytic processing of adhesion proteins from epithelial cells during physiological mammary gland involution, adhesion junctions are cleaved by CAPN1 in breast cancer cell lines promoting cell migration. CAPN isoform overexpression and high enzymatic activity, frequently analyzed in breast tumors, are important but not sufficient conditions to suggest their invasive potential in breast cancer cells. Importantly, data presented here suggest that the subcellular distribution of CAPN1 and CAPN2 is a major issue in target-substrate recognition and therefore, identifying the mechanisms to drive the selected CAPN to the proper subcellular compartment will be an important question to be explored in the near future.

Abbreviations

ALLN, *N*-acetyl-L-leucyl-L-leucyl-norleucine; CAPN, calpain; ECM, extracellular matrix; ER, Estrogen Receptor; ERK, Extracellular Regulated Kinase; esiRNA, small interfering RNA; HER2, Human Epidermal Growth Factor Receptor2; Nt or NH2, amino-terminal domain; PgR, progesterone receptor; PKA, protein kinase A; PLA, proximity ligation assay; RT-qPCR, real-time quantitative PCR.

Author Contribution

L.R.-F. and I.F.-V. performed the experiments. S.S.O. transfected breast cancer cells. C.G. was in charge of mice and obtained the tissue samples. R.Z., J.R.V. and E.R.G.-T. contributed to the study design and data interpretation and drafted the initial report. All authors contributed to the final draft of the paper.

Funding

The present study was supported by grants from Ministerio de Ciencia e Innovación including FEDER [BFU2013-46434-P to J.R.V. and R.Z.] and Instituto de Salud Carlos III including FEDER [PI12/02394 to E.R.

Biochemical Journal (2016) **473** 2893–2909
DOI: 10.1042/BCJ20160198

G.-T.] and Consellería de Educación [GVPROMETEO 2014/II-055]. L.R.-F. and S.S.O. are funded by Consellería de Educación [GVPROMETEO 2014/II-055] and Ministerio de Educación, Cultura y Deporte [FPU13/04976].

Acknowledgements

We thank Sonia Priego for acquiring confocal microscopy images, and Elisa Alonso-Yuste for tissue histology and Isabel Escoms Doñate for her technical assistance while working in her master thesis.

Competing Interests

The Authors declare that there are no competing interests associated with the manuscript.

References

1 Zaragozá, R., García-Trevijano, E.R., Lluch, A., Ribas, G. and Viña, J.R. (2015) Involvement of different networks in mammary gland involution after the pregnancy/lactation cycle: implications in breast cancer. *IUBMB Life* **67**, 227–238 doi:10.1002/iub.1365
2 Watson, C.J. and Kreuzaler, P.A. (2011) Remodeling mechanisms of the mammary gland during involution. *Int. J. Dev. Biol.* **55**, 757–762 doi:10.1387/ijdb.113414cw
3 Stelwagen, K. and Singh, K. (2014) The role of tight junctions in mammary gland function. *J. Mammary Gland Biol. Neoplasia* **19**, 131–138 doi:10.1007/s10911-013-9309-1
4 Nava, P., Kamekura, R. and Nusrat, A. (2013) Cleavage of transmembrane junction proteins and their role in regulating epithelial homeostasis. *Tissue Barriers* **1**, e24783 doi:10.4161/tisb.24783
5 Grabowska, M.M. and Day, M.L. (2012) Soluble E-cadherin: more than a symptom of disease. *Front. Biosci.* **17**, 1948–1964 doi:10.2741/4031
6 Krakhmal, N.V., Zavyalova, M.V., Denisov, E.V., Vtorushin, S.V. and Perelmuter, V.M. (2015) Cancer invasion: patterns and mechanisms. *Acta Naturae* **7**, 17–28 PMID: 26085941
7 Moretti, D., Del Bello, B., Allavena, G. and Maellaro, E. (2014) Calpains and cancer: friends or enemies? *Arch Biochem. Biophys.* **564**, 26–36 doi:10.1016/j.abb.2014.09.018
8 Ho, W.-c., Pikor, L., Gao, Y., Elliott, B.E. and Greer, P.A. (2012) Calpain 2 regulates Akt-FoxO-p27Kip1 protein signaling pathway in mammary carcinoma. *J. Biol. Chem.* **287**, 15458–15465 doi:10.1074/jbc.M112.349308
9 Rios-Doria, J., Day, K.C., Kuefer, R., Rashid, M.G., Chinnaiyan, A.M., Rubin, M.A. et al. (2003) The role of calpain in the proteolytic cleavage of E-cadherin in prostate and mammary epithelial cells. *J. Biol. Chem.* **278**, 1372–1379 doi:10.1074/jbc.M208772200
10 Cortesio, C.L., Chan, K.T., Perrin, B.J., Burton, N.O., Zhang, S., Zhang, Z.-Y. et al. (2008) Calpain 2 and PTP1B function in a novel pathway with Src to regulate invadopodia dynamics and breast cancer cell invasion. *J. Cell Biol.* **180**, 957–971 doi:10.1083/jcb.200708048
11 Rios-Doria, J., Kuefer, R., Ethier, S.P. and Day, M.L. (2004) Cleavage of β-catenin by calpain in prostate and mammary tumor cells. *Cancer Res.* **64**, 7237–7240 doi:10.1158/0008-5472.CAN-04-1048
12 Wu, M., Yu, Z., Fan, J., Caron, A., Whiteway, M. and Shen, S.-H. (2006) Functional dissection of human protease μ-calpain in cell migration using RNAi. *FEBS Lett.* **580**, 3246–3256 doi:10.1016/j.febslet.2006.05.003
13 Benetti, R., Copetti, T., Dell'Orso, S., Melloni, E., Brancolini, C., Monte, M. et al. (2005) The calpain system is involved in the constitutive regulation of β-catenin signaling functions. *J. Biol. Chem.* **280**, 22070–22080 doi:10.1074/jbc.M501810200
14 Ono, Y. and Sorimachi, H. (2012) Calpains — an elaborate proteolytic system. *Biochim. Biophys. Acta* **1824**, 224–236 doi:10.1016/j.bbapap.2011.08.005
15 Sorimachi, H., Hata, S. and Ono, Y. (2011) Impact of genetic insights into calpain biology. *J. Biochem.* **150**, 23–37 doi:10.1093/jb/mvr070
16 Raynaud, F., Marcilhac, A., Chebli, K., Benyamin, Y. and Rossel, M. (2008) Calpain 2 expression pattern and sub-cellular localization during mouse embryogenesis. *Int. J. Dev. Biol.* **52**, 383–388 doi:10.1387/ijdb.072448fr
17 Arnandis, T., Ferrer-Vicens, I., Torres, L., García, C., Garcia-Trevijano, E.R., Zaragoza, R. et al. (2014) Differential functions of calpain 1 during epithelial cell death and adipocyte differentiation in mammary gland involution. *Biochem. J.* **459**, 355–368 doi:10.1042/BJ20130847
18 Arnandis, T., Ferrer-Vicens, I., García-Trevijano, E.R., Miralles, V.J., García, C., Torres, L. et al. (2012) Calpains mediate epithelial-cell death during mammary gland involution: mitochondria and lysosomal destabilization. *Cell Death Differ.* **19**, 1536–1548 doi:10.1038/cdd.2012.46
19 Wang, Y., Briz, V., Chishti, A., Bi, X. and Baudry, M. (2013) Distinct roles for μ-calpain and m-calpain in synaptic NMDAR-mediated neuroprotection and extrasynaptic NMDAR-mediated neurodegeneration. *J. Neurosci.* **33**, 18880–18892 doi:10.1523/JNEUROSCI.3293-13.2013
20 Chou, S.-M., Huang, T.-H., Chen, H.-C. and Li, T.-K. (2011) Calcium-induced cleavage of DNA topoisomerase I involves the cytoplasmic-nuclear shuttling of calpain 2. *Cell. Mol. Life. Sci.* **68**, 2769–2784 doi:10.1007/s00018-010-0591-4
21 Franco, S.J., Rodgers, M.A., Perrin, B.J., Han, J., Bennin, D.A., Critchley, D.R. et al. (2004) Calpain-mediated proteolysis of talin regulates adhesion dynamics. *Nat. Cell Biol.* **6**, 977–983 doi:10.1038/ncb1175
22 Xian, W., Schwertfeger, K.L., Vargo-Gogola, T. and Rosen, J.M. (2005) Pleiotropic effects of FGFR1 on cell proliferation, survival, and migration in a 3D mammary epithelial cell model. *J. Cell Biol.* **171**, 663–673 doi:10.1083/jcb.200505098
23 Holliday, D.L. and Speirs, V. (2011) Choosing the right cell line for breast cancer research. *Breast Cancer Res.* **13**, 215 doi:10.1186/bcr2889
24 Söderberg, O., Gullberg, M., Jarvius, M., Ridderstråle, K., Leuchowius, K.-J., Jarvius, J. et al. (2006) Direct observation of individual endogenous protein complexes in situ by proximity ligation. *Nat. Methods* **3**, 995–1000 doi:10.1038/nmeth947
25 Fornetti, J., Flanders, K.C., Henson, P.M., Tan, A.-C., Borges, V.F. and Schedin, P. (2016) Mammary epithelial cell phagocytosis downstream of TGF-β3 is characterized by adherens junction reorganization. *Cell Death Differ.* **23**, 185–196 doi:10.1038/cdd.2015.82
26 Kulkarni, S., Saju, L., Farver, C. and Tubbs, R. (2012) Calpain4 is required for activation of HER2 in breast cancer cells exposed to trastuzumab and its suppression decreases survival and enhances response. *Int. J. Cancer* **131**, 2420–2432 doi:10.1002/ijc.27510
27 Campbell, R.L. and Davies, P.L. (2012) Structure–function relationships in calpains. *Biochem. J.* **447**, 335–351 doi:10.1042/BJ20120921

28 Chou, J.S., Impens, F., Gevaert, K. and Davies, P.L. (2011) m-Calpain activation in vitro does not require autolysis or subunit dissociation. *Biochim. Biophys. Acta, Proteins Proteomics* **1814**, 864–872 doi:10.1016/j.bbapap.2011.04.007
29 Carragher, N.O. and Frame, M.C. (2002) Calpain: a role in cell transformation and migration. *Int. J. Biochem. Cell Biol.* **34**, 1539–1543 doi:10.1016/S1357-2725(02)00069-9
30 Ito, K., Okamoto, I., Araki, N., Kawano, Y., Nakao, M., Fujiyama, S. et al. (1999) Calcium influx triggers the sequential proteolysis of extracellular and cytoplasmic domains of E-cadherin, leading to loss of β-catenin from cell-cell contacts. *Oncogene* **18**, 7080–7090 doi:10.1038/sj.onc.1203191
31 Reddy, P., Liu, L., Ren, C., Lindgren, P., Boman, K., Shen, Y. et al. (2005) Formation of E-cadherin-mediated cell-cell adhesion activates Akt and mitogen activated protein kinase via phosphatidylinositol 3 kinase and ligand-independent activation of epidermal growth factor receptor in ovarian cancer cells. *Mol. Endocrinol.* **19**, 2564–2578 doi:10.1210/me.2004-0342
32 Neve, R.M., Chin, K., Fridlyand, J., Yeh, J., Baehner, F.L., Fevr, T. et al. (2006) A collection of breast cancer cell lines for the study of functionally distinct cancer subtypes. *Cancer Cell* **10**, 515–527 doi:10.1016/j.ccr.2006.10.008
33 Kao, J., Salari, K., Bocanegra, M., Choi, Y.-L., Girard, L., Gandhi, J. et al. (2009) Molecular profiling of breast cancer cell lines defines relevant tumor models and provides a resource for cancer gene discovery. *PLoS ONE* **4**, e6146 doi:10.1371/journal.pone.0006146
34 Kulkarni, S., Reddy, K.B., Esteva, F.J., Moore, H.C., Budd, G.T. and Tubbs, R.R. (2010) Calpain regulates sensitivity to trastuzumab and survival in HER2-positive breast cancer. *Oncogene* **29**, 1339–1350 doi:10.1038/onc.2009.422
35 Storr, S.J., Woolston, C.M., Barros, F.F.T., Green, A.R., Shehata, M., Chan, S.Y. et al. (2011) Calpain-1 expression is associated with relapse-free survival in breast cancer patients treated with trastuzumab following adjuvant chemotherapy. *Int. J. Cancer* **129**, 1773–1780 doi:10.1002/ijc.25832
36 Storr, S.J., Lee, K.W., Woolston, C.M., Safuan, S., Green, A.R., Macmillan, R.D. et al. (2012) Calpain system protein expression in basal-like and triple-negative invasive breast cancer. *Ann. Oncol.* **23**, 2289–2296 doi:10.1093/annonc/mds176
37 Storr, S.J., Pu, X., Davis, J., Lobo, D., Reece-Smith, A.M., Parsons, S.L. et al. (2013) Expression of the calpain system is associated with poor clinical outcome in gastro-oesophageal adenocarcinomas. *J. Gastroenterol.* **48**, 1213–1221
38 Shao, H., Chou, J., Baty, C.J., Burke, N.A., Watkins, S.C., Stolz, D.B. et al. (2006) Spatial localization of m-Calpain to the plasma membrane by phosphoinositide biphosphate binding during epidermal growth factor receptor-mediated activation. *Mol. Cell Biol.* **26**, 5481–5496. doi:10.1128/MCB.02243-05
39 Leloup, L., Shao, H., Bae, Y.H., Deasy, B., Stolz, D., Roy, P. et al. (2010) m-Calpain activation is regulated by its membrane localization and by its binding to phosphatidylinositol 4,5-bisphosphate. *J. Biol. Chem.* **285**, 33549–33566 doi:10.1074/jbc.M110.123604
40 Glading, A., Uberall, F., Keyse, S.M., Lauffenburger, D.A. and Wells, A. (2001) Membrane proximal ERK signaling is required for M-calpain activation downstream of epidermal growth factor receptor signaling. *J. Biol. Chem.* **276**, 23341–23348 doi:10.1074/jbc.M008847200
41 Glading, A., Chang, P., Lauffenburger, D.A. and Wells, A. (2000) Epidermal growth factor receptor activation of calpain is required for fibroblast motility and occurs via an ERK/MAP kinase signaling pathway. *J. Biol. Chem.* **275**, 2390–2398 doi:10.1074/jbc.275.4.2390